

A BIOCHEMICAL AND CELL BIOLOGICAL CHARACTERIZATION OF
TFAZZIN IN A NOVEL BARTH SYNDROME CELL MODEL

by

Ya-Wen Lu

A dissertation submitted to Johns Hopkins University in conformity with the
requirements for the degree of Doctor of Philosophy

Baltimore, Maryland

December, 2015

© 2015 Ya-Wen Lu
All Rights Reserved

ABSTRACT

Barth syndrome (BTHS) is an X-linked disease characterized by cardio- and skeletal myopathy, hypotonia, growth delay, neutropenia, and 3-methylglutaconic aciduria. Patients have mutations in the *TAZ* gene on chromosome Xq28 (G4.5) most of which are presumed to result in a loss-of-function of the protein product, tafazzin (TAZ). As TAZ is involved in the remodeling of the phospholipid, cardiolipin (CL), the resultant lipid profile in the absence of its function shows decreased CL levels, accumulated monolyso-CL, and the remaining CL contains an altered acyl chain composition. Unfortunately, the lack of an antibody against endogenous TAZ has prevented a detailed cell biologic and biochemical characterization of the endogenous protein. This in turn has impeded a molecular understanding of the protein's role in BTHS pathogenesis. Here, we have developed three mouse monoclonal antibodies capable of detecting endogenous TAZ in mammals. A complicating aspect of mammalian TAZ research is the presence of many predicted alternatively spliced variants, of which only the hTAZ –exon5 was able to fully restore aberrant CL profile in the *Saccharomyces cerevisiae* *Δataz1* mutant. Importantly, each TAZ antibody has the ability to detect every predicted isoform as determined by epitope mapping. Our results also show that only one isoform of TAZ is normally expressed in human fibroblasts, HEK293 Flp-In cells, and mouse heart and liver, despite the reported detection of mRNA corresponding to multiple splice variants.

Using mouse tissues, 293 Flp-In cells, and immortalized fibroblasts derived from healthy and BTHS patients, we demonstrate that mammalian TAZ is a highly protease-resistant and localized to the mitochondria where it associates non-integrally with membranes and assembles in a range of complexes. Like its yeast counterpart, TAZ in

humans and rodents associates with the IMS-facing leaflets of the inner and outer mitochondrial membrane, Finally, using a novel mammalian BTHS cell culture model established *via* TALEN-mediated genome editing, we demonstrate that the loss-of-function mechanisms for two pathogenic alleles, R57L and H69Q, when overexpressed in *taz*^{TALEN} cells, are the same as originally modeled and defined in yeast. Thus, our results reveal that *taz*^{TALEN} cells can serve as a convenient platform to systematically dissect the loss-of-function mechanisms that underlie other BTHS variants, especially those that cannot be modeled in yeast due to lack of conservation. Combined with the generation of antibodies against endogenous TAZ, this work provides a major leap forward in our ability to characterize this enigmatic protein, to assign and discern the functions of TAZ and its numerous variants, and to study its role in CL metabolism.

Advisor: Steven M. Claypool, Ph.D.

Reader: Rajini Rao, Ph.D.

ACKNOWLEDGEMENTS

I would like to thank my parents for believing in me. Without them, I would not be where I am today. To Ya-Lin, my baby sister (the better published Lu), I love you and good luck on getting YOUR Ph.D. I am so proud of you.

To the Claypool Lab members, Ouma Onguka, Elizabeth Calzada, Oluwaseun Ogunbona, Michelle Acoba, Matthew Baile, Selvaraju Kandasamy, and others that I have neglected to mention, thank you all for keeping me sane. I don't think that I will ever be able to experience this kind of dynamism and passion for science and life anywhere else. You guys are a joy to work with! I do, however, want to apologize if you have gained these wizzle-like characteristics:

1. Ability to throw another lab member, preferably one that is not present, under the bus,
2. Difficulty communicating with the Boss (and needed a translator),
3. Constitutively-active tear ducts,
4. Addiction to "repurposing,"
5. Tendency to make farm animal noises, especially of the feline kind,
6. Reluctant habituation of fart-sniffing.

Last but not least, thank you so much, Boss, for all that you have done for me. As my harshest critic and my most enthusiastic supporter, you have given me a graduate experience that I would not give up for anything in the world. Remember, together we do great science! Please stay awesome.

TABLE OF CONTENTS

Abstract	ii
Acknowledgements	iv
Table of Contents	v
List of Tables	viii
List of Figures	ix
Chapter 1: Cardiolipin biosynthesis and regulation in yeast	1
Abstract.....	2
Introduction.....	3
Delivering precursor phospholipids to the IMM.....	5
Synthesizing CL.....	7
Remodeling CL.....	9
Establishing the final distribution of CL.....	11
Perspectives.....	12
Acknowledgements.....	13
Figures.....	14
References.....	17
Chapter 2: Disorders of phospholipid metabolism: an emerging class of mitochondrial disease due to defects in nuclear genes	29
Abstract.....	30
Mitochondria and disease.....	32
Cardiolipin metabolism.....	34
Physiological functions.....	49

Emerging diseases of mitochondrial phospholipid metabolism.....	54
Perspectives.....	71
Acknowledgements.....	72
Figures.....	73
References.....	79
Chapter 3: Defining functional classes of Barth syndrome mutation in humans.....	131
Abstract.....	132
Introduction.....	133
Results.....	136
Discussion.....	145
Materials and methods.....	148
Acknowledgements.....	162
Figures.....	164
Supplementary Figures.....	180
References.....	187
Chapter 4: Future Directions.....	195
References.....	213
Appendix I: Unremodeled and remodeled cardiolipin are functionally indistinguishable in yeast.....	222
Summary.....	223
Introduction.....	224
Results.....	227
Disucssion.....	234

Materials and methods.....	236
Acknowledgements.....	240
Figures.....	241
References.....	251
Curriculum vitae.....	265

LIST OF TABLES

Chapter 1

Table 1	Topology of CL synthesis and remodeling enzymes.....	14
---------	--	----

Chapter 2

N/A

Chapter 3

Table 2	Predicting membrane anchors in TAZ.....	164
---------	---	-----

Table 3	Mitochondrial targeting sequences cannot be conclusively defined in any of the TAZ orthologs.....	165
---------	---	-----

Chapter 4

N/A

Appendix I

Table 4	Molecular species of CL.....	241
---------	------------------------------	-----

Table 5	Molecular species of MLCL.....	242
---------	--------------------------------	-----

LIST OF FIGURES

Chapter 1

- Figure 1.1 The topology of CL biosynthesis and remodeling.....15
- Figure 1.2 Regulatory mechanisms of CL biosynthesis and remodeling.....16

Chapter 2

- Figure 2.1 Mammalian cardiolipin biosynthesis.....73
- Figure 2.2 Mammalian cardiolipin remodeling.....74
- Figure 2.3 Inter-organelle and intra-organelle phospholipid trafficking.....75
- Figure 2.4 Biological functions of cardiolipin.....76
- Figure 2.5 Potential mechanisms of DCMA mitochondrial dysfunction.....77
- Figure 2.6 Potential consequences of the absence of SERAC1 activity.....78

Chapter 3

- Figure 3.1 One isoform of TAZ is expressed and localized to mitochondria in mammalian cells and tissues.....166
- Figure 3.2 Generation of a BTHS cell culture model using TALEN-mediated genome editing.....168
- Figure 3.3 *taz*^{TALEN} cells have altered mitochondrial CL and MLCL profiles as determined by high-performance liquid chromatography-mass spectrometry.....169
- Figure 3.4 Membrane association and assembly of TAZ.....172
- Figure 3.5 Mammalian TAZ is protease resistant and associates with IMS-facing leaflets.....173
- Figure 3.6 Both termini of TAZ are in the IMS.....175

Figure 3.7	The R57L allele is highly unstable.....	177
Figure 3.8	The H69Q mutant is catalytically dead.....	179
Figure 3.S1	Pro13 is conserved within mammals and some vertebrates but not fungi, bacteria, or plants.....	180
Figure 3.S2	Increased bis-monoacylglycerol phosphate (BMP) and decreased phosphatidylinositol (PI) in <i>taz</i> ^{TALEN} mitochondria.....	182
Figure 3.S3	<i>taz</i> ^{TALEN} cells contain modest changes in acyl chain composition of the TAZ substrates, PE and PC.....	183
Figure 3.S4	Altered BMP acylation in mitochondria from <i>taz</i> ^{TALEN} cells.....	185
Figure 3.S5	The unstable R57L allele and the catalytically-null H69Q mutant assemble in high molecular weight complexes.....	186
 Chapter 4		
Figure 4.1	Clustal Omega alignment of human and yeast tafazzin.....	210
Figure 4.2	Protease accessibility of human TAZ heterologously expressed in $\Delta taz1$	211
Figure 4.3	Amino acid compositions of yeast and human tafazzin.....	212
 Appendix I		
Figure A.1	CLD1 is epistatic to <i>TAZI</i> in the CL remodeling pathway by mitochondrial phospholipid analysis.....	243
Figure A.2	CLD1 is epistatic to <i>TAZI</i> in the CL remodeling pathway by respiratory growth analysis.....	244
Figure A.3	$\Delta cld1$ contains unremodeled CL.....	245
Figure A.4	Mitochondrial morphology is not affected by unremodeled CL.....	246
Figure A.5	Mitochondrial morphology is not affected by unremodeled CL.....	247

Figure A.6	OXPHOS function is not affected by unremodeled CL.....	248
Figure A.7	Mitochondrial proton leak is increased in the absence of CL.....	249
Figure A.8	Individual components of OXPHOS are not affected by unremodeled CL...	250

CHAPTER 1

Cardiolipin biosynthesis and regulation in yeast

This chapter is published as a review article at:

Baile MG[#], **Lu YW[#]**, and Claypool SM. The topology and regulation of cardiolipin biosynthesis and remodeling in yeast. *Chem Phys Lipids*. 2014 Apr; 179: 23-31.
[#]co-first authors

ABSTRACT

The signature mitochondrial phospholipid cardiolipin plays an important role in mitochondrial function, and alterations in cardiolipin metabolism are associated with human disease. Topologically, cardiolipin biosynthesis and remodeling are complex. Precursor phospholipids must be transported from the ER, across the mitochondrial outer membrane to the matrix-facing leaflet of the inner membrane, where cardiolipin biosynthesis commences. Post-synthesis, cardiolipin undergoes acyl chain remodeling, requiring additional trafficking steps, before it achieves its final distribution within both mitochondrial membranes. This process is regulated at several points via multiple independent mechanisms. Here, we review the regulation and topology of cardiolipin biosynthesis and remodeling in the yeast *Saccharomyces cerevisiae*. Although cardiolipin metabolism is more complicated in mammals, yeast have been an invaluable model for dissecting the steps required for this process.

KEYWORDS

cardiolipin, remodeling, mitochondria, yeast, regulation, lipid trafficking

ABBREVIATIONS

CCCP, carbonyl cyanide 3-chlorophenylhydrazone; CDP-DAG, CDP-diacylglycerol; CL, cardiolipin; ERMES, ER-mitochondrial encounter structure; IM, inner membrane; IMS, intermembrane space; OM, outer membrane; PA, phosphatidic acid; PG, phosphatidylglycerol; PGP, phosphatidylglycerolphosphate; UAS_{INO}, inositol sensitive upstream activating sequence

INTRODUCTION

The unique phospholipid cardiolipin (CL) is required for the efficiency of a number of mitochondrial processes (1). CL is unique for a number of reasons: 1) unlike most other phospholipids which are synthesized in one or a few cellular locations, then disseminated throughout a cell's membranes, CL by and large remains in the mitochondrion, its site of synthesis; 2) CL is essentially a lipid dimer; it consists of two phosphate headgroups, which are attached by a glycerol moiety, and four acyl chains; and 3) after its synthesis, CL undergoes acyl chain remodeling, where acyl chains are removed by a lipase and replaced by a transacylase or acyltransferase, resulting in the establishment of only a few molecular forms of CL in a cell or tissue. Surprisingly, the acyl chain specificity of the lipase has never been demonstrated (2), and the transacylase tafazzin has no acyl chain specificity (3), although tafazzin from *Drosophila* has been shown to preferentially catalyze transacylation reactions on curved membranes leading to the establishment of CL with unsaturated acyl chains, which were proposed to decrease lipid disorder in areas of high curvature (4). Curiously, the final molecular form of CL varies between organisms and even between cell types within the same organism.

CL serves the cell in multiple capacities: it associates with all the major proteins of the mitochondrial respiratory chain and thereby increases the efficiency of electron flow and ADP/ATP exchange (5-12), modulates the catalytic activities and stability of interacting proteins (7, 12-15), is critical for the biogenesis of mitochondrial proteins (12, 16, 17), facilitates mitochondrial fission/fusion (18-20), and is involved in the maintenance and plenitude of cristae morphology (21-23).

In addition to the importance of CL in promoting and maintaining normal mitochondrial function, alterations in CL metabolism have been associated with ischemia and reperfusion, heart failure, diabetic cardiomyopathy, and Barth syndrome (24-28). Barth syndrome is caused by mutations in tafazzin (*TAZI*), and patients present with cardio- and skeletal myopathy, neutropenia, 3-methylglutaconic aciduria, and abnormal mitochondria (24, 29).

Much of the knowledge of CL biosynthesis and remodeling comes from studies in yeast. In addition to the “usual” advantages of using yeast as a model system (30, 31), yeast are viable in the absence of CL and CL precursor phospholipids (32-36) whereas in higher eukaryotes CL is required for life (37). Although CL biosynthesis and remodeling are highly conserved between yeast and higher eukaryotes, there are still a few differences. There are no orthologs of Gep4p, the phosphatidylglycerolphosphate (PGP) phosphatase, or Cld1p, a CL lipase, in higher eukaryotes (2, 32). However, the phylogenetically unrelated PTPMT1 performs the same function as Gep4p (37); and a calcium-independent phospholipase A₂ has been implicated as a CL lipase (38-40), although its exact role in CL remodeling remains nebulous (41). Additionally, only the tafazzin-mediated CL remodeling pathway exists in yeast, while additional remodeling enzymes have been identified in mammals (reviewed in (1)). Thus, while yeast have been useful in dissecting this process, the complexity of and multitude of players in mammalian CL remodeling suggest that there is still much to discover.

With the recent characterizations of Cld1p, Gep4p and Tam41p (2, 32, 42), it is likely that all of the proteins catalyzing CL synthetic or remodeling reactions have been

identified in yeast; however, many questions regarding the regulation of this process, as well as the topology and trafficking of CL and its precursors, remain (Figure 1.1).

DELIVERING PRECURSOR PHOSPHOLIPIDS TO THE IMM

CL biosynthesis requires CDP-diacylglycerol (CDP-DAG), which is formed from phosphatidic acid (PA) and CTP by a CDP-DAG synthase (43). Yeast contain two CDP-DAG synthases: Cds1p in the ER (44), and the recently characterized Tam41p in the mitochondrial inner membrane (IMM) (42).

Although CDP-DAG (containing an NBD moiety) is able to be translocated from the ER to the IM *in vitro*, this process is inefficient (42). The very low abundance of CL in $\Delta tam41$ yeast (45, 46) suggests that if Cds1p-derived CDP-DAG contributes to CL biosynthesis, its role is very minor. Tam41p is peripherally associated with the matrix side of the IMM (Table 1) (42, 47). Thus, Tam41p activity requires that its substrate, PA, be transported from the ER to the matrix-facing leaflet of the IMM. Phospholipid transport between the ER and mitochondrial outer membrane (OMM) was suggested to be mediated by the ER-mitochondria encounter structure (ERMES) complex which physically tethers the two organelles (48). Indeed, loss of any ERMES complex subunit (Mdm10p, Mdm34, Mdm12p, or Mmm1p) alters the mitochondrial phospholipid profile, including reducing CL (45, 48, 49). However, its direct role in phospholipid transport has recently been challenged (50, 51). Further, defects caused by the loss of a functional ERMES complex can be rescued by expressing an artificial ER-mitochondria tether, suggesting that the ERMES complex facilitates phospholipid transport by forming close contact sites between the two membranes, rather than directly transporting phospholipids

(48, 50, 51). Notably, these studies focused on the transport of phosphatidylserine from the ER to mitochondria (and phosphatidylethanolamine to the ER after is decarboxylation in mitochondria). Thus, the mechanisms of PA and CDP-DAG transport from the ER to mitochondria, and the players involved, including a direct assessment of the role of the ERMES complex, remain to be discovered.

To reach to the IMM, CL precursor phospholipids must traverse the OMM, but little is known about this process. Phospholipid exchange between leaflets of purified OMM vesicles is rapid, suggesting that proteins mediate this process. However, treatment with proteases or with sulfhydryl reactive compounds does not inhibit transbilayer movement across the OMM (52).

PA is transported from the OMM to the IMM by the intermembrane space (IMS) resident protein, Ups1p (53). Mdm35p binds Ups1p, facilitating its import into the IMS and preventing its proteolytic degradation (54, 55). Although Ups1p/Mdm35p dimers can bind negatively charged phospholipids, only PA is transported *in vitro*, demonstrating the specificity of its transport activity. Ups1p is unable to dissociate from membranes containing physiological levels of CL. Thus, the higher amount of CL in the IMM is modeled to confer directionality of PA transport and the ability to limit CL accumulation (53). Once delivered to the IMM, PA must traverse to the matrix side of the IMM. This could be accomplished by an unidentified protein or alternatively, PA may redistribute to both leaflets of the IMM based on the transmembrane pH gradient (56, 57).

SYNTHESIZING CL

The first committed step of CL biosynthesis is the formation of PGP from CDP-DAG and glycerol-3-phosphate by Pgs1p (36). While the topology of Pgs1p has never been formally investigated (Table 1), the presence of an NH₂-terminal presequence, which is able to import the *lacZ* gene product to the matrix (58), suggests that Pgs1p is localized on the matrix side of the IMM. PGP is then dephosphorylated to phosphatidylglycerol (PG) by Gep4p, a protein that is peripherally attached to the matrix side of the IMM (32). In the final step of CL biosynthesis, PG and another CDP-DAG are condensed to form CL by Crd1p (34, 35). Characterization of the rat Crd1p homolog from liver indicates that it is an integral membrane protein and that its active site faces the matrix (59, 60).

Exogenous inositol downregulates phosphatidylcholine and phosphatidylinositol biosynthesis through transcriptional repression via an inositol sensitive upstream activating sequence (UAS_{INO}) (61). Pgs1p activity is similarly reduced in the presence of inositol, but it contains a mutated, nonfunctional UAS_{INO} sequence (62) and *PGSI* mRNA levels are unchanged in the presence of inositol (63). Further, deletion of the UAS_{INO}-binding genes *INO2*, *INO4*, or *OPII* does not affect Pgs1p activity (64), suggesting its inositol-mediated regulation is independent of the *INO2-INO4-OPII* circuit. Indeed, inositol increases Pgs1p phosphorylation, leading to its repressed activity, although the kinase(s) involved has yet to be identified (65). Independent from its inositol-mediated regulation, Pgs1p activity is increased under conditions indicative of mitochondrial biogenesis; its mRNA abundance is highest when cells enter stationary

phase, and its activity is higher in the presence of non-fermentable carbon sources and when cells contain functional mtDNA (63, 66, 67).

Crd1p activity is similarly increased during stationary growth, in the presence of mtDNA, and in the presence of non-fermentable carbon sources, leading to increased CL levels (66, 68-72). This is not surprising considering the importance of CL in a myriad of mitochondrial functions (1); as mitochondrial biogenesis increases, CL levels concurrently increase.

Crd1p activity can be additionally regulated by the matrix pH (73). Treatment of yeast with the protonophore CCCP (which disrupts the pH and electrical gradients across the IMM), but not the K⁺ ionophore valinomycin (which disrupts the electrical gradient but does not affect the matrix pH), decreases Crd1p activity. A decrease in the matrix pH is indicative of less robust electron transport chain activity, coordinating the mitochondrion's energetic requirements with CL biosynthesis. This is further exemplified by the decreases in CL levels that result from defects in respiratory complexes and/or bioenergetic function (73, 74).

Interestingly, while steady state CL levels were reduced in $\Delta taz1$ yeast, synthesis of CL was actually increased in the mutant, concurrent with MLCL accumulation (28). These observations led the group to suggest that *de novo* CL biosynthesis might be regulated by downstream CL acylation/remodeling. Crd1p's activity might therefore be negatively regulated by its own product, and under conditions where CL is decreased or aberrantly acylated, the cell compensates by promoting CL biogenesis.

CL biosynthesis is thus regulated via multiple independent mechanisms: by inositol, which regulates Pgs1p; by mitochondrial biogenesis, which affects Pgs1p and

Crd1p activity; by CL, which may inhibit Crd1p activity; and by the capacity for oxidative phosphorylation, which affects Crd1p.

REMODELING CL

CL remodeling is initiated by the lipase Cld1p in yeast (2), which removes an acyl chain from CL, generating MLCL. Taz1p performs an acyl-CoA independent transacylation reaction, transferring an acyl chain from a phospholipid to a lysophospholipid (generated by a phospholipase), regenerating CL (28, 75, 76).

Cld1p is located on the matrix-facing leaflet of the IM and does not traverse the membrane (69). Surprisingly, the localization of Taz1p is not the same as enzymes upstream in the pathway. In yeast, Taz1p was originally localized to the mitochondrial OMM (77), but was later shown to be present on both the inner and outer membrane, on leaflets facing the IMS (16, 25). Taz1p is an interfacial membrane protein; it contains residues that are embedded in, but not through, the membrane (Claypool 2006).

Cld1p and Taz1p are localized to different sides of the IMM, and neither contains transmembrane domains, suggesting that an as yet unidentified protein(s) transports MLCL generated by Cld1p to the opposite side of the IMM and/or to the OMM. This trafficking of MLCL is expected to occur rapidly after CL deacylation as MLCL does not accumulate in yeast with a functional Taz1p (28, 69). That both Cld1p and Taz1p assemble into higher-order complexes (25, 68, 69), and that their binding partners have been, at best, partially defined, raises the exciting possibility that the protein(s) mediating MLCL translocation physically interacts with Cld1p, Taz1p, or both enzymes, although this has yet to be tested. While proteins mediating phospholipid redistribution between

membrane leaflets have been identified for the plasma membrane, Golgi, and endosomes (78), considerably less is known about this process in the mitochondrion. CL redistribution between IMM leaflets has been observed (56, 60), but the protein(s) responsible has not been identified. So far, phospholipid scramblase 3 (PLS3) is the only mitochondrial protein suggested to facilitate transbilayer lipid trafficking (79), but this has not been formally demonstrated. Further, deletion of its predicted yeast ortholog, *AIM25*, in yeast does not result in MLCL accumulation (data not shown). Importantly, the translocation of phospholipids between membrane leaflets may not be facilitated by specific proteins, but instead non-specifically by the presence of numerous transmembrane proteins, as has been suggested for bacterial membranes and the ER (78, 80, 81).

Similar to Crd1p, Cld1p activity is upregulated in the presence of non-fermentable carbon sources. Cld1p expression increases in lactate-containing media, and is repressed in dextrose-containing media (69), suggesting that CL remodeling is coordinately regulated with biosynthesis. Cld1p is also regulated by changes in the electrochemical gradient, but through a different mechanism and with a different functional outcome than Crd1p regulation. While reduction of the matrix pH decreases Crd1p activity (73), Cld1p activity increases upon dissipation of the electrical potential (69). These differences may provide a mechanism by which CL biosynthesis and remodeling activity can be independently adjusted to fit the requirements of the mitochondrion.

Cld1p is the only protein in the CL remodeling pathway whose activity is known to be regulated (Taz1p expression increases when yeast are grown in the presence of non-fermentable carbon sources (69). Despite the fact that the spatial separation of Cld1p and

Taz1p provides a potential point of regulation, MLCL levels remain unchanged and very low/absent unless Taz1p is non-functional (69), suggesting that the activity of the MLCL flippase and Taz1p is never limiting.

ESTABLISHING THE FINAL DISTRIBUTION OF CL

CL is enriched in the IMM, but is also present on the OMM (16). How it achieves its final distribution in yeast is still unclear. Intriguingly, the presence of a subpopulation of Taz1p on the OMM opens up the possibility that MLCL may be the lipid species trafficked from the IMM to the OMM, where it is then reacylated to form CL (16, 25).

Phospholipid transfer between the OMM and IMM has been suggested to occur at contact sites between the two membranes (82, 83). Recently, the proteins comprising this complex (termed mitochondrial inner membrane organizing system, MICOS) have been identified (84-86). Loss of this complex results in abnormal cristae morphology and loss of cristae junctions. However, the effects on phospholipid transport, the import of the CL precursor PA, or the final distribution of CL, have yet to be studied in contact site mutant yeast strains.

Currently, three proteins have been described that have the ability to traffic/redistribute CL in mammals: the mitochondrial creatine kinase (MtCK) (87), the mitochondrial nucleoside diphosphate kinase (NDPK-D) (87, 88), and phospholipid scramblase 3 (PLS3) (79). However, MtCK has no ortholog in yeast. Yeast also do not contain a mitochondrial-specific ortholog of NDPK-D, although a small portion of the yeast nucleoside diphosphate kinase, Ynk1p, localizes to mitochondria (89). However, if Ynk1p can transport CL between membranes remains to be determined. PLS3 was shown

to redistribute CL between the IMM and OMM in mammalian mitochondria (79), but phospholipid transport between membranes is inconsistent with its role as a scramblase. Thus, it is likely that PLS3 instead coordinates with a CL transport protein, and the altered distribution of CL between the OMM and IMM when PLS3 is overexpressed reflects the increased availability of CL on the IMS-facing leaflet of the IMM.

Three UPS isoforms exist in yeast, although a concrete function has yet to be assigned to Ups2p or Ups3p. It is tempting to speculate that, like Ups1p and PA (53), either of these proteins can transport CL (or MLCL) between the IMM and OMM. Interestingly, total CL levels in *UPS2* and *UPS3* mutants remain largely unaffected (90, 91), but the relative distribution of CL between the IMM and OMM has never been analyzed.

PERSPECTIVES

While most, if not all, of the enzymes involved in CL biosynthesis and remodeling have been identified (at least in yeast), many questions remain. How CL precursors are trafficked, and how CL achieves its final distribution, remains incompletely resolved. The ERMES complex is undoubtedly important for the trafficking of phospholipids between the ER and OMM, but whether it directly transports phospholipids or simply mediates the apposition of the two membranes remains to be answered. OMM/IMM contact sites are potentially important for the movement of both CL precursors and CL itself between mitochondrial membranes, but this is currently an understudied aspect of CL metabolism. Additionally, the proteins mediating CL/MLCL movement, both between membranes and between leaflets of the same membrane, await

identification. The regulation of CL precursor trafficking, except for the potential ability of CL to inhibit Ups1p/Mdm35p-mediated PA import, is unknown. Trafficking steps have the potential to regulate the flux of precursors through the CL pathway, but whether this is the case has yet to be determined. Further, compared to yeast (Figure 2 summarizes modes of regulation identified in yeast), knowledge of these processes and their regulation in mammals is lacking.

ACKNOWLEDGEMENTS

Work in the authors' laboratory is supported by National Institutes of Health grant 1R01HL108882. Y.L. is a predoctoral fellow of the American Heart Association.

TABLE 1 Topology of CL synthesis and remodeling enzymes.

Protein	Localization / Membrane association	Predicted transmembrane domains^a	Biochemical experiments	Refs.
Tam41p	Matrix leaflet of IMM/peripheral	0	Protected from protease in mitoplasts, extracted with carbonate	(92)
Pgs1p	Matrix leaflet of IMM/peripheral	0, 1, 2 ^b	NH ₂ -terminal presequence imports <i>LacZ</i> to mitochondrial matrix	(58)
Gep4p	Matrix leaflet of IMM/peripheral	0	Protected from protease in mitoplasts; extracted with carbonate	(32)
Crd1p	Active site faces the matrix of the IMM/integral	2, 3, 4, 5	Protected from protease in mitoplasts; blocking divalent cation entry into the matrix inhibits CL synthesis ^c	(59)
Cld1p	Matrix leaflet of IMM/non-integral	0, 1, 2	Protected from protease in mitoplasts; partially extracted with carbonate; extracted with high salt concentrations	(69)
Taz1p	IMS-facing leaflet of IMM and OMM/non-integral	0, 1, 2	Degraded by protease in mitoplasts; partially extracted with carbonate; epitope tags throughout the polypeptide face the IMS	(25)

^aTransmembrane predictions were determined using the DAS-TMfilter prediction server (93), TMpred (94), HMMTOP (95), TMHMM (96), and SPLIT (97)

^bMost programs predicted Pgs1p to have 0 transmembrane domains, except TMpred which predicted either 1 or 2 transmembrane segments

^cBiochemical experiments have not been performed on yeast Crd1p. The experiments here analyzed the rat Crd1p homolog

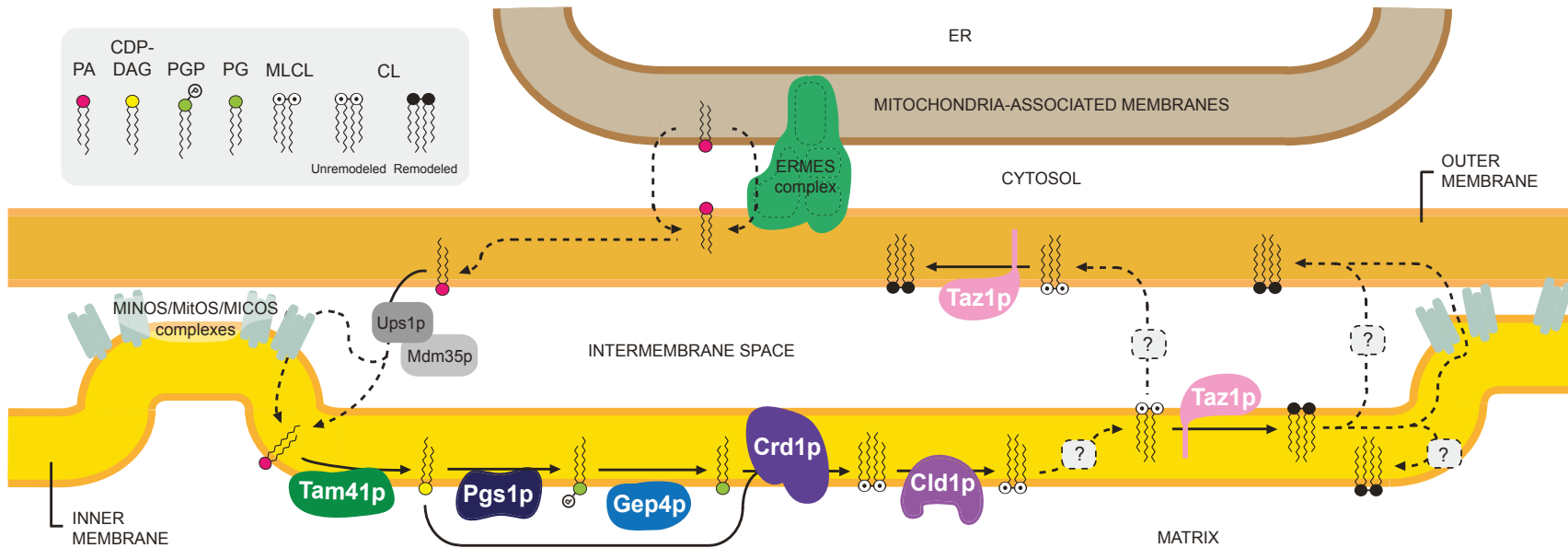


FIGURE 1.1 The topology of CL biosynthesis and remodeling. Phosphatidic acid (PA) is synthesized in the ER and translocates to mitochondria in a process that is influenced by the ERMES (ER-mitochondria encounter structure) complex. Ups1/Mdm35p heterodimers transport PA from the OMM to the IMM, potentially at contact sites (established by MICOS complexes). PA is converted to CDP-diacylglycerol (CDP-DAG) by Tam41p on the matrix-facing leaflet of the IM. CDP-DAG is used to generate phosphatidylglycerolphosphate (PGP) by Pgs1p. PGP is dephosphorylated to phosphatidylglycerol (PG) by Gep4p. PG and another CDP-DAG are condensed to form unremodeled CL by Crd1p. CL is deacylated by Cld1p on the matrix-facing leaflet of the IMM, forming MLCL. *Via* an unknown mechanism, MLCL must flip to the IMS-facing leaflet of the IMM or be transported to the OMM to gain access to the transacylase Taz1p, which regenerates CL. Multiple rounds of deacylation/reacylation result in remodeled CL which is enriched in unsaturated acyl chains. CL achieves its final distribution on both leaflets of the IMM and OMM through currently ill-defined mechanisms. The depicted topology of Pgs1p has not been experimentally verified. Solid lines indicate known pathways. Dashed lines delineate potential but currently unknown phospholipid transport processes.

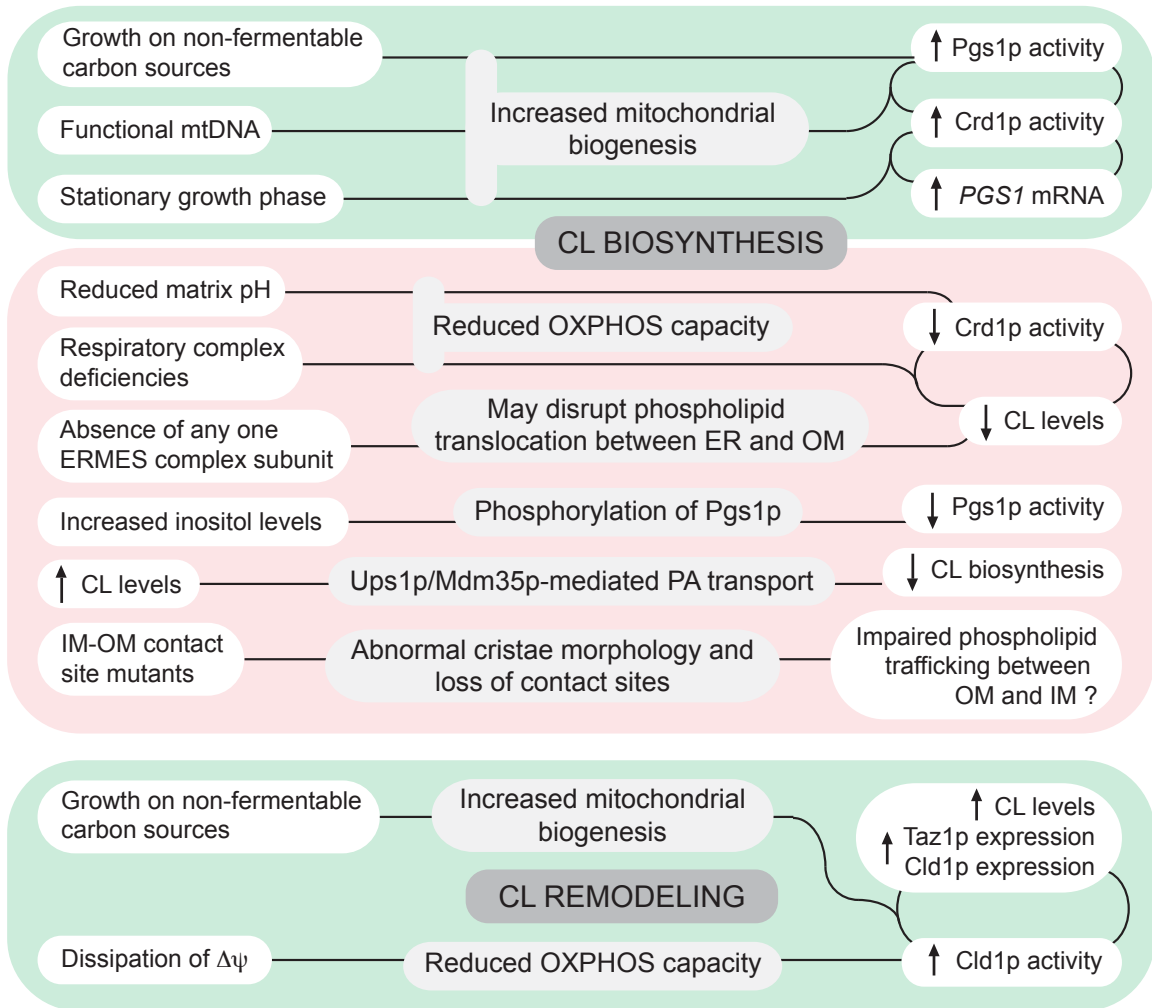


FIGURE 1.2 Regulatory mechanisms of CL biosynthesis and remodeling. The CL biosynthetic pathway is upregulated under conditions favoring mitochondrial biogenesis. In contrast, deficiencies in ERMES (ER-OMM), MICOS (OMM-IMM contact sites) complexes, and components of the electron transport chain, as well as increased levels of inositol and reduced matrix pH, can all lead to a down-regulation of CL biosynthesis. Additionally, CL levels can be modulated by Ups1p/Mdm35p-mediated PA transport. Similar to CL biosynthesis, growth of yeast on respiratory media also promotes CL remodeling by upregulating the activity and/or expression of enzymes in the remodeling pathway. Distinct from CL biosynthesis, dissipation of the electrical potential across the IMM, indicative of reduced OXPHOS capacity, increases Cld1p activity. Green boxes indicates conditions that promote CL biosynthesis and remodeling while red boxes indicate conditions that repress CL biosynthesis.

REFERENCES

- 1 Claypool, S.M. and Koehler, C.M. (2012) The complexity of cardiolipin in health and disease. *Trends Biochem Sci*, **37**, 32-41.
- 2 Beranek, A., Rechberger, G., Knauer, H., Wolinski, H., Kohlwein, S.D. and Leber, R. (2009) Identification of a cardiolipin-specific phospholipase encoded by the gene *CLD1* (*YGR110W*) in yeast. *The Journal of biological chemistry*, **284**, 11572-11578.
- 3 Schlame, M. (2012) Cardiolipin remodeling and the function of tafazzin. *Biochimica et biophysica acta*, **1831**, 582-588.
- 4 Schlame, M., Acehan, D., Berno, B., Xu, Y., Valvo, S., Ren, M., Stokes, D.L. and Epan, R.M. (2012) The physical state of lipid substrates provides transacylation specificity for tafazzin. *Nature chemical biology*, **8**, 862-869.
- 5 Acehan, D., Malhotra, A., Xu, Y., Ren, M., Stokes, D.L. and Schlame, M. (2011) Cardiolipin affects the supramolecular organization of ATP synthase in mitochondria. *Biophysical journal*, **100**, 2184-2192.
- 6 Schwall, C.T., Greenwood, V.L. and Alder, N.N. (2012) The stability and activity of respiratory Complex II is cardiolipin-dependent. *Biochimica et biophysica acta*, **1817**, 1588-1596.
- 7 Claypool, S.M., Oktay, Y., Boonthueung, P., Loo, J.A. and Koehler, C.M. (2008) Cardiolipin defines the interactome of the major ADP/ATP carrier protein of the mitochondrial inner membrane. *The Journal of cell biology*, **182**, 937-950.
- 8 Fry, M. and Green, D.E. (1981) Cardiolipin requirement for electron transfer in complex I and III of the mitochondrial respiratory chain. *The Journal of biological chemistry*, **256**, 1874-1880.
- 9 Yu, C.A. and Yu, L. (1980) Structural role of phospholipids in ubiquinol-cytochrome c reductase. *Biochemistry*, **19**, 5715-5720.

- 10 Schagger, H., Hagen, T., Roth, B., Brandt, U., Link, T.A. and von Jagow, G. (1990) Phospholipid specificity of bovine heart bc1 complex. *European journal of biochemistry / FEBS*, **190**, 123-130.
- 11 Bazan, S., Mileykovskaya, E., Mallampalli, V.K., Heacock, P., Sparagna, G.C. and Dowhan, W. (2013) Cardiolipin-dependent reconstitution of respiratory supercomplexes from purified *Saccharomyces cerevisiae* complexes III and IV. *The Journal of biological chemistry*, **288**, 401-411.
- 12 Jiang, F., Ryan, M.T., Schlame, M., Zhao, M., Gu, Z., Klingenberg, M., Pfanner, N. and Greenberg, M.L. (2000) Absence of cardiolipin in the *crd1* null mutant results in decreased mitochondrial membrane potential and reduced mitochondrial function. *The Journal of biological chemistry*, **275**, 22387-22394.
- 13 Wenz, T., Hielscher, R., Hellwig, P., Schagger, H., Richers, S. and Hunte, C. (2009) Role of phospholipids in respiratory cytochrome bc(1) complex catalysis and supercomplex formation. *Biochimica et biophysica acta*, **1787**, 609-616.
- 14 Gomez, B., Jr. and Robinson, N.C. (1999) Phospholipase digestion of bound cardiolipin reversibly inactivates bovine cytochrome bc1. *Biochemistry*, **38**, 9031-9038.
- 15 Pfeiffer, K., Gohil, V., Stuart, R.A., Hunte, C., Brandt, U., Greenberg, M.L. and Schagger, H. (2003) Cardiolipin stabilizes respiratory chain supercomplexes. *The Journal of biological chemistry*, **278**, 52873-52880.
- 16 Gebert, N., Joshi, A.S., Kutik, S., Becker, T., McKenzie, M., Guan, X.L., Mooga, V.P., Stroud, D.A., Kulkarni, G., Wenk, M.R. *et al.* (2009) Mitochondrial cardiolipin involved in outer-membrane protein biogenesis: implications for Barth syndrome. *Curr Biol*, **19**, 2133-2139.
- 17 Joshi, A.S., Zhou, J., Gohil, V.M., Chen, S. and Greenberg, M.L. (2009) Cellular functions of cardiolipin in yeast. *Biochimica et biophysica acta*, **1793**, 212-218.
- 18 Joshi, A.S., Thompson, M.N., Fei, N., Huttemann, M. and Greenberg, M.L. (2012) Cardiolipin and mitochondrial phosphatidylethanolamine have overlapping functions in

- mitochondrial fusion in *Saccharomyces cerevisiae*. *The Journal of biological chemistry*, **287**, 17589-17597.
- 19 DeVay, R.M., Dominguez-Ramirez, L., Lackner, L.L., Hoppins, S., Stahlberg, H. and Nunnari, J. (2009) Coassembly of Mgm1 isoforms requires cardiolipin and mediates mitochondrial inner membrane fusion. *The Journal of cell biology*, **186**, 793-803.
- 20 Ban, T., Heymann, J.A., Song, Z., Hinshaw, J.E. and Chan, D.C. (2010) OPA1 disease alleles causing dominant optic atrophy have defects in cardiolipin-stimulated GTP hydrolysis and membrane tubulation. *Human molecular genetics*, **19**, 2113-2122.
- 21 Acehan, D., Xu, Y., Stokes, D.L. and Schlame, M. (2007) Comparison of lymphoblast mitochondria from normal subjects and patients with Barth syndrome using electron microscopic tomography. *Lab Invest*, **87**, 40-48.
- 22 Acehan, D., Khuchua, Z., Houtkooper, R.H., Malhotra, A., Kaufman, J., Vaz, F.M., Ren, M., Rockman, H.A., Stokes, D.L. and Schlame, M. (2009) Distinct effects of tafazzin deletion in differentiated and undifferentiated mitochondria. *Mitochondrion*, **9**, 86-95.
- 23 Mileykovskaya, E. and Dowhan, W. (2009) Cardiolipin membrane domains in prokaryotes and eukaryotes. *Biochimica et biophysica acta*, **1788**, 2084-2091.
- 24 Schlame, M. and Ren, M. (2006) Barth syndrome, a human disorder of cardiolipin metabolism. *FEBS letters*, **580**, 5450-5455.
- 25 Claypool, S.M., McCaffery, J.M. and Koehler, C.M. (2006) Mitochondrial mislocalization and altered assembly of a cluster of Barth syndrome mutant tafazzins. *The Journal of cell biology*, **174**, 379-390.
- 26 Chicco, A.J. and Sparagna, G.C. (2007) Role of cardiolipin alterations in mitochondrial dysfunction and disease. *American journal of physiology. Cell physiology*, **292**, C33-44.
- 27 Paradies, G., Ruggiero, F.M., Petrosillo, G. and Quagliariello, E. (1997) Age-dependent decline in the cytochrome c oxidase activity in rat heart mitochondria: role of cardiolipin. *FEBS letters*, **406**, 136-138.

- 28 Gu, Z., Valianpour, F., Chen, S., Vaz, F.M., Hakkaart, G.A., Wanders, R.J. and Greenberg, M.L. (2004) Aberrant cardiolipin metabolism in the yeast *taz1* mutant: a model for Barth syndrome. *Molecular microbiology*, **51**, 149-158.
- 29 Barth, P.G., Scholte, H.R., Berden, J.A., Van der Klei-Van Moorsel, J.M., Luyt-Houwen, I.E., Van 't Veer-Korthof, E.T., Van der Harten, J.J. and Sobotka-Plojhar, M.A. (1983) An X-linked mitochondrial disease affecting cardiac muscle, skeletal muscle and neutrophil leucocytes. *Journal of the neurological sciences*, **62**, 327-355.
- 30 Baile, M.G. and Claypool, S.M. (2013) The power of yeast to model diseases of the powerhouse of the cell. *Front Biosci (Landmark Ed)*, **18**, 241-278.
- 31 Botstein, D. and Fink, G.R. (2011) Yeast: an experimental organism for 21st Century biology. *Genetics*, **189**, 695-704.
- 32 Osman, C., Haag, M., Wieland, F.T., Brugger, B. and Langer, T. (2010) A mitochondrial phosphatase required for cardiolipin biosynthesis: the PGP phosphatase Gep4. *EMBO J*, **29**, 1976-1987.
- 33 Tuller, G., Hrastnik, C., Achleitner, G., Schiefthaler, U., Klein, F. and Daum, G. (1998) YDL142c encodes cardiolipin synthase (Cls1p) and is non-essential for aerobic growth of *Saccharomyces cerevisiae*. *FEBS letters*, **421**, 15-18.
- 34 Jiang, F., Rizavi, H.S. and Greenberg, M.L. (1997) Cardiolipin is not essential for the growth of *Saccharomyces cerevisiae* on fermentable or non-fermentable carbon sources. *Molecular microbiology*, **26**, 481-491.
- 35 Chang, S.C., Heacock, P.N., Mileykovskaya, E., Voelker, D.R. and Dowhan, W. (1998) Isolation and characterization of the gene (CLS1) encoding cardiolipin synthase in *Saccharomyces cerevisiae*. *The Journal of biological chemistry*, **273**, 14933-14941.
- 36 Chang, S.C., Heacock, P.N., Clancey, C.J. and Dowhan, W. (1998) The PEL1 gene (renamed PGS1) encodes the phosphatidylglycero-phosphate synthase of *Saccharomyces cerevisiae*. *The Journal of biological chemistry*, **273**, 9829-9836.

- 37 Zhang, J., Guan, Z., Murphy, A.N., Wiley, S.E., Perkins, G.A., Worby, C.A., Engel, J.L., Heacock, P., Nguyen, O.K., Wang, J.H. *et al.* (2011) Mitochondrial phosphatase PTPMT1 is essential for cardiolipin biosynthesis. *Cell Metab*, **13**, 690-700.
- 38 Malhotra, A., Edelman-Novemsky, I., Xu, Y., Plesken, H., Ma, J., Schlame, M. and Ren, M. (2009) Role of calcium-independent phospholipase A2 in the pathogenesis of Barth syndrome. *Proceedings of the National Academy of Sciences of the United States of America*, **106**, 2337-2341.
- 39 Mancuso, D.J., Sims, H.F., Han, X., Jenkins, C.M., Guan, S.P., Yang, K., Moon, S.H., Pietka, T., Abumrad, N.A., Schlesinger, P.H. *et al.* (2007) Genetic ablation of calcium-independent phospholipase A2gamma leads to alterations in mitochondrial lipid metabolism and function resulting in a deficient mitochondrial bioenergetic phenotype. *The Journal of biological chemistry*, **282**, 34611-34622.
- 40 Schlame, M., Blais, S., Edelman-Novemsky, I., Xu, Y., Montecillo, F., Phoon, C.K., Ren, M. and Neubert, T.A. (2012) Comparison of cardiolipins from *Drosophila* strains with mutations in putative remodeling enzymes. *Chem Phys Lipids*, **165**, 512-519.
- 41 Kiebish, M.A., Yang, K., Liu, X., Mancuso, D.J., Guan, S., Zhao, Z., Sims, H.F., Cerqua, R., Cade, W.T., Han, X. *et al.* (2013) Dysfunctional cardiac mitochondrial bioenergetic, lipidomic, and signaling in a murine model of Barth syndrome. *Journal of lipid research*, **54**, 1312-1325.
- 42 Tamura, Y., Harada, Y., Nishikawa, S., Yamano, K., Kamiya, M., Shiota, T., Kuroda, T., Kuge, O., Sesaki, H., Imai, K. *et al.* (2013) Tam41 is a CDP-diacylglycerol synthase required for cardiolipin biosynthesis in mitochondria. *Cell Metab*, **17**, 709-718.
- 43 Shen, H., Heacock, P.N., Clancey, C.J. and Dowhan, W. (1996) The CDS1 gene encoding CDP-diacylglycerol synthase in *Saccharomyces cerevisiae* is essential for cell growth. *The Journal of biological chemistry*, **271**, 789-795.

- 44 Kuchler, K., Daum, G. and Paltauf, F. (1986) Subcellular and submitochondrial localization of phospholipid-synthesizing enzymes in *Saccharomyces cerevisiae*. *Journal of bacteriology*, **165**, 901-910.
- 45 Tamura, Y., Onguka, O., Hobbs, A.E., Jensen, R.E., Iijima, M., Claypool, S.M. and Sesaki, H. (2012) Role for two conserved intermembrane space proteins, Ups1p and Ups2p, [corrected] in intra-mitochondrial phospholipid trafficking. *The Journal of biological chemistry*, **287**, 15205-15218.
- 46 Kutik, S., Rissler, M., Guan, X.L., Guiard, B., Shui, G., Gebert, N., Heacock, P.N., Rehling, P., Dowhan, W., Wenk, M.R. *et al.* (2008) The translocator maintenance protein Tam41 is required for mitochondrial cardiolipin biosynthesis. *The Journal of cell biology*, **183**, 1213-1221.
- 47 Gallas, M.R., Dienhart, M.K., Stuart, R.A. and Long, R.M. (2006) Characterization of Mmp37p, a *Saccharomyces cerevisiae* mitochondrial matrix protein with a role in mitochondrial protein import. *Molecular biology of the cell*, **17**, 4051-4062.
- 48 Kornmann, B., Currie, E., Collins, S.R., Schuldiner, M., Nunnari, J., Weissman, J.S. and Walter, P. (2009) An ER-mitochondria tethering complex revealed by a synthetic biology screen. *Science*, **325**, 477-481.
- 49 Stroud, D.A., Oeljeklaus, S., Wiese, S., Bohnert, M., Lewandrowski, U., Sickmann, A., Guiard, B., van der Laan, M., Warscheid, B. and Wiedemann, N. (2011) Composition and topology of the endoplasmic reticulum-mitochondria encounter structure. *J Mol Biol*, **413**, 743-750.
- 50 Voss, C., Lahiri, S., Young, B.P., Loewen, C.J. and Prinz, W.A. (2012) ER-shaping proteins facilitate lipid exchange between the ER and mitochondria in *S. cerevisiae*. *J Cell Sci*, **125**, 4791-4799.
- 51 Nguyen, T.T., Lewandowska, A., Choi, J.Y., Markgraf, D.F., Junker, M., Bilgin, M., Ejsing, C.S., Voelker, D.R., Rapoport, T.A. and Shaw, J.M. (2012) Gem1 and ERMES do not

directly affect phosphatidylserine transport from ER to mitochondria or mitochondrial inheritance. *Traffic*, **13**, 880-890.

52 Janssen, M.J., Koorengel, M.C., de Kruijff, B. and de Kroon, A.I. (1999) Transbilayer movement of phosphatidylcholine in the mitochondrial outer membrane of *Saccharomyces cerevisiae* is rapid and bidirectional. *Biochimica et biophysica acta*, **1421**, 64-76.

53 Connerth, M., Tatsuta, T., Haag, M., Klecker, T., Westermann, B. and Langer, T. (2012) Intramitochondrial transport of phosphatidic acid in yeast by a lipid transfer protein. *Science*, **338**, 815-818.

54 Tamura, Y., Iijima, M. and Sesaki, H. (2010) Mdm35p imports Ups proteins into the mitochondrial intermembrane space by functional complex formation. *EMBO J*, **29**, 2875-2887.

55 Potting, C., Wilmes, C., Engmann, T., Osman, C. and Langer, T. (2010) Regulation of mitochondrial phospholipids by Ups1/PRELI-like proteins depends on proteolysis and Mdm35. *EMBO J*, **29**, 2888-2898.

56 Gallet, P.F., Zachowski, A., Julien, R., Fellmann, P., Devaux, P.F. and Maftah, A. (1999) Transbilayer movement and distribution of spin-labelled phospholipids in the inner mitochondrial membrane. *Biochimica et biophysica acta*, **1418**, 61-70.

57 Hope, M.J., Redelmeier, T.E., Wong, K.F., Rodriguez, W. and Cullis, P.R. (1989) Phospholipid asymmetry in large unilamellar vesicles induced by transmembrane pH gradients. *Biochemistry*, **28**, 4181-4187.

58 Dzugasova, V., Obernauerova, M., Horvathova, K., Vachova, M., Zakova, M. and Subik, J. (1998) Phosphatidylglycerolphosphate synthase encoded by the PEL1/PGS1 gene in *Saccharomyces cerevisiae* is localized in mitochondria and its expression is regulated by phospholipid precursors. *Curr Genet*, **34**, 297-302.

59 Schlame, M. and Haldar, D. (1993) Cardiolipin is synthesized on the matrix side of the inner membrane in rat liver mitochondria. *The Journal of biological chemistry*, **268**, 74-79.

- 60 Gallet, P.F., Petit, J.M., Maftah, A., Zachowski, A. and Julien, R. (1997) Asymmetrical distribution of cardiolipin in yeast inner mitochondrial membrane triggered by carbon catabolite repression. *The Biochemical journal*, **324 (Pt 2)**, 627-634.
- 61 Henry, S.A., Kohlwein, S.D. and Carman, G.M. (2012) Metabolism and regulation of glycerolipids in the yeast *Saccharomyces cerevisiae*. *Genetics*, **190**, 317-349.
- 62 Bachhawat, N., Ouyang, Q. and Henry, S.A. (1995) Functional characterization of an inositol-sensitive upstream activation sequence in yeast. A cis-regulatory element responsible for inositol-choline mediated regulation of phospholipid biosynthesis. *The Journal of biological chemistry*, **270**, 25087-25095.
- 63 Zhong, Q. and Greenberg, M.L. (2003) Regulation of phosphatidylglycerophosphate synthase by inositol in *Saccharomyces cerevisiae* is not at the level of PGS1 mRNA abundance. *The Journal of biological chemistry*, **278**, 33978-33984.
- 64 Greenberg, M.L., Hubbell, S. and Lam, C. (1988) Inositol regulates phosphatidylglycerolphosphate synthase expression in *Saccharomyces cerevisiae*. *Molecular and cellular biology*, **8**, 4773-4779.
- 65 He, Q. and Greenberg, M.L. (2004) Post-translational regulation of phosphatidylglycerolphosphate synthase in response to inositol. *Molecular microbiology*, **53**, 1243-1249.
- 66 Gaynor, P.M., Hubbell, S., Schmidt, A.J., Lina, R.A., Minskoff, S.A. and Greenberg, M.L. (1991) Regulation of phosphatidylglycerolphosphate synthase in *Saccharomyces cerevisiae* by factors affecting mitochondrial development. *Journal of bacteriology*, **173**, 6124-6131.
- 67 Shen, H. and Dowhan, W. (1998) Regulation of phosphatidylglycerophosphate synthase levels in *Saccharomyces cerevisiae*. *The Journal of biological chemistry*, **273**, 11638-11642.
- 68 Claypool, S.M., Boontheung, P., McCaffery, J.M., Loo, J.A. and Koehler, C.M. (2008) The cardiolipin transacylase, tafazzin, associates with two distinct respiratory components providing insight into Barth syndrome. *Molecular biology of the cell*, **19**, 5143-5155.

- 69 Baile, M.G., Whited, K. and Claypool, S.M. (2013) Deacylation on the matrix side of the mitochondrial inner membrane regulates cardiolipin remodeling. *Molecular biology of the cell*, **24**, 2008-2020.
- 70 Jiang, F., Gu, Z., Granger, J.M. and Greenberg, M.L. (1999) Cardiolipin synthase expression is essential for growth at elevated temperature and is regulated by factors affecting mitochondrial development. *Molecular microbiology*, **31**, 373-379.
- 71 Jakovcic, S., Getz, G.S., Rabinowitz, M., Jakob, H. and Swift, H. (1971) Cardiolipin content of wild type and mutant yeasts in relation to mitochondrial function and development. *The Journal of cell biology*, **48**, 490-502.
- 72 Su, X. and Dowhan, W. (2006) Regulation of cardiolipin synthase levels in *Saccharomyces cerevisiae*. *Yeast*, **23**, 279-291.
- 73 Gohil, V.M., Hayes, P., Matsuyama, S., Schagger, H., Schlame, M. and Greenberg, M.L. (2004) Cardiolipin biosynthesis and mitochondrial respiratory chain function are interdependent. *The Journal of biological chemistry*, **279**, 42612-42618.
- 74 Zhao, M., Schlame, M., Rua, D. and Greenberg, M.L. (1998) Cardiolipin synthase is associated with a large complex in yeast mitochondria. *The Journal of biological chemistry*, **273**, 2402-2408.
- 75 Xu, Y., Malhotra, A., Ren, M. and Schlame, M. (2006) The enzymatic function of tafazzin. *The Journal of biological chemistry*, **281**, 39217-39224.
- 76 Xu, Y., Kelley, R.I., Blanck, T.J. and Schlame, M. (2003) Remodeling of cardiolipin by phospholipid transacylation. *The Journal of biological chemistry*, **278**, 51380-51385.
- 77 Brandner, K., Mick, D.U., Frazier, A.E., Taylor, R.D., Meisinger, C. and Rehling, P. (2005) Taz1, an outer mitochondrial membrane protein, affects stability and assembly of inner membrane protein complexes: implications for Barth Syndrome. *Molecular biology of the cell*, **16**, 5202-5214.

- 78 van Meer, G., Voelker, D.R. and Feigenson, G.W. (2008) Membrane lipids: where they are and how they behave. *Nature reviews. Molecular cell biology*, **9**, 112-124.
- 79 Liu, J., Dai, Q., Chen, J., Durrant, D., Freeman, A., Liu, T., Grossman, D. and Lee, R.M. (2003) Phospholipid scramblase 3 controls mitochondrial structure, function, and apoptotic response. *Mol Cancer Res*, **1**, 892-902.
- 80 Kol, M.A., de Kroon, A.I., Killian, J.A. and de Kruijff, B. (2004) Transbilayer movement of phospholipids in biogenic membranes. *Biochemistry*, **43**, 2673-2681.
- 81 Kol, M.A., de Kroon, A.I., Rijkers, D.T., Killian, J.A. and de Kruijff, B. (2001) Membrane-spanning peptides induce phospholipid flop: a model for phospholipid translocation across the inner membrane of *E. coli*. *Biochemistry*, **40**, 10500-10506.
- 82 Simbeni, R., Paltauf, F. and Daum, G. (1990) Intramitochondrial transfer of phospholipids in the yeast, *Saccharomyces cerevisiae*. *The Journal of biological chemistry*, **265**, 281-285.
- 83 Blok, M.C., Wirtz, K.W. and Scherphof, G.L. (1971) Exchange of phospholipids between microsomes and inner and outer mitochondrial membranes of rat liver. *Biochimica et biophysica acta*, **233**, 61-75.
- 84 von der Malsburg, K., Muller, J.M., Bohnert, M., Oeljeklaus, S., Kwiatkowska, P., Becker, T., Loniewska-Lwowska, A., Wiese, S., Rao, S., Milenkovic, D. *et al.* (2011) Dual role of mitofilin in mitochondrial membrane organization and protein biogenesis. *Dev Cell*, **21**, 694-707.
- 85 Harner, M., Korner, C., Walther, D., Mokranjac, D., Kaesmacher, J., Welsch, U., Griffith, J., Mann, M., Reggiori, F. and Neupert, W. (2011) The mitochondrial contact site complex, a determinant of mitochondrial architecture. *EMBO J*, **30**, 4356-4370.
- 86 Hoppins, S., Collins, S.R., Cassidy-Stone, A., Hummel, E., Devay, R.M., Lackner, L.L., Westermann, B., Schuldiner, M., Weissman, J.S. and Nunnari, J. (2011) A mitochondrial-focused

genetic interaction map reveals a scaffold-like complex required for inner membrane organization in mitochondria. *The Journal of cell biology*, **195**, 323-340.

87 Epand, R.F., Schlattner, U., Wallimann, T., Lacombe, M.L. and Epand, R.M. (2007) Novel lipid transfer property of two mitochondrial proteins that bridge the inner and outer membranes. *Biophysical journal*, **92**, 126-137.

88 Schlattner, U., Tokarska-Schlattner, M., Ramirez, S., Tyurina, Y.Y., Amoscato, A.A., Mohammadyani, D., Huang, Z., Jiang, J., Yanamala, N., Seffouh, A. *et al.* (2013) Dual function of mitochondrial Nm23-H4 protein in phosphotransfer and intermembrane lipid transfer: a cardiolipin-dependent switch. *The Journal of biological chemistry*, **288**, 111-121.

89 Amutha, B. and Pain, D. (2003) Nucleoside diphosphate kinase of *Saccharomyces cerevisiae*, Ynk1p: localization to the mitochondrial intermembrane space. *The Biochemical journal*, **370**, 805-815.

90 Tamura, Y., Endo, T., Iijima, M. and Sesaki, H. (2009) Ups1p and Ups2p antagonistically regulate cardiolipin metabolism in mitochondria. *The Journal of cell biology*, **185**, 1029-1045.

91 Osman, C., Haag, M., Potting, C., Rodenfels, J., Dip, P.V., Wieland, F.T., Brugger, B., Westermann, B. and Langer, T. (2009) The genetic interactome of prohibitins: coordinated control of cardiolipin and phosphatidylethanolamine by conserved regulators in mitochondria. *The Journal of cell biology*, **184**, 583-596.

92 Tamura, Y., Harada, Y., Yamano, K., Watanabe, K., Ishikawa, D., Ohshima, C., Nishikawa, S., Yamamoto, H. and Endo, T. (2006) Identification of Tam41 maintaining integrity of the TIM23 protein translocator complex in mitochondria. *The Journal of cell biology*, **174**, 631-637.

93 Cserzo, M., Eisenhaber, F., Eisenhaber, B. and Simon, I. (2004) TM or not TM: transmembrane protein prediction with low false positive rate using DAS-TMfilter. *Bioinformatics*, **20**, 136-137.

- 94 Hofmann, K. and Stoffel, W. (1993) TMbase - A database of membrane spanning proteins segments. *Biol. Chem. Hoppe-Seyler*, **374**, 166.
- 95 Tusnady, G.E. and Simon, I. (1998) Principles governing amino acid composition of integral membrane proteins: application to topology prediction. *J Mol Biol*, **283**, 489-506.
- 96 Krogh, A., Larsson, B., von Heijne, G. and Sonnhammer, E.L. (2001) Predicting transmembrane protein topology with a hidden Markov model: application to complete genomes. *J Mol Biol*, **305**, 567-580.
- 97 Juretic, D., Zoranic, L. and Zucic, D. (2002) Basic charge clusters and predictions of membrane protein topology. *J Chem Inf Comput Sci*, **42**, 620-632.

CHAPTER 2

Disorders of phospholipid metabolism: an emerging class of mitochondrial disease due to defects in nuclear genes

This chapter appears as a review article published at:

Lu YW, Claypool SM. Disorders of phospholipid metabolism: an emerging class of mitochondrial disease due to defects in nuclear genes. *Front Genet.* 2015 Feb 3; 6:3.

ABSTRACT

The human nuclear and mitochondrial genomes co-exist within each cell. While the mitochondrial genome encodes for a limited number of proteins, transfer RNAs, and ribosomal RNAs, the vast majority of mitochondrial proteins are encoded in the nuclear genome. Of the multitude of mitochondrial disorders known to date, only a fifth are maternally inherited. The recent characterization of the mitochondrial proteome therefore serves as an important step towards delineating the nosology of a large spectrum of phenotypically heterogeneous diseases. Following the identification of the first nuclear gene defect to underlie a mitochondrial disorder, a plenitude of genetic variants that provoke mitochondrial pathophysiology have been molecularly elucidated and classified into six categories that impact: 1) oxidative phosphorylation (subunits and assembly factors); 2) mitochondrial DNA maintenance and expression; 3) mitochondrial protein import and assembly; 4) mitochondrial quality control (chaperones and proteases); 5) iron-sulfur cluster homeostasis; and 6) mitochondrial dynamics (fission and fusion). Here, we propose that an additional class of genetic variant be included in the classification schema to acknowledge the role of genetic defects in phospholipid biosynthesis, remodeling, and metabolism in mitochondrial pathophysiology. This seventh class includes a small but notable group of nuclear-encoded proteins whose dysfunction impacts normal mitochondrial phospholipid metabolism. The resulting human disorders present with a diverse array of pathologic consequences that reflect the variety of functions that phospholipids have in mitochondria and highlight the important role of proper membrane homeostasis in mitochondrial biology.

KEYWORDS

mitochondrial disease, phospholipid metabolism, cardiolipin, Barth syndrome, MEGDEL, DCMA, Sengers syndrome, hereditary spastic paraplegia.

MITOCHONDRIA AND DISEASE

The mitochondrion is the primary generator of adenosine triphosphate (ATP) in eukaryotes. In addition to oxidative phosphorylation (OXPHOS), the mitochondrion is involved in a wide range of essential cellular processes. The organelle is the home for the tricarboxylic acid cycle, fatty acid beta-oxidation, iron-sulfur cluster biogenesis, a portion of the urea cycle, and steps in the porphyrin and pyrimidine biosynthetic pathways. Moreover, mitochondria have important roles in Ca^{2+} buffering and thus, Ca^{2+} signaling, are a major producer (a consequence of OXPHOS) and scavenger of reactive oxygen species (ROS), and are intimately involved in programmed cell death (1, 2). Finally, the mitochondrion directly contributes to cellular phospholipid metabolism by hosting machinery that can produce at least four distinct phospholipids: phosphatidic acid (PA), phosphatidylglycerol (PG), cardiolipin (CL), and phosphatidylethanolamine (PE). Given the myriad of roles the mitochondrion plays in maintaining cellular homeostasis, it is no surprise that defects in mitochondrial function lead to a broad spectrum of diseases (3).

Mitochondrial disorders, first recognized in 1962 (4), are the most common source of inborn errors of metabolism (5-7). Primary mitochondrial disorders can be caused by mutation of genes encoded by either mitochondrial (mt)DNA or nuclear (n)DNA (but whose protein product resides in the mitochondrion). Thus, while the discovery of pathogenic mtDNA mutations in the 1980s greatly facilitated understanding of maternally-inherited OXPHOS disease (8, 9), the clinical and genetic heterogeneity of mitochondrial disease still complicates efforts to diagnose, manage, and treat affected patients (3, 10, 11).

Human mtDNA encodes 13 OXPHOS subunits, 22 transfer RNAs, and two ribosomal RNAs (12). In contrast, 99% of the mitochondrial proteome, which consists of over 1000 proteins (11, 13-20), is encoded by the nuclear genome. Thus, not surprisingly, disorders that are caused by pathogenic mtDNA mutations (identified in 30 of the 37 mtDNA-encoded proteins (21)) only comprise a fifth of the known mitochondrial diseases (22).

Mitochondrial dysfunction is not only defined by specific defects in mtDNA or in OXPHOS-associated processes. Mutations in enzymes involved in any number of the mitochondrion's essential functions can lead to mitochondrial disease. Genetic variants that drive mitochondrial pathophysiology have been broadly classified into six categories: 1) OXPHOS-related (subunits and assembly factors) (23); 2) mtDNA maintenance and expression (24); 3) mitochondrial biogenesis (25); 4) mitochondrial quality control (chaperones and proteases) (26); 5) iron-sulfur cluster homeostasis (27); and 6) mitochondrial dynamics (fission and fusion) (28). These categories are delineated by the pathways in which the impacted proteins partake but do not predict in any way known, the clinical presentation caused by any given genetic mutation.

Here, we propose that an additional class of genetic variant be included in the classification schema to acknowledge the role of defects in mitochondrial phospholipid metabolism as a cause of mitochondrial disease. This seventh class will encompass a small but notable group of Mendelian-inherited disorders that specifically impact normal mitochondrial phospholipid metabolism and thus highlight the important role of proper membrane homeostasis in mitochondrial physiology. PA, PG, CL, and PE have parts, if not all, of their biosynthetic pathways localized to the mitochondrion. Combined with the essential import of extra-mitochondrial phosphatidylcholine, phosphatidylserine and

phosphatidylinositol, the mitochondrion requires and maintains a highly articulated lipid trafficking network. Therefore, it is no surprise that disruption of mitochondrial phospholipid metabolism can lead to mitochondrial dysfunction.

While the mitochondrion hosts a major PE biosynthetic pathway, to date, an inherited disease directly impinging on mitochondrial PE metabolism has not been demonstrated. As such, the biology of this important phospholipid will not be covered here. Instead, this review will only focus on those phospholipids which are impacted by mutations in genes encoded by the nuclear genome with defined or emerging roles in mitochondrial phospholipid metabolism.

CARDIOLIPIN METABOLISM

Mitochondrial membranes and asymmetry

Each mitochondrion has two highly specialized membranes, the outer mitochondrial membrane (OMM) and inner mitochondrial membrane (IMM), delineating two aqueous compartments, a dense internal matrix and an intermembrane space (IMS). Characteristic to mitochondrial membranes is a low phospholipid to protein ratio relative to other organelle membranes, high PC and PE content, cumulatively accounting for up to 80% of total lipid phosphorous, low amounts of sterols and sphingolipids, and enrichment of a unique phospholipid, CL (29).

Commonly known as the signature phospholipid of mitochondria, CL is a phospholipid dimer that consists of a pair phosphatidic acids, each with two fatty acyl chains, bridged by a central glycerol moiety (30, 31). The presence of four acyl chains per molecule provides the opportunity for an incredible diversity of CL molecular forms

while the two phosphate groups confer upon the lipid a net -1 charge at physiological pH (32). CL, like PE and PA, is a non-bilayer forming phospholipid; these lipids have much smaller hydrophilic head group diameters than their hydrophobic acyl chains, making them cone-shaped. Non-bilayer lipids participate in membrane fusion events (33), facilitate membrane bending (34), and can impart order to surrounding lipids (35). This distinguishes them from bilayer forming lipids that have head groups and acyl chains that are of similar diameter.

Each mitochondrial membrane has a distinct protein population and phospholipid composition (13-19, 36-40). In fact, the protein to phospholipid ratio differs significantly between the IMM and OMM, with the IMM being significantly more proteinaceous (41-43). When purified, OMM and IMM vesicles have different shapes, structures, and lipid compositions (37, 44). Notably, the OMM has relatively less CL than the IMM (36, 45). Even within a membrane bilayer, there is asymmetry in the lipid composition between the two leaflets (42, 46-50). For instance, most of the associated PE and all of the low amounts of CL are on the cytoplasmic-facing side of OMM (46).

The high protein to phospholipid ratio in the IMM reflects the sheer magnitude of essential processes that occur in its context. Embedded in the IMM is the OXPHOS system, three distinct translocation machineries (TIM22, TIM23, and OXA1), carrier proteins that mediate the flux of metabolites across the IMM, quality control proteases, and phospholipid metabolizing enzymes. In spite of this protein density, the IMM is an intact diffusion barrier that enforces the proton gradient generated by the electron transport chain. The stored power of the electrochemical gradient across the IMM is central to mitochondrial biology. Not only is it used as the source of energy for ATP

production and harnessed to drive numerous transport processes, but in fact, the electrochemical gradient is required for mitochondrial biogenesis itself (51). Therefore, maintaining a proper lipid composition is likely not only required to support the functionality of the numerous proteins and protein complexes embedded in the IMM but also to maintain its crucial barrier function.

PA pools potentially used for CL production

CL biosynthesis begins with PA, a common substrate in triacylglycerol and glycerolipid metabolism. Reflecting this central role, PA can be made in a multitude of ways. Worth mentioning from the outset is that the source of PA used for CL biosynthesis has yet to be experimentally established; given the apparent redundancy, we anticipate that more than one PA-producing pathway will be at play.

De novo biosynthesis of PA is catalyzed by glycerophosphate acyltransferases (GPATs) that are localized to the mitochondrial OMM (GPAT1/2) (52-54) or ER (GPAT3/4) (55, 56). GPATs transfer acyl groups from acyl-CoA donors to the *sn*-1 position of glycerol-3-phosphate generating lyso-PA (LPA). Whether and how the mitochondrial and ER GPAT isoforms contribute to mitochondrial phospholipid metabolism is currently unresolved. The LPA that is generated on either the OMM or within the mitochondria-associated membrane (MAM, (57, 58)) subcompartment of the ER can be acylated by LPA acyltransferases (LPAATs). In mammals, there are four LPAAT isoforms that differ in their tissue distribution and acyl-CoA specificities (some LPAATs can additionally acylate other lyso-lipids) (59-64). In addition to the defined LPAATs, other lyso-phospholipid acyltransferases are able to esterify LPA to some degree (65).

Another potential source of PA is mitochondrial phospholipase D (MitoPLD), a divergent member of the PLD superfamily localized to the OMM that can hydrolyze CL to PA *in vitro* (66). Similar to yeast, mammals can also produce PA *via* the dihydroxyacetone phosphate pathway in the peroxisome (67). All of the discussed pathways of PA synthesis are located outside of, or on the outside of, mitochondria. However, the recent identification of acylglycerol kinase (AGK) in the IMS suggests that PA may be produced inside the mitochondrion (16). AGK, previously termed MuLK for multi-substrate lipid kinase (68), phosphorylates diacylglycerol (DAG) and monoacylglycerol generating PA and LPA (68, 69). AGK activity is modulated by surface charge (*via* Mg²⁺) and stimulated, in a dose-dependent manner, by CL (68). Moreover, overexpression of AGK in the human prostate cancer PC-3 model results in increased mitochondrial PA although CL levels are unchanged (69). Thus, whether PA made by AGK inside of the mitochondrion can and does access the downstream CL biosynthetic machinery is unclear.

Cardiolipin biosynthesis

Upon gaining access to the matrix side of the IMM (discussed later), PA is converted to cytidine diphosphate-DAG (CDP-DAG) and pyrophosphate upon reaction with cytidine triphosphate (CTP; Figure 2.1). The reaction is catalyzed by CDP-DAG synthases (CDS), whose activities have been demonstrated in yeast ER and mitochondria (70, 71). It has been recently established that the conserved IMM resident Tam41p is the mitochondrial CDP-DAG synthase whose activity provides CDP-DAG for CL biosynthesis (72-74). Accordingly, CDS proteins in the ER provide CDP-DAG that is

used for phospholipid biosynthesis therein while TAMM41 supplies the CL pathway (29).

Also localized on the matrix-facing leaflet of the membrane are downstream enzymes in PG and CL biosynthesis. The committed step of this pathway is catalyzed by phosphatidylglycerol phosphate (PGP) synthase (PGS1), which forms PGP from CDP-DAG and glycerol 3-phosphate (75). After PGP is synthesized, it is rapidly dephosphorylated to PG by PTPMT1 (76, 77) of the protein tyrosine phosphatase family that shares no primary sequence similarity to the yeast PGP phosphatase, Gep4p (78). Notably, at steady state, PG is present at extremely low levels (1-2%) relative to the other major mitochondrial phospholipids (79), indicating that newly-synthesized PG is quickly consumed by downstream pathways. Finally, cardiolipin synthase (CLS), an integral IMM protein with its active site facing the matrix (80), condenses PG with another molecule of CDP-DAG to generate nascent unremodeled CL (81-83).

Cardiolipin remodeling

Cardiolipin biosynthetic enzymes exhibit no or only limited acyl chain specificity (81, 82, 84). The general lack of acyl chain specificity in CL biosynthesis is significant as it is in direct contrast to the observation that in any given tissue (except the brain (85)), there exists a dominant homogeneous molecular form of CL that is characterized by the incorporation of unsaturated fatty acyl chains (86) and molecular symmetry with respect to the two chiral centers of CL (87). In mammals, CL is predominantly composed of unsaturated 18-carbon linoleic acid (18:2). The enrichment in this particular species is exemplified by human heart where 18:2-linoleic acid constitutes up to 90% of the acyl chains in CL, yielding the abundant and stereotypical tetralinoleoyl-CL species (87, 88).

However, it is notable that the final acyl chain composition of CL in different tissues is not the same; this observation has led to the hypothesis that the final acyl chain composition of CL is tailored to the unique demands of its host tissue (85, 87, 89).

As such, the generation of CL molecular species that accumulate at steady state requires the active remodeling of CL shortly after its *de novo* synthesis (90, 91). To initiate the remodeling process, a lipase removes an acyl chain from CL generating monolyso-CL (MLCL) that is subsequently re-acylated by one of several enzymes (Figure 2.2). Through a series of such reactions at each position in CL, a tissue-specific homogeneous pool of CL is generated that is characterized by molecular symmetry and a higher degree of acyl chain unsaturation.

Phospholipases

In yeast, the recently identified cardiolipin deacylase, Cld1p, initiates CL remodeling and preferentially catalyzes the hydrolysis of palmitic acid (16:0) from newly synthesized CL, forming MLCL (92, 93). In the absence of Cld1p, the acyl chain composition of CL shifts to palmitic acid (16:0) residues at the expense of palmitoleic (16:1) and oleic (18:1) acid moieties (92, 93). Cld1p associates with the matrix-facing leaflet of the IMM and lacks any membrane spanning segments (94), placing the initiation of CL remodeling on the same side of the IMM as its biosynthesis.

Although there are no orthologs of Cld1p in higher eukaryotes, evidence points to Ca^{2+} -independent phospholipases A_2 (iPLA₂) as being involved in mammalian CL remodeling. The PLA₂ family of enzymes catalyzes the hydrolysis of membrane glycerophospholipids at the *sn*-2 position, generating free fatty acids and lyso-lipids.

Interestingly, all of the PLA₂ isoforms capable of hydrolyzing CL *in vitro* have different specificities for CL molecular species (95).

iPLA_{2g} is membrane-bound, dually localized to the mitochondrion and peroxisome, and participates in CL metabolism (96). In the hearts and skeletal muscle of *ipla2g*^{-/-} mice, CL levels are reduced and the acyl chain pattern is altered (97, 98). However, the absence of iPLA_{2g} in *taz* knockdown mice does not prevent the accumulation of MLCL as predicted if iPLA_{2g} functions immediately upstream of TAZ (99).

Ablation of another mitochondrially-localized iPLA₂ family member, iPLA_{2-VIA}, in *taz*^{-/-} flies, partially restores MLCL:CL ratios, a biochemical hallmark of TAZ dysfunction, and rescues male sterility (100-102). Still, the CL acyl chain pattern in single *ipla2-via*^{-/-} flies is not significantly different from wild type (wt) flies, suggesting that like murine iPLA_{2g}, iPLA_{2-VIA} activity is not obligately required to initiate the remodeling process. Thus, which phospholipase(s) functions upstream of mammalian TAZ remains an open and important question. Once identified, basic biochemical and cell biological characterization will further establish the topology of CL remodeling. For instance, it is anticipated that the lipase(s) that initiates CL remodeling will reside in the same compartment as the enzyme that subsequently re-acylates MLCL; it is worthwhile to note that although iPLA_{2g} localizes to the mitochondrion, its submitochondrial distribution has not been formally demonstrated. If the lipase and its substrate do not co-localize, then appropriate trafficking steps of the lipid substrate (CL or MLCL) will be inferred. A consideration of the basic cell biology of the lipase(s) required for CL

remodeling is particularly relevant given that all three enzymes that can re-acylate MLCL reside in distinct cellular compartments.

Trans/acyltransferases

In mammals, there are at least three enzymes that have the capacity to re-acylate MLCL: TAZ, MLCL acyltransferase 1 (MLCLAT1), and acyl-CoA:lysocardiolipin acyltransferase-1 (ALCAT1), of which only TAZ is evolutionarily conserved from yeast to higher eukaryotes (103-106). All evidence to date indicates that the MLCL transacylase, TAZ, is responsible for the vast majority of physiological CL remodeling. TAZ deficiency is biochemically characterized by increased MLCL, the remodeling intermediate, decreased CL, both the substrate and product, and an abnormal acyl chain pattern of the remaining CL (101, 107-111). However, the mechanism by which TAZ establishes the steady state CL acyl chain composition is unresolved; TAZ catalyzes a reversible transacylation that exhibits no intrinsic acyl chain specificity, acts on acyl chains at both *sn*-1 and *sn*-2 positions, and can use any number of phospholipids and their lyso-derivatives as fatty acyl donors and acceptors, respectively (103, 112). Notably, heterologous expression of human TAZ in *taz*^{-/-} flies or *Dtaz1* yeast generates CL with acyl chain patterns typical of *Drosophila melanogaster* and yeast, respectively, and not humans (110, 113). This suggests that the characteristic fatty acid profile of CL may not be conferred by the substrate specificity of TAZ. Interestingly, recombinant fly TAZ can generate the physiologically-relevant tetralinoleoyl-CL species from MLCL but only under experimental conditions that promote non-bilayer membranes (114). This suggests that unique membrane physical states such as regions of high curvature, can confer upon TAZ acyl chain specificity. Other mechanisms that are hypothesized to play a role in the

TAZ-based establishment of CL molecular species include the specificity of enzymes immediately upstream of TAZ that initiate the remodeling process and thus dictate which substrates are available to TAZ (92), as well as the dietary intake of fatty acids (115).

Presently, the submitochondrial localization of endogenous mammalian TAZ has not been documented. Yeast Taz1p associates with the IMS-facing leaflets of the OMM and the IMM as an interfacial protein (37, 111, 116). This is in sharp contrast to the deacylase, Cld1p that initiates CL remodeling and is localized to the matrix-facing IMM leaflet (94). Topologically, this means that MLCL produced on the matrix-side of the IMM in yeast has to flip across the membrane and/or be transported to the OMM, to access TAZ for remodeling (117). As TAZ is the only CL remodeling enzyme that is conserved in eukaryotes, it is anticipated that mammalian TAZ will be similarly localized in the organelle. Therefore, determining the submitochondrial localization of the upstream phospholipase in mammals will establish the CL and MLCL trafficking steps needed to access TAZ for remodeling (117).

In mammals, MLCLAT1, which associates with the matrix side of the IMM (118), does not encounter the same problem of substrate access as TAZ. MLCLAT1 was originally identified in porcine liver mitochondria as a 74-kDa protein (104) that corresponds to the COOH terminus of the human trifunctional protein (TFP) alpha (a) (105). The TFP complex consists of a- and b-subunits that catalyze the last three steps of mitochondrial long-chain fatty acid beta-oxidation thus providing a significant source of cellular energy (118, 119). Pathogenic mutations in either TFP subunit are associated with beta-oxidation disorders, where patients suffer from cardiomyopathy and skeletal myopathy (120-122). Interestingly, recombinant TFPa is soluble when expressed alone,

in contrast to its partner TFPb, suggesting that it may contain a function independent of its association with TFPb that may be described by MLCLAT1 (123). Presently, the gene encoding MLCLAT1 has not been definitively determined. That MLCLAT1 is likely a splice variant of TFPa is suggested by the fact that knockdown using RNAi targeting the NH₂-terminal portion of TFPa, absent in MLCLAT1, reduces TFPa, but not MLCLAT1 mRNA levels (124). However, whether RNAi targeting a shared region between TFPa and MLCLAT1 can reduce the expression of both genes has not been established.

Both recombinant human TFPa and MLCLAT1 can bind MLCL *in vitro* and are able to incorporate linoleoyl-(18:2), oleoyl- (18:1), and palmitoyl-(16:1) CoA into MLCL (105, 123, 124). When either protein is overexpressed in BTHS lymphoblasts, there is increased incorporation of linoleic acid in CL (105, 124). However, TFPa overexpression does not generate a CL profile that reflects its *in vitro* specificity. Thus, while TFPa and/or MLCLAT1 can participate in CL remodeling, especially in the absence of TAZ function when the levels of MLCL are high, the exact contribution of this acyltransferase(s) to physiological CL remodeling is unclear.

Finally, ALCAT1 acylates MLCL and dilyso-CL *in vivo* and can use a number of lyso-phospholipids as acyl acceptors *in vitro* (125-127). Depending on the acyl acceptor, tissue type, and species, ALCAT1 has been described to preferentially incorporate long chain unsaturated fatty acyl chains or promiscuously accept all acyl-CoA derivatives (125, 127). As such, ALCAT1 lacks the specificity expected of an enzyme with a critical role in physiological CL remodeling. Notably, ALCAT1 resides in the ER MAMs (125, 127). Therefore, for ALCAT1 to participate in CL metabolism, CL and/or MLCL must

travel from the IMM to at least the external leaflet of the OMM, if the active site of ALCAT1, which has not been determined, faces the cytosol.

The absence of TAZ causes alterations in CL molecular species in every model tested to date (87, 92, 100, 101, 103, 107, 109, 110, 128-139). In contrast, the loss of MLCLAT1/TFPa or ALCAT1 does not consistently result in changes in the steady state acyl chain composition of CL (140-142). Thus, it is unlikely that either MLCLAT1/TFPa or ALCAT1 significantly contributes to the steady state CL acyl chain profile under normal conditions. These results further underscore the predominant role of TAZ in physiological CL remodeling

Phospholipid trafficking steps required for CL metabolism

Once made, PA must travel to the matrix side of the IMM to gain access to the CL biosynthetic machinery. If made in the ER, this requires movement of PA from ER to OMM, flipping between OMM leaflets, movement from the OMM to the IMM, and finally flipping to the matrix-facing IMM leaflet. Inter-organelle contacts have recently emerged as being critically important for mitochondrial phospholipid metabolism. In yeast, there are at least two distinct structures that contribute to the physical association of ER and mitochondria (Figure 2.3). The first described complex is the ER-mitochondria encounter structure (ERMES) (143). A second ER-mitochondria tether, the ER-membrane protein complex (EMC), that is distinct from ERMES, was recently identified in yeast (144). When either EMC or ERMES subunits are missing, the number and length of ER-mitochondria contacts are reduced and mitochondria are unable to support growth on respiratory media (143-146). Also, a synthetic mitochondria-ER tether similarly rescues the defects caused by the absence of EMC or ERMES. While EMC may play a

more direct role in phospholipid trafficking (144), EMC and ERMES complexes likely have both overlapping and distinct functions in phospholipid transfer between the ER and mitochondria (144, 147).

The ERMES subunits are conserved in fungi but not in metazoans. In contrast, the close apposition of ER and mitochondria is conserved (148). In mammals, IP₃ receptor/GRP75/VDAC1-containing complexes (149), mitofusin-2 (150), and several other proteins have roles in ER-mitochondria tethering (151, 152). Moreover, the newly described EMC is conserved but its role in ER-mitochondrion tethering has only been tested in yeast. The diversity of players implicated in this inter-organelle association provides strong evidence of the physiological importance of such contacts.

The existence of vacuolar and mitochondrial contacts, termed vCLAMPs (vacuole and mitochondrial patch), recently identified in yeast, further highlights the importance of inter-organelle associations for mitochondrial phospholipid metabolism (153, 154). Simultaneous deletion of ERMES and vCLAMP components is synthetically lethal. Deletion of vCLAMP and repression of ERMES impairs PA trafficking into mitochondria and results in a 40% reduction in CL levels (154). A recent report describing mitofusin 2-mediated contacts between mouse melanosomes (a lysosomal-like compartment in pigment cells) and mitochondria (155), suggests that there may be similar vacuolar-tethering mechanisms in mammals.

Analogous to inter-organelle tethers, regions of close physical apposition between the IMM and OMM are important for lipid trafficking across the IMS (41, 156), although the underlying mechanism(s) is unknown. In addition, IMM-OMM contact sites have roles in energy transduction from the mitochondrial matrix to the cytosol (157) and

precursor protein import (158). MICOS (mitochondrial contact site and cristae organizing system) is a hetero-oligomeric protein complex that is embedded in the IMM but interacts with several distinct OMM proteins (159-163). Depletion of the conserved mitofilin/Fcj1p (yeast formation of cristae junction 1) subunit, which constitutes the MICOS core, results in an expanded IMM surface, dramatic loss of cristae junctions, and the remaining cristae are stacked, lamellar, and aberrantly disconnected from the OMM (159, 162, 164, 165). Recently, apolipoprotein O (APOO) and APOO-like protein (APOOL) were identified as potential subunits of the bovine MICOS complex (166). The IMS-facing APOOL specifically binds CL *in vitro* and its knockdown results in morphological phenotypes similar to yeast MICOS mutants (166). Thus, MICOS complexes are key determinants of cristae morphology that contain subunits capable of binding CL (159, 160, 162). Whether these two properties are leveraged in the context of phospholipid trafficking between the IMM and OMM is presently unclear although it is interesting to note that biochemically isolated IMM-OMM contact sites are enriched in CL (41, 43).

The movement of PA from the OMM to the IMM is mediated by the IMS-resident Ups1p/PRELI-like proteins (167, 168). *In vitro*, the yeast Ups1p/Mdm35p dimer (169, 170) binds numerous anionic phospholipids but only transports PA (167). The directionality of PA transport is likely conferred by the fact that Ups1p remains tightly bound to membranes containing physiological amounts of CL, leading to Ups1p's subsequent degradation. These observations suggest a mechanism for regulating CL biosynthesis by limiting precursor trafficking between the two membranes when CL levels are bountiful (167). Whether transport of PA by the Ups1p/PRELI-like proteins

utilizes in some manner MICOS or is instead mechanistically distinct is at present unknown.

Once PA is transported to the IMM, or if synthesized in this compartment by AGK, the transbilayer movement of PA to the matrix-leaflet is required for PA to gain access to the CL biosynthetic enzymes. How this is achieved is presently not known but could involve a specific protein or protein complex. However, the requirement for a specific PA transporter does not seem obligate as a transmembrane pH gradient is sufficient to disseminate PA across both IMM leaflets (171, 172).

Since CL is made in the context of the matrix leaflet and can eventually be exposed on the OMM, mechanisms must be present to facilitate the movement of CL intra-mitochondrially. Scramblases are Ca^{2+} -dependent, ATP-independent bidirectional transporters that equilibrate lipids unevenly distributed across a bilayer (173). As such, a scramblase could serve to redistribute CL made on the matrix-side, between IMM leaflets. Alternatively, phospholipid translocation between membrane leaflets may not be mediated by specific proteins, but instead facilitated by the presence of numerous transmembrane proteins (especially in the context of the IMM) in a non-specific manner, as suggested for bacterial and ER membranes (174, 175).

Albeit minor, CL is a normal constituent of the OMM and can traffic to the OMM following certain stimuli (176, 177). Phospholipid scramblase 3 (PLS3) is the only known mitochondrial scramblase (178-180) and *in vitro*, murine and human PLS3 catalyze the Ca^{2+} -dependent flip-flop of CL in proteoliposomes (180). However, it is unclear whether PLS3 functions *in vivo* as a CL scramblase or instead mediates the movement of CL from the IMM to the OMM. PLS3 overexpression increases

mitochondrial mass, *CLS* transcription, CL synthesis, and CL externalization to the OMM (179, 181). Conversely, overexpression of a catalytically-dead *pls3* allele or *PLS3* knockdown reduces CL externalization following UV irradiation or rotenone poisoning, respectively (176, 181). How does PLS3 activity contribute to movement of CL to the OMM? If PLS3 is a true scramblase, then the equilibration of CL between the leaflets of the IMM may be required for the subsequent ability of CL to traffic to the OMM. Alternatively, PLS3 may instead directly participate in the movement of CL between mitochondrial membranes. Future studies are needed to clarify the role of PLS3 in this process.

Another potential mechanism by which lipids can be transferred from the IMM to the OMM involves the NM23-H4/NDPK-D (nucleotide diphosphate kinase isoform D) (182). NM23-H4 is the only mitochondrially-targeted member of a family of NDPKs whose role in phosphotransfer is well-established. NM23-H4 has been additionally implicated in the trafficking of anionic phospholipids (in particular CL) between the IMM and the OMM (183). Interestingly, the levels of CL can functionally switch NM23-H4 between phosphotransfer and lipid transfer modes (184). Normally, the lipid transfer mode is inhibited by anionic lipids, including CL, and the protein operates as a nucleotide kinase. However, when CL levels are low (due to mitochondrial dysfunction), NM23-H4's lipid transfer function is de-repressed and the protein cross-links the IMS-facing leaflets of the IMM and OMM. Subsequently, NM23-H4 facilitates the thermodynamically-unfavorable movement of negatively-charged lipids across the aqueous IMS.

While a role for both NM23-H4 and PLS3 in the stimulated externalization of CL on the OMM is clearly emerging, whether either or both enzymes participate in the routine processes of CL biosynthesis and remodeling is not known. Given its MAM-residence, it is tempting to speculate that NM23-H4 and/or PLS3 may be involved in ALCAT1-based CL remodeling.

PHYSIOLOGICAL FUNCTIONS

Phospholipids play a myriad of roles in cellular and mitochondrial physiology that are beyond the scope of any single review. The following section is focused on recently discovered roles and guided by those physiological functions of mitochondrial lipids, that when disturbed, may contribute to human disease. Of note, the diversity of functions attributed to the discussed mitochondrial phospholipids is reflected by the vast array of pathogenic mechanisms that underlie this cohort of mitochondrial diseases.

Phosphatidic acid

The dynamic appearance and disappearance of PA on the OMM is a recently established determinant of mitochondrial fusion and fission. Overexpressed MitoPLD generates PA on the OMM, promoting mitochondrial fusion and subsequent aggregation (66), while loss of MitoPLD leads to fragmented mitochondria (185). PA generated by MitoPLD recruits the PA phosphatase, lipin-1. Lipin-1 dephosphorylates PA to DAG which stimulates mitochondrial fission while simultaneously removing the pro-fusogenic accumulation of PA on the OMM (185, 186). Interestingly, *mitopl^d* flies (187) and mice (185, 188) have defects in the biogenesis of Piwi-interacting (pi)RNAs that have a role in providing a germline-specific defense against retrotransposon activity (189). Male

mitopld^{-/-} flies are sterile, typical of flies lacking piRNAs (190), lose nuages (191), sites where piRNA production and processing is thought to occur, and have de-repressed retrotransposons in their testes (187, 188). Moreover, *lipin-1*^{-/-} mice have elevated PA on the mitochondrial surface and significantly increased nuage formation (185). Genetic evidence therefore strongly supports a role for PA and/or DAG at the OMM in piRNA production (185). However, the exact role of MitoPLD with respect to the mitochondrial phospholipid pool is unclear.

The importance of the dynamic regulation of PA on the OMM is further substantiated by the recent characterization of PA-PLA₁ (192). *In vitro*, PA-PLA₁, preferentially deacylates PA to LPA (193). PA-PLA₁ overexpression or depletion in HeLa cells causes mitochondrial fragmentation and elongation, respectively (192). Interestingly, co-expression of PA-PLA₁ and MitoPLD prevents the accumulation of PA on the OMM surface and the morphological defects associated with MitoPLD overexpression alone (192). Similar to *mitopld*^{-/-} and *lipin-1*^{-/-} mice, *pa-pla1*^{-/-} mice have a defect in spermatogenesis that correlates with mitochondrial disorganization (192). Finally, diminution of *ddhd2*, a related iPLA₁ family member with a similar specificity for PA as PA-PLA₁, causes mitochondrial elongation in mouse embryonic fibroblasts (192).

Phosphatidylglycerol

Besides being a required intermediate in CL biosynthesis, PG is also a precursor for bis(monoacylglycerol)phosphate (BMP; (194)), a class of phospholipid that is highly enriched in late endosomes and lysosomes (195-197). While BMP is found in many tissues and cells, it is usually present at less than 1% of the total phospholipid mass (198,

199). BMP is a structural isomer of PG and is thought to function in the maintenance and regulation of endosomal/lysosomal membrane dynamics and cholesterol trafficking (200-203). However, its exact biological role(s) is unresolved.

Cardiolipin

The absolute requirement of PG and/or CL for life is underscored by the observation that *ptpmt1*^{-/-} mice die in utero before embryonic day 8.5 (76). Reflecting this importance, CL has a multitude of functional roles in mitochondria (Figure 2.4). CL is highly enriched in cardiac tissues making up 15-20% of the total phospholipid phosphorus mass of the heart (204, 205). Its relative abundance in cells and tissues with high energetic demands point to CL as being intimately involved in maintaining mitochondrial structure and function. Indeed, it interacts with numerous mitochondrial proteins, including all OXPHOS complexes and most mitochondrial solute carriers, and is often required for their functional reconstitution in liposomes (206-212). In addition, CL is proposed to function as a proton trap that helps funnel pumped protons towards the ATP synthase to generate ATP (32). An association with CL promotes the assembly of membrane proteins into oligomeric complexes (206, 213-217). Indeed, CL is important for the assembly and function of IMM and OMM translocases and thus, mitochondrial biogenesis (37, 218, 219). CL is also critically important for stabilizing respiratory supercomplexes (SC), supramolecular assemblies built from respiratory complexes I, III and IV (220). These SCs are thought to increase the efficiency of electron transfer between the respiratory chain components by substrate channeling mechanisms (221, 222), thereby maximizing OXPHOS. Further, SC assembly shortens the distance traveled by mobile electron carriers, minimizing ROS leakage and reducing oxidative damage.

Finally, CL-binding stimulates the activity of dynamin-related GTPases with pivotal roles in IMM fusion and mitochondrial fission (223-225). All of these CL-supported functions have been discussed extensively in several excellent reviews (106, 226-231).

Both apoptosis and mitophagy, a macro-autophagic process that is pre-emptive to cell death *via* apoptosis, are signaled in part by the externalization of CL to the OMM. The movement of CL to the OMM is thought to involve the scramblase PLS3 and/or NM23-H4 and may occur preferentially at IMM-OMM contact sites thought to be enriched in CL (41, 43). Overexpression of NM23-H4, but not a CL-binding mutant, increases apoptotic markers that may be ascribed to increased CL externalization on the OMM (184). CL on the OMM attracts and activates caspase-8 (177) and aids in pro-apoptotic Bax insertion into and permeabilization of the OMM (232, 233). In preparations of giant unilamellar vesicles lacking CL, caspase-8 is unable to interact with vesicle membranes, a step necessary for caspase-8 activation and subsequent recruitment of tBid (234, 235). Yeast mitochondria lacking CL are protected from the bioenergetic perturbations normally induced upon incubation with tBid (236) underscoring the importance of CL for tBid function. Furthermore, CL peroxidation by cytochrome c promotes the release of a number of pro-apoptotic factors, including cytochrome c, following OMM permeabilization (237). Under conditions of mild mitochondrial dysfunction, CL is externalized on the OMM where it promotes the specific destruction of the mitochondrion by mitophagy (176). siRNA knockdown of the scramblase PLS3 or CL synthase CLS in neuronal cells, diminishes CL externalization and the number of mitochondrially-associated autophagic markers, and attenuates chemically-induced mitophagy (176). As CL externalization is important for both apoptosis and mitophagy,

there is likely to be a threshold level of mitochondrial damage (severity of insult and percentage of mitochondrial pool impacted) above which apoptosis is executed and below which the affected mitochondria are selectively removed. In addition, qualitative and/or quantitative differences in the CL exposed on the OMM may influence how this lipid signal is interpreted by the cell.

Remodeled *versus* unremodeled CL

While the role and functional consequence of MLCAT1-based remodeling is presently unresolved, TAZ- and ALCAT1-mediated CL remodeling are associated with very different physiologic outcomes. In the absence of TAZ, the acyl chain composition of CL is significantly diversified and molecular symmetry is lost (87). Thus, TAZ has a preeminent role in dictating the final collection of acyl chains attached to CL under physiological conditions. The final acyl chain pattern of CL, which is tissue-specific, is thought to be critical for normal mitochondrial physiology by supporting some combination of the functions attributed to CL. However, *Dcld1* yeast, which fail to initiate CL remodeling and accumulate normal amounts of unremodeled CL, have wt OXPHOS activity and normal mitochondrial morphology (92, 238). These results question the idea that TAZ-based CL remodeling produces “optimized” CL species that promote mitochondrial fitness, and instead suggests that CL remodeling may actually accomplish other physiologically important functions that either were not tested (92, 238) or have not yet been discovered.

In contrast to TAZ-based CL remodeling, CL remodeled by ALCAT1 predisposes mitochondria to damage. In mouse myoblasts, ALCAT1 overexpression increases the amount of CL enriched with docosahexaenoic acid (22:6) at the expense of linoleic acid

(18:2) (140), consistent with alterations in CL species that are observed in aging rat hearts (the latter additionally contain 20:4 arachidonic acid (239)). The increased acyl chain unsaturation in these CL forms makes them peroxidation-prone and increases the susceptibility of mitochondria to undergo apoptosis (140, 239, 240). As such, ALCAT1 seems to perform “pathogenic” remodeling of CL. Consistent with this, ALCAT1 overexpression, also noted in mouse models of metabolic disease, increases the rate of ATP, and consequently, ROS production during oxidative stress (140). Conversely, ablation of ALCAT1 elevates tetralinoleoyl-CL content in the heart (140), prevents the onset of disease, increases insulin resistance, mitigates OXPHOS dysfunction by increasing complex I activity, restores mtDNA fidelity, alleviates fusion defects and associated mitochondrial fragmentation, and re-establishes mitochondrial quality control (140, 241-243). Combined, this suggests that CL remodeled by ALCAT1 may exacerbate and/or signal mitochondrial dysfunction in disease pathogenesis (242).

EMERGING DISEASES OF MITOCHONDRIAL PHOSPHOLIPID

METABOLISM

With the recent application of next generation sequencing methodologies, new disease-causing genes are being implicated in mitochondrial disorders each year. For the remainder of this review, we describe a new category of mitochondrial disorder that is caused by nuclear defects that specifically alter mitochondrial phospholipid metabolism. We anticipate that the diseases discussed below represent the tip of the iceberg and that more disorders that impinge on mitochondrial phospholipid metabolism will be identified in the near future.

Tafazzin mutations leading to Barth syndrome

Mutations in the gene that encodes the MLCL transacylase, TAZ, lead to Barth syndrome (BTHS) (244-246). BTHS is the founding member of this new class of mitochondrial disease and thus not surprisingly, is the best characterized. This X-linked multisystem disorder presents with cardiomyopathy, skeletal muscle weakness, neutropenia, growth retardation, and 3-methylglutaconic aciduria (3-MGA), and can be fatal if not diagnosed early (244, 247, 248) (one isolated case of BTHS in a female patient has been reported (249)). 3-MGA-uria is a heterogeneous group of syndromes characterized by an increased excretion of 3-methylglutaconic and 3-methylglutaric acids, breakdown products of leucine catabolism (250). Additional features such as isolated left ventricular noncompaction, ventricular arrhythmia, motor delay, exercise intolerance, poor appetite, fatigue, hypoglycemia, lactic acidosis, and hyperammonemia have also been described in BTHS patients (251, 252). Patient heart, liver, and skeletal muscle biopsies contain malformed mitochondria with tightly stacked or circular bundles of cristae (139, 244, 253, 254). In patient-derived lymphoblasts, mitochondria have dramatically reduced inner membranes, collapsed cristae, and are often fragmented (138, 255). *TAZ* (G4.5) contains 11 exons, is localized on a gene-rich region on Xq28, and is highly expressed in cardiac and skeletal tissues (246). Pathogenic *taz* variants identified to date encompass splice site mutations, insertions, deletions, as well as missense and nonsense mutations (247) (a current list of known genetic variants is maintained by the Barth syndrome foundation; <https://www.barthsyndrome.org/science>).

Efforts to understand BTHS pathogenesis are complicated by the complete lack of genotype-phenotype correlations. Patients with the same mutation, or even siblings

sharing the same mutation, can manifest with extremely disparate symptoms. A case in point is that of a 51 year old proband, the oldest BTHS patient reported, and his 3 year old grandnephew (256). Although they harbor the same mutation, the boy presented with cardinal manifestations of BTHS (including congestive heart failure that required a heart transplant at 11 months of age) while the great uncle was 43 years old when he was diagnosed with myopathy. These observations highlight the importance of modifying factors as key determinants in BTHS disease progression.

Furthermore, links between different mutations and severity of disease have not been established for BTHS. Model organisms can help bridge this gap. Using a yeast BTHS model, 21 distinct pathogenic missense mutations have been modeled in yeast Taz1p and their loss-of-function mechanism defined. This effort has identified seven classes of BTHS mutant defined by their loss-of-function mechanisms (108, 111, 257). Briefly, the seven classes comprise of variants that are 1) nonfunctional truncated products resulting from frameshifts or aberrant splicing, 2) mislocalized within mitochondria and aggregation-prone, 3) aberrantly assembled, 4) catalytically dead, 5) hypomorphic alleles with residual transacylase activity, 6) unable to engage in stable productive assemblies, or 7) temperature-sensitive. Systematic analyses of pathogenic variants in this manner can provide important mechanistic insight into the clinical heterogeneity of BTHS. The next step in attaining this goal is to verify that the defined loss-of-function mechanisms are conserved in an appropriate mammalian model. Such a model is additionally needed to characterize pathogenic alleles that cannot be modeled in yeast due to a lack of conservation.

There are a number of BTHS models presently available. Importantly, every BTHS model has the characteristic biochemical defects that underlie BTHS – increased MLCL, decreased CL, and an abnormal acyl chain composition of the remaining CL. In addition to yeast, other cellular BTHS models include patient-derived fibroblasts (258), lymphocytes (87, 138), and iPSCs (135, 136), and *taz*-depleted rodent (131, 259, 260) and human cell lines (177). Animal models of BTHS include *taz*-depleted zebrafish (261) and mice (137, 262, 263), and *taz*^{-/-} flies (132).

Cellular models of BTHS show dysmorphic changes in mitochondrial morphology and energetic defects (131, 133, 255). In patient-derived lymphoblasts (133, 138), iPSCs (136), and fibroblasts (258), there is low basal respiration, reduced membrane potential, and compromised coupling of OXPHOS. Respiratory SCs are decreased and there is a shift in SC assembly from large “respirasomes” to smaller, and presumably, less efficient SCs (133, 136, 264). Therefore, it is postulated that these alterations in respiratory chain assembly diminish respiratory efficiency and consequently, augment ROS production. While basal respiration is unaffected in the shRNA-inducible *taz* knockdown mouse, maximal uncoupled respiration is reduced; whether this reflects changes in respiratory SC stability has not been demonstrated (265). Enzymatic analyses of respiratory chain complexes using cardiomyocytes derived from the *taz* knockdown mouse indicate that complex III is impaired (265), suggestive of a similar bioenergetic dysfunction as noted in the cellular models. In *taz*-depleted mice (137, 262, 263) and zebrafish (261), cardiac defects are observed that recapitulate many of the relevant cardiac parameters noted in BTHS patients. With respect to zebrafish, *taz* knockdown severely impairs zebrafish development and the degree of cardiac

dysmorphology is proportional to the morpholino dose. In addition to impaired cardiac function, *taz* knockdown mice have abnormal skeletal muscle ultrastructure (132, 137) consistent with *taz*^{-/-} flies that also have impaired muscle functions (131, 132). Recently, cardiomyocytes differentiated from BTHS patient iPSCs have been generated (135, 136). In these cells, there is structural destabilization of respiratory SCs that correlates with reduced respiratory complex activities (136). When wt cells are seeded onto engineered chips, they form sarcomeres and contract; in contrast, the ability of BTHS-derived cardiomyocytes to form organized sarcomeric arrays is severely impacted as is their contractility (135). Therefore, results from the myriad of BTHS models indicate that the lipid abnormalities that occur in the absence of TAZ result in OXPHOS dysfunction associated with SC destabilization. OXPHOS dysfunction increases the production of ROS and in sum, these impairments compromise heart development and function.

As already discussed, the stimulated externalization of CL onto the OMM is an important event that can alternatively trigger apoptosis or mitophagy. It is thus notable that BTHS-derived lymphocytes are resistant to mitochondrial-dependent apoptosis due to an impaired ability to recruit and activate caspase-8 (133, 177). Interestingly, *caspase-8*^{-/-} mice die *in utero* and the embryos have heart abnormalities that include thin and disorganized trabeculae (266), phenotypes also observed upon *taz* depletion *in utero* (263). Thus, defects in caspase-8 activity may contribute to the cardiomyopathy in BTHS. The relative capacity of BTHS mitochondria to be consumed by mitophagy has not been reported. However, BTHS lymphocytes have more mitochondria that are individually less functional (133) suggesting that mitochondrial homeostasis may indeed be perturbed in BTHS and contribute to disease progression.

Importantly, the detailed biochemical and cell biologic characterization of the numerous BTHS models have begun to identify potential avenues for therapeutic intervention. For instance, suppression of mitochondrial ROS attenuates the energetic and functional decline caused by *taz*-depletion in rodent cardiac myocytes (260) and corrects the sarcomere organization and contractile function of induced BTHS cardiomyocytes (135). Genetic and/or pharmacologic targeting of the lipase that initiates CL remodeling in yeast, flies, and patient lymphoblasts prevents, to varying degrees, the mitochondrial dysfunction caused by the absence of TAZ and can additionally rescue the sterility of male *taz*^{-/-} flies (92, 102, 238). These results suggest that the mitochondrial dysfunction stemming from TAZ deficiency is not likely due to reduced remodeled CL, but instead caused by the increased abundance of MLCL and/or the low total amounts of CL. As such, drugs that can scavenge mitochondrial ROS or prevent the accumulation of MLCL (inhibit the activity of the upstream deacylase(s); enhance the activity of other putative MLCL remodelers; augment a pathway that degrades MLCL) could be used to the potential therapeutic benefit of BTHS patients.

DNAJC19 mutations leading to dilated cardiomyopathy with ataxia (DCMA) syndrome

To date, only two mutations have been identified in *DNAJC19* (DnaJ/Hsp40 homolog, subfamily C, member 19) that are associated with DCMA (267, 268), an autosomal recessive disorder that presents with early onset dilated cardiomyopathy, non-progressive cerebellar ataxia leading to motor delays, testicular dysgenesis, growth failure, and elevated levels of 3-MGA. Additional features include microcytic anemia, mild to borderline non-progressive mental retardation, hepatic steatosis, and occasional

optic atrophy (267-269). DCMA shares with BTHS certain clinical features including left ventricular noncompaction with spongy and trabeculated myocardium (269). However, unlike in BTHS, DCMA patients do not exhibit neutropenia or skeletal myopathy (245).

DNAJC19 is on chromosome 3q26.33 (267). The gene consists of six exons and is ubiquitously expressed as a 525 bp transcript with a minor 435 bp form, lacking exon 4, in all tissues tested and control fibroblasts (267). The consanguineous Canadian Dariusleut Hutterite families all have an exon4 splicing defect while two Finnish brothers have a frameshift mutation resulting in a truncated protein (267, 268). Consistent with these mutations, only the shorter transcript is expressed in fibroblasts from one Hutterite patient (267) and *DNAJC19* protein is not detected in fibroblasts derived from the Finnish siblings (268). Since there are only two genetic variants of *DNAJC19* linked to DCMA, it is not possible to describe genotype-phenotype correlations in this disorder. Still, in a retrospective study of the Hutterite patients that all share the same mutation (269), 13 of the 17 patients developed dilated cardiomyopathy and 10 later died. Interestingly, three patients had resolved or stabilized cardiomyopathy and another four did not present with cardiac defects at all. Thus, there is significant clinical variability with respect to this particular DCMA allele.

DNAJC19 is associated with the matrix-facing leaflet of the IMM via a predicted NH₂-terminal transmembrane region (141) and contains a conserved DNAJ domain at the COOH terminus, in contrast to other conventional DNAJ-proteins with an NH₂-terminal J-domain. DNAJ domain-containing proteins typically act as molecular chaperones for Hsp70/Hsp40s and prevent protein aggregation by aiding in the folding and assembly of newly synthesized proteins (270, 271). Sequence alignment indicates that *DNAJC19* is

orthologous to yeast Pam18p, a constituent of the TIM23 import machinery (272). In yeast, the Pam18p and Mdj2p proteins are essential components of the TIM23 translocation machinery (273), interacting with mitochondrial Hsp70p, Pam16p, and Tim44p to form the presequence translocase-associated motor complex (274-279). This subcomplex associates with the core TIM23 translocon (consisting of Tim23p, Tim17p, Tim50p and variably, Tim21p) and mediates import of precursors destined for the matrix in an ATP- and membrane potential-dependent manner (219, 280-284). Thus, DNAJC19 may, like yeast Pam18p, stimulate the ATPase activity of mtHsp70 and stabilize mtHsp70 binding to incoming peptides. For an excellent review on mitochondrial protein translocation, refer to (51).

Consistent with a role in protein import, DNAJC19 interacts with MAGMAS, the conserved mammalian ortholog of yeast Pam16p that is essential for development (285-288). MAGMAS is structurally similar to DNAJC19 but peripherally associated with the matrix-leaflet of the IMM. The interaction between DNAJC19 and MAGMAS occurs via their reciprocal J-domains and is required to recruit DNAJC19 to the core TIM23 translocon (289). MAGMAS then associates with TIM17, a subunit of the TIM23 core, to form the TIM23 translocation machinery (290, 291). Interestingly, there are three distinct forms of TIM23 translocon that incorporate different TIM17 isoforms and associate with either DNAJC15 (TIM17a; translocase A), another co-chaperone of the same Hsp40-type (292, 293), or DNAJC19 (TIM17b₁ and TIM17b₂; translocase Bs). Of the three versions of TIM23, translocase Bs are critical for basal mitochondrial biogenesis (e.g. OXPHOS, iron-sulfur cluster biogenesis, mtDNA copy number, and maintenance of mitochondrial membrane potential) while translocase A plays a dispensable, albeit supportive role when

translocase Bs are absent (291). In light of these results, defects in mitochondrial presequence protein import and consequently, mitochondrial biogenesis, may represent the mechanism of DCMA pathogenesis.

Recently, however, human and murine DNAJC19 were found to additionally interact with PHB complexes (141). PHB complexes are large hetero-oligomeric complexes composed of PHB1 and PHB2 subunits (294) that are involved in cristae morphogenesis (295) and modeled to function as lipid scaffolds in the IMM, redistributing lipids (such as CL (296)) and delineating functional membrane domains (297). In yeast, *Dphb1* is synthetically lethal with *Dcrd1* highlighting the importance of conserved PHB complexes in CL metabolism (298). Interestingly, *DNAJC19*-depletion in HEK293T cells shifts the CL acyl profile to longer and less saturated chains; however, CL levels are unaffected and MLCL does not accumulate (141). Moreover, while a functional DNAJ-domain is not required for DNAJC19 to interact with PHB complexes, it is necessary to rescue the changes in CL molecular composition that occur upon *DNAJC19* knockdown (141). In contrast, *PHB2* knockdown results in the same three biochemical alterations that characterize BTHS (increased MLCL, decreased CL, and changes in CL acyl chain composition), although the increase in MLCL is significantly less than in *TAZ* knockdown cells (141). Concomitant knockdown of *PHB2* or *DNAJC19* with *TAZ* does not alter the accumulation of MLCL that occurs upon depletion of *TAZ* alone, indicating that neither PHB complexes nor DNAJC19 are required to generate the substrate, MLCL, used by TAZ. Combined, these results suggest unexpected roles for both PHB complexes and DNAJC19 in CL remodeling and further indicate that their functions in this regard, are at least partially distinct. TAZ does not interact with PHB2 or

DNAJC19 directly (141). Thus, the ability of PHB/DNAJC19 complexes to define specific membrane domains, such as those with negative curvature, is postulated to confer acyl chain specificity to TAZ (114, 141). In the absence of such privileged domains, TAZ remodeling still occurs, it just lacks acyl chain specificity.

In sum, it appears that DNAJC19 has dual functions in the regulation of CL remodeling and mitochondrial protein biogenesis (Figure 2.5). A key question that remains unresolved is whether both activities contribute to DCMA disease pathogenesis. Presently lacking is any information regarding the lipid profile and protein import functionality of mitochondria isolated from actual DCMA patients; such data is needed to better understand the underlying pathogenic mechanism. If similar alterations in CL are detected in DCMA patient cells, future studies will be needed to define how DNAJC19/PHB complexes regulate the collection of acyl chains attached to CL and relate these changes to mitochondrial dysfunction. This latter question is all the more interesting and relevant given that in yeast, flies, and mammalian cells, genetically and/or pharmacologically preventing production of MLCL by targeting the lipase that begins the remodeling cascade rescues the multitude of phenotypes attributed to TAZ deficiency (92, 102, 238).

SERAC1 mutations leading to MEGDEL syndrome

Evidence that PG, like CL, undergoes physiologically important remodeling was recently provided by the identification of *serine active site containing 1 (SERAC1)* mutations that cause autosomal recessive MEGDEL syndrome (3-MGA-uria, sensorineural deafness, encephalopathy, and neuroradiological evidence of progressive Leigh-like syndrome (299, 300). In addition to classical MEGDEL symptoms, an

increasing list of clinical phenotypes have been associated with *SERAC1* mutations; infantile mitochondrial hepatopathy, psychomotor and developmental delay, bilateral optic nerve atrophy, myoclonic epilepsy, and microcephaly (301-304). Similar to BTHS and DCMA, MEGDEL patients have 3-MGA-uria and variable mitochondrial dysfunction.

SERAC1 is located on chromosome 6q25.3 and the encoded protein resides in the MAM (299). *SERAC1* is a predicted single-pass transmembrane protein that is 654 amino acids long and translated from 17 exons into three isoforms (299). The protein is a member of the PGAP (post-GPI attachment to protein 1)-like protein domain family and contains an a/b-hydrolase fold and a highly conserved serine-lipase domain (299). To date, 18 different mutations have been described in 24 patients, many of which are frameshift, nonsense, or missense mutations within or upstream of the lipase domain (299, 301-307). Of note, a patient recently described with severe, early onset MEGDEL symptoms harbors compound frameshift and stop-gain heterozygous mutations upstream of the lipase domain (301). In contrast to patients with variants within the lipase domain, which may allow for a protein with residual activity, the production of truncated *SERAC1* completely lacking the lipase domain from both alleles may account for the severity of the particular patient's phenotype.

SERAC1 is implicated in changing the acyl chain composition of CL's precursor, PG. Specifically, MEGDEL patient fibroblasts have elevated concentrations of PG-34:1 and lower concentrations of PG-36:1; the acyl chain compositions of the other major phospholipid classes, with the notable exception of CL, are normal (299). The inability to convert PG-34:1 to PG-36:1 results in the accumulation of PG-34:1 and subsequent

incorporation of PG with these acyl chain species into CL. Thus, in MEGDEL patients, CL levels are normal but the acyl chain composition of CL is altered (299). As in the case of DNAJC19 deficiency, if and how normal levels of CL of abnormal acyl chain composition affects mitochondrial function is at present unclear. Notably, most MEGDEL patient tissues and fibroblasts exhibit OXPHOS dysfunction (299, 300, 302, 303, 305-307), though the degree of impairment and the affected respiratory chain component(s) varies. Moreover, ROS production is increased and catalase levels decreased in fibroblasts derived from at least one MEGDEL patient (307); therefore, similar to BTHS, defective OXPHOS function may cause an imbalance in redox homeostasis in MEGDEL patients. However, additional basic work is required to define whether increased ROS production and reduced scavenging is a consistent feature associated with SERAC1 dysfunction, exactly how defective SERAC1 variably impairs OXPHOS, and if the changes noted in the acyl chain composition of CL in MEGDEL patients are detrimental to mitochondrial functionality.

It is curious to note that endogenous TAZ, which is presumably functional in MEGDEL patients, is unable to correct the unusual CL acyl chains that accumulate in the absence of SERAC1 function. PG is a precursor of CL and therefore contributes directly to the collection of acyl chains associated with pre-remodeled CL. Since other phospholipids have normal acyl chain compositions in MEGDEL patients (299), in theory, TAZ should still be able to generate “normal” CL. One possible explanation for this discrepancy is that perhaps the CL that accumulates in MEGDEL patients is not a substrate for the lipase that functions upstream of TAZ to initiate CL remodeling.

While SERAC1 defects do not affect the abundance or acyl chain pattern of phosphatidylcholine, phosphatidylserine, or PE, it does significantly reduce levels of BMP (299), a lipid implicated in endosomal/lysosomal homeostasis and function (200) (Figure 2.6). BMP levels regulate cholesterol trafficking with low intracellular BMP causing accumulation of free cholesterol in late endosomes. Indeed, SERAC1 patient fibroblasts accumulate unesterified cholesterol (303, 305) and patient biopsies show dramatically disorganized striated muscle ultrastructure with abnormal mitochondria and lysosomal accumulation of neutral fat droplets (299, 302). It is presently not clear how a change in the acyl chain composition of PG translates into lower amounts of BMP especially since the molecular composition of BMP in MEGDEL patients is not altered relative to controls (299). Also unclear is how PG produced on the matrix side of the IMM gains access to SERAC1, which resides in the MAM. As our understanding of how SERAC1 regulates the acyl chain composition of CL and the production of BMP is in its infancy, future basic work is needed to develop assorted models designed to better understand these processes and how their disturbance cause the numerous MEGDEL syndrome phenotypes.

Acylglycerol kinase mutations leading to Sengers syndrome

Sengers syndrome is caused by the absence of the IMS-residing acylglycerol kinase (AGK) (20, 308, 309). Symptoms of Sengers syndrome may present at birth, childhood, or early adulthood and its clinical manifestations range from being severe, causing death in infancy, to mild, allowing survival into adulthood (309, 310). This autosomal-recessive disorder is characterized by congenital cataracts, hypertrophic cardiomyopathy, skeletal myopathy, exercise intolerance, lactic acidosis, and increased

urinary 3-MGA; though motor development is delayed, mental development of the affected individuals are normal (311). Hence, the phenotypic spectrum associated with Sengers syndrome substantially overlaps with both Barth and DCMA syndromes. Sengers syndrome was originally thought to be due to deficiencies in the level and/or function of adenine nucleotide translocase 1 (ANT1) (312). ANT1 is the heart/muscle isoform of the mitochondrial ADP/ATP exchanger that plays a fundamental role in OXPHOS by mediating the flux of ADP and ATP across the IMM (313). However, genetic analyses excluded mutations in the *ANT1* gene; as such, it was subsequently proposed that transcriptional, translational, or posttranslational events might be responsible for the lower amounts of ANT1 observed in patient (312). Recently, two groups localized the defect *via* exome sequencing, not in or around *ANT1*, but instead to the *AGK* locus on chromosome 7q34 (20, 309).

The *AGK* gene contains 17 exons and encodes for a 422 amino acid protein; it is a mitochondrial membrane-associated, multi-substrate lipid kinase that contains domains that are highly homologous to sphingosine kinase-2 as well as DAG kinase (68, 69, 314). When phylogenetic analyses of AGK were undertaken, sequence comparisons to other lipid kinases such as DAG, ceramide, and sphingosine kinases revealed that despite containing a highly conserved DAG kinase catalytic domain, human and murine AGK segregate to a unique branch and are not members of any previously described lipid kinase family (68).

Like Barth and DCMA syndromes, genotype-phenotype correlations in Sengers syndrome are not readily apparent. For instance, there are Sengers syndrome patients who are nonsyndromic or do not develop lactic acidosis (315), and siblings who share the

same mutation but present with very different disease courses (one had the severe form of disease and died at 15 months of age while the other brother, at 3 years old, was without skeletal myopathy or physical limitations (316)). Thus, the etiology of Sengers syndrome is also likely to involve genetic modifiers that can significantly affect disease progression and severity.

However, there is evidence that a genotype-phenotype correlation for Sengers syndrome patients potentially exists (308). Two forms of the syndrome have been described, a severe neonatal form that leads to infantile death (317) and a more benign, but chronic, form that has allowed survival into the fourth decade (310). The former disease type is always associated with homozygous *AGK* nonsense mutations while in the latter, patients usually harbor at least one splice site variant or a start codon mutation, but not doubly null/missense alleles (308). Presumably, aberrant splicing of the COOH terminal exons (in or after the DAG kinase domain) produces proteins with residual AGK activity while inactivation of the canonical start site allows for initiation at an alternative/cryptic start site (318). In support of this possible genotype-phenotype relation, the oldest surviving patients (>35 years) carry either heterozygous start site and stop codon mutations or a homozygous mutation affecting exon 15-16 splicing (310, 319).

A role for AGK in the assembly, stability and/or regulation of OXPHOS components such as ANT1 and complex I has been speculated (308, 320). OXPHOS defects in patient samples have been variable (20, 308, 309, 312, 315, 316, 320, 321). In the more severe cases, ANT1 and complex I levels are low and the mtDNA copy number reduced. However, in the milder cases, OXPHOS function is spared. Curiously, ANT1

levels are normal in undifferentiated myoblasts but are dramatically reduced upon myoblast differentiation (309). This observation is notable as it suggests that ANT1 stability is compromised during muscle fiber differentiation in Sengers syndrome patients. While the exact molecular function of AGK is not known, its potential role in CL metabolism is consistent with the varied bioenergetic impairments, structurally abnormal mitochondria, and lipid and glycogen deposits in patient-derived skeletal and cardiac muscle (311, 316). A comprehensive phospholipid analysis has not been performed for Sengers syndrome cells and/or tissues. Therefore, whether the absence of AGK function correlates with disturbances in phospholipid metabolism has not yet been established. If AGK generates PA that contributes substantially to TAMM41's substrate pool (Figure 2.1), then the absence of AGK function should significantly impact downstream PG and CL synthesis. Given the aforementioned results concerning the relative stability of ANT1 in undifferentiated *versus* differentiated myoblasts, the choice of cell/tissue to analyze is likely to be critically important in uncovering if and how AGK participates in mitochondrial phospholipid metabolism. Such information is anticipated to shed crucial light onto Sengers syndrome disease pathogenesis.

Phosphatidic acid-preferring phospholipase A₁ mutations leading to hereditary spastic paraplegia

Mutations in the phospholipase A₁ family members *DDHD1* (322-324) and *DDHD2* (325-329) have recently been linked to autosomal-recessive forms of hereditary spastic paraplegia (HSP). HSPs are an extremely heterogeneous group of inherited neurological disorders that are classified by patients who present with (complex HSP) or without (uncomplicated or pure HSP) neurological defects. Pure HSP is characterized by

progressive spasticity and weakness of the lower limbs. In complex HSP, spastic paraplegia is compounded with neurological and systemic abnormalities such as dementia, intellectual disability, ataxia, and neuropathy, amongst others (see (330) for comprehensive discussion of HSP and spastic paraplegia variants). Furthermore, there is varied disease onset, progression, and “functional plateaus” (a point at which there is very little further disability) between the HSPs and as such, there is very little genotype-phenotype correlation in this heterogeneous disorder.

HSP has been linked to over 50 genetic loci, covering all chromosomes, of which only 22 genes have been identified so far (330, 331). Two of the identified disease-associated genes are *DDHD1* and *DDHD2* that encode protein products with PA-phospholipase A₁ activity. *DDHD1* is localized to chromosome 14q21.1, contains 12 exons (322) and encodes for the 872 amino acid protein, PA-PLA₁. Initial characterization identified substantial PA-PLA₁ activity in bovine brain and testis that corresponds to the two tissues with the highest *DDHD1* mRNA expression (332, 333). In humans, these two tissues, along with heart and skeletal muscle, additionally contain high levels of *DDHD2*, a more ubiquitously expressed DDHD family member (334-336). *DDHD2* is both cytosolic and membrane-associated (334, 337). Located on chromosome 8p11.23 and containing 18 exons, *DDHD2* is expressed as two major mRNA transcripts that correspond to the full length 711 amino acid protein and another that lacks the COOH terminal DDHD phospholipase domain. When patient *ddhd2* mutants were overexpressed in and partially purified from HEK293T, PA-PLA₁ activity was either low or absent compared to overexpressed wt *DDHD2* (329). Notably, depletion of PA-PLA₁ activity (*DDHD1* or *DDHD2*) in some, but not all cells, can cause mitochondrial

elongation (192, 326, 337), presumably due to unopposed fusion. Thus, one might expect that the balance between fission and fusion may be disturbed in some cells in patients with *ddhd1* or *ddhd2* mutations with an overall shift towards too much fusion. As active fission is a crucial process for clearance of damaged mitochondria by mitophagy, unopposed fusion could drive the accumulation of dysfunctional mitochondria (338). Consistent with the possible accretion of sub-optimal mitochondria, respiration and ATP levels are decreased and cytosolic ROS increased in *ddhd1* patient-derived lymphoblasts (322). Unfortunately, PA levels and mitochondrial morphology have not been documented in either *ddhd1* or *ddhd2* patient-derived cells (322) but there are no major changes in phospholipids in *ddhd2*^{-/-} mouse brains (339).

It is unclear whether or not depletion of DDHD1 or DDHD2 can directly affect mitochondrial dynamics by accumulating pro-fusogenic PA on the OMM. Given their similar substrate specificity, they may have redundant roles in this regard. Still, there might be functional differences for these two PA phospholipases that are dictated by their expression patterns and subcellular distributions. As such, future studies are needed to investigate the potential causative link between dysregulation of PA metabolism on the OMM with disease pathogenesis for these subtypes of HSP.

PERSPECTIVES

Phospholipids are not simply cellular barriers that delineate cells and organelles thus allowing biochemical pathways to be compartmentalized and cross-regulated. Although predominantly synthesized in the ER, some phospholipids, such as PG and CL, are exclusively made in the mitochondrion, while others, such as PE, involve a pathway

that begins in the ER but is completed in the cell's powerhouse. In mitochondria, phospholipids are important for an impressive array of functions. Indeed, when phospholipid levels, molecular species, or distribution within the mitochondrion is affected, as is the case for the diseases discussed herein, mitochondrial dysfunction ensues. Barth syndrome was the first known inborn error of mitochondrial phospholipid metabolism. Since the identification of *TAZ* as the causative gene for BTHS, exome sequencing and basic research have both contributed to the recent addition of new diseases that impinge upon mitochondrial lipid metabolism. We propose to classify these disorders as a new category of mitochondrial disease that specifically impacts phospholipid homeostasis. The clinical heterogeneity of patient phenotypes reflects the variety of functions that phospholipids partake in and their fundamental importance for mitochondrial physiology. Future work needs to focus on developing appropriate models for these diseases. As exemplified by BTHS, the availability and in-depth characterization of such models will contribute enormously to our understanding of each disease process and identify potential therapeutic strategies. Further, such basic work should help us better understand disease mechanisms and provide explanations for shared and distinct phenotypes.

ACKNOWLEDGEMENTS

We thank the Claypool lab for critical reading of the manuscript. This work was supported by National Institutes of Health Grants R00HL089185 and R01GM111548 (S.M.C.), and a pre-doctoral fellowship from the American Heart Association (Y.L.).

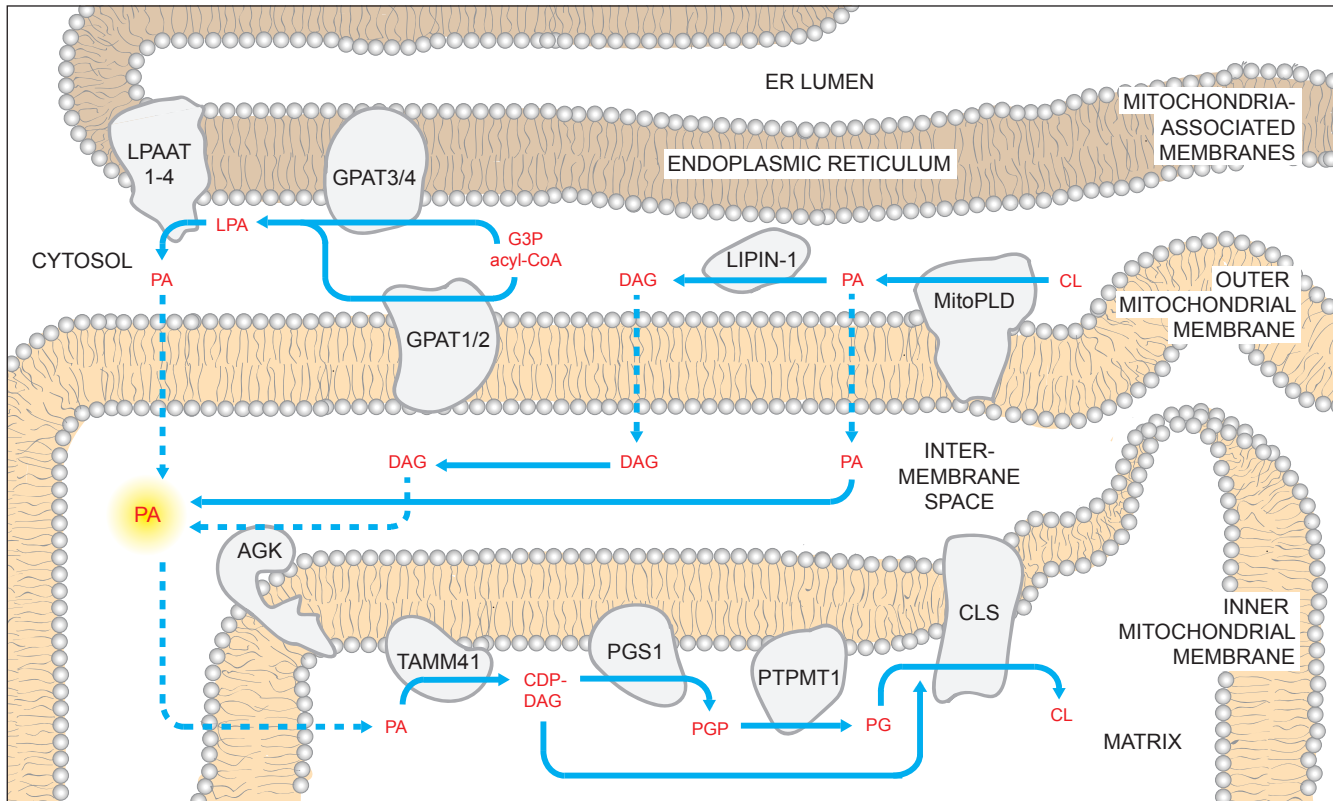


FIGURE 2.1 Mammalian cardiolipin biosynthesis. CL biosynthesis likely involves PA sourced from multiple pathways. PA can be generated by LPAATs which acylate LPA; LPA can be made using glycerol 3-phosphate (G3P) and acyl-CoAs by mitochondrial and ER GPATs. Additionally, PA can be made on the OMM through the hydrolysis of CL by MitoPLD. In the OMM, PA recruits the phosphatase lipin-1 which dephosphorylates PA into DAG. In turn, DAG may traffic across the OMM and be phosphorylated by AGK forming PA in the context of the IMS-side of the IMM. Regardless of where it is made, PA must reach the matrix side of the IMM to gain access to the core CL biosynthetic machinery. Here, PA is converted to CDP-DAG by TAMM41, thus providing the precursor for the committed step in CL biosynthesis, PGP synthesis by PGS1. PGP is rapidly dephosphorylated by PTPMT1 and the produced PG is condensed with CDP-DAG by CLS generating CL. Dashed arrows describe uncharacterized steps and pathways.

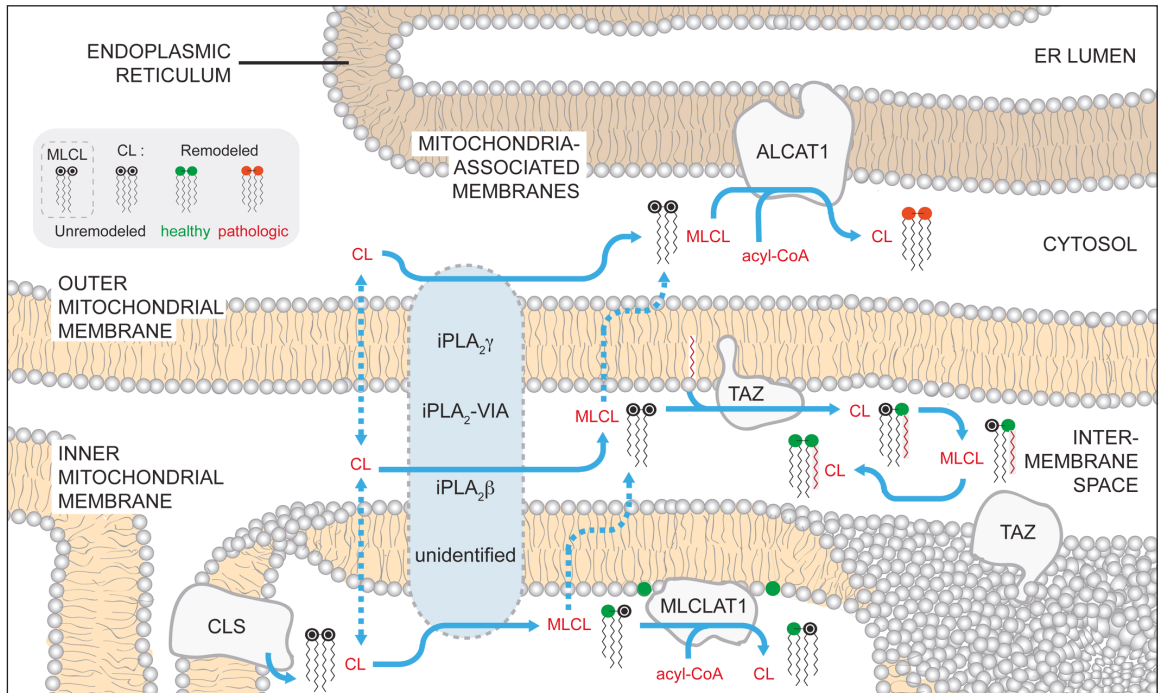


FIGURE 2.2 Mammalian cardiolipin remodeling. CL that is synthesized by CLS on the matrix-facing leaflet of the IMM can be remodeled by three different pathways. While no single enzyme has been demonstrated to be required to initiate CL remodeling in mammals, several phospholipases of the iPLA₂ family have been demonstrated to have a role in the process. Additionally, the submitochondrial localization of the phospholipases and the mechanisms by which CL gains access to these enzymes are unknown. After a fatty acyl chain is hydrolyzed from CL, generating MLCL, MLCL can be acylated back to CL by acyltransferases or transacylases. MLCLAT1 on the matrix-leaflet of the IMM, TAZ on the IMS-facing leaflets of the OMM and IMM, and ALCAT1 on the ER MAM all have the capacity to re-acylate MLCL. The acyltransferases, ALCAT1 and MLCLAT1, use acyl-CoAs as an acyl chain donor to acylate MLCL. In contrast, the transacylase TAZ uses acyl chains donated from other phospholipids. The activity of TAZ is required to establish the steady state physiological CL molecular form. In contrast, the CL formed by ALCAT1 is more sensitive to oxidative damage and associated with pathologic states. Dashed arrows describe uncharacterized steps and pathways. In the phospholipid key, unremodeled CL corresponds to the newly synthesized CL that enters the pathway at the point of CLS (black head group). CL can undergo either physiologically-relevant CL remodeling (green head group) or pathological remodeling (red head group).

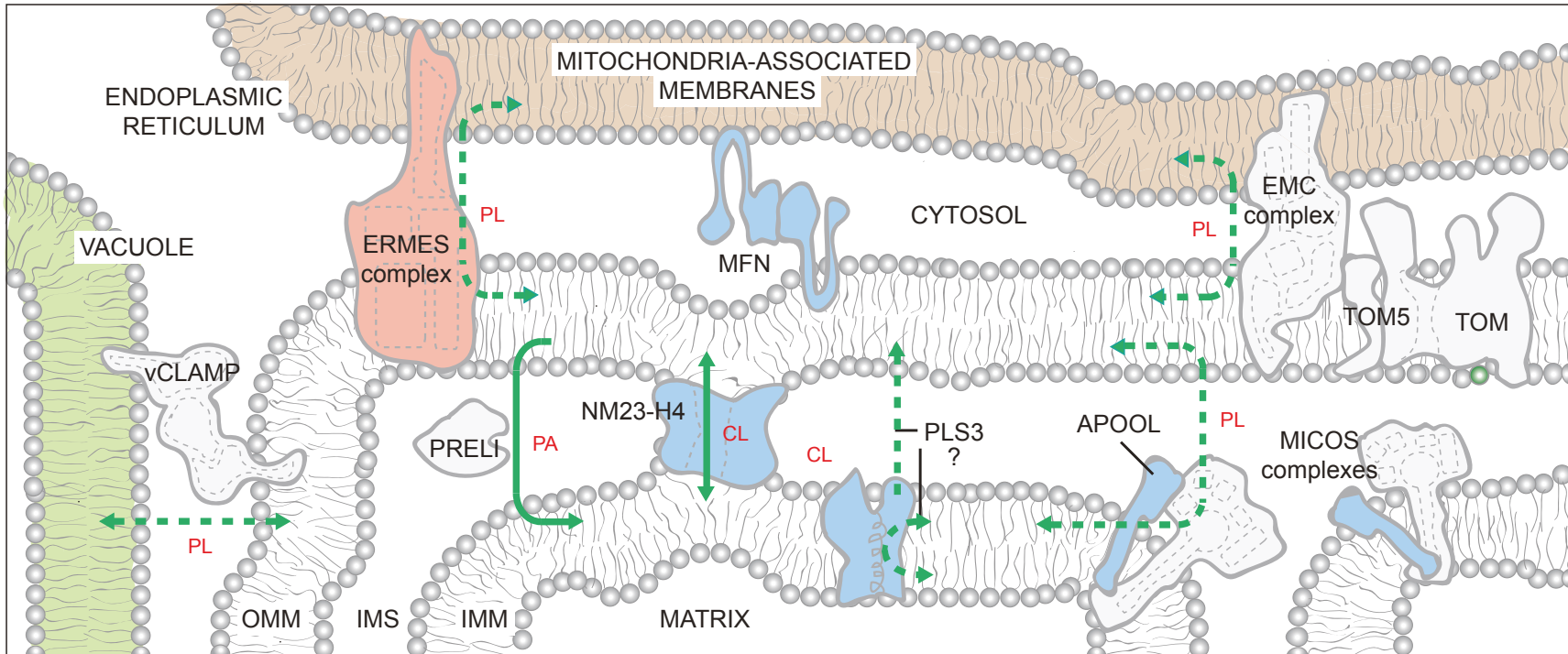


FIGURE 2.3 Inter-organelle and intra-organelle phospholipid trafficking. The existence of ER- and vacuole-mitochondria contacts is highly conserved from yeast to humans. By generating closely appositioned membranes, the inter-organelle and intra-organelle tethers are hypothesized to promote movement of lipids across the aqueous cytosol and IMS, respectively. Within the mitochondrion, phospholipid trafficking may involve contacts between the OMM and the IMM mediated by MICOS complexes or NM23-H4. In addition, PRELI transports PA from the OMM to the IMM. PLS3 activity stimulates CL externalization on OMM. It may directly transport CL from the IMM to the OMM or instead function as a scramblase that redistributes CL between both leaflets of the IMM. CL now exposed to IMS-side of IMM would then be transported to the OMM by other mechanisms. With the possible exception of EMC, it is presently unclear if any of the known tethers has specificity for a defined phospholipid(s); as such, they are shown to promote the flux of phospholipids (PL) in bulk. If a specific phospholipid is impacted by mutations in a complex/protein (levels and/or composition), the lipid is indicated. Solid lines indicate known transport mechanisms. Dashed lines describe possible trafficking routes and/or highlight transport events whose mechanisms have not been resolved. The ERMES complex is found only in yeast and color-coded pink. For the remaining proteins/complexes, those found only in mammals are in blue and those that are likely to be conserved across species are colored grey. See text for additional details.

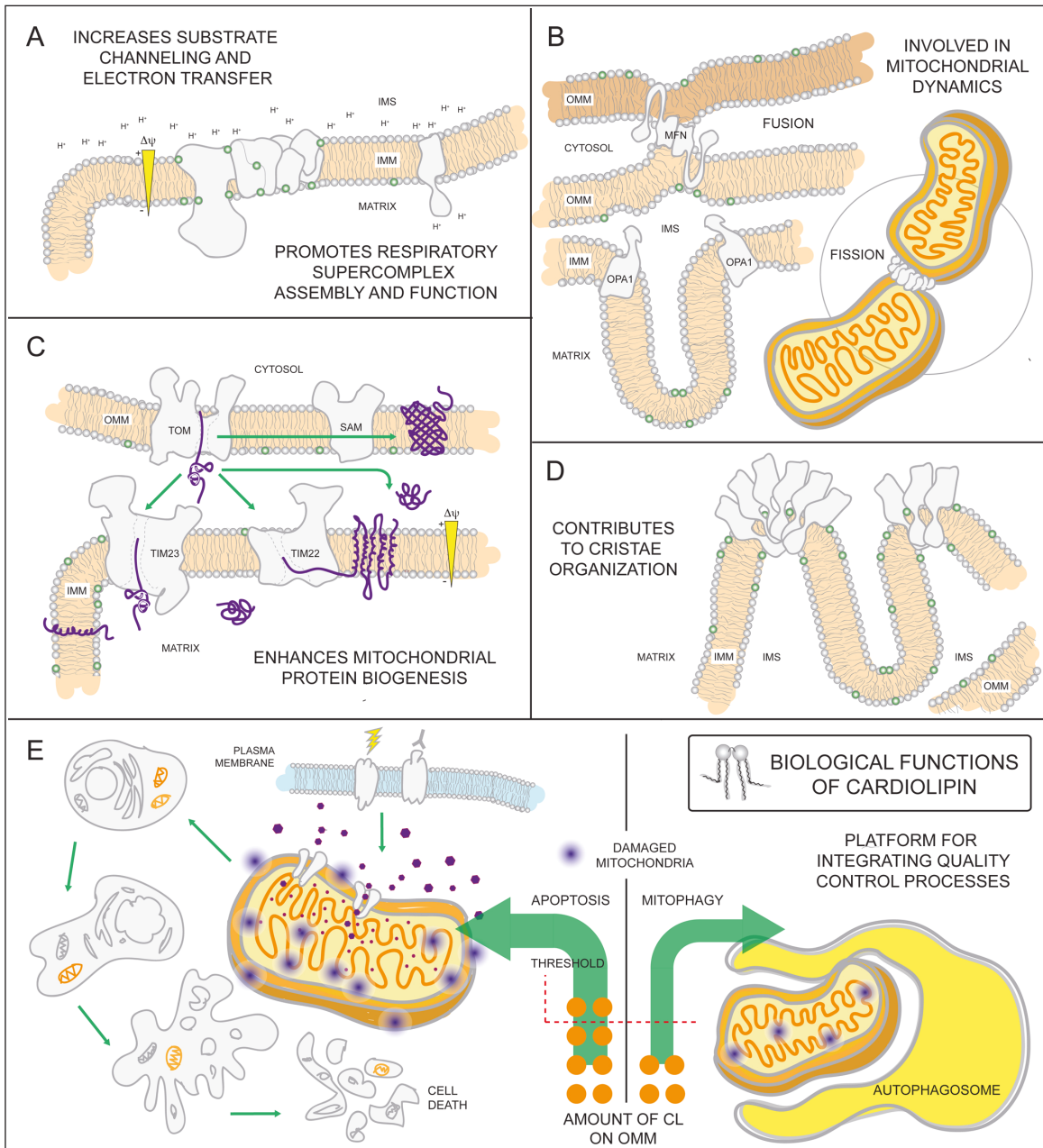


FIGURE 2.4 Biological functions of cardiolipin. As the signature phospholipid of the mitochondrion, CL is intimately involved in a number of mitochondrial processes. (A) Anionic CL on the IMM can function as a proton trap by attracting (and providing) a local pool of protons that can be funneled towards the ATP synthase. Moreover, CL is associated with every OXPHOS component and can promote their assembly into respiratory supercomplexes. Such supramolecular assemblies are thought to enhance electron transfer and reduce ROS leakage from the electron transport chain. (B) CL associates with dynamin-related GTPases that are intimately involved in fusion and fission and (C) contributes to the assembly and function of IMM and OMM translocases vital for mitochondrial biogenesis. (D) Besides enhancing OXPHOS by stabilizing SCs, CL also promotes the assembly of ATP synthase oligomers that provide a structural scaffold required for establishing the characteristic shape of mitochondrial cristae. (E) Externalization of CL on the surface of the mitochondrion is involved in signaling the execution of either mitophagy or apoptotic cell death.

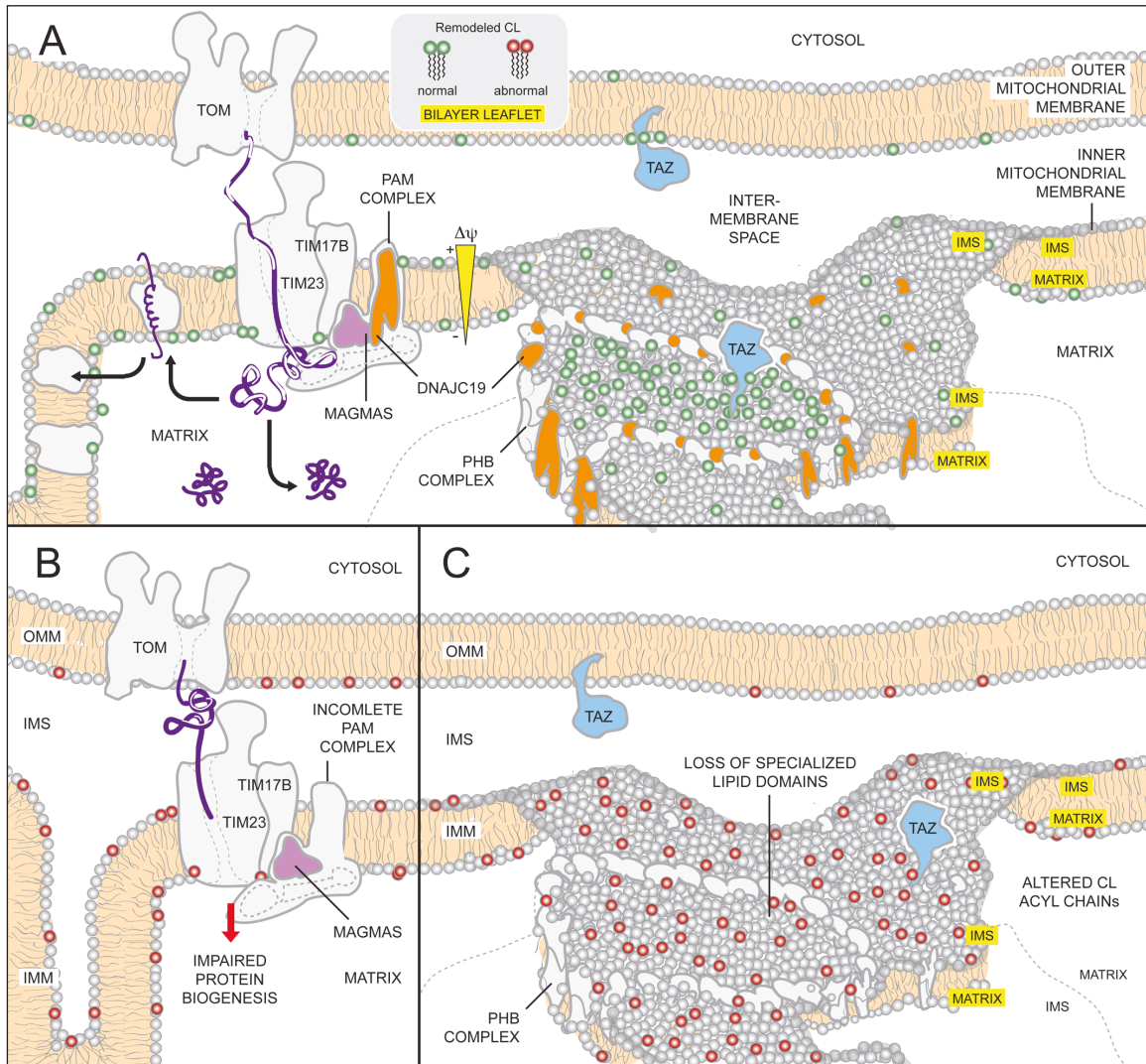


FIGURE 2.5 Potential mechanisms of DCMA mitochondrial dysfunction. (A) Under physiological conditions, DNAJC19 is targeted to TIM17B by MAGMAS and associates with components of the TIM23 translocation machinery, forming translocase B. DNAJC19 is homologous to yeast Pam18p which stimulates mHsp70 activity of the PAM (presequence-associated motor) complex and stabilizes binding of incoming precursors. Moreover, DNAJC19 also interacts with prohibitin-2 (PHB) of the PHB complexes. PHB1/PHB2 oligomers form ring-like complexes that are modeled to delineate specialized membrane domains. Functional segregation of CL and TAZ in such domains may confer acyl chain specificity to TAZ, allowing it to perform physiologically-relevant CL remodeling (green). Thus, DNAJC19 may participate in both mitochondrial presequence protein import as well as formation of membrane domains that are important for TAZ-based CL remodeling. (B) In the absence of DNAJC19, the ability of the TIM23 machinery to import proteins across the IMM may be compromised. Consequently, the biogenesis of mitochondrial proteins, such as subunits of respiratory complexes, may be reduced. (C) Further, loss of DNAJC19 prevents the PHB complex-based generation of privileged membrane domains. In the absence of such domains, TAZ remodeling, which may still occur, lacks specificity (red). For clarity, not all components of the TOM, TIM, and PAM complexes are depicted.

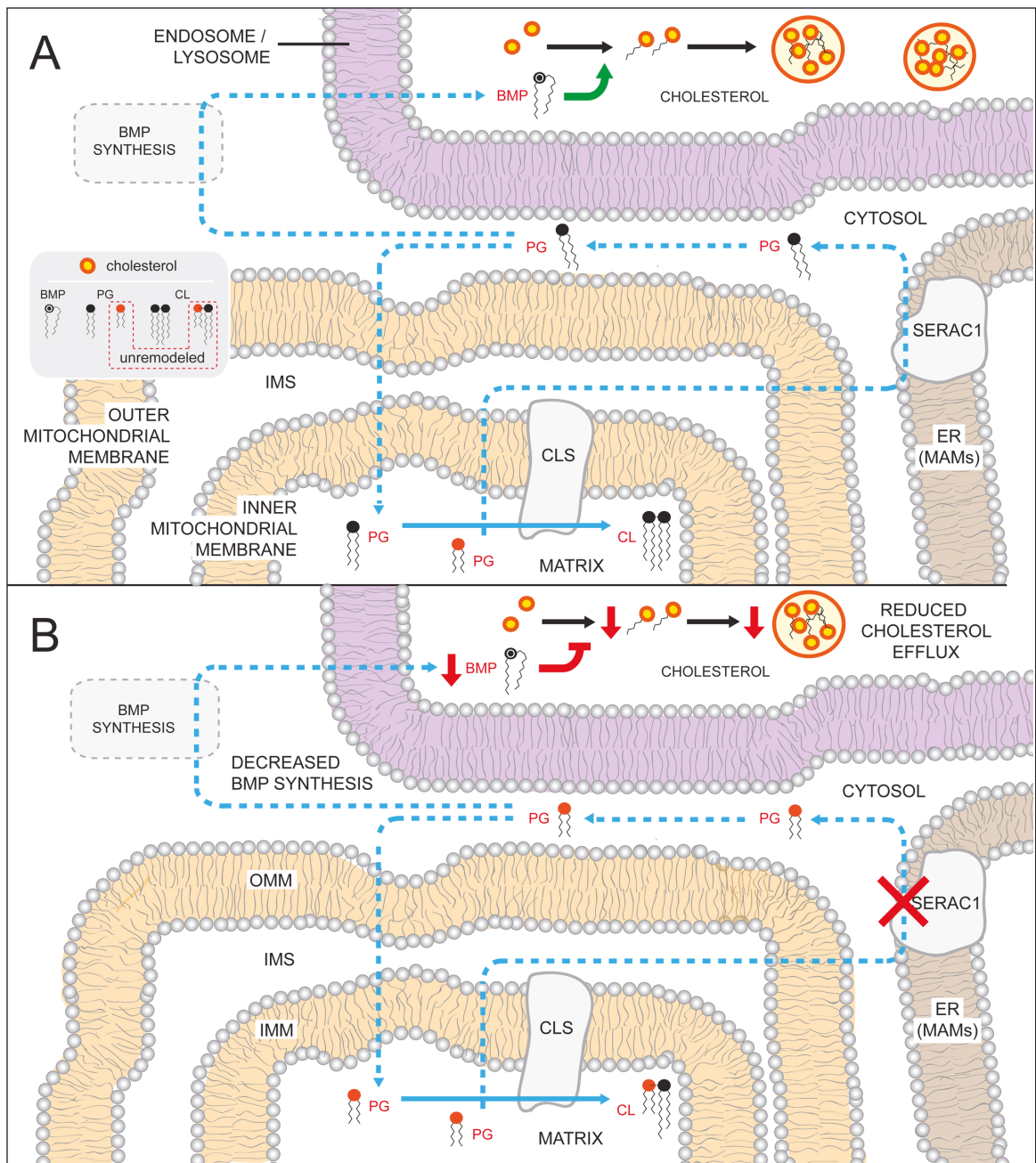


FIGURE 2.6 Potential consequences of the absence of SERAC1 activity. (A) PG that is generated on the matrix-leaflet of the IMM is trafficked out of the mitochondrion and remodeled by SERAC1 on the ER MAMs. Remodeled PG can subsequently serve as substrate for BMP and CL synthesis. BMP in the endosomal/lysosomal compartments regulates (green arrow) cholesterol esterification and trafficking out of the compartment. (B) In the absence of a functional SERAC1, PG is not remodeled and accumulates shorter acyl chain moieties. The decrease in acyl chain length somehow reduces overall BMP levels, perhaps because the unremodeled PG is a poor precursor for BMP synthesis. Reduced BMP levels in the endosome/lysosome impairs cholesterol esterification (inhibition in red) and leads to decreased (red arrows) cholesterol efflux. The lack of SERAC1 also changes the steady state composition of CL acyl chains. Blue arrows denote enzymatic reactions and lipid movements. Dashed arrows describe uncharacterized steps and pathways.

REFERENCES

- 1 Green, D.R. and Kroemer, G. (2004) The pathophysiology of mitochondrial cell death. *Science*, **305**, 626-629.
- 2 Kroemer, G., Petit, P., Zamzami, N., Vayssiere, J.L. and Mignotte, B. (1995) The biochemistry of programmed cell death. *FASEB journal : official publication of the Federation of American Societies for Experimental Biology*, **9**, 1277-1287.
- 3 Wong, L.J. (2007) Diagnostic challenges of mitochondrial DNA disorders. *Mitochondrion*, **7**, 45-52.
- 4 Luft, R., Ikkos, D., Palmieri, G., Ernster, L. and Afzelius, B. (1962) A case of severe hypermetabolism of nonthyroid origin with a defect in the maintenance of mitochondrial respiratory control: a correlated clinical, biochemical, and morphological study. *The Journal of clinical investigation*, **41**, 1776-1804.
- 5 Schaefer, A.M., McFarland, R., Blakely, E.L., He, L., Whittaker, R.G., Taylor, R.W., Chinnery, P.F. and Turnbull, D.M. (2008) Prevalence of mitochondrial DNA disease in adults. *Annals of neurology*, **63**, 35-39.
- 6 Naviaux, R.K. (2004) Developing a systematic approach to the diagnosis and classification of mitochondrial disease. *Mitochondrion*, **4**, 351-361.
- 7 Foundation, T.U.M.D. (2014), Pittsburg, Vol. 2014.
- 8 Holt, I.J., Harding, A.E. and Morgan-Hughes, J.A. (1988) Deletions of muscle mitochondrial DNA in patients with mitochondrial myopathies. *Nature*, **331**, 717-719.
- 9 Wallace, D.C., Singh, G., Lott, M.T., Hodge, J.A., Schurr, T.G., Lezza, A.M., Elsas, L.J., 2nd and Nikoskelainen, E.K. (1988) Mitochondrial DNA mutation associated with Leber's hereditary optic neuropathy. *Science*, **242**, 1427-1430.

- 10 DaRe, J.T., Vasta, V., Penn, J., Tran, N.T. and Hahn, S.H. (2013) Targeted exome sequencing for mitochondrial disorders reveals high genetic heterogeneity. *BMC medical genetics*, **14**, 118.
- 11 Calvo, S.E. and Mootha, V.K. (2010) The mitochondrial proteome and human disease. *Annual review of genomics and human genetics*, **11**, 25-44.
- 12 Anderson, S., Bankier, A.T., Barrell, B.G., de Bruijn, M.H., Coulson, A.R., Drouin, J., Eperon, I.C., Nierlich, D.P., Roe, B.A., Sanger, F. *et al.* (1981) Sequence and organization of the human mitochondrial genome. *Nature*, **290**, 457-465.
- 13 Pagliarini, D.J., Calvo, S.E., Chang, B., Sheth, S.A., Vafai, S.B., Ong, S.E., Walford, G.A., Sugiana, C., Boneh, A., Chen, W.K. *et al.* (2008) A mitochondrial protein compendium elucidates complex I disease biology. *Cell*, **134**, 112-123.
- 14 Mootha, V.K., Bunkenborg, J., Olsen, J.V., Hjerrild, M., Wisniewski, J.R., Stahl, E., Bolouri, M.S., Ray, H.N., Sihag, S., Kamal, M. *et al.* (2003) Integrated analysis of protein composition, tissue diversity, and gene regulation in mouse mitochondria. *Cell*, **115**, 629-640.
- 15 Johnson, D.T., Harris, R.A., French, S., Blair, P.V., You, J., Bemis, K.G., Wang, M. and Balaban, R.S. (2007) Tissue heterogeneity of the mammalian mitochondrial proteome. *American journal of physiology. Cell physiology*, **292**, C689-697.
- 16 Hung, V., Zou, P., Rhee, H.W., Udeshi, N.D., Cracan, V., Svinkina, T., Carr, S.A., Mootha, V.K. and Ting, A.Y. (2014) Proteomic mapping of the human mitochondrial intermembrane space in live cells via ratiometric APEX tagging. *Molecular cell*, **55**, 332-341.

- 17 Rhee, H.W., Zou, P., Udeshi, N.D., Martell, J.D., Mootha, V.K., Carr, S.A. and Ting, A.Y. (2013) Proteomic mapping of mitochondria in living cells via spatially restricted enzymatic tagging. *Science*, **339**, 1328-1331.
- 18 Zahedi, R.P., Sickmann, A., Boehm, A.M., Winkler, C., Zufall, N., Schonfisch, B., Guiard, B., Pfanner, N. and Meisinger, C. (2006) Proteomic analysis of the yeast mitochondrial outer membrane reveals accumulation of a subclass of preproteins. *Molecular biology of the cell*, **17**, 1436-1450.
- 19 Taylor, S.W., Fahy, E., Zhang, B., Glenn, G.M., Warnock, D.E., Wiley, S., Murphy, A.N., Gaucher, S.P., Capaldi, R.A., Gibson, B.W. *et al.* (2003) Characterization of the human heart mitochondrial proteome. *Nature biotechnology*, **21**, 281-286.
- 20 Calvo, S.E., Compton, A.G., Hershman, S.G., Lim, S.C., Lieber, D.S., Tucker, E.J., Laskowski, A., Garone, C., Liu, S., Jaffe, D.B. *et al.* (2012) Molecular diagnosis of infantile mitochondrial disease with targeted next-generation sequencing. *Science translational medicine*, **4**, 118ra110.
- 21 Ye, K., Lu, J., Ma, F., Keinan, A. and Gu, Z. (2014) Extensive pathogenicity of mitochondrial heteroplasmy in healthy human individuals. *Proceedings of the National Academy of Sciences of the United States of America*, **111**, 10654-10659.
- 22 Dimauro, S. and Davidzon, G. (2005) Mitochondrial DNA and disease. *Annals of medicine*, **37**, 222-232.
- 23 Ugalde, C., Moran, M., Blazquez, A., Arenas, J. and Martin, M.A. (2009) Mitochondrial disorders due to nuclear OXPHOS gene defects. *Advances in experimental medicine and biology*, **652**, 85-116.

- 24 Jacobs, H.T. and Turnbull, D.M. (2005) Nuclear genes and mitochondrial translation: a new class of genetic disease. *Trends in genetics : TIG*, **21**, 312-314.
- 25 Perez-Martinez, X., Funes, S., Camacho-Villasana, Y., Marjavaara, S., Tavares-Carreon, F. and Shingu-Vazquez, M. (2008) Protein synthesis and assembly in mitochondrial disorders. *Current topics in medicinal chemistry*, **8**, 1335-1350.
- 26 Koppen, M. and Langer, T. (2007) Protein degradation within mitochondria: versatile activities of AAA proteases and other peptidases. *Critical reviews in biochemistry and molecular biology*, **42**, 221-242.
- 27 Lill, R., Hoffmann, B., Molik, S., Pierik, A.J., Rietzschel, N., Stehling, O., Uzarska, M.A., Webert, H., Wilbrecht, C. and Muhlenhoff, U. (2012) The role of mitochondria in cellular iron-sulfur protein biogenesis and iron metabolism. *Biochimica et biophysica acta*, **1823**, 1491-1508.
- 28 Chen, H. and Chan, D.C. (2009) Mitochondrial dynamics--fusion, fission, movement, and mitophagy--in neurodegenerative diseases. *Human molecular genetics*, **18**, R169-176.
- 29 Horvath, S.E. and Daum, G. (2013) Lipids of mitochondria. *Progress in lipid research*, **52**, 590-614.
- 30 Lecocq, J. and Ballou, C.E. (1964) On the Structure of Cardiolipin. *Biochemistry*, **3**, 976-980.
- 31 Schlame, M., Rua, D. and Greenberg, M.L. (2000) The biosynthesis and functional role of cardiolipin. *Progress in lipid research*, **39**, 257-288.
- 32 Haines, T.H. and Dencher, N.A. (2002) Cardiolipin: a proton trap for oxidative phosphorylation. *FEBS letters*, **528**, 35-39.

- 33 Verkleij, A.J., Leunissen-Bijvelt, J., de Kruijff, B., Hope, M. and Cullis, P.R. (1984) Non-bilayer structures in membrane fusion. *Ciba Foundation symposium*, **103**, 45-59.
- 34 Gruner, S.M. (1985) Intrinsic curvature hypothesis for biomembrane lipid composition: a role for nonbilayer lipids. *Proceedings of the National Academy of Sciences of the United States of America*, **82**, 3665-3669.
- 35 Zeczycki, T.N., Whelan, J., Hayden, W.T., Brown, D.A. and Shaikh, S.R. (2014) Increasing levels of cardiolipin differentially influence packing of phospholipids found in the mitochondrial inner membrane. *Biochemical and biophysical research communications*, **450**, 366-371.
- 36 Daum, G. and Vance, J.E. (1997) Import of lipids into mitochondria. *Progress in lipid research*, **36**, 103-130.
- 37 Gebert, N., Joshi, A.S., Kutik, S., Becker, T., McKenzie, M., Guan, X.L., Mooga, V.P., Stroud, D.A., Kulkarni, G., Wenk, M.R. *et al.* (2009) Mitochondrial cardiolipin involved in outer-membrane protein biogenesis: implications for Barth syndrome. *Current biology : CB*, **19**, 2133-2139.
- 38 Zinser, E., Sperka-Gottlieb, C.D., Fasch, E.V., Kohlwein, S.D., Paltauf, F. and Daum, G. (1991) Phospholipid synthesis and lipid composition of subcellular membranes in the unicellular eukaryote *Saccharomyces cerevisiae*. *Journal of bacteriology*, **173**, 2026-2034.
- 39 Colbeau, A., Nachbaur, J. and Vignais, P.M. (1971) Enzymic characterization and lipid composition of rat liver subcellular membranes. *Biochimica et biophysica acta*, **249**, 462-492.

- 40 Zinser, E. and Daum, G. (1995) Isolation and biochemical characterization of organelles from the yeast, *Saccharomyces cerevisiae*. *Yeast*, **11**, 493-536.
- 41 Ardail, D., Privat, J.P., Egret-Charlier, M., Levrat, C., Lerme, F. and Louisot, P. (1990) Mitochondrial contact sites. Lipid composition and dynamics. *The Journal of biological chemistry*, **265**, 18797-18802.
- 42 Sperka-Gottlieb, C.D., Hermetter, A., Paltauf, F. and Daum, G. (1988) Lipid topology and physical properties of the outer mitochondrial membrane of the yeast, *Saccharomyces cerevisiae*. *Biochimica et biophysica acta*, **946**, 227-234.
- 43 Simbeni, R., Pon, L., Zinser, E., Paltauf, F. and Daum, G. (1991) Mitochondrial membrane contact sites of yeast. Characterization of lipid components and possible involvement in intramitochondrial translocation of phospholipids. *The Journal of biological chemistry*, **266**, 10047-10049.
- 44 Hovius, R., Lambrechts, H., Nicolay, K. and de Kruijff, B. (1990) Improved methods to isolate and subfractionate rat liver mitochondria. Lipid composition of the inner and outer membrane. *Biochimica et biophysica acta*, **1021**, 217-226.
- 45 de Kroon, A.I., Dolis, D., Mayer, A., Lill, R. and de Kruijff, B. (1997) Phospholipid composition of highly purified mitochondrial outer membranes of rat liver and *Neurospora crassa*. Is cardiolipin present in the mitochondrial outer membrane? *Biochimica et biophysica acta*, **1325**, 108-116.
- 46 Hovius, R., Thijssen, J., van der Linden, P., Nicolay, K. and de Kruijff, B. (1993) Phospholipid asymmetry of the outer membrane of rat liver mitochondria. Evidence for the presence of cardiolipin on the outside of the outer membrane. *FEBS letters*, **330**, 71-76.

- 47 Cheneval, D., Muller, M., Toni, R., Ruetz, S. and Carafoli, E. (1985) Adriamycin as a probe for the transversal distribution of cardiolipin in the inner mitochondrial membrane. *The Journal of biological chemistry*, **260**, 13003-13007.
- 48 Gallet, P.F., Petit, J.M., Maftah, A., Zachowski, A. and Julien, R. (1997) Asymmetrical distribution of cardiolipin in yeast inner mitochondrial membrane triggered by carbon catabolite repression. *The Biochemical journal*, **324 (Pt 2)**, 627-634.
- 49 Krebs, J.J., Hauser, H. and Carafoli, E. (1979) Asymmetric distribution of phospholipids in the inner membrane of beef heart mitochondria. *The Journal of biological chemistry*, **254**, 5308-5316.
- 50 Harb, J.S., Comte, J. and Gautheron, D.C. (1981) Asymmetrical orientation of phospholipids and their interactions with marker enzymes in pig heart mitochondrial inner membrane. *Archives of biochemistry and biophysics*, **208**, 305-318.
- 51 Chacinska, A., Koehler, C.M., Milenkovic, D., Lithgow, T. and Pfanner, N. (2009) Importing mitochondrial proteins: machineries and mechanisms. *Cell*, **138**, 628-644.
- 52 Wang, S., Lee, D.P., Gong, N., Schwerbrock, N.M., Mashek, D.G., Gonzalez-Baro, M.R., Stapleton, C., Li, L.O., Lewin, T.M. and Coleman, R.A. (2007) Cloning and functional characterization of a novel mitochondrial N-ethylmaleimide-sensitive glycerol-3-phosphate acyltransferase (GPAT2). *Archives of biochemistry and biophysics*, **465**, 347-358.
- 53 Lewin, T.M., Schwerbrock, N.M., Lee, D.P. and Coleman, R.A. (2004) Identification of a new glycerol-3-phosphate acyltransferase isoenzyme, mtGPAT2, in mitochondria. *The Journal of biological chemistry*, **279**, 13488-13495.

- 54 Yet, S.F., Lee, S., Hahm, Y.T. and Sul, H.S. (1993) Expression and identification of p90 as the murine mitochondrial glycerol-3-phosphate acyltransferase. *Biochemistry*, **32**, 9486-9491.
- 55 Chen, Y.Q., Kuo, M.S., Li, S., Bui, H.H., Peake, D.A., Sanders, P.E., Thibodeaux, S.J., Chu, S., Qian, Y.W., Zhao, Y. *et al.* (2008) AGPAT6 is a novel microsomal glycerol-3-phosphate acyltransferase. *The Journal of biological chemistry*, **283**, 10048-10057.
- 56 Nagle, C.A., Vergnes, L., Dejong, H., Wang, S., Lewin, T.M., Reue, K. and Coleman, R.A. (2008) Identification of a novel sn-glycerol-3-phosphate acyltransferase isoform, GPAT4, as the enzyme deficient in *Agpat6*^{-/-} mice. *Journal of lipid research*, **49**, 823-831.
- 57 Gaigg, B., Simbeni, R., Hrastnik, C., Paltauf, F. and Daum, G. (1995) Characterization of a microsomal subfraction associated with mitochondria of the yeast, *Saccharomyces cerevisiae*. Involvement in synthesis and import of phospholipids into mitochondria. *Biochimica et biophysica acta*, **1234**, 214-220.
- 58 Vance, J.E. (1990) Phospholipid synthesis in a membrane fraction associated with mitochondria. *The Journal of biological chemistry*, **265**, 7248-7256.
- 59 Eto, M., Shindou, H. and Shimizu, T. (2014) A novel lysophosphatidic acid acyltransferase enzyme (LPAAT4) with a possible role for incorporating docosahexaenoic acid into brain glycerophospholipids. *Biochemical and biophysical research communications*, **443**, 718-724.
- 60 Aguado, B. and Campbell, R.D. (1998) Characterization of a human lysophosphatidic acid acyltransferase that is encoded by a gene located in the class III

region of the human major histocompatibility complex. *The Journal of biological chemistry*, **273**, 4096-4105.

61 West, J., Tompkins, C.K., Balantac, N., Nudelman, E., Meengs, B., White, T., Bursten, S., Coleman, J., Kumar, A., Singer, J.W. *et al.* (1997) Cloning and expression of two human lysophosphatidic acid acyltransferase cDNAs that enhance cytokine-induced signaling responses in cells. *DNA and cell biology*, **16**, 691-701.

62 Lu, B., Jiang, Y.J., Zhou, Y., Xu, F.Y., Hatch, G.M. and Choy, P.C. (2005) Cloning and characterization of murine 1-acyl-sn-glycerol 3-phosphate acyltransferases and their regulation by PPARalpha in murine heart. *The Biochemical journal*, **385**, 469-477.

63 Prasad, S.S., Garg, A. and Agarwal, A.K. (2011) Enzymatic activities of the human AGPAT isoform 3 and isoform 5: localization of AGPAT5 to mitochondria. *Journal of lipid research*, **52**, 451-462.

64 Schmidt, J.A., Yvone, G.M. and Brown, W.J. (2010) Membrane topology of human AGPAT3 (LPAAT3). *Biochemical and biophysical research communications*, **397**, 661-667.

65 Agarwal, A.K. (2012) Lysophospholipid acyltransferases: 1-acylglycerol-3-phosphate O-acyltransferases. From discovery to disease. *Current opinion in lipidology*, **23**, 290-302.

66 Choi, S.Y., Huang, P., Jenkins, G.M., Chan, D.C., Schiller, J. and Frohman, M.A. (2006) A common lipid links Mfn-mediated mitochondrial fusion and SNARE-regulated exocytosis. *Nature cell biology*, **8**, 1255-1262.

- 67 Hajra, A.K. and Bishop, J.E. (1982) Glycerolipid biosynthesis in peroxisomes via the acyl dihydroxyacetone phosphate pathway. *Annals of the New York Academy of Sciences*, **386**, 170-182.
- 68 Waggoner, D.W., Johnson, L.B., Mann, P.C., Morris, V., Guastella, J. and Bajjalieh, S.M. (2004) MuLK, a eukaryotic multi-substrate lipid kinase. *The Journal of biological chemistry*, **279**, 38228-38235.
- 69 Bektas, M., Payne, S.G., Liu, H., Goparaju, S., Milstien, S. and Spiegel, S. (2005) A novel acylglycerol kinase that produces lysophosphatidic acid modulates cross talk with EGFR in prostate cancer cells. *The Journal of cell biology*, **169**, 801-811.
- 70 Kuchler, K., Daum, G. and Paltauf, F. (1986) Subcellular and submitochondrial localization of phospholipid-synthesizing enzymes in *Saccharomyces cerevisiae*. *Journal of bacteriology*, **165**, 901-910.
- 71 Shen, H., Heacock, P.N., Clancey, C.J. and Dowhan, W. (1996) The CDS1 gene encoding CDP-diacylglycerol synthase in *Saccharomyces cerevisiae* is essential for cell growth. *The Journal of biological chemistry*, **271**, 789-795.
- 72 Kutik, S., Rissler, M., Guan, X.L., Guiard, B., Shui, G., Gebert, N., Heacock, P.N., Rehling, P., Dowhan, W., Wenk, M.R. *et al.* (2008) The translocator maintenance protein Tam41 is required for mitochondrial cardiolipin biosynthesis. *The Journal of cell biology*, **183**, 1213-1221.
- 73 Tamura, Y., Harada, Y., Nishikawa, S., Yamano, K., Kamiya, M., Shiota, T., Kuroda, T., Kuge, O., Sesaki, H., Imai, K. *et al.* (2013) Tam41 is a CDP-diacylglycerol synthase required for cardiolipin biosynthesis in mitochondria. *Cell metabolism*, **17**, 709-718.

- 74 Tamura, Y., Harada, Y., Yamano, K., Watanabe, K., Ishikawa, D., Ohshima, C., Nishikawa, S., Yamamoto, H. and Endo, T. (2006) Identification of Tam41 maintaining integrity of the TIM23 protein translocator complex in mitochondria. *The Journal of cell biology*, **174**, 631-637.
- 75 Chang, S.C., Heacock, P.N., Clancey, C.J. and Dowhan, W. (1998) The PEL1 gene (renamed PGS1) encodes the phosphatidylglycero-phosphate synthase of *Saccharomyces cerevisiae*. *The Journal of biological chemistry*, **273**, 9829-9836.
- 76 Zhang, J., Guan, Z., Murphy, A.N., Wiley, S.E., Perkins, G.A., Worby, C.A., Engel, J.L., Heacock, P., Nguyen, O.K., Wang, J.H. *et al.* (2011) Mitochondrial phosphatase PTPMT1 is essential for cardiolipin biosynthesis. *Cell metabolism*, **13**, 690-700.
- 77 Xiao, J., Engel, J.L., Zhang, J., Chen, M.J., Manning, G. and Dixon, J.E. (2011) Structural and functional analysis of PTPMT1, a phosphatase required for cardiolipin synthesis. *Proceedings of the National Academy of Sciences of the United States of America*, **108**, 11860-11865.
- 78 Osman, C., Haag, M., Wieland, F.T., Brugger, B. and Langer, T. (2010) A mitochondrial phosphatase required for cardiolipin biosynthesis: the PGP phosphatase Gep4. *The EMBO journal*, **29**, 1976-1987.
- 79 Daum, G. (1985) Lipids of mitochondria. *Biochimica et biophysica acta*, **822**, 1-42.
- 80 Schlame, M. and Haldar, D. (1993) Cardiolipin is synthesized on the matrix side of the inner membrane in rat liver mitochondria. *The Journal of biological chemistry*, **268**, 74-79.

- 81 Chen, D., Zhang, X.Y. and Shi, Y. (2006) Identification and functional characterization of hCLS1, a human cardiolipin synthase localized in mitochondria. *The Biochemical journal*, **398**, 169-176.
- 82 Chang, S.C., Heacock, P.N., Mileykovskaya, E., Voelker, D.R. and Dowhan, W. (1998) Isolation and characterization of the gene (CLS1) encoding cardiolipin synthase in *Saccharomyces cerevisiae*. *The Journal of biological chemistry*, **273**, 14933-14941.
- 83 Lu, B., Xu, F.Y., Jiang, Y.J., Choy, P.C., Hatch, G.M., Grunfeld, C. and Feingold, K.R. (2006) Cloning and characterization of a cDNA encoding human cardiolipin synthase (hCLS1). *Journal of lipid research*, **47**, 1140-1145.
- 84 Houtkooper, R.H., Akbari, H., van Lenthe, H., Kulik, W., Wanders, R.J., Frentzen, M. and Vaz, F.M. (2006) Identification and characterization of human cardiolipin synthase. *FEBS letters*, **580**, 3059-3064.
- 85 Cheng, H., Mancuso, D.J., Jiang, X., Guan, S., Yang, J., Yang, K., Sun, G., Gross, R.W. and Han, X. (2008) Shotgun lipidomics reveals the temporally dependent, highly diversified cardiolipin profile in the mammalian brain: temporally coordinated postnatal diversification of cardiolipin molecular species with neuronal remodeling. *Biochemistry*, **47**, 5869-5880.
- 86 Schlame, M., Brody, S. and Hostetler, K.Y. (1993) Mitochondrial cardiolipin in diverse eukaryotes. Comparison of biosynthetic reactions and molecular acyl species. *European journal of biochemistry / FEBS*, **212**, 727-735.
- 87 Schlame, M., Ren, M., Xu, Y., Greenberg, M.L. and Haller, I. (2005) Molecular symmetry in mitochondrial cardiolipins. *Chemistry and physics of lipids*, **138**, 38-49.

- 88 Schlame, M. and Otten, D. (1991) Analysis of cardiolipin molecular species by high-performance liquid chromatography of its derivative 1,3-bisphosphatidyl-2-benzoyl-sn-glycerol dimethyl ester. *Analytical biochemistry*, **195**, 290-295.
- 89 Han, X., Yang, K., Yang, J., Cheng, H. and Gross, R.W. (2006) Shotgun lipidomics of cardiolipin molecular species in lipid extracts of biological samples. *Journal of lipid research*, **47**, 864-879.
- 90 Eichberg, J. (1974) The reacylation of deacylated derivatives of diphosphatidylglycerol by microsomes and mitochondria from rat liver. *The Journal of biological chemistry*, **249**, 3423-3429.
- 91 Schlame, M. and Rustow, B. (1990) Lysocardiolipin formation and reacylation in isolated rat liver mitochondria. *The Biochemical journal*, **272**, 589-595.
- 92 Baile, M.G., Sathappa, M., Lu, Y.W., Pryce, E., Whited, K., McCaffery, J.M., Han, X., Alder, N.N. and Claypool, S.M. (2014) Unremodeled and remodeled cardiolipin are functionally indistinguishable in yeast. *The Journal of biological chemistry*, **289**, 1768-1778.
- 93 Beranek, A., Rechberger, G., Knauer, H., Wolinski, H., Kohlwein, S.D. and Leber, R. (2009) Identification of a cardiolipin-specific phospholipase encoded by the gene CLD1 (YGR110W) in yeast. *The Journal of biological chemistry*, **284**, 11572-11578.
- 94 Baile, M.G., Whited, K. and Claypool, S.M. (2013) Deacylation on the matrix side of the mitochondrial inner membrane regulates cardiolipin remodeling. *Molecular biology of the cell*, **24**, 2008-2020.

- 95 Hsu, Y.H., Dumlao, D.S., Cao, J. and Dennis, E.A. (2013) Assessing phospholipase A2 activity toward cardiolipin by mass spectrometry. *PloS one*, **8**, e59267.
- 96 Mancuso, D.J., Jenkins, C.M. and Gross, R.W. (2000) The genomic organization, complete mRNA sequence, cloning, and expression of a novel human intracellular membrane-associated calcium-independent phospholipase A(2). *The Journal of biological chemistry*, **275**, 9937-9945.
- 97 Mancuso, D.J., Sims, H.F., Han, X., Jenkins, C.M., Guan, S.P., Yang, K., Moon, S.H., Pietka, T., Abumrad, N.A., Schlesinger, P.H. *et al.* (2007) Genetic ablation of calcium-independent phospholipase A2gamma leads to alterations in mitochondrial lipid metabolism and function resulting in a deficient mitochondrial bioenergetic phenotype. *The Journal of biological chemistry*, **282**, 34611-34622.
- 98 Yoda, E., Hachisu, K., Taketomi, Y., Yoshida, K., Nakamura, M., Ikeda, K., Taguchi, R., Nakatani, Y., Kuwata, H., Murakami, M. *et al.* (2010) Mitochondrial dysfunction and reduced prostaglandin synthesis in skeletal muscle of Group VIB Ca²⁺-independent phospholipase A2gamma-deficient mice. *Journal of lipid research*, **51**, 3003-3015.
- 99 Kiebish, M.A., Yang, K., Liu, X., Mancuso, D.J., Guan, S., Zhao, Z., Sims, H.F., Cerqua, R., Cade, W.T., Han, X. *et al.* (2013) Dysfunctional cardiac mitochondrial bioenergetic, lipidomic, and signaling in a murine model of Barth syndrome. *Journal of lipid research*, **54**, 1312-1325.
- 100 Houtkooper, R.H., Turkenburg, M., Poll-The, B.T., Karall, D., Perez-Cerda, C., Morrone, A., Malvagia, S., Wanders, R.J., Kulik, W. and Vaz, F.M. (2009) The

enigmatic role of tafazzin in cardiolipin metabolism. *Biochimica et biophysica acta*, **1788**, 2003-2014.

101 Houtkooper, R.H., Rodenburg, R.J., Thiels, C., van Lenthe, H., Stet, F., Poll-The, B.T., Stone, J.E., Steward, C.G., Wanders, R.J., Smeitink, J. *et al.* (2009) Cardiolipin and monolysocardiolipin analysis in fibroblasts, lymphocytes, and tissues using high-performance liquid chromatography-mass spectrometry as a diagnostic test for Barth syndrome. *Analytical biochemistry*, **387**, 230-237.

102 Malhotra, A., Edelman-Novemsky, I., Xu, Y., Plesken, H., Ma, J., Schlame, M. and Ren, M. (2009) Role of calcium-independent phospholipase A2 in the pathogenesis of Barth syndrome. *Proceedings of the National Academy of Sciences of the United States of America*, **106**, 2337-2341.

103 Xu, Y., Malhotra, A., Ren, M. and Schlame, M. (2006) The enzymatic function of tafazzin. *The Journal of biological chemistry*, **281**, 39217-39224.

104 Taylor, W.A. and Hatch, G.M. (2003) Purification and characterization of monolysocardiolipin acyltransferase from pig liver mitochondria. *The Journal of biological chemistry*, **278**, 12716-12721.

105 Taylor, W.A. and Hatch, G.M. (2009) Identification of the human mitochondrial linoleoyl-coenzyme A monolysocardiolipin acyltransferase (MLCL AT-1). *The Journal of biological chemistry*, **284**, 30360-30371.

106 Claypool, S.M. and Koehler, C.M. (2012) The complexity of cardiolipin in health and disease. *Trends in biochemical sciences*, **37**, 32-41.

107 Valianpour, F., Mitsakos, V., Schlemmer, D., Towbin, J.A., Taylor, J.M., Ekert, P.G., Thorburn, D.R., Munnich, A., Wanders, R.J., Barth, P.G. *et al.* (2005)

Monolysocardiolipins accumulate in Barth syndrome but do not lead to enhanced apoptosis. *Journal of lipid research*, **46**, 1182-1195.

108 Claypool, S.M., Whited, K., Srijumnong, S., Han, X. and Koehler, C.M. (2011) Barth syndrome mutations that cause tafazzin complex lability. *The Journal of cell biology*, **192**, 447-462.

109 Gu, Z., Valianpour, F., Chen, S., Vaz, F.M., Hakkaart, G.A., Wanders, R.J. and Greenberg, M.L. (2004) Aberrant cardiolipin metabolism in the yeast taz1 mutant: a model for Barth syndrome. *Molecular microbiology*, **51**, 149-158.

110 Vaz, F.M., Houtkooper, R.H., Valianpour, F., Barth, P.G. and Wanders, R.J. (2003) Only one splice variant of the human TAZ gene encodes a functional protein with a role in cardiolipin metabolism. *The Journal of biological chemistry*, **278**, 43089-43094.

111 Claypool, S.M., McCaffery, J.M. and Koehler, C.M. (2006) Mitochondrial mislocalization and altered assembly of a cluster of Barth syndrome mutant tafazzins. *The Journal of cell biology*, **174**, 379-390.

112 Malhotra, A., Xu, Y., Ren, M. and Schlame, M. (2009) Formation of molecular species of mitochondrial cardiolipin. 1. A novel transacylation mechanism to shuttle fatty acids between sn-1 and sn-2 positions of multiple phospholipid species. *Biochimica et biophysica acta*, **1791**, 314-320.

113 Xu, Y., Zhang, S., Malhotra, A., Edelman-Novemsky, I., Ma, J., Kruppa, A., Cernicica, C., Blais, S., Neubert, T.A., Ren, M. *et al.* (2009) Characterization of tafazzin splice variants from humans and fruit flies. *The Journal of biological chemistry*, **284**, 29230-29239.

- 114 Schlame, M., Acehan, D., Berno, B., Xu, Y., Valvo, S., Ren, M., Stokes, D.L. and Epand, R.M. (2012) The physical state of lipid substrates provides transacylation specificity for tafazzin. *Nature chemical biology*, **8**, 862-869.
- 115 Stavrovskaya, I.G., Bird, S.S., Marur, V.R., Sniatynski, M.J., Baranov, S.V., Greenberg, H.K., Porter, C.L. and Kristal, B.S. (2013) Dietary macronutrients modulate the fatty acyl composition of rat liver mitochondrial cardiolipins. *Journal of lipid research*, **54**, 2623-2635.
- 116 Brandner, K., Mick, D.U., Frazier, A.E., Taylor, R.D., Meisinger, C. and Rehling, P. (2005) Taz1, an outer mitochondrial membrane protein, affects stability and assembly of inner membrane protein complexes: implications for Barth Syndrome. *Molecular biology of the cell*, **16**, 5202-5214.
- 117 Baile, M.G., Lu, Y.W. and Claypool, S.M. (2014) The topology and regulation of cardiolipin biosynthesis and remodeling in yeast. *Chemistry and physics of lipids*, **179**, 25-31.
- 118 Carpenter, K., Pollitt, R.J. and Middleton, B. (1992) Human liver long-chain 3-hydroxyacyl-coenzyme A dehydrogenase is a multifunctional membrane-bound beta-oxidation enzyme of mitochondria. *Biochemical and biophysical research communications*, **183**, 443-448.
- 119 Uchida, Y., Izai, K., Orii, T. and Hashimoto, T. (1992) Novel fatty acid beta-oxidation enzymes in rat liver mitochondria. II. Purification and properties of enoyl-coenzyme A (CoA) hydratase/3-hydroxyacyl-CoA dehydrogenase/3-ketoacyl-CoA thiolase trifunctional protein. *The Journal of biological chemistry*, **267**, 1034-1041.

- 120 Sims, H.F., Brackett, J.C., Powell, C.K., Treem, W.R., Hale, D.E., Bennett, M.J., Gibson, B., Shapiro, S. and Strauss, A.W. (1995) The molecular basis of pediatric long chain 3-hydroxyacyl-CoA dehydrogenase deficiency associated with maternal acute fatty liver of pregnancy. *Proceedings of the National Academy of Sciences of the United States of America*, **92**, 841-845.
- 121 Ushikubo, S., Aoyama, T., Kamijo, T., Wanders, R.J., Rinaldo, P., Vockley, J. and Hashimoto, T. (1996) Molecular characterization of mitochondrial trifunctional protein deficiency: formation of the enzyme complex is important for stabilization of both alpha- and beta-subunits. *American journal of human genetics*, **58**, 979-988.
- 122 IJlst, L., Wanders, R.J., Ushikubo, S., Kamijo, T. and Hashimoto, T. (1994) Molecular basis of long-chain 3-hydroxyacyl-CoA dehydrogenase deficiency: identification of the major disease-causing mutation in the alpha-subunit of the mitochondrial trifunctional protein. *Biochimica et biophysica acta*, **1215**, 347-350.
- 123 Fould, B., Garlatti, V., Neumann, E., Fenel, D., Gaboriaud, C. and Arlaud, G.J. (2010) Structural and functional characterization of the recombinant human mitochondrial trifunctional protein. *Biochemistry*, **49**, 8608-8617.
- 124 Taylor, W.A., Mejia, E.M., Mitchell, R.W., Choy, P.C., Sparagna, G.C. and Hatch, G.M. (2012) Human trifunctional protein alpha links cardiolipin remodeling to beta-oxidation. *PloS one*, **7**, e48628.
- 125 Cao, J., Liu, Y., Lockwood, J., Burn, P. and Shi, Y. (2004) A novel cardiolipin-remodeling pathway revealed by a gene encoding an endoplasmic reticulum-associated acyl-CoA:lysocardiolipin acyltransferase (ALCAT1) in mouse. *The Journal of biological chemistry*, **279**, 31727-31734.

- 126 Cao, J., Shen, W., Chang, Z. and Shi, Y. (2009) ALCAT1 is a polyglycerophospholipid acyltransferase potently regulated by adenine nucleotide and thyroid status. *American journal of physiology. Endocrinology and metabolism*, **296**, E647-653.
- 127 Zhao, Y., Chen, Y.Q., Li, S., Konrad, R.J. and Cao, G. (2009) The microsomal cardiolipin remodeling enzyme acyl-CoA lysocardiolipin acyltransferase is an acyltransferase of multiple anionic lysophospholipids. *Journal of lipid research*, **50**, 945-956.
- 128 Vreken, P., Valianpour, F., Nijtmans, L.G., Grivell, L.A., Plecko, B., Wanders, R.J. and Barth, P.G. (2000) Defective remodeling of cardiolipin and phosphatidylglycerol in Barth syndrome. *Biochemical and biophysical research communications*, **279**, 378-382.
- 129 Valianpour, F., Wanders, R.J., Overmars, H., Vreken, P., Van Gennip, A.H., Baas, F., Plecko, B., Santer, R., Becker, K. and Barth, P.G. (2002) Cardiolipin deficiency in X-linked cardioskeletal myopathy and neutropenia (Barth syndrome, MIM 302060): a study in cultured skin fibroblasts. *The Journal of pediatrics*, **141**, 729-733.
- 130 Schlame, M., Kelley, R.I., Feigenbaum, A., Towbin, J.A., Heerdt, P.M., Schieble, T., Wanders, R.J., DiMauro, S. and Blanck, T.J. (2003) Phospholipid abnormalities in children with Barth syndrome. *Journal of the American College of Cardiology*, **42**, 1994-1999.
- 131 Acehan, D., Khuchua, Z., Houtkooper, R.H., Malhotra, A., Kaufman, J., Vaz, F.M., Ren, M., Rockman, H.A., Stokes, D.L. and Schlame, M. (2009) Distinct effects of

tafazzin deletion in differentiated and undifferentiated mitochondria. *Mitochondrion*, **9**, 86-95.

132 Xu, Y., Condell, M., Plesken, H., Edelman-Novemsky, I., Ma, J., Ren, M. and Schlame, M. (2006) A Drosophila model of Barth syndrome. *Proceedings of the National Academy of Sciences of the United States of America*, **103**, 11584-11588.

133 Gonzalvez, F., D'Aurelio, M., Boutant, M., Moustapha, A., Puech, J.P., Landes, T., Arnaune-Pelloquin, L., Vial, G., Taleux, N., Slomianny, C. *et al.* (2013) Barth syndrome: cellular compensation of mitochondrial dysfunction and apoptosis inhibition due to changes in cardiolipin remodeling linked to tafazzin (TAZ) gene mutation. *Biochimica et biophysica acta*, **1832**, 1194-1206.

134 van Werkhoven, M.A., Thorburn, D.R., Gedeon, A.K. and Pitt, J.J. (2006) Monolysocardiolipin in cultured fibroblasts is a sensitive and specific marker for Barth Syndrome. *Journal of lipid research*, **47**, 2346-2351.

135 Wang, G., McCain, M.L., Yang, L., He, A., Pasqualini, F.S., Agarwal, A., Yuan, H., Jiang, D., Zhang, D., Zangi, L. *et al.* (2014) Modeling the mitochondrial cardiomyopathy of Barth syndrome with induced pluripotent stem cell and heart-on-chip technologies. *Nature medicine*, **20**, 616-623.

136 Dudek, J., Cheng, I.F., Balleininger, M., Vaz, F.M., Streckfuss-Bomeke, K., Hubscher, D., Vukotic, M., Wanders, R.J., Rehling, P. and Guan, K. (2013) Cardiolipin deficiency affects respiratory chain function and organization in an induced pluripotent stem cell model of Barth syndrome. *Stem cell research*, **11**, 806-819.

137 Acehan, D., Vaz, F., Houtkooper, R.H., James, J., Moore, V., Tokunaga, C., Kulik, W., Wansapura, J., Toth, M.J., Strauss, A. *et al.* (2011) Cardiac and skeletal

muscle defects in a mouse model of human Barth syndrome. *The Journal of biological chemistry*, **286**, 899-908.

138 Xu, Y., Sutachan, J.J., Plesken, H., Kelley, R.I. and Schlame, M. (2005) Characterization of lymphoblast mitochondria from patients with Barth syndrome. *Laboratory investigation; a journal of technical methods and pathology*, **85**, 823-830.

139 Bissler, J.J., Tsoras, M., Goring, H.H., Hug, P., Chuck, G., Tombragel, E., McGraw, C., Schlotman, J., Ralston, M.A. and Hug, G. (2002) Infantile dilated X-linked cardiomyopathy, G4.5 mutations, altered lipids, and ultrastructural malformations of mitochondria in heart, liver, and skeletal muscle. *Laboratory investigation; a journal of technical methods and pathology*, **82**, 335-344.

140 Li, J., Romestaing, C., Han, X., Li, Y., Hao, X., Wu, Y., Sun, C., Liu, X., Jefferson, L.S., Xiong, J. *et al.* (2010) Cardiolipin remodeling by ALCAT1 links oxidative stress and mitochondrial dysfunction to obesity. *Cell metabolism*, **12**, 154-165.

141 Richter-Dennerlein, R., Korwitz, A., Haag, M., Tatsuta, T., Dargazanli, S., Baker, M., Decker, T., Lamkemeyer, T., Rugarli, E.I. and Langer, T. (2014) DNAJC19, a mitochondrial cochaperone associated with cardiomyopathy, forms a complex with prohibitins to regulate cardiolipin remodeling. *Cell metabolism*, **20**, 158-171.

142 Schlame, M., Blais, S., Edelman-Novemsky, I., Xu, Y., Montecillo, F., Phoon, C.K., Ren, M. and Neubert, T.A. (2012) Comparison of cardiolipins from *Drosophila* strains with mutations in putative remodeling enzymes. *Chemistry and physics of lipids*, **165**, 512-519.

- 143 Kornmann, B., Currie, E., Collins, S.R., Schuldiner, M., Nunnari, J., Weissman, J.S. and Walter, P. (2009) An ER-mitochondria tethering complex revealed by a synthetic biology screen. *Science*, **325**, 477-481.
- 144 Lahiri, S., Chao, J.T., Tavassoli, S., Wong, A.K., Choudhary, V., Young, B.P., Loewen, C.J. and Prinz, W.A. (2014) A Conserved Endoplasmic Reticulum Membrane Protein Complex (EMC) Facilitates Phospholipid Transfer from the ER to Mitochondria. *PLoS biology*, **12**, e1001969.
- 145 Kornmann, B., Osman, C. and Walter, P. (2011) The conserved GTPase Gem1 regulates endoplasmic reticulum-mitochondria connections. *Proceedings of the National Academy of Sciences of the United States of America*, **108**, 14151-14156.
- 146 Tamura, Y., Onguka, O., Hobbs, A.E., Jensen, R.E., Iijima, M., Claypool, S.M. and Sesaki, H. (2012) Role for two conserved intermembrane space proteins, Ups1p and Ups2p, [corrected] in intra-mitochondrial phospholipid trafficking. *The Journal of biological chemistry*, **287**, 15205-15218.
- 147 Nguyen, T.T., Lewandowska, A., Choi, J.Y., Markgraf, D.F., Junker, M., Bilgin, M., Ejsing, C.S., Voelker, D.R., Rapoport, T.A. and Shaw, J.M. (2012) Gem1 and ERMES do not directly affect phosphatidylserine transport from ER to mitochondria or mitochondrial inheritance. *Traffic*, **13**, 880-890.
- 148 Csordas, G., Renken, C., Varnai, P., Walter, L., Weaver, D., Buttle, K.F., Balla, T., Mannella, C.A. and Hajnoczky, G. (2006) Structural and functional features and significance of the physical linkage between ER and mitochondria. *The Journal of cell biology*, **174**, 915-921.

- 149 Matsuzaki, H., Fujimoto, T., Tanaka, M. and Shirasawa, S. (2013) Tespa1 is a novel component of mitochondria-associated endoplasmic reticulum membranes and affects mitochondrial calcium flux. *Biochemical and biophysical research communications*, **433**, 322-326.
- 150 de Brito, O.M. and Scorrano, L. (2008) Mitofusin 2 tethers endoplasmic reticulum to mitochondria. *Nature*, **456**, 605-610.
- 151 Csordas, G., Varnai, P., Golenar, T., Roy, S., Purkins, G., Schneider, T.G., Balla, T. and Hajnoczky, G. (2010) Imaging interorganelle contacts and local calcium dynamics at the ER-mitochondrial interface. *Molecular cell*, **39**, 121-132.
- 152 Merkwirth, C. and Langer, T. (2008) Mitofusin 2 builds a bridge between ER and mitochondria. *Cell*, **135**, 1165-1167.
- 153 Honscher, C., Mari, M., Auffarth, K., Bohnert, M., Griffith, J., Geerts, W., van der Laan, M., Cabrera, M., Reggiori, F. and Ungermann, C. (2014) Cellular metabolism regulates contact sites between vacuoles and mitochondria. *Developmental cell*, **30**, 86-94.
- 154 Elbaz-Alon, Y., Rosenfeld-Gur, E., Shinder, V., Futerman, A.H., Geiger, T. and Schuldiner, M. (2014) A dynamic interface between vacuoles and mitochondria in yeast. *Developmental cell*, **30**, 95-102.
- 155 Daniele, T., Hurbain, I., Vago, R., Casari, G., Raposo, G., Tacchetti, C. and Schiaffino, M.V. (2014) Mitochondria and melanosomes establish physical contacts modulated by Mfn2 and involved in organelle biogenesis. *Current biology : CB*, **24**, 393-403.

- 156 Schlattner, U., Tokarska-Schlattner, M., Rousseau, D., Boissan, M., Mannella, C., Epand, R. and Lacombe, M.L. (2014) Mitochondrial cardiolipin/phospholipid trafficking: the role of membrane contact site complexes and lipid transfer proteins. *Chemistry and physics of lipids*, **179**, 32-41.
- 157 Nicolay, K., Rojo, M., Wallimann, T., Demel, R. and Hovius, R. (1990) The role of contact sites between inner and outer mitochondrial membrane in energy transfer. *Biochimica et biophysica acta*, **1018**, 229-233.
- 158 Vogel, F., Bornhövd, C., Neupert, W. and Reichert, A.S. (2006) Dynamic subcompartmentalization of the mitochondrial inner membrane. *The Journal of Cell Biology*, **175**, 237-247.
- 159 Harner, M., Korner, C., Walther, D., Mokranjac, D., Kaesmacher, J., Welsch, U., Griffith, J., Mann, M., Reggiori, F. and Neupert, W. (2011) The mitochondrial contact site complex, a determinant of mitochondrial architecture. *The EMBO journal*, **30**, 4356-4370.
- 160 Hoppins, S., Collins, S.R., Cassidy-Stone, A., Hummel, E., Devay, R.M., Lackner, L.L., Westermann, B., Schuldiner, M., Weissman, J.S. and Nunnari, J. (2011) A mitochondrial-focused genetic interaction map reveals a scaffold-like complex required for inner membrane organization in mitochondria. *The Journal of cell biology*, **195**, 323-340.
- 161 van der Laan, M., Bohnert, M., Wiedemann, N. and Pfanner, N. (2012) Role of MINOS in mitochondrial membrane architecture and biogenesis. *Trends in cell biology*, **22**, 185-192.

- 162 von der Malsburg, K., Muller, J.M., Bohnert, M., Oeljeklaus, S., Kwiatkowska, P., Becker, T., Loniewska-Lwowska, A., Wiese, S., Rao, S., Milenkovic, D. *et al.* (2011) Dual role of mitofilin in mitochondrial membrane organization and protein biogenesis. *Developmental cell*, **21**, 694-707.
- 163 Pfanner, N., van der Laan, M., Amati, P., Capaldi, R.A., Caudy, A.A., Chacinska, A., Darshi, M., Deckers, M., Hoppins, S., Icho, T. *et al.* (2014) Uniform nomenclature for the mitochondrial contact site and cristae organizing system. *The Journal of cell biology*, **204**, 1083-1086.
- 164 John, G.B., Shang, Y., Li, L., Renken, C., Mannella, C.A., Selker, J.M., Rangell, L., Bennett, M.J. and Zha, J. (2005) The mitochondrial inner membrane protein mitofilin controls cristae morphology. *Molecular biology of the cell*, **16**, 1543-1554.
- 165 Mun, J.Y., Lee, T.H., Kim, J.H., Yoo, B.H., Bahk, Y.Y., Koo, H.S. and Han, S.S. (2010) *Caenorhabditis elegans* mitofilin homologs control the morphology of mitochondrial cristae and influence reproduction and physiology. *Journal of cellular physiology*, **224**, 748-756.
- 166 Weber, T.A., Koob, S., Heide, H., Wittig, I., Head, B., van der Blik, A., Brandt, U., Mittelbronn, M. and Reichert, A.S. (2013) APOOL is a cardiolipin-binding constituent of the Mitofilin/MINOS protein complex determining cristae morphology in mammalian mitochondria. *PloS one*, **8**, e63683.
- 167 Connerth, M., Tatsuta, T., Haag, M., Klecker, T., Westermann, B. and Langer, T. (2012) Intramitochondrial transport of phosphatidic acid in yeast by a lipid transfer protein. *Science*, **338**, 815-818.

- 168 Potting, C., Tatsuta, T., Konig, T., Haag, M., Wai, T., Aaltonen, M.J. and Langer, T. (2013) TRIAP1/PRELI complexes prevent apoptosis by mediating intramitochondrial transport of phosphatidic acid. *Cell metabolism*, **18**, 287-295.
- 169 Potting, C., Wilmes, C., Engmann, T., Osman, C. and Langer, T. (2010) Regulation of mitochondrial phospholipids by Ups1/PRELI-like proteins depends on proteolysis and Mdm35. *The EMBO journal*, **29**, 2888-2898.
- 170 Tamura, Y., Iijima, M. and Sesaki, H. (2010) Mdm35p imports Ups proteins into the mitochondrial intermembrane space by functional complex formation. *The EMBO journal*, **29**, 2875-2887.
- 171 Gallet, P.F., Zachowski, A., Julien, R., Fellmann, P., Devaux, P.F. and Maftah, A. (1999) Transbilayer movement and distribution of spin-labelled phospholipids in the inner mitochondrial membrane. *Biochimica et biophysica acta*, **1418**, 61-70.
- 172 Hope, M.J., Redelmeier, T.E., Wong, K.F., Rodriguez, W. and Cullis, P.R. (1989) Phospholipid asymmetry in large unilamellar vesicles induced by transmembrane pH gradients. *Biochemistry*, **28**, 4181-4187.
- 173 Contreras, F.X., Sanchez-Magraner, L., Alonso, A. and Goni, F.M. (2010) Transbilayer (flip-flop) lipid motion and lipid scrambling in membranes. *FEBS letters*, **584**, 1779-1786.
- 174 Kol, M.A., de Kroon, A.I., Killian, J.A. and de Kruijff, B. (2004) Transbilayer movement of phospholipids in biogenic membranes. *Biochemistry*, **43**, 2673-2681.
- 175 Kol, M.A., de Kroon, A.I., Rijkers, D.T., Killian, J.A. and de Kruijff, B. (2001) Membrane-spanning peptides induce phospholipid flop: a model for phospholipid translocation across the inner membrane of *E. coli*. *Biochemistry*, **40**, 10500-10506.

- 176 Chu, C.T., Ji, J., Dagda, R.K., Jiang, J.F., Tyurina, Y.Y., Kapralov, A.A., Tyurin, V.A., Yanamala, N., Shrivastava, I.H., Mohammadyani, D. *et al.* (2013) Cardiolipin externalization to the outer mitochondrial membrane acts as an elimination signal for mitophagy in neuronal cells. *Nature cell biology*, **15**, 1197-1205.
- 177 Gonzalez, F., Schug, Z.T., Houtkooper, R.H., MacKenzie, E.D., Brooks, D.G., Wanders, R.J., Petit, P.X., Vaz, F.M. and Gottlieb, E. (2008) Cardiolipin provides an essential activating platform for caspase-8 on mitochondria. *The Journal of cell biology*, **183**, 681-696.
- 178 Liu, J., Chen, J., Dai, Q. and Lee, R.M. (2003) Phospholipid scramblase 3 is the mitochondrial target of protein kinase C delta-induced apoptosis. *Cancer research*, **63**, 1153-1156.
- 179 Van, Q., Liu, J., Lu, B., Feingold, K.R., Shi, Y., Lee, R.M. and Hatch, G.M. (2007) Phospholipid scramblase-3 regulates cardiolipin de novo biosynthesis and its resynthesis in growing HeLa cells. *The Biochemical journal*, **401**, 103-109.
- 180 Zhou, Q., Sims, P.J. and Wiedmer, T. (1998) Identity of a conserved motif in phospholipid scramblase that is required for Ca²⁺-accelerated transbilayer movement of membrane phospholipids. *Biochemistry*, **37**, 2356-2360.
- 181 Liu, J., Dai, Q., Chen, J., Durrant, D., Freeman, A., Liu, T., Grossman, D. and Lee, R.M. (2003) Phospholipid scramblase 3 controls mitochondrial structure, function, and apoptotic response. *Molecular cancer research : MCR*, **1**, 892-902.
- 182 Milon, L., Meyer, P., Chiadmi, M., Munier, A., Johansson, M., Karlsson, A., Lascu, I., Capeau, J., Janin, J. and Lacombe, M.L. (2000) The human nm23-H4 gene

product is a mitochondrial nucleoside diphosphate kinase. *The Journal of biological chemistry*, **275**, 14264-14272.

183 Tokarska-Schlattner, M., Boissan, M., Munier, A., Borot, C., Mailleau, C., Speer, O., Schlattner, U. and Lacombe, M.L. (2008) The nucleoside diphosphate kinase D (NM23-H4) binds the inner mitochondrial membrane with high affinity to cardiolipin and couples nucleotide transfer with respiration. *The Journal of biological chemistry*, **283**, 26198-26207.

184 Schlattner, U., Tokarska-Schlattner, M., Ramirez, S., Tyurina, Y.Y., Amoscato, A.A., Mohammadyani, D., Huang, Z., Jiang, J., Yanamala, N., Seffouh, A. *et al.* (2013) Dual function of mitochondrial Nm23-H4 protein in phosphotransfer and intermembrane lipid transfer: a cardiolipin-dependent switch. *The Journal of biological chemistry*, **288**, 111-121.

185 Huang, H., Gao, Q., Peng, X., Choi, S.Y., Sarma, K., Ren, H., Morris, A.J. and Frohman, M.A. (2011) piRNA-associated germline nuage formation and spermatogenesis require MitoPLD profusogenic mitochondrial-surface lipid signaling. *Developmental cell*, **20**, 376-387.

186 Reue, K. and Dwyer, J.R. (2009) Lipin proteins and metabolic homeostasis. *Journal of lipid research*, **50 Suppl**, S109-114.

187 Pane, A., Wehr, K. and Schupbach, T. (2007) zucchini and squash encode two putative nucleases required for rasiRNA production in the Drosophila germline. *Developmental cell*, **12**, 851-862.

188 Watanabe, T., Chuma, S., Yamamoto, Y., Kuramochi-Miyagawa, S., Totoki, Y., Toyoda, A., Hoki, Y., Fujiyama, A., Shibata, T., Sado, T. *et al.* (2011) MITOPLD is a

mitochondrial protein essential for nuage formation and piRNA biogenesis in the mouse germline. *Developmental cell*, **20**, 364-375.

189 Gunawardane, L.S., Saito, K., Nishida, K.M., Miyoshi, K., Kawamura, Y., Nagami, T., Siomi, H. and Siomi, M.C. (2007) A slicer-mediated mechanism for repeat-associated siRNA 5' end formation in *Drosophila*. *Science*, **315**, 1587-1590.

190 He, Z., Kokkinaki, M., Pant, D., Gallicano, G.I. and Dym, M. (2009) Small RNA molecules in the regulation of spermatogenesis. *Reproduction*, **137**, 901-911.

191 Russell, L. and Frank, B. (1978) Ultrastructural characterization of nuage in spermatocytes of the rat testis. *The Anatomical record*, **190**, 79-97.

192 Baba, T., Kashiwagi, Y., Arimitsu, N., Kogure, T., Edo, A., Maruyama, T., Nakao, K., Nakanishi, H., Kinoshita, M., Frohman, M.A. *et al.* (2014) Phosphatidic acid (PA)-preferring phospholipase A1 regulates mitochondrial dynamics. *The Journal of biological chemistry*, **289**, 11497-11511.

193 Higgs, H.N. and Glomset, J.A. (1994) Identification of a phosphatidic acid-preferring phospholipase A1 from bovine brain and testis. *Proceedings of the National Academy of Sciences*, **91**, 9574-9578.

194 Hullin-Matsuda, F., Kawasaki, K., Delton-Vandenbroucke, I., Xu, Y., Nishijima, M., Lagarde, M., Schlame, M. and Kobayashi, T. (2007) De novo biosynthesis of the late endosome lipid, bis(monoacylglycero)phosphate. *Journal of lipid research*, **48**, 1997-2008.

195 Mobius, W., van Donselaar, E., Ohno-Iwashita, Y., Shimada, Y., Heijnen, H.F., Slot, J.W. and Geuze, H.J. (2003) Recycling compartments and the internal vesicles of

multivesicular bodies harbor most of the cholesterol found in the endocytic pathway.

Traffic, **4**, 222-231.

196 Poorthuis, B.J. and Hostetler, K.Y. (1976) Studies on the subcellular localization and properties of bis(monoacylglyceryl)phosphate biosynthesis in rat liver. *The Journal of biological chemistry*, **251**, 4596-4602.

197 Wherrett, J.R. and Huterer, S. (1972) Enrichment of bis-(monoacylglyceryl) phosphate in lysosomes from rat liver. *The Journal of biological chemistry*, **247**, 4114-4120.

198 Simon, G. and Rouser, G. (1969) Species variations in phospholipid class distribution of organs. II. Heart and skeletal muscle. *Lipids*, **4**, 607-614.

199 Mason, R.J., Stossel, T.P. and Vaughan, M. (1972) Lipids of alveolar macrophages, polymorphonuclear leukocytes, and their phagocytic vesicles. *The Journal of clinical investigation*, **51**, 2399-2407.

200 Hullin-Matsuda, F., Luquain-Costaz, C., Bouvier, J. and Delton-Vandenbroucke, I. (2009) Bis(monoacylglycerol)phosphate, a peculiar phospholipid to control the fate of cholesterol: Implications in pathology. *Prostaglandins, leukotrienes, and essential fatty acids*, **81**, 313-324.

201 Gallala, H.D. and Sandhoff, K. (2011) Biological function of the cellular lipid BMP-BMP as a key activator for cholesterol sorting and membrane digestion. *Neurochemical research*, **36**, 1594-1600.

202 Kobayashi, T., Beuchat, M.H., Lindsay, M., Frias, S., Palmiter, R.D., Sakuraba, H., Parton, R.G. and Gruenberg, J. (1999) Late endosomal membranes rich in lysobisphosphatidic acid regulate cholesterol transport. *Nature cell biology*, **1**, 113-118.

- 203 Kobayashi, T., Stang, E., Fang, K.S., de Moerloose, P., Parton, R.G. and Gruenberg, J. (1998) A lipid associated with the antiphospholipid syndrome regulates endosome structure and function. *Nature*, **392**, 193-197.
- 204 Pangborn, M. (1942) Isolation and purification of a serologically active phospholipid from beef heart. *The Journal of biological chemistry*, **143**, 247-256.
- 205 Hostetler, K.Y., Galesloot, J.M., Boer, P. and Van Den Bosch, H. (1975) Further studies on the formation of cardiolipin and phosphatidylglycerol in rat liver mitochondria. Effect of divalent cations and the fatty acid composition of CDP-diglyceride. *Biochimica et biophysica acta*, **380**, 382-389.
- 206 Claypool, S.M., Oktay, Y., Boontheung, P., Loo, J.A. and Koehler, C.M. (2008) Cardiolipin defines the interactome of the major ADP/ATP carrier protein of the mitochondrial inner membrane. *The Journal of cell biology*, **182**, 937-950.
- 207 Cheneval, D., Muller, M. and Carafoli, E. (1983) The mitochondrial phosphate carrier reconstituted in liposomes is inhibited by doxorubicin. *FEBS letters*, **159**, 123-126.
- 208 Eble, K.S., Coleman, W.B., Hantgan, R.R. and Cunningham, C.C. (1990) Tightly associated cardiolipin in the bovine heart mitochondrial ATP synthase as analyzed by ³¹P nuclear magnetic resonance spectroscopy. *The Journal of biological chemistry*, **265**, 19434-19440.
- 209 Shinzawa-Itoh, K., Aoyama, H., Muramoto, K., Terada, H., Kurauchi, T., Tadehara, Y., Yamasaki, A., Sugimura, T., Kurono, S., Tsujimoto, K. *et al.* (2007) Structures and physiological roles of 13 integral lipids of bovine heart cytochrome c oxidase. *The EMBO journal*, **26**, 1713-1725.

- 210 Claypool, S.M. (2009) Cardiolipin, a critical determinant of mitochondrial carrier protein assembly and function. *Biochimica et biophysica acta*, **1788**, 2059-2068.
- 211 Beyer, K. and Klingenberg, M. (1985) ADP/ATP carrier protein from beef heart mitochondria has high amounts of tightly bound cardiolipin, as revealed by ³¹P nuclear magnetic resonance. *Biochemistry*, **24**, 3821-3826.
- 212 Schwall, C.T., Greenwood, V.L. and Alder, N.N. (2012) The stability and activity of respiratory Complex II is cardiolipin-dependent. *Biochimica et biophysica acta*, **1817**, 1588-1596.
- 213 Acehan, D., Malhotra, A., Xu, Y., Ren, M., Stokes, D.L. and Schlame, M. (2011) Cardiolipin affects the supramolecular organization of ATP synthase in mitochondria. *Biophysical journal*, **100**, 2184-2192.
- 214 Strauss, M., Hofhaus, G., Schroder, R.R. and Kuhlbrandt, W. (2008) Dimer ribbons of ATP synthase shape the inner mitochondrial membrane. *The EMBO journal*, **27**, 1154-1160.
- 215 Zhang, M., Mileykovskaya, E. and Dowhan, W. (2002) Gluing the respiratory chain together. Cardiolipin is required for supercomplex formation in the inner mitochondrial membrane. *The Journal of biological chemistry*, **277**, 43553-43556.
- 216 Althoff, T., Mills, D.J., Popot, J.L. and Kuhlbrandt, W. (2011) Arrangement of electron transport chain components in bovine mitochondrial supercomplex I1III2IV1. *The EMBO journal*, **30**, 4652-4664.
- 217 Pfeiffer, K., Gohil, V., Stuart, R.A., Hunte, C., Brandt, U., Greenberg, M.L. and Schagger, H. (2003) Cardiolipin stabilizes respiratory chain supercomplexes. *The Journal of biological chemistry*, **278**, 52873-52880.

- 218 Jiang, F., Ryan, M.T., Schlame, M., Zhao, M., Gu, Z., Klingenberg, M., Pfanner, N. and Greenberg, M.L. (2000) Absence of cardiolipin in the *crd1* null mutant results in decreased mitochondrial membrane potential and reduced mitochondrial function. *The Journal of biological chemistry*, **275**, 22387-22394.
- 219 van der Laan, M., Meinecke, M., Dudek, J., Hutu, D.P., Lind, M., Perschil, I., Guiard, B., Wagner, R., Pfanner, N. and Rehling, P. (2007) Motor-free mitochondrial presequence translocase drives membrane integration of preproteins. *Nature cell biology*, **9**, 1152-1159.
- 220 Schagger, H. and Pfeiffer, K. (2000) Supercomplexes in the respiratory chains of yeast and mammalian mitochondria. *The EMBO journal*, **19**, 1777-1783.
- 221 Lapuente-Brun, E., Moreno-Loshuertos, R., Acin-Perez, R., Latorre-Pellicer, A., Colas, C., Balsa, E., Perales-Clemente, E., Quiros, P.M., Calvo, E., Rodriguez-Hernandez, M.A. *et al.* (2013) Supercomplex assembly determines electron flux in the mitochondrial electron transport chain. *Science*, **340**, 1567-1570.
- 222 Acin-Perez, R., Fernandez-Silva, P., Peleato, M.L., Perez-Martos, A. and Enriquez, J.A. (2008) Respiratory active mitochondrial supercomplexes. *Molecular cell*, **32**, 529-539.
- 223 Ban, T., Heymann, J.A., Song, Z., Hinshaw, J.E. and Chan, D.C. (2010) OPA1 disease alleles causing dominant optic atrophy have defects in cardiolipin-stimulated GTP hydrolysis and membrane tubulation. *Human molecular genetics*, **19**, 2113-2122.
- 224 Bustillo-Zabalbeitia, I., Montessuit, S., Raemy, E., Basanez, G., Terrones, O. and Martinou, J.C. (2014) Specific interaction with cardiolipin triggers functional activation of Dynamin-Related Protein 1. *PloS one*, **9**, e102738.

- 225 Montessuit, S., Somasekharan, S.P., Terrones, O., Lucken-Ardjomande, S., Herzig, S., Schwarzenbacher, R., Manstein, D.J., Bossy-Wetzel, E., Basanez, G., Meda, P. *et al.* (2010) Membrane remodeling induced by the dynamin-related protein Drp1 stimulates Bax oligomerization. *Cell*, **142**, 889-901.
- 226 Osman, C., Voelker, D.R. and Langer, T. (2011) Making heads or tails of phospholipids in mitochondria. *The Journal of cell biology*, **192**, 7-16.
- 227 Joshi, A.S., Zhou, J., Gohil, V.M., Chen, S. and Greenberg, M.L. (2009) Cellular functions of cardiolipin in yeast. *Biochimica et biophysica acta*, **1793**, 212-218.
- 228 Chicco, A.J. and Sparagna, G.C. (2007) Role of cardiolipin alterations in mitochondrial dysfunction and disease. *American journal of physiology. Cell physiology*, **292**, C33-44.
- 229 Houtkooper, R.H. and Vaz, F.M. (2008) Cardiolipin, the heart of mitochondrial metabolism. *Cellular and molecular life sciences : CMLS*, **65**, 2493-2506.
- 230 Lewis, R.N. and McElhaney, R.N. (2009) The physicochemical properties of cardiolipin bilayers and cardiolipin-containing lipid membranes. *Biochimica et biophysica acta*, **1788**, 2069-2079.
- 231 Sparagna, G.C. and Lesnefsky, E.J. (2009) Cardiolipin remodeling in the heart. *Journal of cardiovascular pharmacology*, **53**, 290-301.
- 232 Kuwana, T., Mackey, M.R., Perkins, G., Ellisman, M.H., Latterich, M., Schneider, R., Green, D.R. and Newmeyer, D.D. (2002) Bid, Bax, and lipids cooperate to form supramolecular openings in the outer mitochondrial membrane. *Cell*, **111**, 331-342.

- 233 Lucken-Ardjomande, S., Montessuit, S. and Martinou, J.C. (2008) Contributions to Bax insertion and oligomerization of lipids of the mitochondrial outer membrane. *Cell death and differentiation*, **15**, 929-937.
- 234 Jalmar, O., Francois-Moutal, L., Garcia-Saez, A.J., Perry, M., Granjon, T., Gonzalez, F., Gottlieb, E., Ayala-Sanmartin, J., Klosgen, B., Schwille, P. *et al.* (2013) Caspase-8 binding to cardiolipin in giant unilamellar vesicles provides a functional docking platform for bid. *PloS one*, **8**, e55250.
- 235 Jalmar, O., Garcia-Saez, A.J., Berland, L., Gonzalez, F. and Petit, P.X. (2010) Giant unilamellar vesicles (GUVs) as a new tool for analysis of caspase-8/Bid-FL complex binding to cardiolipin and its functional activity. *Cell death & disease*, **1**, e103.
- 236 Gonzalez, F., Pariselli, F., Dupaigne, P., Budihardjo, I., Lutter, M., Antonsson, B., Diolez, P., Manon, S., Martinou, J.C., Gubern, M. *et al.* (2005) tBid interaction with cardiolipin primarily orchestrates mitochondrial dysfunctions and subsequently activates Bax and Bak. *Cell death and differentiation*, **12**, 614-626.
- 237 Kagan, V.E., Tyurin, V.A., Jiang, J., Tyurina, Y.Y., Ritov, V.B., Amoscato, A.A., Osipov, A.N., Belikova, N.A., Kapralov, A.A., Kini, V. *et al.* (2005) Cytochrome c acts as a cardiolipin oxygenase required for release of proapoptotic factors. *Nature chemical biology*, **1**, 223-232.
- 238 Ye, C., Lou, W., Li, Y., Chatzisprou, I.A., Huttemann, M., Lee, I., Houtkooper, R.H., Vaz, F.M., Chen, S. and Greenberg, M.L. (2014) Deletion of the cardiolipin-specific phospholipase Cld1 rescues growth and life span defects in the tafazzin mutant: implications for Barth syndrome. *The Journal of biological chemistry*, **289**, 3114-3125.

- 239 Paradies, G., Petrosillo, G., Paradies, V. and Ruggiero, F.M. (2009) Role of cardiolipin peroxidation and Ca²⁺ in mitochondrial dysfunction and disease. *Cell calcium*, **45**, 643-650.
- 240 Watkins, S.M., Carter, L.C. and German, J.B. (1998) Docosahexaenoic acid accumulates in cardiolipin and enhances HT-29 cell oxidant production. *Journal of lipid research*, **39**, 1583-1588.
- 241 Liu, X., Ye, B., Miller, S., Yuan, H., Zhang, H., Tian, L., Nie, J., Imae, R., Arai, H., Li, Y. *et al.* (2012) Ablation of ALCAT1 mitigates hypertrophic cardiomyopathy through effects on oxidative stress and mitophagy. *Molecular and cellular biology*, **32**, 4493-4504.
- 242 Wang, L., Liu, X., Nie, J., Zhang, J., Kimball, S.R., Zhang, H., Zhang, W.J., Jefferson, L.S., Cheng, Z., Ji, Q. *et al.* (2014) ALCAT1 controls mitochondrial etiology of fatty liver diseases, linking defective mitophagy to hepatosteatosis. *Hepatology*, in press.
- 243 Li, J., Liu, X., Wang, H., Zhang, W., Chan, D.C. and Shi, Y. (2012) Lysocardiolipin acyltransferase 1 (ALCAT1) controls mitochondrial DNA fidelity and biogenesis through modulation of MFN2 expression. *Proceedings of the National Academy of Sciences of the United States of America*, **109**, 6975-6980.
- 244 Barth, P.G., Scholte, H.R., Berden, J.A., Van der Klei-Van Moorsel, J.M., Luyt-Houwen, I.E., Van 't Veer-Korthof, E.T., Van der Harten, J.J. and Sobotka-Plojhar, M.A. (1983) An X-linked mitochondrial disease affecting cardiac muscle, skeletal muscle and neutrophil leucocytes. *Journal of the neurological sciences*, **62**, 327-355.

- 245 Barth, P.G., Valianpour, F., Bowen, V.M., Lam, J., Duran, M., Vaz, F.M. and Wanders, R.J. (2004) X-linked cardioskeletal myopathy and neutropenia (Barth syndrome): an update. *American journal of medical genetics. Part A*, **126A**, 349-354.
- 246 Bione, S., D'Adamo, P., Maestrini, E., Gedeon, A.K., Bolhuis, P.A. and Toniolo, D. (1996) A novel X-linked gene, G4.5. is responsible for Barth syndrome. *Nature genetics*, **12**, 385-389.
- 247 Johnston, J., Kelley, R.I., Feigenbaum, A., Cox, G.F., Iyer, G.S., Funanage, V.L. and Proujansky, R. (1997) Mutation characterization and genotype-phenotype correlation in Barth syndrome. *American journal of human genetics*, **61**, 1053-1058.
- 248 Kelley, R.I., Cheatham, J.P., Clark, B.J., Nigro, M.A., Powell, B.R., Sherwood, G.W., Sladky, J.T. and Swisher, W.P. (1991) X-linked dilated cardiomyopathy with neutropenia, growth retardation, and 3-methylglutaconic aciduria. *The Journal of pediatrics*, **119**, 738-747.
- 249 Cosson, L., Toutain, A., Simard, G., Kulik, W., Matyas, G., Guichet, A., Blasco, H., Maakaroun-Vermesse, Z., Vaillant, M.C., Le Caignec, C. *et al.* (2012) Barth syndrome in a female patient. *Molecular genetics and metabolism*, **106**, 115-120.
- 250 Wysocki, S.J., Wilkinson, S.P., Hahnel, R., Wong, C.Y. and Panegyres, P.K. (1976) 3-Hydroxy-3-methylglutaric aciduria, combined with 3-methylglutaconic aciduria. *Clinica chimica acta; international journal of clinical chemistry*, **70**, 399-406.
- 251 Steward, C.G., Newbury-Ecob, R.A., Hastings, R., Smithson, S.F., Tsai-Goodman, B., Quarrell, O.W., Kulik, W., Wanders, R., Pennock, M., Williams, M. *et al.* (2010) Barth syndrome: an X-linked cause of fetal cardiomyopathy and stillbirth. *Prenatal diagnosis*, **30**, 970-976.

- 252 Ichida, F., Tsubata, S., Bowles, K.R., Haneda, N., Uese, K., Miyawaki, T., Dreyer, W.J., Messina, J., Li, H., Bowles, N.E. *et al.* (2001) Novel gene mutations in patients with left ventricular noncompaction or Barth syndrome. *Circulation*, **103**, 1256-1263.
- 253 Orstavik, K.H., Orstavik, R.E., Naumova, A.K., D'Adamo, P., Gedeon, A., Bolhuis, P.A., Barth, P.G. and Toniolo, D. (1998) X chromosome inactivation in carriers of Barth syndrome. *American journal of human genetics*, **63**, 1457-1463.
- 254 Hodgson, S., Child, A. and Dyson, M. (1987) Endocardial fibroelastosis: possible X linked inheritance. *Journal of medical genetics*, **24**, 210-214.
- 255 Acehan, D., Xu, Y., Stokes, D.L. and Schlame, M. (2007) Comparison of lymphoblast mitochondria from normal subjects and patients with Barth syndrome using electron microscopic tomography. *Laboratory investigation; a journal of technical methods and pathology*, **87**, 40-48.
- 256 Ronvelia, D., Greenwood, J., Platt, J., Hakim, S. and Zaragoza, M.V. (2012) Intrafamilial variability for novel TAZ gene mutation: Barth syndrome with dilated cardiomyopathy and heart failure in an infant and left ventricular noncompaction in his great-uncle. *Molecular genetics and metabolism*, **107**, 428-432.
- 257 Whited, K., Baile, M.G., Currier, P. and Claypool, S.M. (2013) Seven functional classes of Barth syndrome mutation. *Human molecular genetics*, **22**, 483-492.
- 258 Barth, P.G., Van den Bogert, C., Bolhuis, P.A., Scholte, H.R., van Gennip, A.H., Schutgens, R.B. and Ketel, A.G. (1996) X-linked cardioskeletal myopathy and neutropenia (Barth syndrome): respiratory-chain abnormalities in cultured fibroblasts. *Journal of inherited metabolic disease*, **19**, 157-160.

- 259 He, Q. (2010) Tafazzin knockdown causes hypertrophy of neonatal ventricular myocytes. *American journal of physiology. Heart and circulatory physiology*, **299**, H210-216.
- 260 He, Q., Harris, N., Ren, J. and Han, X. (2014) Mitochondria-targeted antioxidant prevents cardiac dysfunction induced by tafazzin gene knockdown in cardiac myocytes. *Oxidative medicine and cellular longevity*, **2014**, 654198.
- 261 Khuchua, Z., Yue, Z., Batts, L. and Strauss, A.W. (2006) A zebrafish model of human Barth syndrome reveals the essential role of tafazzin in cardiac development and function. *Circulation research*, **99**, 201-208.
- 262 Soustek, M.S., Falk, D.J., Mah, C.S., Toth, M.J., Schlame, M., Lewin, A.S. and Byrne, B.J. (2011) Characterization of a transgenic short hairpin RNA-induced murine model of Tafazzin deficiency. *Human gene therapy*, **22**, 865-871.
- 263 Phoon, C.K., Acehan, D., Schlame, M., Stokes, D.L., Edelman-Novemsky, I., Yu, D., Xu, Y., Viswanathan, N. and Ren, M. (2012) Tafazzin knockdown in mice leads to a developmental cardiomyopathy with early diastolic dysfunction preceding myocardial noncompaction. *Journal of the American Heart Association*, **1**.
- 264 McKenzie, M., Lazarou, M., Thorburn, D.R. and Ryan, M.T. (2006) Mitochondrial respiratory chain supercomplexes are destabilized in Barth Syndrome patients. *Journal of molecular biology*, **361**, 462-469.
- 265 Powers, C., Huang, Y., Strauss, A. and Khuchua, Z. (2013) Diminished Exercise Capacity and Mitochondrial bc1 Complex Deficiency in Tafazzin-Knockdown Mice. *Frontiers in physiology*, **4**, 74.

- 266 Varfolomeev, E.E., Schuchmann, M., Luria, V., Chiannikulchai, N., Beckmann, J.S., Mett, I.L., Rebrikov, D., Brodianski, V.M., Kemper, O.C., Kollet, O. *et al.* (1998) Targeted disruption of the mouse Caspase 8 gene ablates cell death induction by the TNF receptors, Fas/Apo1, and DR3 and is lethal prenatally. *Immunity*, **9**, 267-276.
- 267 Davey, K.M., Parboosingh, J.S., McLeod, D.R., Chan, A., Casey, R., Ferreira, P., Snyder, F.F., Bridge, P.J. and Bernier, F.P. (2006) Mutation of DNAJC19, a human homologue of yeast inner mitochondrial membrane co-chaperones, causes DCMA syndrome, a novel autosomal recessive Barth syndrome-like condition. *Journal of medical genetics*, **43**, 385-393.
- 268 Ojala, T., Polinati, P., Manninen, T., Hiippala, A., Rajantie, J., Karikoski, R., Suomalainen, A. and Tyni, T. (2012) New mutation of mitochondrial DNAJC19 causing dilated and noncompaction cardiomyopathy, anemia, ataxia, and male genital anomalies. *Pediatric research*, **72**, 432-437.
- 269 Sparkes, R., Patton, D. and Bernier, F. (2007) Cardiac features of a novel autosomal recessive dilated cardiomyopathic syndrome due to defective importation of mitochondrial protein. *Cardiology in the young*, **17**, 215-217.
- 270 Ohtsuka, K. and Hata, M. (2000) Mammalian HSP40/DNAJ homologs: cloning of novel cDNAs and a proposal for their classification and nomenclature. *Cell stress & chaperones*, **5**, 98-112.
- 271 Mayer, M.P. and Bukau, B. (2005) Hsp70 chaperones: cellular functions and molecular mechanism. *Cellular and molecular life sciences : CMLS*, **62**, 670-684.

- 272 Mokranjac, D., Sichting, M., Neupert, W. and Hell, K. (2003) Tim14, a novel key component of the import motor of the TIM23 protein translocase of mitochondria. *The EMBO journal*, **22**, 4945-4956.
- 273 Mokranjac, D., Sichting, M., Popov-Celeketic, D., Berg, A., Hell, K. and Neupert, W. (2005) The import motor of the yeast mitochondrial TIM23 preprotein translocase contains two different J proteins, Tim14 and Mdj2. *The Journal of biological chemistry*, **280**, 31608-31614.
- 274 Kozany, C., Mokranjac, D., Sichting, M., Neupert, W. and Hell, K. (2004) The J domain-related cochaperone Tim16 is a constituent of the mitochondrial TIM23 preprotein translocase. *Nature structural & molecular biology*, **11**, 234-241.
- 275 Frazier, A.E., Dudek, J., Guiard, B., Voos, W., Li, Y., Lind, M., Meisinger, C., Geissler, A., Sickmann, A., Meyer, H.E. *et al.* (2004) Pam16 has an essential role in the mitochondrial protein import motor. *Nature structural & molecular biology*, **11**, 226-233.
- 276 D'Silva, P.R., Schilke, B., Hayashi, M. and Craig, E.A. (2008) Interaction of the J-protein heterodimer Pam18/Pam16 of the mitochondrial import motor with the translocon of the inner membrane. *Molecular biology of the cell*, **19**, 424-432.
- 277 Moro, F., Okamoto, K., Donzeau, M., Neupert, W. and Brunner, M. (2002) Mitochondrial protein import: molecular basis of the ATP-dependent interaction of MtHsp70 with Tim44. *The Journal of biological chemistry*, **277**, 6874-6880.
- 278 Truscott, K.N., Voos, W., Frazier, A.E., Lind, M., Li, Y., Geissler, A., Dudek, J., Muller, H., Sickmann, A., Meyer, H.E. *et al.* (2003) A J-protein is an essential subunit of the presequence translocase-associated protein import motor of mitochondria. *The Journal of cell biology*, **163**, 707-713.

- 279 Schneider, H.C., Berthold, J., Bauer, M.F., Dietmeier, K., Guiard, B., Brunner, M. and Neupert, W. (1994) Mitochondrial Hsp70/MIM44 complex facilitates protein import. *Nature*, **371**, 768-774.
- 280 Bomer, U., Meijer, M., Maarse, A.C., Honlinger, A., Dekker, P.J., Pfanner, N. and Rassow, J. (1997) Multiple interactions of components mediating preprotein translocation across the inner mitochondrial membrane. *The EMBO journal*, **16**, 2205-2216.
- 281 Moro, F., Sirrenberg, C., Schneider, H.C., Neupert, W. and Brunner, M. (1999) The TIM17.23 preprotein translocase of mitochondria: composition and function in protein transport into the matrix. *The EMBO journal*, **18**, 3667-3675.
- 282 Geissler, A., Chacinska, A., Truscott, K.N., Wiedemann, N., Brandner, K., Sickmann, A., Meyer, H.E., Meisinger, C., Pfanner, N. and Rehling, P. (2002) The mitochondrial presequence translocase: an essential role of Tim50 in directing preproteins to the import channel. *Cell*, **111**, 507-518.
- 283 Chacinska, A., Lind, M., Frazier, A.E., Dudek, J., Meisinger, C., Geissler, A., Sickmann, A., Meyer, H.E., Truscott, K.N., Guiard, B. *et al.* (2005) Mitochondrial presequence translocase: switching between TOM tethering and motor recruitment involves Tim21 and Tim17. *Cell*, **120**, 817-829.
- 284 Yamamoto, H., Esaki, M., Kanamori, T., Tamura, Y., Nishikawa, S. and Endo, T. (2002) Tim50 is a subunit of the TIM23 complex that links protein translocation across the outer and inner mitochondrial membranes. *Cell*, **111**, 519-528.
- 285 Gonczy, P., Echeverri, C., Oegema, K., Coulson, A., Jones, S.J., Copley, R.R., Duperon, J., Oegema, J., Brehm, M., Cassin, E. *et al.* (2000) Functional genomic analysis

of cell division in *C. elegans* using RNAi of genes on chromosome III. *Nature*, **408**, 331-336.

286 Jubinsky, P.T., Short, M.K., Mutema, G. and Witte, D.P. (2003) Developmental expression of Magmas in murine tissues and its co-expression with the GM-CSF receptor. *The journal of histochemistry and cytochemistry : official journal of the Histochemistry Society*, **51**, 585-596.

287 Jubinsky, P.T., Messer, A., Bender, J., Morris, R.E., Ciruolo, G.M., Witte, D.P., Hawley, R.G. and Short, M.K. (2001) Identification and characterization of Magmas, a novel mitochondria-associated protein involved in granulocyte-macrophage colony-stimulating factor signal transduction. *Experimental hematology*, **29**, 1392-1402.

288 D'Silva, P.R., Schilke, B., Walter, W. and Craig, E.A. (2005) Role of Pam16's degenerate J domain in protein import across the mitochondrial inner membrane. *Proceedings of the National Academy of Sciences of the United States of America*, **102**, 12419-12424.

289 Sinha, D., Joshi, N., Chittoor, B., Samji, P. and D'Silva, P. (2010) Role of Magmas in protein transport and human mitochondria biogenesis. *Human molecular genetics*, **19**, 1248-1262.

290 Mehawej, C., Delahodde, A., Legeai-Mallet, L., Delague, V., Kaci, N., Desvignes, J.P., Kibar, Z., Capo-Chichi, J.M., Chouery, E., Munnich, A. *et al.* (2014) The impairment of MAGMAS function in human is responsible for a severe skeletal dysplasia. *PLoS genetics*, **10**, e1004311.

291 Sinha, D., Srivastava, S., Krishna, L. and D'Silva, P. (2014) Unraveling the intricate organization of mammalian mitochondrial presequence translocases: existence

of multiple translocases for maintenance of mitochondrial function. *Molecular and cellular biology*, **34**, 1757-1775.

292 Hatle, K.M., Gummadidala, P., Navasa, N., Bernardo, E., Dodge, J., Silverstrim, B., Fortner, K., Burg, E., Suratt, B.T., Hammer, J. *et al.* (2013) MCJ/DnaJC15, an endogenous mitochondrial repressor of the respiratory chain that controls metabolic alterations. *Molecular and cellular biology*, **33**, 2302-2314.

293 Schusdziarra, C., Blamowska, M., Azem, A. and Hell, K. (2013) Methylation-controlled J-protein MCJ acts in the import of proteins into human mitochondria. *Human molecular genetics*, **22**, 1348-1357.

294 Tatsuta, T., Model, K. and Langer, T. (2005) Formation of membrane-bound ring complexes by prohibitins in mitochondria. *Molecular biology of the cell*, **16**, 248-259.

295 Merkwirth, C., Dargazanli, S., Tatsuta, T., Geimer, S., Lower, B., Wunderlich, F.T., von Kleist-Retzow, J.C., Waisman, A., Westermann, B. and Langer, T. (2008) Prohibitins control cell proliferation and apoptosis by regulating OPA1-dependent cristae morphogenesis in mitochondria. *Genes & development*, **22**, 476-488.

296 Christie, D.A., Lemke, C.D., Elias, I.M., Chau, L.A., Kirchhof, M.G., Li, B., Ball, E.H., Dunn, S.D., Hatch, G.M. and Madrenas, J. (2011) Stomatin-like protein 2 binds cardiolipin and regulates mitochondrial biogenesis and function. *Molecular and cellular biology*, **31**, 3845-3856.

297 Osman, C., Merkwirth, C. and Langer, T. (2009) Prohibitins and the functional compartmentalization of mitochondrial membranes. *Journal of cell science*, **122**, 3823-3830.

- 298 Osman, C., Haag, M., Potting, C., Rodenfels, J., Dip, P.V., Wieland, F.T., Brugger, B., Westermann, B. and Langer, T. (2009) The genetic interactome of prohibitins: coordinated control of cardiolipin and phosphatidylethanolamine by conserved regulators in mitochondria. *The Journal of cell biology*, **184**, 583-596.
- 299 Wortmann, S.B., Vaz, F.M., Gardeitchik, T., Vissers, L.E., Renkema, G.H., Schuurs-Hoeijmakers, J.H., Kulik, W., Lammens, M., Christin, C., Kluijtmans, L.A. *et al.* (2012) Mutations in the phospholipid remodeling gene SERAC1 impair mitochondrial function and intracellular cholesterol trafficking and cause dystonia and deafness. *Nature genetics*, **44**, 797-802.
- 300 Wortmann, S., Rodenburg, R.J., Huizing, M., Loupatty, F.J., de Koning, T., Kluijtmans, L.A., Engelke, U., Wevers, R., Smeitink, J.A. and Morava, E. (2006) Association of 3-methylglutaconic aciduria with sensori-neural deafness, encephalopathy, and Leigh-like syndrome (MEGDEL association) in four patients with a disorder of the oxidative phosphorylation. *Molecular genetics and metabolism*, **88**, 47-52.
- 301 Lumish, H.S., Yang, Y., Xia, F., Wilson, A. and Chung, W.K. (2014) The Expanding MEGDEL Phenotype: Optic Nerve Atrophy, Microcephaly, and Myoclonic Epilepsy in a Child with SERAC1 Mutations. *JIMD reports*, in press.
- 302 Wedatilake, Y., Plagnol, V., Anderson, G., Paine, S., Clayton, P., Jacques, T. and Rahman, S. (2014) Tubular aggregates caused by serine active site containing 1 (SERAC1) mutations in a patient with a mitochondrial encephalopathy. *Neuropathology and applied neurobiology*, in press.
- 303 Sarig, O., Goldsher, D., Nousbeck, J., Fuchs-Telem, D., Cohen-Katsenelson, K., Iancu, T.C., Manov, I., Saada, A., Sprecher, E. and Mandel, H. (2013) Infantile

mitochondrial hepatopathy is a cardinal feature of MEGDEL syndrome (3-methylglutaconic aciduria type IV with sensorineural deafness, encephalopathy and Leigh-like syndrome) caused by novel mutations in SERAC1. *American journal of medical genetics. Part A*, **161**, 2204-2215.

304 Vilarinho, S., Choi, M., Jain, D., Malhotra, A., Kulkarni, S., Pashankar, D., Phatak, U., Patel, M., Bale, A., Mane, S. *et al.* (2014) Individual exome analysis in diagnosis and management of paediatric liver failure of indeterminate aetiology. *Journal of hepatology*, **61**, 1056-1063.

305 Tort, F., Garcia-Silva, M.T., Ferrer-Cortes, X., Navarro-Sastre, A., Garcia-Villoria, J., Coll, M.J., Vidal, E., Jimenez-Almazan, J., Dopazo, J., Briones, P. *et al.* (2013) Exome sequencing identifies a new mutation in SERAC1 in a patient with 3-methylglutaconic aciduria. *Molecular genetics and metabolism*, **110**, 73-77.

306 Dweikat, I.M., Abdelrazeq, S., Ayeshe, S. and Jundi, T. (2014) MEGDEL Syndrome in a Child From Palestine: Report of a Novel Mutation in SERAC1 Gene. *Journal of child neurology*, in press.

307 Karkucinska-Wieckowska, A., Lebedzinska, M., Jurkiewicz, E., Pajdowska, M., Trubicka, J., Szymanska-Debinska, T., Suski, J., Pinton, P., Duszynski, J., Pronicki, M. *et al.* (2011) Increased reactive oxygen species (ROS) production and low catalase level in fibroblasts of a girl with MEGDEL association (Leigh syndrome, deafness, 3-methylglutaconic aciduria). *Folia neuropathologica / Association of Polish Neuropathologists and Medical Research Centre, Polish Academy of Sciences*, **49**, 56-63.

308 Haghghi, A., Haack, T.B., Atiq, M., Mottaghi, H., Haghghi-Kakhki, H., Bashir, R.A., Ahting, U., Feichtinger, R.G., Mayr, J.A., Rotig, A. *et al.* (2014) Sengers

- syndrome: six novel AGK mutations in seven new families and review of the phenotypic and mutational spectrum of 29 patients. *Orphanet journal of rare diseases*, **9**, 119.
- 309 Mayr, J.A., Haack, T.B., Graf, E., Zimmermann, F.A., Wieland, T., Haberberger, B., Superti-Furga, A., Kirschner, J., Steinmann, B., Baumgartner, M.R. *et al.* (2012) Lack of the mitochondrial protein acylglycerol kinase causes Sengers syndrome. *American journal of human genetics*, **90**, 314-320.
- 310 van Ekeren, G.J., Stadhouders, A.M., Smeitink, J.A. and Sengers, R.C. (1993) A retrospective study of patients with the hereditary syndrome of congenital cataract, mitochondrial myopathy of heart and skeletal muscle and lactic acidosis. *European journal of pediatrics*, **152**, 255-259.
- 311 Sengers, R.C., Trijbels, J.M., Willems, J.L., Daniels, O. and Stadhouders, A.M. (1975) Congenital cataract and mitochondrial myopathy of skeletal and heart muscle associated with lactic acidosis after exercise. *The Journal of pediatrics*, **86**, 873-880.
- 312 Jordens, E.Z., Palmieri, L., Huizing, M., van den Heuvel, L.P., Sengers, R.C., Dorner, A., Ruitenbeek, W., Trijbels, F.J., Valsson, J., Sigfusson, G. *et al.* (2002) Adenine nucleotide translocator 1 deficiency associated with Sengers syndrome. *Annals of neurology*, **52**, 95-99.
- 313 Li, K., Warner, C.K., Hodge, J.A., Minoshima, S., Kudoh, J., Fukuyama, R., Maekawa, M., Shimizu, Y., Shimizu, N. and Wallace, D.C. (1989) A human muscle adenine nucleotide translocator gene has four exons, is located on chromosome 4, and is differentially expressed. *The Journal of biological chemistry*, **264**, 13998-14004.

- 314 Topham, M.K. and Prescott, S.M. (1999) Mammalian diacylglycerol kinases, a family of lipid kinases with signaling functions. *The Journal of biological chemistry*, **274**, 11447-11450.
- 315 Aldahmesh, M.A., Khan, A.O., Mohamed, J.Y., Alghamdi, M.H. and Alkuraya, F.S. (2012) Identification of a truncation mutation of acylglycerol kinase (AGK) gene in a novel autosomal recessive cataract locus. *Human mutation*, **33**, 960-962.
- 316 Siriwardena, K., Mackay, N., Levandovskiy, V., Blaser, S., Raiman, J., Kantor, P.F., Ackerley, C., Robinson, B.H., Schulze, A. and Cameron, J.M. (2013) Mitochondrial citrate synthase crystals: novel finding in Sengers syndrome caused by acylglycerol kinase (AGK) mutations. *Molecular genetics and metabolism*, **108**, 40-50.
- 317 Smeitink, J.A., Sengers, R.C., Trijbels, J.M., Ruitenbeek, W., Daniels, O., Stadhouders, A.M. and Kock-Jansen, M.J. (1989) Fatal neonatal cardiomyopathy associated with cataract and mitochondrial myopathy. *European journal of pediatrics*, **148**, 656-659.
- 318 Starck, S.R., Jiang, V., Pavon-Eternod, M., Prasad, S., McCarthy, B., Pan, T. and Shastri, N. (2012) Leucine-tRNA initiates at CUG start codons for protein synthesis and presentation by MHC class I. *Science*, **336**, 1719-1723.
- 319 Lalive d'Epina, S., Rampini, S., Arbenz, U., Steinmann, B. and Gitzelmann, R. (1986) [Infantile cataract, hypertrophic cardiomyopathy and lactic acidosis following minor muscular exertion--a little known metabolic disease]. *Klinische Monatsblätter für Augenheilkunde*, **189**, 482-485.
- 320 Pitkanen, S., Merante, F., McLeod, D.R., Applegarth, D., Tong, T. and Robinson, B.H. (1996) Familial cardiomyopathy with cataracts and lactic acidosis: a defect in

complex I (NADH-dehydrogenase) of the mitochondria respiratory chain. *Pediatric research*, **39**, 513-521.

321 Morava, E., Sengers, R., Ter Laak, H., Van Den Heuvel, L., Janssen, A., Trijbels, F., Cruysberg, H., Boelen, C. and Smeitink, J. (2004) Congenital hypertrophic cardiomyopathy, cataract, mitochondrial myopathy and defective oxidative phosphorylation in two siblings with Sengers-like syndrome. *European journal of pediatrics*, **163**, 467-471.

322 Tesson, C., Nawara, M., Salih, M.A., Rossignol, R., Zaki, M.S., Al Balwi, M., Schule, R., Mignot, C., Obre, E., Bouhouche, A. *et al.* (2012) Alteration of fatty-acid-metabolizing enzymes affects mitochondrial form and function in hereditary spastic paraplegia. *American journal of human genetics*, **91**, 1051-1064.

323 Liguori, R., Giannoccaro, M.P., Arnoldi, A., Citterio, A., Tonon, C., Lodi, R., Bresolin, N. and Bassi, M.T. (2014) Impairment of brain and muscle energy metabolism detected by magnetic resonance spectroscopy in hereditary spastic paraparesis type 28 patients with DDHD1 mutations. *Journal of neurology*, **261**, 1789-1793.

324 Bouslam, N., Benomar, A., Azzedine, H., Bouhouche, A., Namekawa, M., Klebe, S., Charon, C., Durr, A., Ruberg, M., Brice, A. *et al.* (2005) Mapping of a new form of pure autosomal recessive spastic paraplegia (SPG28). *Annals of neurology*, **57**, 567-571.

325 Citterio, A., Arnoldi, A., Panzeri, E., D'Angelo, M.G., Filosto, M., Dilena, R., Arrigoni, F., Castelli, M., Maghini, C., Germiniasi, C. *et al.* (2014) Mutations in CYP2U1, DDHD2 and GBA2 genes are rare causes of complicated forms of hereditary spastic paraparesis. *Journal of neurology*, **261**, 373-381.

- 326 Schuurs-Hoeijmakers, J.H., Geraghty, M.T., Kamsteeg, E.J., Ben-Salem, S., de Bot, S.T., Nijhof, B., van de, V., II, van der Graaf, M., Nobau, A.C., Otte-Holler, I. *et al.* (2012) Mutations in DDHD2, encoding an intracellular phospholipase A(1), cause a recessive form of complex hereditary spastic paraplegia. *American journal of human genetics*, **91**, 1073-1081.
- 327 Gonzalez, M., Nampoothiri, S., Kornblum, C., Oteyza, A.C., Walter, J., Konidari, I., Hulme, W., Speziani, F., Schols, L., Zuchner, S. *et al.* (2013) Mutations in phospholipase DDHD2 cause autosomal recessive hereditary spastic paraplegia (SPG54). *European journal of human genetics : EJHG*, **21**, 1214-1218.
- 328 Magariello, A., Citrigno, L., Zuchner, S., Gonzalez, M., Patitucci, A., Sofia, V., Conforti, F.L., Pappalardo, I., Mazzei, R., Ungaro, C. *et al.* (2014) Further evidence that DDHD2 gene mutations cause autosomal recessive hereditary spastic paraplegia with thin corpus callosum. *European journal of neurology : the official journal of the European Federation of Neurological Societies*, **21**, e25-26.
- 329 Doi, H., Ushiyama, M., Baba, T., Tani, K., Shiina, M., Ogata, K., Miyatake, S., Fukuda-Yuzawa, Y., Tsuji, S., Nakashima, M. *et al.* (2014) Late-onset spastic ataxia phenotype in a patient with a homozygous DDHD2 mutation. *Scientific reports*, **4**, 7132.
- 330 Fink, J.K. (2013) Hereditary spastic paraplegia: clinico-pathologic features and emerging molecular mechanisms. *Acta neuropathologica*, **126**, 307-328.
- 331 Finsterer, J., Loscher, W., Quasthoff, S., Wanschitz, J., Auer-Grumbach, M. and Stevanin, G. (2012) Hereditary spastic paraplegias with autosomal dominant, recessive, X-linked, or maternal trait of inheritance. *Journal of the neurological sciences*, **318**, 1-18.

- 332 Higgs, H.N. and Glomset, J.A. (1994) Identification of a phosphatidic acid-preferring phospholipase A1 from bovine brain and testis. *Proc Natl Acad Sci U S A*, **91**, 9574-9578.
- 333 Higgs, H.N., Han, M.H., Johnson, G.E. and Glomset, J.A. (1998) Cloning of a phosphatidic acid-preferring phospholipase A1 from bovine testis. *The Journal of biological chemistry*, **273**, 5468-5477.
- 334 Sato, S., Inoue, H., Kogure, T., Tagaya, M. and Tani, K. (2010) Golgi-localized KIAA0725p regulates membrane trafficking from the Golgi apparatus to the plasma membrane in mammalian cells. *FEBS letters*, **584**, 4389-4395.
- 335 Nakajima, K., Sonoda, H., Mizoguchi, T., Aoki, J., Arai, H., Nagahama, M., Tagaya, M. and Tani, K. (2002) A novel phospholipase A1 with sequence homology to a mammalian Sec23p-interacting protein, p125. *The Journal of biological chemistry*, **277**, 11329-11335.
- 336 Morikawa, R.K., Aoki, J., Kano, F., Murata, M., Yamamoto, A., Tsujimoto, M. and Arai, H. (2009) Intracellular phospholipase A1gamma (iPLA1gamma) is a novel factor involved in coat protein complex I- and Rab6-independent retrograde transport between the endoplasmic reticulum and the Golgi complex. *The Journal of biological chemistry*, **284**, 26620-26630.
- 337 Baba, T., Yamamoto, A., Tagaya, M. and Tani, K. (2013) A lysophospholipid acyltransferase antagonist, CI-976, creates novel membrane tubules marked by intracellular phospholipase A1 KIAA0725p. *Molecular and cellular biochemistry*, **376**, 151-161.

338 Twig, G., Elorza, A., Molina, A.J., Mohamed, H., Wikstrom, J.D., Walzer, G., Stiles, L., Haigh, S.E., Katz, S., Las, G. *et al.* (2008) Fission and selective fusion govern mitochondrial segregation and elimination by autophagy. *The EMBO journal*, **27**, 433-446.

339 Inloes, J.M., Hsu, K.L., Dix, M.M., Viader, A., Masuda, K., Takei, T., Wood, M.R. and Cravatt, B.F. (2014) The hereditary spastic paraplegia-related enzyme DDHD2 is a principal brain triglyceride lipase. *Proceedings of the National Academy of Sciences of the United States of America*, **111**, 14924-14929.

CHAPTER 3

Defining functional classes of Barth syndrome mutation in humans

This chapter is a version of a manuscript currently under revision at Human Molecular Genetics:

Lu YW[#], Galbraith L, Herndon JD, Lu YL, Pras-Raves M, Vervaart M, van Kampen A, Luyf A, Koehler CM, McCaffery JM, Gottlieb E, Vaz FM, Claypool SM. Defining functional classes of Barth syndrome mutation in humans. *In revision*.
[#] first author

ABSTRACT

The X-linked disease Barth syndrome (BTHS) is caused by mutations in *TAZ*; *TAZ* is the main determinant of the final acyl chain composition of the mitochondrial-specific phospholipid, cardiolipin. To date, a detailed characterization of endogenous *TAZ* has only been performed in yeast. Further, why a given BTHS-associated missense mutation impairs *TAZ* function has only been determined in a yeast model of this human disease. Presently, the detailed characterization of yeast tafazzin harboring individual BTHS mutations at evolutionarily conserved residues has identified seven distinct loss-of-function mechanisms caused by patient-associated missense alleles. However, whether the biochemical consequences associated with individual mutations also occur in the context of human *TAZ* in a validated mammalian model has not been demonstrated. Here, utilizing newly established monoclonal antibodies capable of detecting endogenous *TAZ*, we demonstrate that mammalian *TAZ*, like its yeast counterpart, is localized to the mitochondrion where it adopts an extremely protease-resistant fold, associates non-integrally with intermembrane space-facing membranes and assembles in a range of complexes. Even though multiple isoforms are expressed at the mRNA level, only a single polypeptide that co-migrates with the human isoform lacking exon 5 is expressed in human skin fibroblasts, HEK293 cells, and murine heart and liver mitochondria. Finally, using a new genome-edited mammalian BTHS cell culture model, we demonstrate that the loss-of-function mechanisms for two BTHS alleles that represent two of the seven functional classes of BTHS mutation as originally defined in yeast, are the same when modeled in human *TAZ*.

INTRODUCTION

The boundaries of cells and organelles are marked by membranes that differ in their phospholipid and protein compositions. The collection of phospholipids, including their associated fatty acyl chains, that establish a defined membrane-bound compartment confer unique membrane properties (curvature and rigidity) and contribute to numerous functions that occur at/across the membrane surface (transport and signaling) or within the space that it confines. As such, changes in membrane lipid composition can directly impact numerous fundamental cellular processes. A particularly salient example of the importance of proper lipid composition for organelle function is provided by the mitochondrion, the powerhouse of the cell, and its signature phospholipid, cardiolipin (CL).

CL is required for a diversity of basic processes that are central to mitochondrial biology (1). In fact, CL is of such fundamental importance that mammalian development fails *in utero* in its absence (2). CL is a dimer of two phosphatidic acids linked together by a glycerol bridge. CL associates with numerous mitochondrial proteins, including every oxidative phosphorylation (OXPHOS) complex/component, many solute carriers, and translocases in both the outer and inner mitochondrial membranes (3-5). Collectively, these interactions with CL stabilize individual proteins and multisubunit complexes, and can stimulate enzyme activity either directly (e.g. serve a catalytic function (6)) or secondarily (e.g. promote the assembly of individual respiratory complexes into more efficient supercomplexes (7-9)). Finally, CL serves as a signal that is detected by CL-binding proteins with downstream consequences that range from mitochondrial fission

and inner mitochondrial membrane (IMM) fusion (10, 11) to apoptosis and mitophagy (12, 13).

The biosynthesis of CL occurs through a reaction series that is highly conserved from yeast to humans (14). With respect to its acyl chain composition, the CL that is newly produced is not what accumulates at steady state, which is highly homogeneous and characterized by increased acyl chain unsaturation and molecular symmetry (15). The steady state form of CL is established by an acyl chain remodeling process that begins with the removal of a fatty acyl chain from CL by a deacylase(s), generating monolysocardiolipin (MLCL), which is then re-acylated by the evolutionarily conserved MLCL transacylase, tafazzin (TAZ) (16). Mutations in *TAZ* result in the X-linked cardio- and skeletal myopathy, Barth syndrome (BTHS) (17, 18). In the absence of TAZ, there is less CL, the remodeling precursor and product, and more MLCL, the remodeling intermediate (19). Further, the CL that remains has an abnormal acyl chain profile (15, 20). These BTHS-associated changes in mitochondrial phospholipid composition destabilize respiratory supercomplexes, reduce OXPHOS efficiency, increase reactive oxygen species production, and impair sarcomere organization (21-24).

BTHS is the founding member of a new class of mitochondrial disorder that results from nuclear defects that impact mitochondrial phospholipid metabolism (25). Notably, some of the disorders, including dilated cardiomyopathy with ataxia (DCMA), Sengers, and MEGDEL syndromes, in this new class of mitochondrial disease share some biochemical phenotypes with BTHS. In each case, changes in the acyl chain pattern, abundance, and or submitochondrial distribution of CL are postulated to contribute to disease pathogenesis (26-29). However, their exact pathogenic mechanisms have not

been established and thus the basis for the shared and unique phenotypes of this cohort of syndromes is presently unclear.

Currently, a detailed topological map of tafazzin-based CL remodeling has only been drawn in the yeast *Saccharomyces cerevisiae*. In yeast, all of the steps up to and including the initiation of the remodeling process occur on the matrix side of the IMM (14). In contrast, yeast Taz1 is anchored to both the IMM and outer mitochondrial membrane (OMM) facing the intermembrane space (IMS) by virtue of a membrane anchor that protrudes into but not completely through the lipid bilayer (30). Thus, in yeast, CL remodeling involves an obligate trafficking step of MLCL from one side of the IMM to the other. Further, a yeast BTHS model has been exploited to determine the disease pathogenicity of a multitude of patient-associated missense alleles. To date, seven distinct pathogenic loss-of-function (LOF) mechanisms have been identified (30-32). Thus at present, our understanding of the basic cell biology of this clinically important remodeling pathway and the biochemical abnormalities associated with any genetic lesion linked to BTHS is based solely on work in yeast.

Here, we show that mammalian TAZ is localized to the mitochondrion where it adopts an extremely protease-resistant fold, associates non-integrally with IMS-facing membranes, and assembles in a range of complexes. Even though multiple isoforms are expressed at the transcript level, only a single TAZ polypeptide that co-migrates with the human isoform lacking exon 5 is detected in mitochondria isolated from human skin fibroblasts, HEK293 cells, and murine heart and liver. Utilizing a newly established mammalian BTHS cell model, we determined that the two pathogenic mutations tested result in the same biochemical consequences when modeled in human TAZ as originally

defined in yeast. Interestingly, overexpression of the unstable R57L mutant which lacks transacylase activity *in vitro*, partially rescues the mitochondrial CL and MLCL abnormalities of the *taz* deficient cells *in vivo*, suggesting that strategies aimed at stabilizing this mutant allele could be of therapeutic benefit.

RESULTS

Mammalian TAZ is localized to the mitochondrion

The absence of antibodies capable of detecting endogenous TAZ has significantly impeded progress in our understanding of BTHS pathogenesis. To overcome this obstacle, three TAZ-specific mouse monoclonal antibodies (mAb; 2G3F7, 3D7F11, and 2C2C9) were generated. Critically, each mAb detected endogenous TAZ in fibroblast cell extracts from healthy controls (C109) but not two BTHS patients (TAZ001 and TAZ003) (Figure 3.1A). TAZ001 encodes a truncated 50 amino acid protein while TAZ003 has a single R57L missense allele in TAZ (20). Using these new reagents, endogenous TAZ co-fractionated with mitochondria (Figure 3.1B) and was detected in both human and murine mitochondria (Figure 3.1C).

Human TAZ mRNA is present as a number of splice variants (20, 33). To determine the capacity of the three mAbs to detect different TAZ isoforms, the epitope recognized by each mAb was mapped; each of the three mAbs binds an epitope that is present in a different exon (Figure 3.1D). Moreover, they each have the capacity to recognize every predicted isoform based on mRNA analyses (20, 33). Following immunoprecipitation of TAZ with one mAb (3D7F11), only a single TAZ band was detected by immunoblot using a second mAb (2C2C9) in control but not BTHS cell

extracts (Figure 3.1E). Finally, based on co-migration with assorted human TAZ isoforms expressed in *taz1Δ* yeast (34), all of the cells and tissues surveyed only express TAZ lacking exon 5 (TAZ-ex5; exon 5 is missing in rodents so full-length murine TAZ already lacks exon 5) (Figure 3.1F). Thus, TAZ-ex5 is likely the major isoform expressed at the protein level *in vivo*.

Generation of a mammalian BTHS cell model

To establish a new mammalian BTHS cell culture model, we utilized TALEN-mediated genome editing in 293 Flp-In cells to introduce genetic lesions within *TAZ* exon 1. Two *taz*^{TALEN} clones were identified that had undetectable levels of TAZ protein (Figure 3.2B) and which contained genomic deletions in the targeted locus (Figure 3.2A). In both *taz*^{TALEN}.2 and 19, a proline that is highly conserved in mammals but not in fungi, is deleted (Figure 3.S1); in addition, there was a missense mutation (V12A) identified in *taz*^{TALEN}.19 and five additional amino acids removed (amino acids 11-16) in *taz*^{TALEN}.2. Surprisingly, neither deletion altered the overall reading frame of TAZ. Based on *in silico* analyses (Table 2), we hypothesize that Pro13 is either a critical determinant of a non-bilayer spanning membrane anchor and/or essential for TAZ folding and stability. Consistent with these possibilities, proteosomal inhibition with MG132 did not stabilize TAZ in either *taz*^{TALEN} cell line (Figure 3.2C). The lack of protein expression did not reflect differences in TAZ mRNA levels (Figure 3.2D). Moreover, the expression of representative proteins of each mitochondrial subcompartment and every OXPHOS complex was the same in mitochondria isolated from each *taz*^{TALEN} cell line as WT (Figures 3.2E and F). Of note, the expression of PHB2 and DNAJC19, proteins functionally linked to TAZ (28), was also not altered in either *taz*^{TALEN} cell line. Finally,

as matrix-targeted Su9-DHFR was imported into mitochondria isolated from both *taz*^{TALEN} cells at rates similar to that of WT mitochondria, the membrane potential across the IMM is not grossly impaired in the *taz*^{TALEN} cells (Figures 3.2G and H).

Next, the phospholipid composition of mitochondria isolated from WT and *taz*^{TALEN} cells was determined by mass spectrometry. An increased MLCL:CL ratio is a biochemical hallmark of TAZ deficiency (35). Importantly, mitochondria from each *taz*^{TALEN} cell contained a significantly increased MLCL:CL ratio (Figure 3.3C) that was largely driven by an accumulation of MLCL (Figure 3.3B). The amount of CL was not significantly changed (Figure 3.3A). TAZ-based CL remodeling is a major determinant of the final acyl chain composition of CL at the steady state, which is typified by the inclusion of more unsaturated acyl chains compared to pre-remodeled CL. While there were only modest changes in CL acyl chain length in the *taz*^{TALEN} cells (Figure 3.3E), the amount of CL containing fewer double bonds was significantly increased (Figure 3.3F). Moreover, the relative abundance of unsaturated acyl chains for CL molecules of a given length was consistently lower in *taz*^{TALEN} than in WT mitochondria (Figures 3.3G-K). In addition to its dramatically increased abundance, there were also notable changes in the acyl chain profile of the remodeling intermediate MLCL in mitochondria isolated from both *taz*^{TALEN} cells (Figures 3.3L-O). Specifically, MLCL with longer acyl chains that contained fewer double bonds accumulated in the absence of TAZ activity. Other alterations in the mitochondrial lipidome that were consistent features of mitochondria from both *taz*^{TALEN} cells included an increased abundance of phosphatidylglycerol (PG, Figure 3.3D), bis-monoacylglycerol phosphate, reduced levels of phosphatidylinositol, and subtle changes in the acyl chain length and saturation of phosphatidylcholine (PC) and

phosphatidylethanolamine, two lipid classes that can be used by TAZ as acyl chain donors for MLCL re-acylation (16) (Figures 3.S2-S4). Collectively, these results validate the *ta ζ* ^{TALEN} cells as new cellular BTHS models.

Mammalian TAZ is a membrane protein that assembles in high molecular weight complexes

Yeast Taz1 associates with the IMS-side of the IMM and OMM by virtue of a membrane anchor that extends into but not through the lipid bilayer (30). To determine if human TAZ is similarly membrane-associated, mitochondrial extracts from 293 Flp-In or C109 fibroblasts were sonicated and centrifuged to obtain the pellet, containing membrane-associated proteins, and the supernatant, containing soluble proteins. TAZ, like TIM23 and TOM20, was detected in the pellet fraction (Figure 3.4A). Next, alkali extraction was performed. As expected, the integral proteins TIM23 and TOM20 were largely retained in the pellet whereas the peripheral cytochrome c (CYT C) was quantitatively released into the supernatant (Figure 3.4B). Like yeast Taz1, human TAZ was steadily released into the supernatant as the pH increased, suggesting a similar mode of membrane association (Figure 3.4C). Alternatively, analogous to succinate dehydrogenase subunit A (SDHA), TAZ membrane association may be determined by an interaction with a yet-to-be identified integral membrane protein.

As yeast Taz1 engages in a range of macromolecular complexes (30, 36), the assembly of mammalian TAZ was examined by 2D blue native (BN)/SDS-PAGE. In both human and murine mitochondria, TAZ assembled in a range of complexes (Figure 3.4D). In sum, these results demonstrate that mammalian TAZ associates with

mitochondrial membranes and engages in macromolecular complexes in a manner that is highly reminiscent of its yeast ortholog.

Mammalian TAZ is highly protease resistant and localized to IMS-facing leaflets

Next, we determined the submitochondrial localization of TAZ. First, mitochondria from 293 Flp-In cells were titrated with increasing amounts of digitonin, causing the sequential release of soluble IMS proteins, soluble matrix proteins, membrane proteins of the OMM, and finally IMM-embedded proteins into the supernatant (Figures 3.5A and B). The fractionation profile of human TAZ overlapped with both IMM and OMM proteins (Figure 3.5B) suggesting that like yeast Taz1, human TAZ associates with both the IMM and OMM (4, 30, 37).

Second, a protease-protection assay was performed to determine if human TAZ is associated with IMS-facing membranes as predicted based on results in yeast. In brief, human and murine mitochondria were incubated in iso-osmotic buffer, low osmotic buffer, or low osmotic buffer supplemented with detergent, with each permutation performed in the absence or presence of the non-specific protease mixture, pronase E (Figure 3.5C). Accordingly, OMM proteins facing the cytosol (e.g. TOM20) are accessible to added protease in each condition, residents of the IMS (TIM23; TIM23 is an IMM protein with a large domain exposed to the IMS) are degraded by added protease following osmotic rupture of the OMM (low osmotic buffer) and detergent solubilization, and matrix proteins (GRP75) are only degraded upon addition of detergent with protease. Like the matrix marker GRP75, in every source of mitochondria tested, mammalian TAZ was only degraded by pronase after detergent solubilization. These results thus suggest

that mammalian TAZ is localized to the matrix-facing leaflet of the IMM, the opposite side of the IMM as yeast Taz1.

This conclusion, however, is predicated on TAZ being sensitive to protease. Thus, another potential explanation for the observed pattern is that perhaps TAZ adopts a highly protease-resistant fold that becomes accessible to proteolytic cleavage only in the presence of detergent. To test the idea that TAZ is protease-resistant, we compared its sensitivity to proteases upon addition of detergent with or without prior heat denaturation (Figure 3.5D). When solubilized with SDS, heat denaturation increased the sensitivity of TAZ to degradation by each protease. One potential explanation for the resistance of TAZ to proteolytic degradation is that it forms aggregates. However, using a sequential detergent solubility assay where TAZ was readily solubilized with digitonin (protein aggregates resist solubilization even when re-extracted with TX-100), TAZ does not form protein aggregates (Figure 3.5E).

In light of TAZ's protease resistance, the assays performed cannot conclusively establish the topology of membrane-associated TAZ. Therefore, we performed an *in organello* import assay in which radiolabeled TAZ precursor was incubated with WT mitochondria in the presence or absence of a membrane potential and non-imported precursor removed with trypsin (Figure 3.5F). Import of TAZ was time-dependent but membrane potential-independent. The TAZ precursor was not processed upon import consistent with the failure of most *in silico* programs (Table 3) to predict a mitochondrial presequence cleavage site. Critically, ³⁵S-TAZ precursor was readily degraded by trypsin following incubation with mitochondria on ice and disruption of the OMM (compare lanes 7 and 8). Finally, following import in the presence of a membrane potential,

disruption of the OMM in the presence of trypsin drastically decreased the ^{35}S -TAZ detected (lane 6). Thus, the protease resistance of TAZ observed at steady state occurs after it is imported into the mitochondrial IMS.

To gain further insight into the topology of TAZ, epitope tags were added to either termini of TAZ (CNAP-TAZ and TAZ-3XFLAG for NH_2 - or COOH -terminal tagged TAZ, respectively) (Figure 3.6A). Upon transfection into the $\text{ta}\bar{z}^{\text{TALEN}}$.19 cell line, each construct was expressed similar to untagged WT TAZ (Figure 3.6B) and importantly, rescued the altered MLCL:CL ratio of this TAZ-deficient model (Figures 3.6C and D). The sensitivity of the appended epitope tags to proteolytic degradation was determined in intact mitochondria, following OMM rupture, or in the presence of detergent. Like the IMS marker TIM23, which is anchored to the IMM but exposes a large domain in the IMS, the NH_2 -terminal epitope of CNAP-TAZ became sensitive to added protease when the OMM was disrupted (Figure 3.6F). In contrast, 3XFLAG added to the COOH terminus of TAZ was resistant to proteolytic degradation unless detergent was included (Figure 3.6F). Thus, either the COOH terminus of TAZ is in the matrix, implying that TAZ has a membrane spanning domain contrary to expectations based on its alkali extraction profile (Figures 3.4B and C), or alternatively, the added tag is incorporated in the core protease-resistant structure of TAZ. To distinguish between these two possibilities, we transfected the $\text{ta}\bar{z}^{\text{TALEN}}$.19 cell line with TAZ harboring a COOH -terminal APEX2 tag (38, 39). APEX2 encodes an engineered ascorbate peroxidase that can be used in electron microscopy studies to localize a tagged protein (38, 39). TAZ-APEX2 was expressed normally and functional based on the restored MLCL:CL ratio (Figures 3.6B-D). When $\text{ta}\bar{z}^{\text{TALEN}}$.19 cells expressing TAZ-APEX2 were labeled *in vivo*

with H₂O₂ in the presence of 3,3'-diaminobenzidine (DAB), electron micrographs captured DAB staining in the mitochondrial IMS (Figure 3.6G). In contrast, peroxide treatment of *taz*^{TALEN} cells expressing untagged TAZ resulted in micrographs with little contrast and no staining. Our combined results indicate that mammalian TAZ adopts a highly protease-resistant structure following its import into the mitochondrial IMS where it non-integrally associates with mitochondrial membranes with both termini exposed to the IMS.

The R57L allele encodes an unstable protein

TAZ003 fibroblasts harbor an R57L missense mutation that was previously classified in yeast (K65L) as a temperature-sensitive allele (Figure 3.7A) (20, 32). As such, the inability to detect TAZ in TAZ003 cells could provide evidence that like in yeast, the R57L allele is intrinsically unstable. To determine if the R57L allele encodes an unstable polypeptide, we re-introduced into the two *taz*^{TALEN} cell lines WT TAZ, R57L, and an H69Q TAZ mutant that in yeast encodes a catalytically-null polypeptide (32). The 5-6 subclones that were isolated per construct per parental cell line displayed little variability in TAZ expression for a given TAZ allele (Figure 3.7B). Consistent with the possibility that the R57L allele is intrinsically unstable, its steady state expression in clones from both *taz*^{TALEN} cells was dramatically reduced compared to WT TAZ-expressing cells. The reduced expression was not reflected at the transcript level (Figure 3.7C), did not result from impaired import into the mitochondrial IMS (Figure 3.7D), and was not restored upon proteosomal inhibition (Figures 3.7E and 3.S5A). Moreover, when cytosolic protein synthesis was inhibited with cycloheximide, R57L had a much shorter

half-life ($t_{1/2}$) than WT TAZ (Figures 3.7F and 3.S5B). Thus, as previously characterized in a yeast BTHS model (32), the R57L BTHS variant encodes an unstable protein.

The H69Q allele is catalytically-null

The H69Q mutation disrupts a highly conserved HXXXXD acyltransferase motif. When modeled in yeast, the equivalent H77Q mutation results in a protein that behaves biochemically and cell biologically like WT Taz1 but that is completely devoid of transacylase activity (32). As expected, expression of H69Q in whole cell extracts (Figure 3.7B) and isolated mitochondria (Figure 3.8A) was similar to WT TAZ. The H69Q allele was imported into the mitochondrial IMS (Figure 3.8B) and assembled in complexes (Figures 3.8C and 3.S5C) just like WT TAZ. The preserved complex formation of the H69Q mutant indicates that TAZ assembly is insensitive to increased MLCL or changes in CL acylation. To directly measure the transacylase activity of WT and mutant TAZ, isolated mitochondria were incubated with ^{14}C -labeled lyso-PC and its conversion to PC monitored (Figure 3.8D). Overexpression of WT TAZ resulted in dramatically increased transacylase activity. In stark contrast, mitochondria overexpressing H69Q (or R57L) lacked any detectable transacylase activity above background. Finally, while WT TAZ restored the MLCL:CL ratio of both $\text{taz}^{\text{TALEN}}$ cell lines to normal, overexpression of the H69Q mutant did not (Figures 3.8E-G). Therefore, the H69Q variant encodes a catalytically inactive polypeptide in both mammals and yeast. Intriguingly, overexpression of the R57L mutant, which was devoid of transacylase activity *in vitro* (Figure 3.8D) did partially improve the MLCL:CL ratio of both $\text{taz}^{\text{TALEN}}$ cell lines *in vivo* (Figures 3.8E-G) indicating that prior to its degradation, it retained some residual catalytic activity. Consistently, the R57L allele was still assembled normally (Figure

3.S5C). Collectively, these results suggest that the LOF mechanisms that underlie certain missense mutations are conserved in yeast and mammalian BTHS models.

DISCUSSION

We have determined that CL remodeling is organized in topologically similar ways in mammals and yeast. Like in yeast, mammalian TAZ is localized to the IMS-facing leaflets of the OMM and IMM. Thus, the main determinant of the final CL acyl chain pattern, TAZ, resides on the opposite side of the IMM as the CL biosynthetic machinery. In yeast, the lipase that functions upstream of Taz1, Cld1, is peripherally associated with the matrix side of the IMM (40). At present, the identity and detailed localization of the mammalian lipase(s) that functions upstream of human TAZ to initiate CL remodeling has not been defined. The rationale for the localization and topology of TAZ-based CL remodeling in yeast and mammals is presently unclear but is presumed to be important for it to function properly. Notably, besides dictating the final acyl chain pattern of CL, the physiological functions of this conserved remodeling pathway remain elusive (41).

Overall, our work suggests that human and yeast TAZ, whose polypeptides are only 18% identical and 41% conserved, are remarkably similar biochemically. Not only is their submitochondrial localization the same, yeast and mammalian TAZ also interact with mitochondrial membranes in a similar manner which in yeast involves a membrane anchor that extends into but not completely through the lipid bilayer (30). Further, both yeast and mammalian TAZ assemble in a range of complexes that appear qualitatively quite comparable (36). Previously, we demonstrated that yeast Taz1 does not associate

with itself but does interact with the ATP synthase as well as the major mitochondrial ADP/ATP carrier, Aac2 (36). Thus, it is possible that these interactions will be evolutionarily conserved. However, it is important to mention that the vast majority of the yeast Taz1 interactome remains undocumented and the noted interactions between yeast Taz1 and the ATP synthase or Aac2 are clearly sub-stoichiometric. The composition of all of the mammalian TAZ-associated complexes is similarly unknown but is something we are actively investigating.

Critically, another feature shared between yeast and mammalian TAZ are the LOF mechanisms associated with distinct pathogenic mutations. Using a novel BTHS cell model, the LOF mechanism for the two tested pathogenic mutations were conserved as modeled in yeast or human TAZ. In patient-derived TAZ003 cells, the protein product of the R57L allele is undetectable. When overexpressed in *taz*^{TALEN} cells, the R57L mutant localized properly and assembled normally (Figures 3.S5A-C), but accumulated to a much lesser extent and had a significantly shorter half-life than WT TAZ. The corresponding yeast mutant, K65L, is a temperature-sensitive allele that becomes unstable and loses activity at non-permissive temperature (32). Interestingly, even though the R57L allele lacked *in vitro* activity, its overexpression did improve the MLCL:CL ratio in both *taz*^{TALEN} cells (Figure 3.7G). Therefore, small molecules capable of stabilizing the R57L mutant could increase its activity and thus represent viable therapeutic options. Importantly, dysfunctional conservation extends to the H69Q mutation. In yeast, the corresponding H77Q mutant is identical to WT Taz1 in every way tested except that it is devoid of transacylase activity (32). As predicted from yeast, the H69Q mutant allele closely resembled WT TAZ except that it was catalytically-null.

TAZ is a promiscuous transacylase that can utilize a range of lyso-lipid substrates and phospholipid acyl chain donors. Moreover, TAZ itself lacks intrinsic acyl chain specificity which raises the obvious question of how a non-specific enzyme can generate CL that typically has a specific collection of acyl chains. Recent experiments have suggested that the physical state of phospholipid membranes can affect the substrate specificity of TAZ. Under experimental conditions that mimic high membrane curvature, have an increased proportion of non-bilayer lipids, or perturbed bilayer states, TAZ gains the capacity to generate the physiologically-relevant CL molecular form that contains four attached 18:2 linoleic acids (42). In mitochondria, such privileged lipid domains may be delineated by the recently described prohibitin/DNAJC19 complexes (28). The ring-shaped prohibitin complexes, composed of PHB1 and PHB2 subunits and including DNAJC19 (28), form protein and lipid scaffolds within the IMM that contribute to cristae morphogenesis and cell proliferation (43). Surprisingly, knockdown of either PHB2 or DNAJC19, which do not interact with TAZ, changes the acyl chain pattern of CL similar to TAZ depletion (28). Depletion of either protein with TAZ does not prevent the accumulation of MLCL. These findings suggest that PHB/DNAJC19 complexes participate in CL remodeling after the process is initiated. Since MLCL does not accumulate, TAZ is still active when PHB2 or DNAJC19 expression is reduced. Although both completely traverse the IMM bilayer, the majority of the DNAJC19 polypeptide resides in the matrix. Thus, how PHB/DNAJC19 complexes could modulate TAZ specificity remains unclear based on the submitochondrial localization and interfacial membrane association of TAZ as defined previously in yeast and here in mammals. Given our placement of mammalian TAZ on the IMS-leaflet of the IMM, it is

tempting to speculate that PHB/DNAJC19 complexes sequester TAZ within membrane domains with physical properties (high membrane curvature) that confer acyl chain specificity to TAZ. While the exact details of how PHB/DNAJC19 complexes modulate the specificity of TAZ-mediated CL remodeling is undefined, the functional relationship between PHB/DNAJC19 complexes and TAZ is underscored by the fact that mutations in DNAJC19 result in DCMA, a disease that shares many clinical features with BTHS (25, 26). Our results thus establish a framework to dissect the functional relationship between PHB/DNAJC19 complexes and TAZ which may in turn reveal the basis for the shared and distinct phenotypes of BTHS and DCMA.

MATERIALS AND METHODS

Molecular Biology

The human TAZ ORF lacking exon 5 was amplified by PCR using cDNA from HeLa cells and subcloned first into pBSK (Stratagene) and then into pcDNA5/FRT (Invitrogen). The R57L and H69Q mutations were introduced into the parental pcDNA5/FRT_{hTAZ} plasmid *via* overlap extension (44). TAZ with an NH₂ terminal CNAP tag (45) or COOH terminal 3XFLAG or APEX2 tags were introduced into the parental pcDNA5/FRT_{hTAZ} plasmid *via* overlap extension (44). For TAZAPEX2, pcDNA3APEX2-NES (39), a gift from Alice Ting (Addgene plasmid # 49386), was used as template. For *in vitro* transcription/translation, WT TAZ and the R57L and H69Q alleles were subcloned into pSP64. The sequence of every construct was verified by DNA sequencing. The TALEN binding pair recognizes sequences in TAZ exon1 that are separated by 16 nucleotides and immediately downstream of the start site (Life

Technologies). The two constructs, which are fused to the truncated FokI nuclease, were subcloned into pcDNA3.1 and pEF6/V5-HisA (Life Technologies) generating pcDNA3TAZ1-R and pEF6ATAZ1-L, respectively.

Cell Culture

All cells were grown at 37°C, 5% CO₂. Control (C109) and BTHS patient fibroblasts (TAZ001 and TAZ003) (20) were maintained in DMEM (Cellgro) containing 10% fetal bovine serum (FBS, Hyclone), 2 mM L-glutamine (Gibco), and 50 units/L penicillin-streptomycin (Gibco). HEK293 Flp-In cells (Invitrogen) were grown in DMEM containing 10% FBS, 2 mM L-glutamine, and 100 µg/ml zeocin (Invitrogen). To establish a BTHS cell model, 293 Flp-In cells grown in medium lacking antibiotic but supplemented with 50 µg/ml uridine, were transfected with a 1:1 ratio of pcDNA3TAZ1-R and pEF6ATAZ1-L using FuGENE 6 (Promega), selected with 0.5 mg/ml G418 and 5 µg/ml blasticidinS (Cellgro) for 1 week, and single colonies isolated by ring cloning. Individual clones were maintained in the same medium as used for the parental 293 Flp-In cells and the inclusion of uridine found to not be essential. Whole cell extracts derived from candidate clones were harvested and analyzed by SDS-PAGE and immunoblot. Stable *taz*^{TALEN} rescue cell lines were generated by co-transfecting the two *taz*^{TALEN} cell lines with pOG44 (expressing the Flp-recombinase) and the relevant pcDNA5/FRT plasmid (WT, CNAP-TAZ, TAZ-3XFLAG, TAZ-APEX2, R57L, H69Q) at a ratio of 9:1 using FuGENE 6. Transfected cells were selected using 200 µg/ml hygromycin B (Invitrogen), individual clones recovered by ring cloning, expanded, and screened by immunoblot. Equal numbers of individual clones per construct were combined to establish a pooled clonal population that was then used in all subsequent analyses. Each

pooled population was derived from at least 5 individual clones except for *taz*^{TALEN}.19 overexpressing CNAP-TAZ which was established from 3 clones. Mycoplasma contamination was routinely monitored and not detected.

Purification of recombinant human TAZ

The entire open reading frame of *TAZ* lacking exon5 was cloned into the pET28a vector (Novagen) downstream of the 6xHis tag, induced at 37°C for 4 hours with 1 mM IPTG in C41 (DE3) *Escherichia coli*, and inclusion bodies separated from native protein extracts by centrifugation at 22,000 ×g for 1 hour at 4°C. Lipids and debris were removed from the inclusion bodies by resuspending the pellet with 7-10 mls of wash buffer (50 mM Tris-HCl, pH 7.0, 2.5 mM EDTA, 1 M urea, 1% (v/v) Triton X-100) per gram of cells using a dounce homogenizer followed by centrifugation at 22,000 ×g for 30 minutes at 4°C. This wash step was repeated three times until the supernatant was clear. A final wash was performed using wash buffer lacking urea and Triton X-100. The final recovered protein pellet was resuspended using a dounce homogenizer with 4 ml of extraction buffer (50 mM HEPES-KOH, pH 7.5, 5 mM EDTA, 8 M guanidine-HCl, 2 mM β-mercaptoethanol) per gram of cells and clarified by centrifugation at 100,000 ×g for 1 hour at 4°C. The solubilized inclusion bodies were mixed 1:1 with ddH₂O, His₆-TAZ purified using Ni²⁺ agarose (Qiagen), and bound material recovered under denaturing conditions.

Antibodies

Custom monoclonal antibodies against human TAZ-ex5 were produced by Genscript using purified recombinant protein as antigen. Three hybridomas – 2C2C9,

3D7F11, and 2G3F7 – that secrete TAZ-reactive antibodies were established. Antibodies against the following proteins were: GRP75 (Antibodies Inc. 75-127); β -actin (A5441) and TIMM9 (WH0026520M1) (Sigma); topoisomerase I (Developmental Studies Hybridoma Bank CPTC-TOP1-1-S); calreticulin 3 (sc-134295) and TOM20 (sc-11415) (Santa Cruz); HLA-B (Epitomics 2389-1); TIM23 (611332), CYCS (556433), SMAC/DIABLO (612246), and cyclin D1 (556470) (BD); UQCRC2 (ab14745), ACO2 (ab129069), VDAC1 (ab15895), and COX4 (ab16056) (Abcam); SDHA (Invitrogen 4592000); PHB2 (BioLegend 611802); DNAJC19 (ProteinTech 12096-1-AP); and NDUFB6 (Molecular Probes, discontinued). F1 β was a kind gift from Dr. Peter Pedersen (Johns Hopkins School of Medicine) and the ANT2/5H7 (46) antibody was raised against the yeast ADP/ATP carrier, Aac2, but conveniently cross-reacts with human and murine ANT2. Goat anti-rabbit or mouse secondary antibodies conjugated to horseradish peroxidase were also used (31460 and 62-6520; Pierce).

Whole cell extraction

Confluent culture dishes were washed twice with ice-cold PBS and lysed with RIPA lysis buffer (1% (v/v) Triton X-100, 20 mM HEPES-KOH, pH 7.4, 50 mM NaCl, 1 mM EDTA, 2.5 mM MgCl₂, 0.1% (w/v) SDS) spiked with 1 mM PMSF for 30 minutes at 4°C with rotation. Insoluble material was removed by centrifugation for 30 minutes at 21,000 $\times g$ at 4°C, the supernatant collected, and protein quantified using a bichichronic acid (BCA) assay (Pierce).

Immunoblotting

SDS-PAGE and immunoblotting was performed as previously described (47). Images were captured with a Fluorchem Q (Cell Biosciences, Inc) quantitative digital imaging system and quantitation performed using the indicated software. Images were processed in Adobe Photoshop with only linear adjustments in contrast and brightness and assembled in Adobe Illustrator.

Preparation of subcellular fractions

Fibroblasts and 293 Flp-In cells were seeded onto four 150 mm×25 mm tissue-culture dishes and allowed to expand to confluency. Two days prior to mitochondrial isolation, the cells were switched from dextrose- to galactose-based media (DMEM without glucose, Gibco; supplemented with 10 mM galactose, Sigma). Mitochondria were isolated on ice (with ice-cold buffers) using a protocol adapted from (48). Briefly, after aspirating spent media from dishes, cells were scraped off in PBS and centrifuged at 600 ×g for 10 minutes. After washing the cells once more with PBS, the pelleted cells were resuspended in 3 ml isolation buffer (IB_c, 10 mM Tris-MOPS, 1 mM EGTA/Tris, pH 7.4, 200 mM sucrose) and homogenized with 40-45 strokes in a motor-driven tightly fitting Teflon Potter-Elvehjem at 1,600 rpm. Cell lysates were then centrifuged twice at 600 ×g for 10 minutes; the resulting pellet is the nuclear fraction. Mitochondria were recovered from the supernatant by centrifugation at 7,000 ×g for 10 minutes. The mitochondrial pellet was resuspended to a volume that fits a 1.5 ml microcentrifuge tube; after an additional 7,000 ×g spin, a 10,000 ×g clarifying spin was performed to obtain crude mitochondria. The supernatant from the prior 7,000 ×g spin contains cytosolic, lysosomal, and ER fractions which were further sub-fractionated as follows. Lysosomes were pelleted after a 20,000 ×g spin for 30 minutes and resuspended in a residual amount

of IB_c. The remaining supernatant was centrifuged at 40,000 ×g for another 30 minutes to obtain plasma membranes. Further centrifugation of the obtained S40 (100,000 ×g for 1 hour) resulted in the isolation of ER (pellet) and cytosolic fractions (supernatant). Heart and liver mitochondria from 10-12 week old female FVB mice were isolated on ice using a protocol adapted from (49, 50). Briefly, tissues were rinsed with ice-cold CP1 (100 mM KCl, 50 mM MOPS, pH 7.4, 5 mM MgSO₄, 1 mM EGTA, 1 mM ATP), minced with scissors and washed several times with CP1 before resuspension in CP2 (CP1 supplemented with 2 mg/ml BSA). Tissues were then homogenized using a Polytron (three 2.5 second pulses on medium setting; Fisher PowerGen 1000 large bore homogenizer). The homogenate was centrifuged at 580 ×g for 7 minutes at 4°C and the resultant supernatant contained either liver mitochondria or in the case of heart tissue, subsarcolemmal mitochondria (SSM), while the pellet contained heart interfibrillar mitochondria (IFM). Liver and SSM supernatants were repeatedly centrifuged at 580 ×g until there were no visible cell/debris pelleting. A final clarifying spin at 3,000 ×g for 7 minutes was performed before resuspending the mitochondrial pellets in KME (100 mM KCl, 50 mM MOPS, 1 mM EGTA). To extract IFM mitochondria, the pellet was resuspended in CP1 containing 5 mg trypsin per gram tissue with mixing, for 10 minutes on ice. The trypsin was inactivated with an equivalent volume of CP2 before centrifugation at 7,500 ×g for 7 minutes at 4°C. For our purposes (to maximize heart mitochondrial yield) the resultant pellet was resuspended in CP2, clarified with a 3,000 ×g spin before being resuspended in KME and combined with the SSM mitochondria. Organellar and mitochondrial fractions were quantitated using a BCA assay. Mitochondria were resuspended to 10 mg/ml in IB_c (cells) or KME (tissues) and if not

used immediately, aliquoted, snap frozen with liquid N₂, and stored at -80°C for downstream analyses.

Epitope-Mapping

A peptide scan consisting of 15mer peptides with an 11 amino acid overlap between adjacent peptides that spans the entire 262 amino acid TAZ protein was generated by JPT Peptide Technologies. The membrane was moistened with methanol prior to immunoblotting and the membrane subsequently regenerated with 100 mM β-mercaptoethanol, 1% (w/v) SDS, 62.5 mM Tris-HCl, pH 6.7, two more times to map epitopes bound by the different TAZ monoclonal antibodies. The epitopes recognized by each of the three monoclonal antibodies were determined by densitometry analysis of the immunoreactive PepSpots.

Immunoprecipitation

The TAZ monoclonal antibody, 3D7F11, or normal mouse serum was conjugated to protein G-sepharose using the Seize X Protein A Immunoprecipitation kit and protocol (Pierce). Confluent T75 cm² flasks of the indicated cells were lysed with 1 ml RIPA lysis buffer and protein extracts quantified as described above. 1.5 mg cellular extract per cell line was diluted to 1 ml with protease inhibitor-spiked lysis buffer and rotated with 90 μl normal mouse serum-conjugated beads for 1 hour at 4°C. After centrifugation at 376 ×g for 5 minutes at 4°C, the pre-cleared lysates were transferred to tubes containing 90 μl 3D7F11-conjugated beads and rotated at 4°C for 4 hours. Following low speed centrifugation as before, unbound extract was collected for analysis and the bound material (both the pre-clear and IP beads) was sequentially washed (10 minutes rotating

per wash) twice with Wash Buffer (0.1% (v/v) Triton X-100, 20 mM HEPES-KOH, pH 7.4, 50 mM NaCl, 1 mM EDTA, 2.5 mM MgCl₂, 0.1% (w/v) SDS; 1 ml per wash), twice with High Salt Wash Buffer (0.1% (v/v) Triton X-100, 20 mM HEPES-KOH, pH 7.4, 500 mM NaCl, 1 mM EDTA, 2.5 mM MgCl₂, 0.05% (w/v) deoxycholate; 1 ml per wash) and once with Low Salt Wash Buffer (0.1% (v/v) Triton X-100, 20 mM HEPES-KOH, pH 7.4, 1 mM EDTA, 2.5 mM MgCl₂, 0.05% (w/v) deoxycholate; 1 ml per wash). To elute bound material, three sequential elutions were performed using 0.1 M glycine, pH 2.8, and the pooled eluates were neutralized with 50 µl 1 M Tris-Cl, pH 8.0. Eluates were transferred to a spin column (Pierce 1824826) and centrifuged for 2 minutes at 376 ×g to reduce resin carry-over. Finally, the unbound extracts (pre-clear and IP beads) and eluates were TCA-precipitated (20% (v/v) TCA with 0.07% (v/v) deoxycholate) for 1 hour on ice, the pellet fractions resuspended in a 1:1 mix of 2X reducing sample buffer and 0.1 M NaOH, and boiled for 5 minutes.

Genotyping *taz*^{TALEN} cells

Genomic DNA was extracted using the Genra Puregene Cell Kit (Qiagen) and the genomic region surrounding the target site (exon1 extending into exon2, encompassing the ATG) was PCR amplified, digested with XbaI/HindIII (NEB), and ligated into pBSK(-). Transformants were analyzed by Sanger sequencing. As 293 cells are hypotriploid, sequences of at least 10 individual clones for each of the two *taz*^{TALEN} cell lines were obtained, revealing disruption of TAZ downstream of the initiation codon.

Quantitative RT-PCR

Total RNA was isolated from WT, $ta\zeta^{\text{TALEN}}$, and $ta\zeta^{\text{TALEN}}$ overexpressing *TAZ* alleles using the PureLink RNA Mini Kit with DNase treatment (Invitrogen). 25 ng of RNA was analyzed in 20 μl reactions using the EXPRESS One-Step SYBR GreenER qRT-PCR Kit (Life Technologies) with 7500 Real-Time PCR Systems (Applied Biosystems) according to the manufacturer's instructions. Each reaction, including non-template controls, was performed at least in duplicate with a minimum of three different biological replicates and contained 50 nM ROX and 200 nM each of forward and reverse gene-specific primers designed with Primer3 (51). The reaction conditions were as follows: 5 minutes at 50°C, 2 minutes at 95°C, followed by 40 two-temperature cycles (15 seconds at 95°C and 1 minute at 60°C) and melt curve profiling. Expression of *TAZ* was analyzed by the comparative C_T ($\Delta\Delta C_T$) method ($X_{\text{Test}}/X_{\text{GAPDH}}=2^{-\Delta\Delta C_T}$) with *GAPDH* as an endogenous reference gene. Values were represented as mean $\Delta\Delta C_T \pm \text{SEM}$ or fold change ($2^{\Delta\Delta C_T}$) \pm SD relative to *TAZ* expression in 293 Flp-In cells (Prism 6).

Import

Radiolabeled precursors were produced using an SP6 Quick Coupled Transcription/Translation system (Promega) spiked with Easy-Tag L-³⁵S-methionine (PerkinElmer). Radiolabeled precursors were incubated in import buffer (20 mM HEPES-KOH, pH 7.4, 250 mM sucrose, 80 mM KOAc, 5 mM MgOAc, 10 mM succinate, and 5 mM methionine) with freshly isolated mitochondria for the indicated amount of time at 37°C or 4°C, as specified. To dissipate the mitochondrial proton-motive force, mitochondria were pre-incubated with 1 μM valinomycin and 5 μM carbonyl cyanide *m*-chlorophenyl hydrazine for 5 minutes at 37°C. Import was stopped with an equal volume of ice-cold import buffer containing 20 $\mu\text{g/ml}$ trypsin. Where

indicated, the OMM was ruptured as already described in the presence of 20 µg/ml trypsin. Following 30 minutes on ice, 100 µg/ml soybean trypsin inhibitor was added and mitochondria were re-isolated by centrifugation at 21,000 ×g for 5 minutes at 4°C. 100% of each time point and 5% of imported precursors were resolved on 12% SDS-PAGE gels and analyzed by phosphoimaging.

Lipidomics

A defined amount of internal standards (0.1 nmol of CL(14:0)₄, 0.2 nmol of BMP(14:0)₂, 2.0 nmol of PC(14:0)₂, 0.1 nmol of PG(14:0)₂, 5.0 nmol of PS(14:0)₂, 0.5 nmol of PE(14:0)₂, 1.0 nmol of PA(14:0)₂, 2.0 nmol of SM(14:0)₂, 0.02 nmol of LPG(14:0), 0.1 nmol of LPE(14:0), 0.5 nmol of LPC(14:0), 0.1 nmol of LPA(14:0) (Avanti Polar Lipids) dissolved in 120 µl of chloroform/methanol (1:1, v/v) and 1.5 ml of chloroform/methanol (1:1, v/v) were added to 1 mg mitochondria. Subsequently, the mixture was sonicated in a water bath for 5 minutes, followed by centrifugation at 15,000 ×g for 5 minutes. The organic layer was transferred to a glass vial and dried under a nitrogen stream at 60°C. Subsequently, the residue was dissolved in 200 µl of chloroform/methanol/water (50:45:5, v/v/v) containing 0.01% of NH₄OH, and 10 µl of the solution was injected into the liquid chromatography-mass spectrometry (LC/MS) system. LC/MS analysis was performed as described in (35). In negative mode, mass spectra of phospholipid molecular species were obtained by continuous scanning from m/z 380 to 1500 with a scan time of 2 seconds. In positive mode, mass spectra of PC, LPC and SM were obtained by continuous scanning for product ions with m/z 184 from m/z 400 to 1000. Mass spectra for PE, LPE and PE plasmalogens were obtained by scanning on neutral losses of 141 from m/z 400 to 1000. The raw LC/MS data were

converted to mzXML format using msConvert (52) for the negative scan data and ReAdW for the positive specific scan data. Details on the metabolic data pre-processing pipeline will be described elsewhere (manuscript in preparation). Briefly, the dataset was processed using a semi-automated xcms-based metabolomics workflow (53) written in the R language and statistical environment (<http://www.r-project.org/>). The workflow comprises pre-processing (peak-finding and quantification), identification of metabolites, isotope correction, normalization/scaling based on internal added standards and statistical analysis of the results.

Membrane association assays

Sonication experiments utilized 0.2 mg mitochondria and were performed in the absence of KCl as described (40). The supernatant and membrane fractions were separated by ultracentrifugation at 175,000 $\times g$ using a TLA120.1 rotor for 30 minutes at 4°C. Carbonate extraction was performed as described (30) except that 0.5 ml of 0.1 M Na₂CO₃ at the indicated pH was added to 0.1 mg mitochondria, and following 30 minutes on ice, the pellet and supernatant fractions were separated by centrifugation at 175,000 $\times g$ for 15 minutes at 4°C using a TLA120.1 rotor.

Blue native (BN) gel electrophoresis

Mitochondria were solubilized for 30 minutes on ice in 20 mM HEPES-KOH, 10% glycerol, 50 mM NaCl, 1 mM EDTA, 2.5 mM MgCl₂, pH 7.4 supplemented with 1% (w/v) (mouse tissues) or 1.25 % (w/v) (human cells) digitonin (Biosynth International, Inc) and protease inhibitors. Extracts were clarified by centrifugation for 30 minutes at 21,000 $\times g$ at 4°C and analyzed by 2D BN/SDS-PAGE exactly as described (45).

Digitonin fractionation assay

Digitonin-based submitochondrial localization was adapted from (40). In brief, 0.1 mg mitochondria were resuspended in 50 μ l SEHK buffer (250 mM sucrose, 5 mM EDTA, pH 7.0, 10 mM HEPES-KOH, pH 7.4, 200 mM KCl) supplemented with 0-0.5% digitonin and 1 mM PMSF. Following a brief vortex on level 1, samples were incubated for 2 minutes on ice and solubilization stopped by adding 450 μ l cold SEHK buffer. Solubilized proteins were separated from the membrane pellets by centrifugation at 100,000 \times g for 10 minutes at 4°C. After the supernatant was TCA-precipitated, the membrane and supernatant-derived pellets were resuspended in equal volumes of reducing sample buffer.

Protease-based assays

Freshly isolated mammalian mitochondria (0.2 mg) from cells or tissues were resuspended in iso-osmotic IB_c or KME buffers, respectively. To rupture the OMM, mitochondria (0.2 mg) were resuspended in 5 mM Tris-Cl, pH 7.5 for 30 minutes on ice; 0.5% (v/v) deoxycholate was added to further solubilize the IMM. Each of these conditions was performed in the absence and presence of 125 μ g/ml pronase E. Pronase was inhibited with 5 mM PMSF and samples precipitated with 20% (v/v) TCA and 0.07% (v/v) deoxycholate, incubated at 60°C for 5 minutes followed by an hour on ice. Samples were centrifuged at 21,000 \times g for 10 minutes at 4°C, washed with 1 ml of cold acetone, resuspended in a 1:1 mix of 2X reducing sample buffer:0.1M NaOH and boiled for 5 minutes. To determine sensitivity to assorted proteases following heat denaturation, mitochondria (0.2 mg) were resuspended in 5 mM Tris-Cl, pH 7.5 containing 0.1% (v/v) SDS, kept on ice or incubated at 95°C for 5 minutes, and then 5 mM Tris-Cl, pH 7.5 with

0.1% SDS containing 250 $\mu\text{g/ml}$ pronase E, 200 $\mu\text{g/ml}$ proteinase K, or 40 $\mu\text{g/ml}$ trypsin added. Following a 30 minute incubation on ice, pronase E and proteinase K were inhibited with 5 mM PMSF and trypsin with 100 $\mu\text{g/ml}$ soybean trypsin inhibitor. Every sample was precipitated with 20% (v/v) TCA and 0.07% (v/v) deoxycholate, incubated at 60°C for 5 minutes followed by an hour on ice. Samples were centrifuged at 21,000 $\times g$ for 10 minutes at 4°C, washed with 1 ml of cold acetone, resuspended in a 1:1 mix of 2X reducing sample buffer:0.1M NaOH and boiled for 5 minutes.

Protein aggregation assay

Protein aggregation was determined in mitochondria (0.2 mg) isolated from 293 Flp-In cells exactly as previously described (31).

Phospholipid labeling and analyses

Cells were seeded onto 60 mm dishes or 6 well plates and allowed to grow to 50-70% confluency at 37°C, 5% CO₂. Following aspiration, regular media spiked with 2.5 $\mu\text{Ci/ml}$ ³²P_i was added and the cells incubated at 37°C, 5% CO₂ for 24 hrs. Cells were washed twice with ice cold 1X PBS, detached in 0.8 ml IB_c buffer using a cell scraper, transferred to a microfuge tube, collected at 600 $\times g$ 5 min at 4°C, and resuspended in 0.1 ml IB_c buffer. Phospholipids were extracted from equal amounts of labeled cells, determined by liquid scintillation, as described (30) except that 0.9% (w/v) NaCl was used to initiate phase separation instead of ddH₂O. Samples were resuspended in chloroform, loaded onto ADAMANT TLC plates (Machery-Nagel), resolved once in chloroform:ethanol:H₂O:trimethylamine (30:35:7:35, v/v/v/v), and phospholipids visualized using a K-screen and FX-Imager (Bio-Rad Laboratories).

Electron microscopy

Cells were seeded onto 100 mm dishes and allowed to grow to ~70% confluence before fixing with 3.0% formaldehyde and 1.5% glutaraldehyde in 0.1 M sodium cacodylate, 5 mM CaCl₂, 2.5% (w/v) sucrose, pH 7.4, for 1 hour at RT. Cells were washed three times for 15 minutes each with 0.1 M sodium cacodylate, 2.5% (w/v) sucrose, pH 7.4, and another three times for 5 minutes each with 50 mM Tris-HCl, 7.5% (w/v) sucrose, pH 7.4, prior to labeling with 0.5 mg/mL DAB and 0.015% H₂O₂ in 50 mM Tris-HCl, 7.5% (w/v) sucrose, pH 7.4 for 20 to 60 minutes. The labeling reaction was stopped by rinsing cells twice with 50 mM Tris-HCl, 7.5% (w/v) sucrose, pH 7.4, and once with 0.1 M sodium cacodylate, pH 7.4, 5 mM CaCl₂, 2.5% (w/v) sucrose, before scraping cells into needle tubes. Cells were pelleted progressively by spinning from 3,000 rpm to 12,000 rpm over the course of an hour and the pellet was post-fixed in 1% OsO₄, 1% potassium ferrocyanide in 0.1 M sodium cacodylate, 5 mM CaCl₂, pH 7.4 for 45 minutes at RT. The pellets were washed thoroughly with 0.1 M sodium cacodylate, pH 7.4, 5 mM CaCl₂, 2.5% (w/v) sucrose several times until solution becomes clear, dehydrated through a graded series of ice-cold ethanol, and subsequently embedded in Epon resin. Sections were cut on a Reichert Ultracut T ultramicrotome and observed on an FEI Tecnai 12 transmission electron microscope at 100 kV. Images were captured with a Soft Imaging System Megaview III digital camera and figures were assembled in Adobe Photoshop with only linear adjustments in contrast and brightness.

Cycloheximide chase

Cell culture medium lacking antibiotics but containing 100 µg/ml cycloheximide was added to confluent 6-well plates and incubated at 37°C, 5% CO₂. At the designated

times, cells were solubilized with 100 μ l 1% (w/v) SDS and diluted to 0.5% SDS, 1% β -mercaptoethanol with 2% (v/v) β -mercaptoethanol. After denaturing the lysates at 100°C for 10 minutes, protein was quantified using the Bradford method (Bio-Rad).

Transacylation assay

The transacylase assays were performed as previously described (16, 32) using 1 nmol of 1-[¹⁴C]palmitoyl-2-lyso-PC (0.05 mCi; PerkinElmerLife Sciences) per reaction in 0.2 ml reaction buffer (10 mM β -mercaptoethanol, 0.5 mM EDTA, 50 mM Tris, pH 7.4). To initiate the reactions, ~125 μ g mitochondria (the exact amount was determined by the BCA assay) were added, the reactions vortexed on high for 1 second, and incubated with shaking at 220 rpm for 5 minutes at 37°C. Lipid extraction, thin layer chromatography separation, image acquisition and analyses were executed as described (32).

Data analysis

Band densitometry analyses were performed using Quantity One (Bio-Rad) or Image J (54). With the exception of the data in Fig 2D and 7D, statistical analyses were performed using SigmaPlot 11 software (Systat Software) and all comparisons performed by t test or one-way analysis of variance with Holm-Sidak pairwise comparisons. For Fig 2D and 7D, comparisons were performed using one-way analysis of variance with Geisser-Greenhouse correction Tukey's multiple comparison test available in the Prism 6 software (GraphPad). All graphs report the mean \pm SEM.

ACKNOWLEDGMENTS

We are grateful to Kim-Vy Nguyen (Andrew Ewald lab) for providing all the mouse tissues used for experiments in this paper. This work was supported by a grant from the Barth Syndrome Foundation (S.M.C.), National Institutes of Health Grants R00HL089185 and R01HL108882 (S.M.C.), R01GM061721 (C.M.K.), and Biochemistry, Cellular, and Molecular Biology Program Training Grant T32GM007445 (Y-W.L.), and a pre-doctoral fellowship from the American Heart Association (Y-W.L.).

CONFLICT OF INTEREST STATEMENT

There are no conflicts of interest to declare.

ABBREVIATIONS

BTHS, Barth syndrome; CL, cardiolipin; IMM, inner mitochondrial membrane; IMS, intermembrane space; MLCL, monolysocardiolipin; LOF, loss-of-function; mAb, monoclonal antibody; OMM, outer mitochondrial membrane; OXPHOS, oxidative phosphorylation; PC, phosphatidylcholine; PG, phosphatidylglycerol.

Table 2: Predicting membrane anchors in TAZ. *In silico* prediction of membrane anchors using different program algorithms. Some programs have algorithms that predict the existence of membrane domains but do not define the residues involved. Most of the listed algorithms perform searches for transmembrane stretches; however, because our experimental evidence is not consistent with TAZ containing a transmembrane region, we will refer to these stretches as potential membrane anchors. Membrane anchors that were weakly predicted are in paranthesis.

	Human	Mouse	Zebrafish	Fly	Yeast	References
Philius ^a	14-35; (168-183)	Globular	Globular	134-156	Globular	(55)
SOSUI	No TMs predicted	No TMs predicted	No TMs predicted	No TMs predicted	No TMs predicted	(56)
TMHMM v2.0	15-35	15-35	No	136-158	No	(57)
HMMTOP	9-28	15-34	No	135-158	26-44	(58)
MINNOU	15-41	16-40	15-40	135-158	22-47	(59)
Phobius ^b	15-34	15-34	Non-cytoplasmic	135-158	26-47	(60)
SPLIT 4.0	No TMs predicted	No TMs predicted	No TMs predicted	135-157	No TMs predicted	(61)
TOPCONS	15-35	15-35	16-36	92-112	7-27	(62)
OCTOPUS	15-35	15-35	15-35	92-112	7-27	(63)
SCAMPIseq	15-35	15-35	No	No	No	(64)
SCAMPImsa	15-35	15-35	15-35	92-112	7-27	(64)
PRODIV	16-36	16-36	16-36	92-112	10-30	(65)
PRO	16-36	16-36	16-36	No	10-30	(65)
DAS-TMfilter ^c	16-31; (178-181)	17-31; (178-181)	No	138-157; (230-239)	29-46; (222-229)	(66)
waveTM	7-35	16-40	7-35	135-158	29-44	(67)
TopPred II ^d	11-31	15-35	(19-39, 169-189)	139-159; (226-246)	27-47	(68)
TMpred ^e	14-35; (164-184)	15-35; (164-184)	19-39; (165-184)	135-158; (195-214, 227-245)	26-47; (77-98, 112-135)	(69)

^a transmembrane regions with a confidence score greater than 0.5 is listed followed by regions with scores below 0.5 in parentheses

^b non-cytoplasmic (or cytoplasmic) means that the prediction contains no membrane helices but provides the most probable location and orientation of transmembrane helices in the sequence

^c all proteins were predicted to be non-transmembrane proteins using reference library 32 with long output; however, using the hydropathy scores generated from the query sequence, segments containing hydrophobicity scores greater than 2 are chosen and presented; segments containing amino acids that score greater than 3 are listed first followed by those segments that have scores of only 2+ in parentheses

^d transmembranes predicted with certainty are listed followed by putative membrane-spanning segment in parentheses

^e significant transmembrane regions are listed followed by weakly predicted stretches in parentheses

Table 3: Mitochondrial targeting sequences cannot be conclusively defined in any of the TAZ orthologs. *In silico* prediction of mitochondrial targeting peptides present within various TAZ orthologs using different program algorithms. Note that in some programs, the algorithm predicts the presence or absence, or probability, of a targeting peptide but not necessarily the exact residues that define the signal sequence.

Species Uniprot	Human Q16635-3	Mouse Q91WF0	Zebrafish Q6PUS0	Fly Q9V6G5	Yeast Q06510	References
TargetP1.1 ^a	1-26 SP	1-26 SP	1-115 mTP	1-39 mTP	No	(70)
MitoProt II ^b	0.5487 Not pred	0.6897 Not pred	0.7713 C-20	0.3962 C-39	0.6007 Not pred	(71)
PSORT II (Gavel) ^c	None found	C-24	C-32	C-51	None found	(72)
PSORT II (kNN) ^d	8.7%	17.4%	17.4%	17.4%	30.4%	(73)
TPpred 2.0 ^e	None found 0.927	None found 0.851	None found 0.834	None found 0.83	None found 0.996	(74)
Predotar ^f	0.03	0.34	0.00	0.34	0.00	(75)
iPSORT ^g	None found	None found	None found	None found	None found	(76)
MitoFates ^h	No (0.003) C-58 (MPP ⁱ)	No (0.016) C-15 (MPP)	No (0.206) C-23 (MPP)	Yes (0.392) C-42 (MPP)	No (0.012) C-26 (MPP); C-27 (lcp55)	(77)

^a predicts the subcellular localization of proteins based on the predicted presence of chloroplasts transit peptide (cTP), mitochondrial targeting peptide (mTP) or secretory pathway signal peptide (SP)

^b the probability that the protein will be exported to the mitochondria is indicated, along with the potential cleavage site (C-#), if available

^c searches for consensus patterns around mitochondrial targeting peptide cleavage sites (C-#)

^d *k*-nearest neighbor algorithm for assessing the probability that the query is localized to the mitochondria

^e predicts cleavage sites of mitochondrial targeting peptides (prediction score)

^f provides a probability estimate as to whether the sequence contains a mitochondrial (shown), plastid or ER targeting sequence

^g searches for N-terminal sorting signals and predicts whether or not it contains a signal peptide, a mitochondrial targeting peptide, or a chloroplast transit peptide

^h predicts putative mitochondrial presequences (probability score), cleavage site(s) (C-#), and the mitochondrial protease that is likely involved

ⁱ MPP, matrix processing peptidase

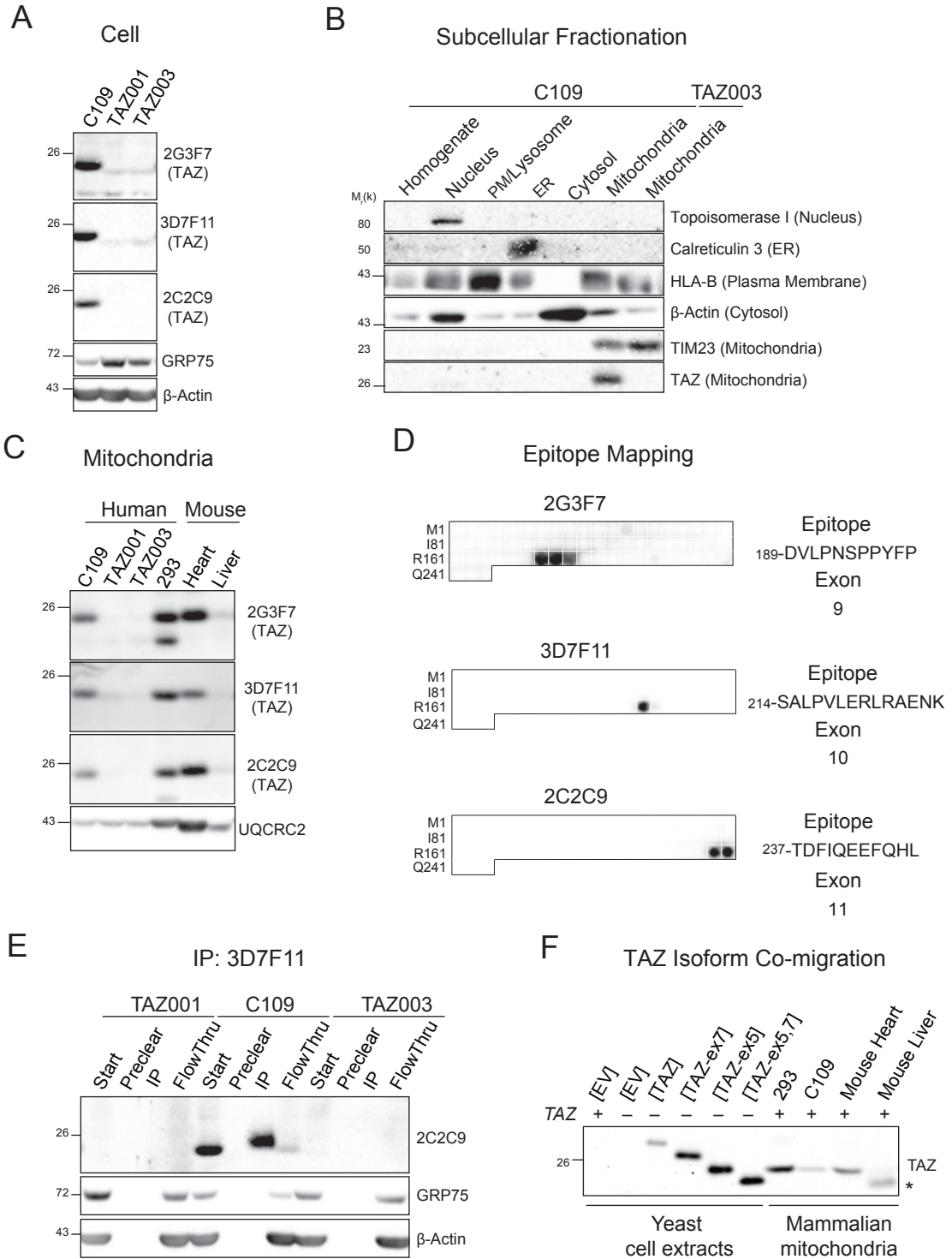


FIGURE 3.1 One isoform of TAZ is expressed and localized to mitochondria in mammalian cells and tissues. [See next page for figure legends.]

FIGURE 3.1 One isoform of TAZ is expressed and localized to mitochondria in mammalian cells and tissues. (A) Whole cell extracts (50 µg) from healthy control (C109) and BTHS patient fibroblasts (TAZ001 and TAZ003) were immunoblotted with three different mAbs generated against recombinant human TAZ. (B) Subcellular fractions (50 µg) derived from C109 cells immunoblotted as indicated. (C) Mitochondrial extracts (50 µg) from the indicated source immunoblotted with the TAZ mAbs. (D) The epitope recognized by each TAZ mAb was determined by peptide array. The exon that harbors each epitope is indicated. (E) TAZ was immunoprecipitated with 3D7F11 from 1.5 mg of the indicated cell extracts. 50 µg starting material and non-binding flow through and 100% of bound material (Preclear and IP) were immunoblotted using 2C2C9. (F) Whole cell extracts from WT or *taz1*Δ yeast transformed as indicated and mitochondrial extracts from the designated source immunoblotted for TAZ. EV, empty vector. *, nonspecific band.

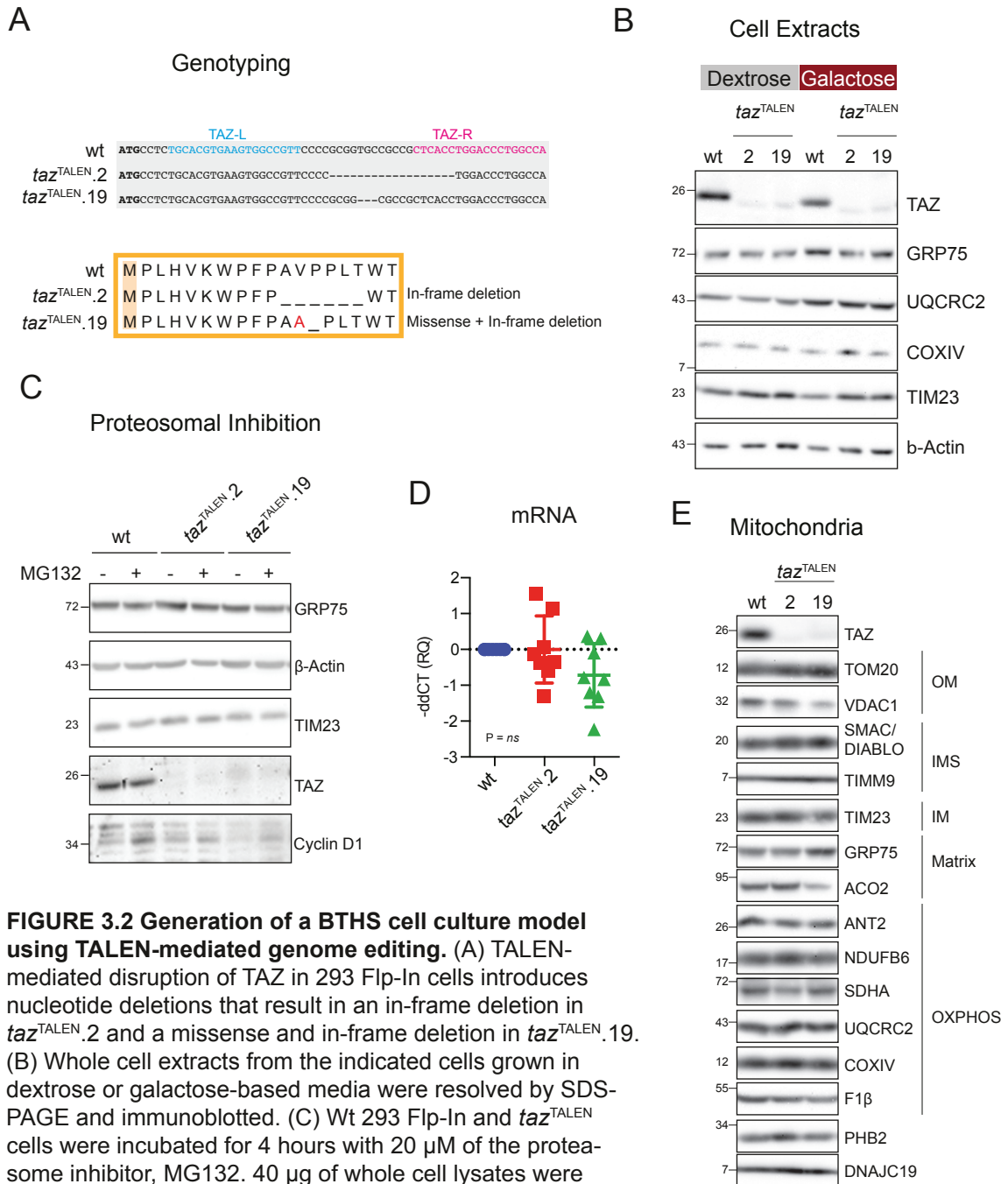


FIGURE 3.2 Generation of a BTHS cell culture model using TALEN-mediated genome editing. (A) TALEN-mediated disruption of TAZ in 293 Flp-In cells introduces nucleotide deletions that result in an in-frame deletion in *taz*^{TALEN.2} and a missense and in-frame deletion in *taz*^{TALEN.19}. (B) Whole cell extracts from the indicated cells grown in dextrose or galactose-based media were resolved by SDS-PAGE and immunoblotted. (C) Wt 293 Flp-In and *taz*^{TALEN} cells were incubated for 4 hours with 20 μM of the proteasome inhibitor, MG132. 40 μg of whole cell lysates were resolved by SDS-PAGE and immunoblotted for the indicated proteins. Cyclin D1, a target of the ubiquitin-proteasome pathway (78), is used as a positive control. (D) Relative mRNA levels of TAZ in wt (293 Flp-In) and each *taz*^{TALEN} cell. Data was analyzed by the comparative CT (ΔΔCT) method, represented as mean ΔΔCT ± SEM n = 8 relative to WT expression level, which was set to 0. [See next page for F-H and figure legends.]

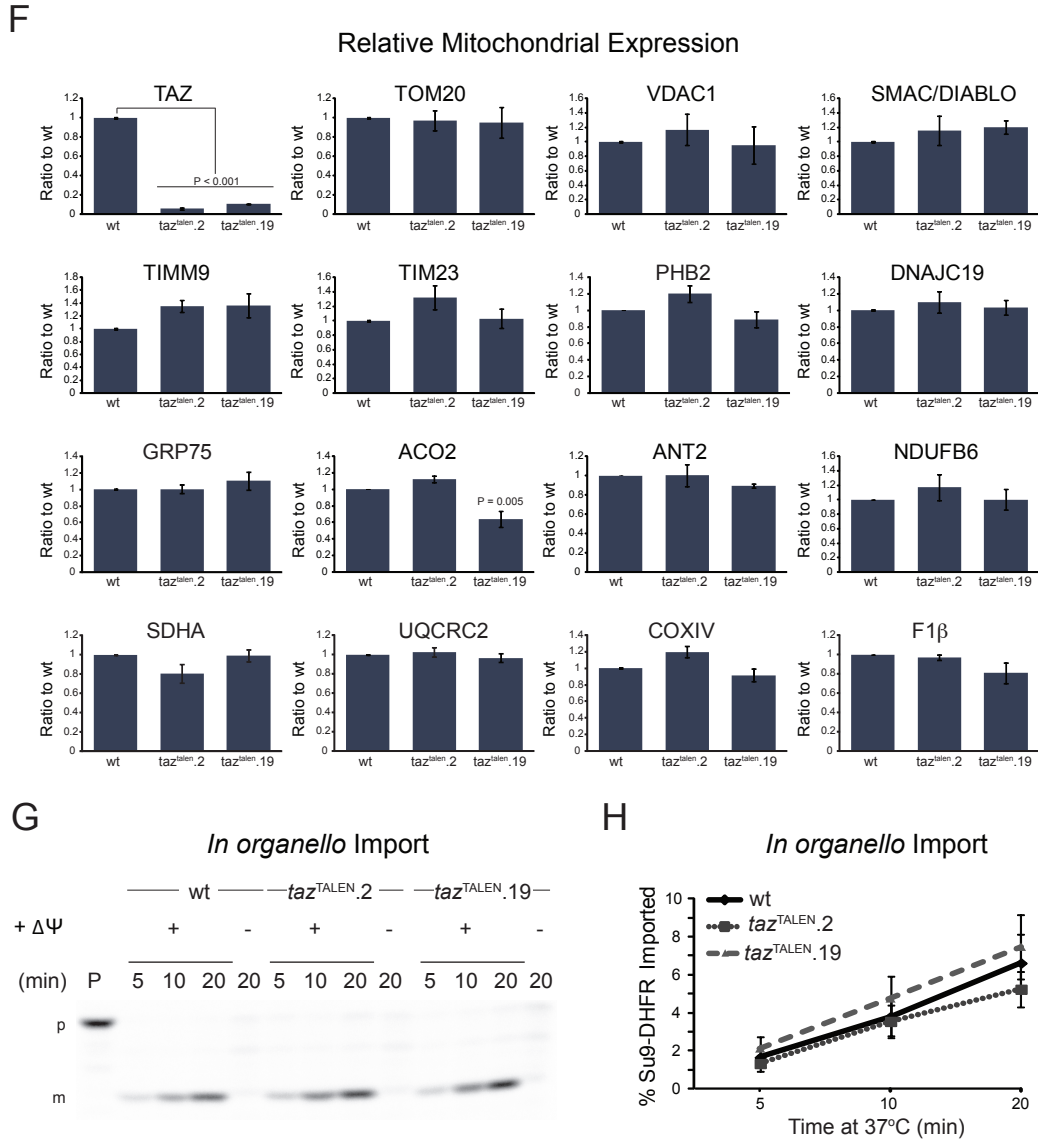


FIGURE 3.2 Generation of a BTBS cell culture model using TALEN-mediated genome editing. (E) Mitochondria (50 μg) from the designated source were immunoblotted as listed. (F) Protein expression in (E) was quantified by densitometry and normalized to wt levels (mean ± SEM; n = 3). Significant differences are indicated. (G) *In organello* import of radiolabeled [³⁵S]-Su9-DHFR into wt 293 Flp-In and *taz*^{TALEN} mitochondria in the presence or absence of a membrane potential. Following import, mitochondria were osmotically ruptured, treated with trypsin, resolved by SDS-PAGE, and bands detected by phosphoimaging. P, precursor (5% of precursor protein + 100 μg mitochondria); p, precursor; m, mature. (H) The percentage of precursor imported at each time point was calculated (mean ± SEM; n = 3). See also Fig S3.1 and Table 2.

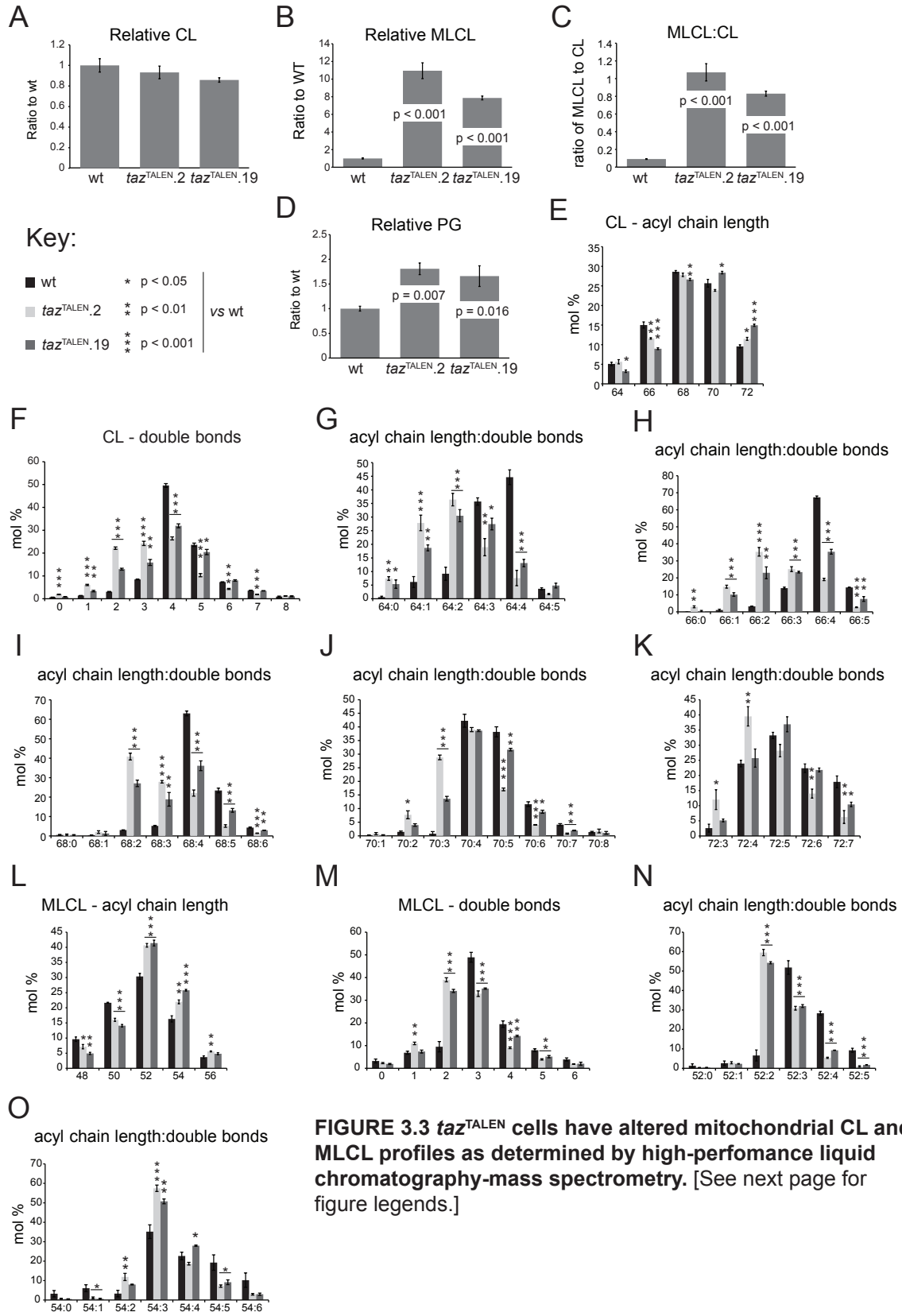


FIGURE 3.3 *taz*^{TALEN} cells have altered mitochondrial CL and MLCL profiles as determined by high-performance liquid chromatography-mass spectrometry. [See next page for figure legends.]

FIGURE 3.3 *faz*^{TALEN} cells have altered mitochondrial CL and MLCL profiles as determined by high-performance liquid chromatography-mass spectrometry. The relative amounts of CL (A), MLCL (B), and PG (D) was determined by high-performance liquid chromatography-mass spectrometry. (C) The ratio of MLCL:CL as determined from (A and B). The abundance of CL (E) and MLCL (L) of a given acyl chain length (E,L) or containing the indicated number of double bonds (F, M), was determined as a percentage of the total amount of CL or MLCL. The distribution of double bonds per acyl chain length for CL (G-K) and MLCL (N-O) expressed as a percent of the sum of all species of the indicated length. All data are the mean \pm SEM (n = 3). Significant differences are indicated. See also Figures 3.S2-3.S4.

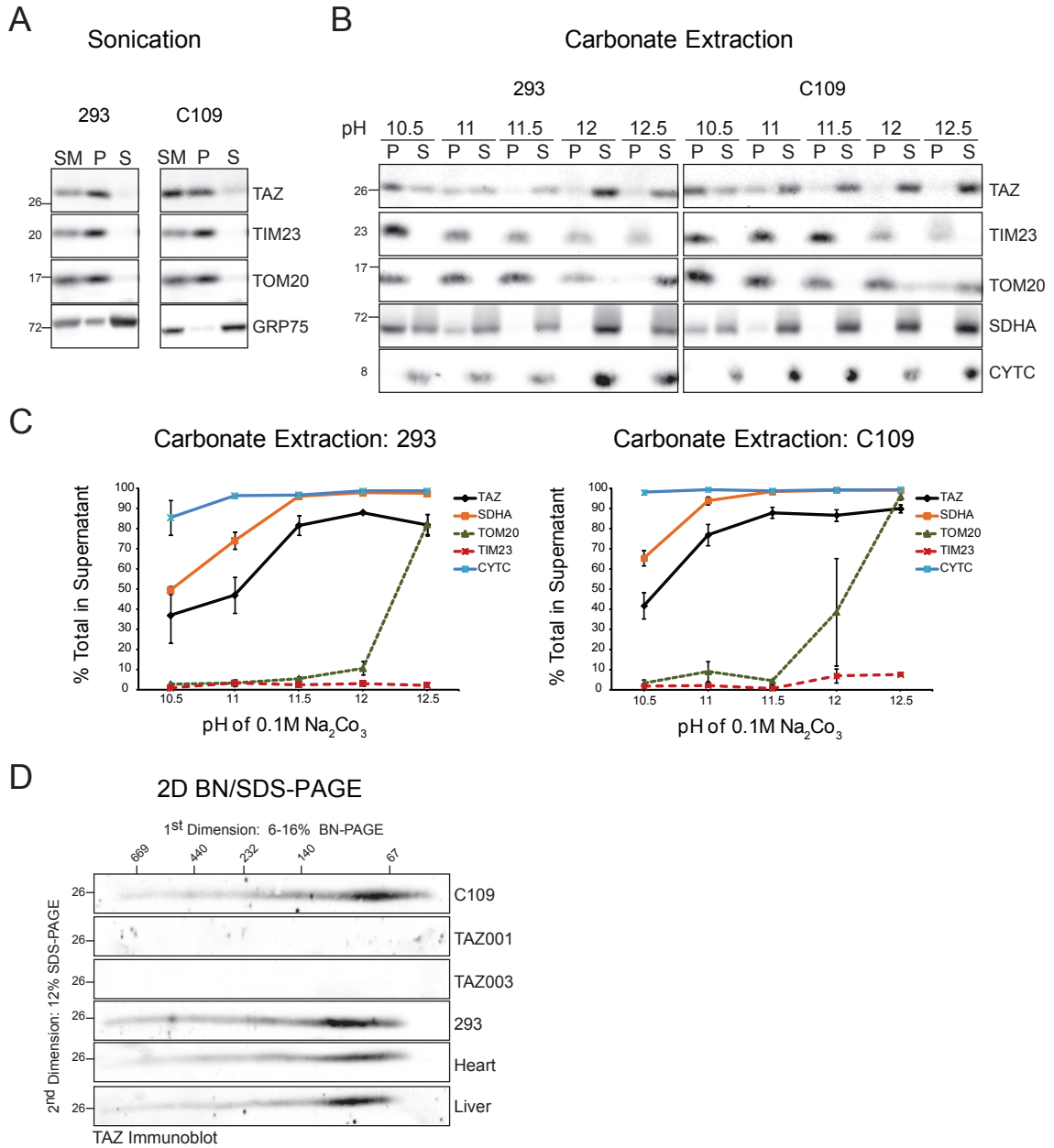


FIGURE 3.4 Membrane association and assembly of TAZ. (A) Mitochondria were sonicated and equal volumes of the pellet (P) and TCA-precipitated supernatant (S) fractions were immunoblotted as indicated. SM, starting material. (B) Mitochondria were incubated in 0.1 M Na_2CO_3 of the listed pH. Integral proteins (P) were separated from released proteins (S) by ultracentrifugation and equal volumes of each were immunoblotted as indicated. (C) Quantified band intensities of the P and S fractions were plotted as the percentage of total protein released into the supernatant for each pH (mean \pm SEM; $n = 3$ (C109) or 4 (293)). (D) Mitochondria from control and BTHS fibroblasts (450 μg), 293 Flp-In cells (200 μg), and mouse heart and liver (200 μg) were solubilized with digitonin, separated by 2D BN/SDS-PAGE, and immunoblotted for TAZ.

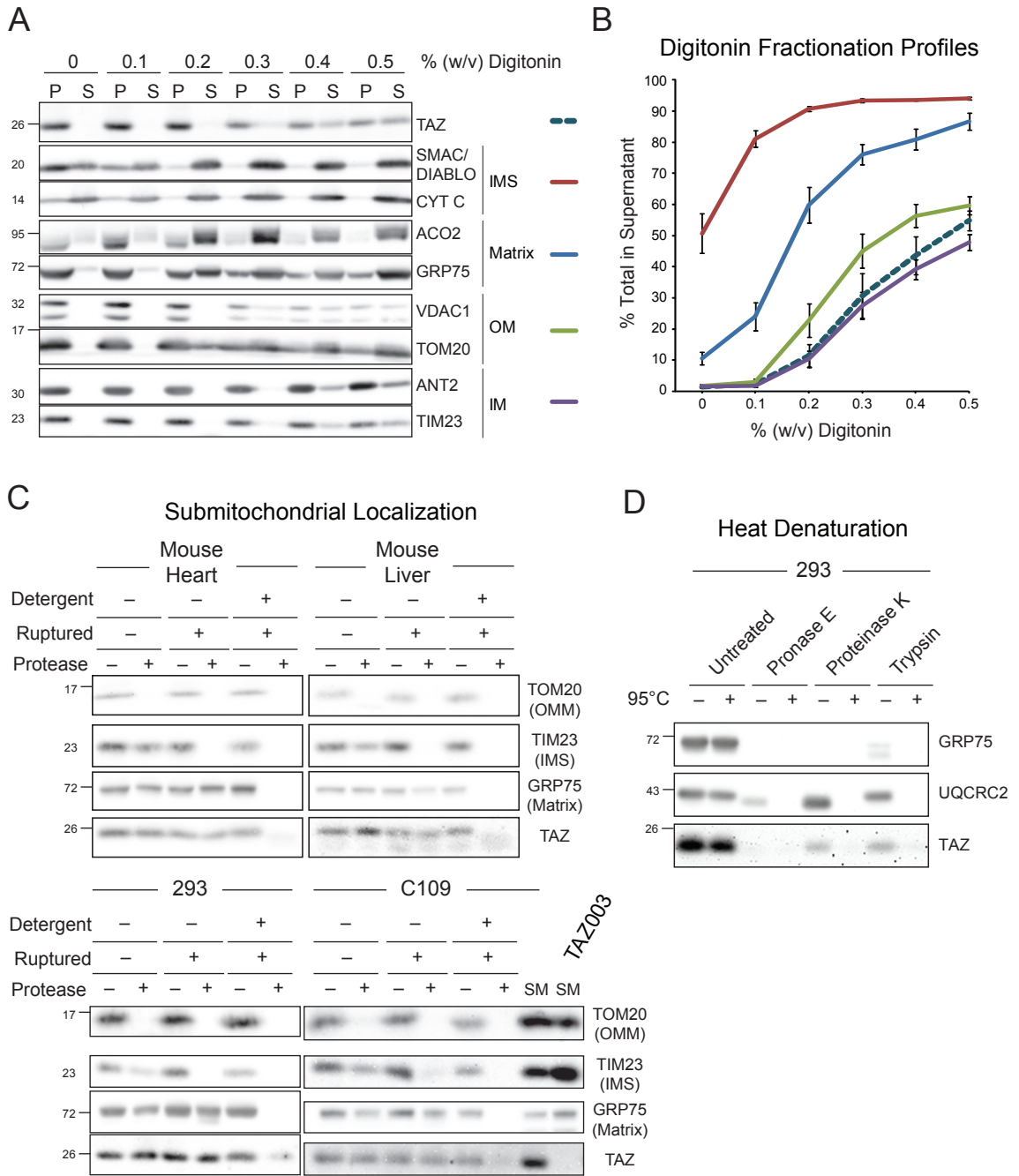


FIGURE 3.5 Mammalian TAZ is protease resistant and associates with IMS-facing leaflets.
 [See next page for F and figure legends.]

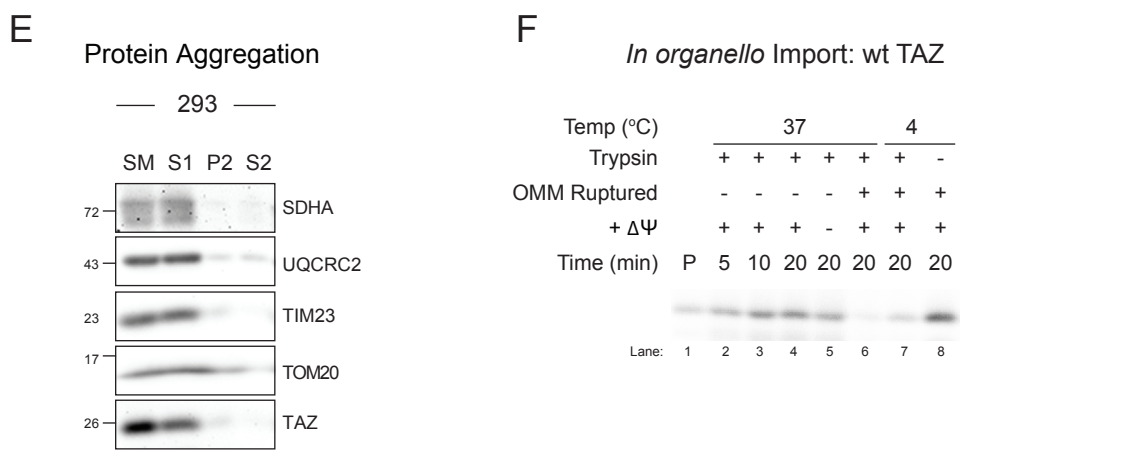


FIGURE 3.5 Mammalian TAZ is protease resistant and associates with IMS-facing leaflets.

(A) Mitochondria were titrated with increasing amounts of digitonin to differentially solubilize mitochondrial compartments. After centrifugation, equal volumes of the pellet (P) and supernatant (S) fractions were resolved by SDS-PAGE and immunoblotted. (B) Quantified band intensities for two markers per compartment were combined and plotted as the percent detected in supernatant (mean \pm SEM; $n = 7$). (C) Mitochondria, osmotically ruptured mitoplasts, or detergent-solubilized mitochondria from the indicated source were incubated without or with protease, resolved by SDS-PAGE, and immunoblotted. (D) Mitochondria were solubilized with 0.1% (w/v) SDS and where indicated, heated at 95°C for 5 minutes prior to adding pronase E, proteinase K, or trypsin. Equal volumes of each sample were resolved by SDS-PAGE and immunoblotted. (E) Mitochondria were solubilized with digitonin and fractionated into a supernatant (S1) and pellet (P1) by centrifugation. Material not extracted by digitonin (P1) was further solubilized with TX-100 and separated into a supernatant (S2) and pellet (P2) by centrifugation. Fractions were resolved by SDS-PAGE and immunoblotted as indicated. (F) *In organello* import of radiolabeled [³⁵S]-TAZ into 293 Flp-In mitochondria at the indicated temperature in the presence or absence of a membrane potential. Following import, mitochondria were treated with trypsin, resolved by SDS-PAGE, and bands detected by phosphoimaging. Where indicated, mitochondria were osmotically ruptured in the presence or absence of trypsin. P, precursor (5% of precursor protein + 100 μ g mitochondria).

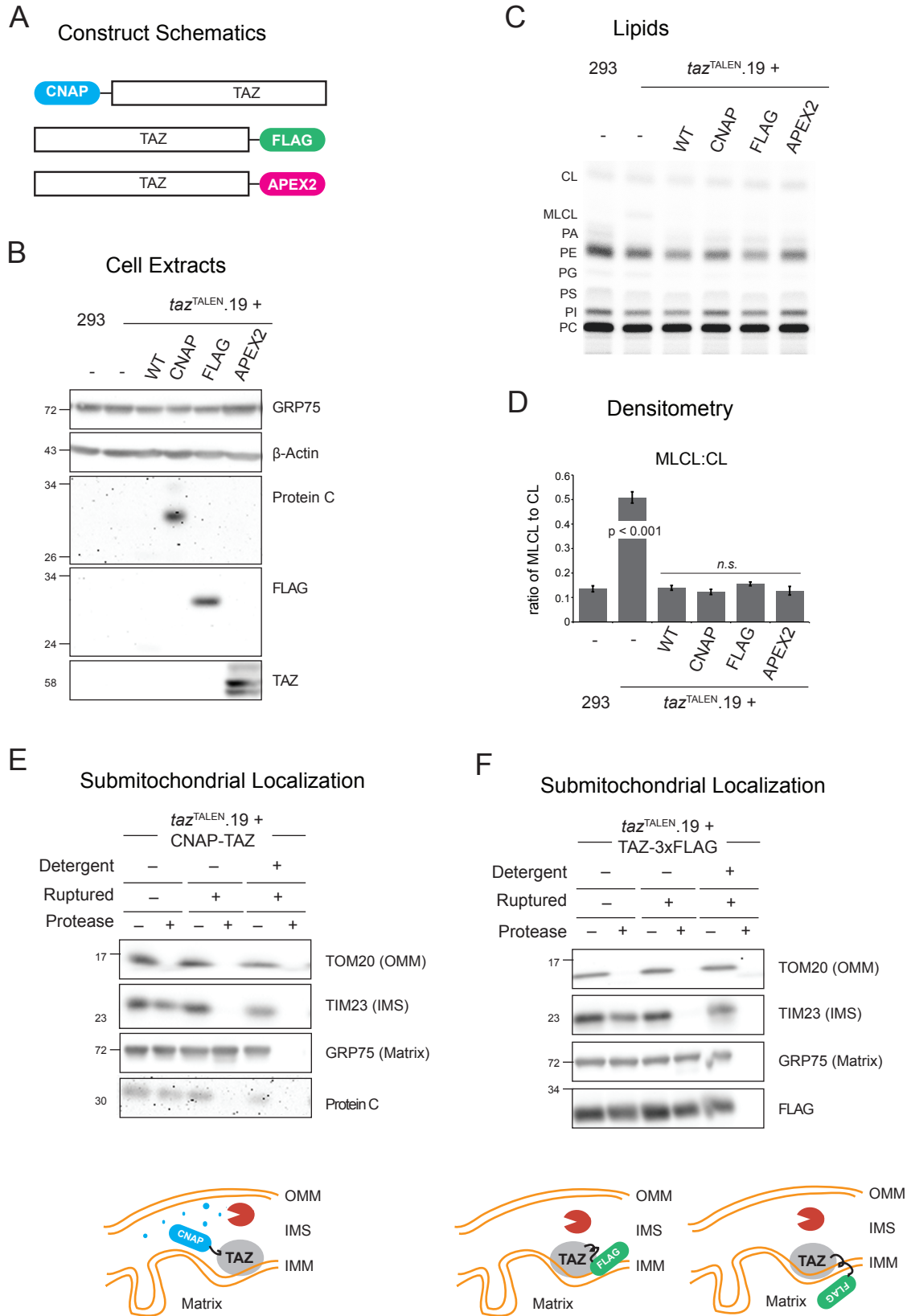
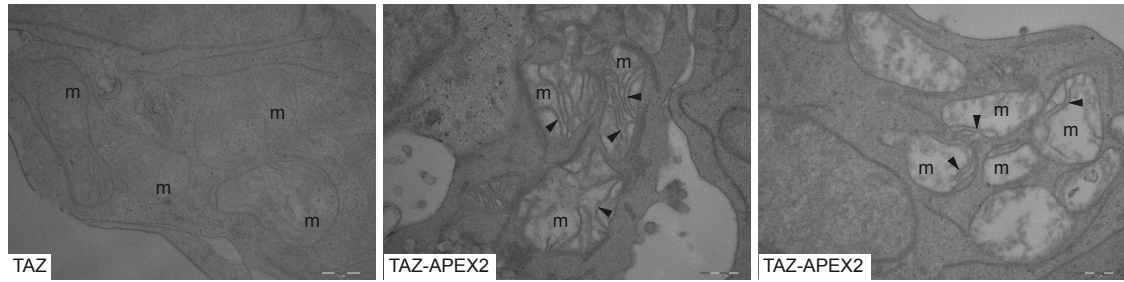


FIGURE 3.6 Both termini of TAZ are in the IMS. [See next page for G-H and figure legends.]

G EM - TAZ-APEX2



H Topology of Mammalian TAZ

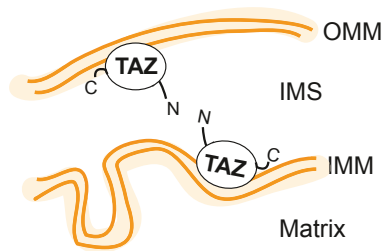


FIGURE 3.6 Both termini of TAZ are in the IMS.

(A) Cartoon of epitope tagged TAZ constructs. (B) Whole cell extracts (30 μ g) were immunoblotted for the indicated proteins. (C) Phospholipids from the indicated cells were labeled with 32 Pi and separated by TLC. (D) Quantification of the MLCL:CL ratio (mean \pm SEM; n=3). Significant differences compared to wt 293 Flp-In cells were determined by one-way ANOVA. n.s. = differences not significant. (E and F) The protease accessibility of epitope tags added to the NH₂ (E) or COOH (F) termini of TAZ was determined as in Fig 3.5C. (G) *taz*^{TALEN}.19 cells overexpressing WT or TAZ-APEX2 were labeled in vivo with H₂O₂ and DAB followed by OsO₄ and EM imaging. Scale bar, (H) Cartoon summary of the topology and membrane association of TAZ.

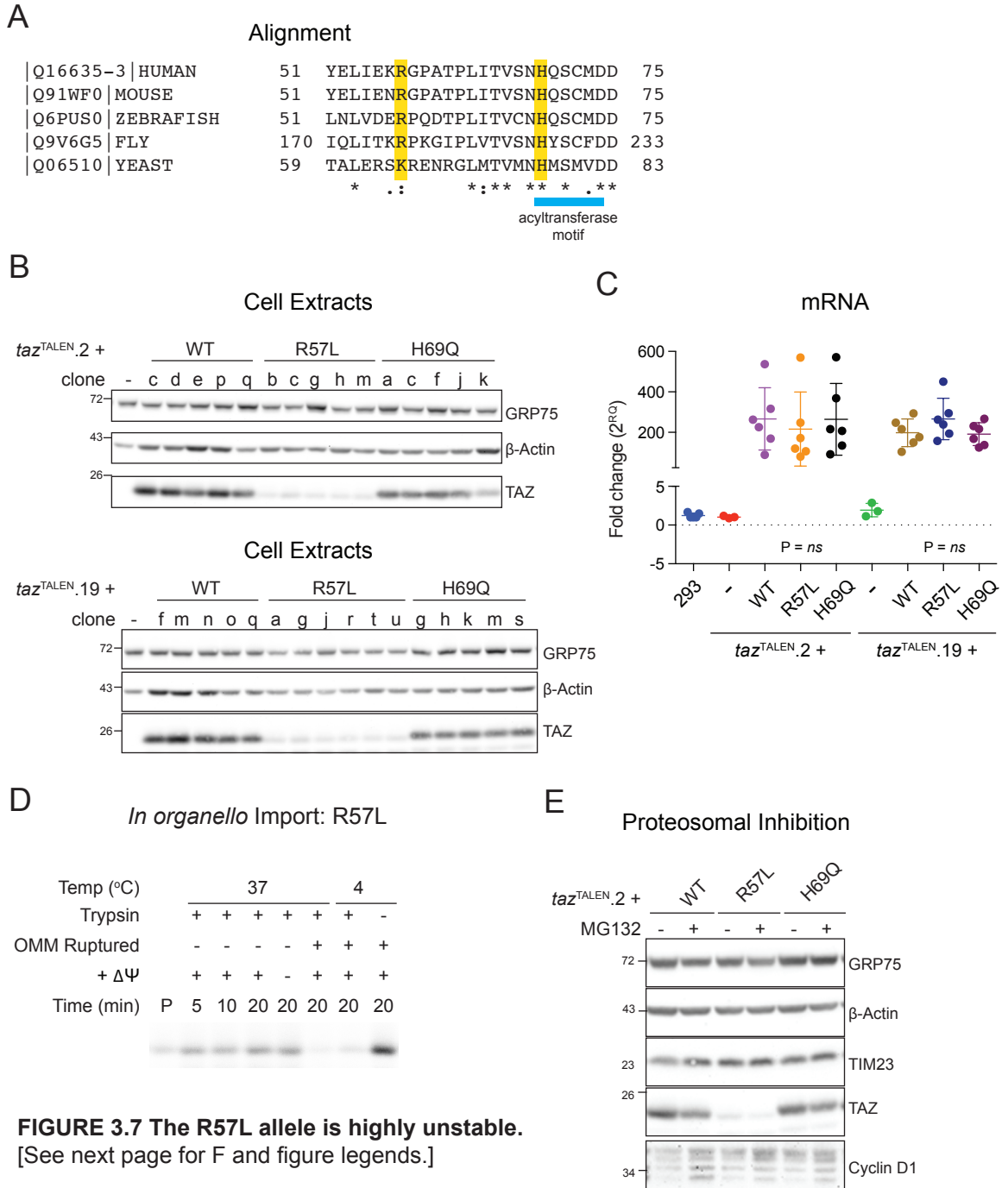


FIGURE 3.7 The R57L allele is highly unstable.
[See next page for F and figure legends.]

F

In vivo Degradation: Cell Extracts

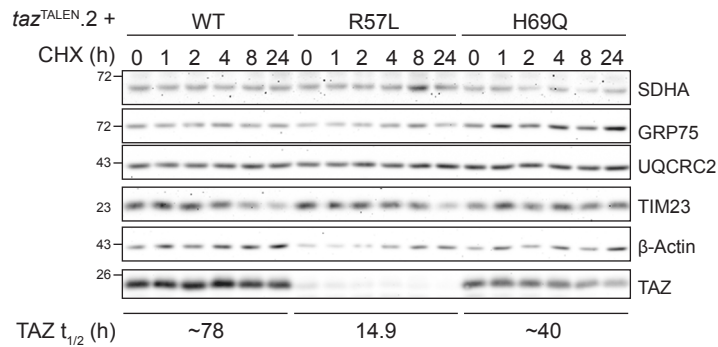


FIGURE 3.7 The R57L allele is highly unstable. (A) Sequence alignment of TAZ from the indicated species encompassing human Arg57 and His69 (highlighted) and the HXXXXD motif (underlined). (B) Whole cell extracts (20 μ g) from 5-6 clones transfected with the indicated TAZ alleles were immunoblotted. (C) Relative mRNA levels of TAZ analyzed by the comparative CT ($\Delta\Delta$ CT) method, represented as mean fold change ($2^{\Delta\Delta$ CT) \pm SD $n \geq 4$ relative to 293 Flp-In TAZ expression. (D) *In organello* import of radiolabeled precursor R57L TAZ into freshly isolated 293 Flp-In mitochondria as described in Fig. 3.5F. (E) *taz*^{TALEN} cells overexpressing WT, R57L and H69Q alleles were incubated for 4 hours with 20 μ M of the proteasome inhibitor, MG132. 40 μ g of whole cell lysates were resolved by SDS-PAGE and immunoblotted for the indicated proteins. (F) Whole cell extracts (20 μ g) were collected after incubation with cycloheximide for the indicated times, and the amount of TAZ remaining assessed by immunoblot. The half-lives of the indicated TAZ alleles were calculated using the mean of five individual repetitions. See also Fig. 3.S5.

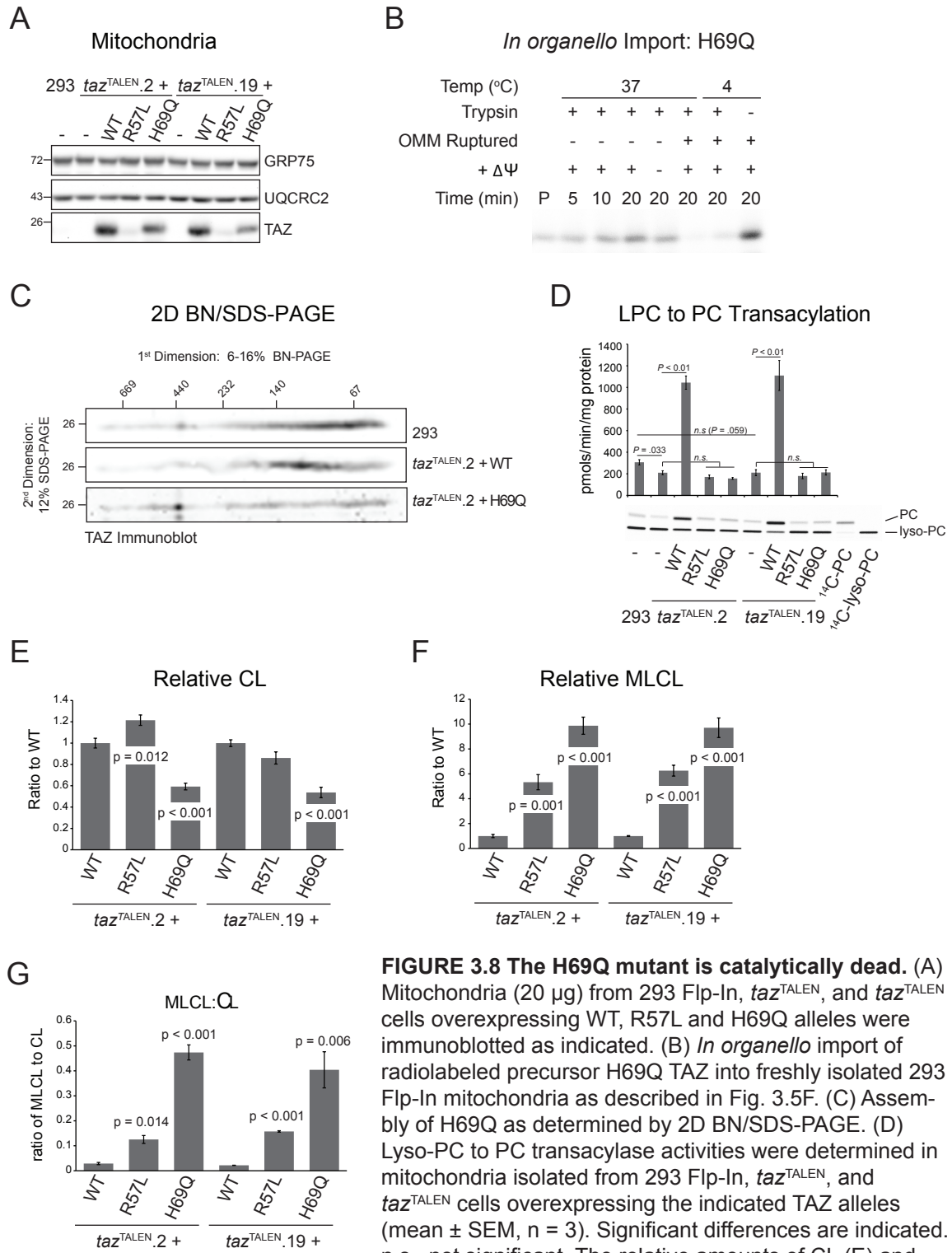


FIGURE 3.8 The H69Q mutant is catalytically dead. (A) Mitochondria (20 μ g) from 293 Flp-In, taz^{TALEN} , and taz^{TALEN} cells overexpressing WT, R57L and H69Q alleles were immunoblotted as indicated. (B) *In organello* import of radiolabeled precursor H69Q TAZ into freshly isolated 293 Flp-In mitochondria as described in Fig. 3.5F. (C) Assembly of H69Q as determined by 2D BN/SDS-PAGE. (D) Lyso-PC to PC transacylase activities were determined in mitochondria isolated from 293 Flp-In, taz^{TALEN} , and taz^{TALEN} cells overexpressing the indicated TAZ alleles (mean \pm SEM, $n = 3$). Significant differences are indicated. n.s., not significant. The relative amounts of CL (E) and MLCL (F), and the subsequent MLCL:CL ratio (G), in taz^{TALEN} cells overexpressing WT, R57L, and H69Q were determined as previously described. See also Figure 3.S5.

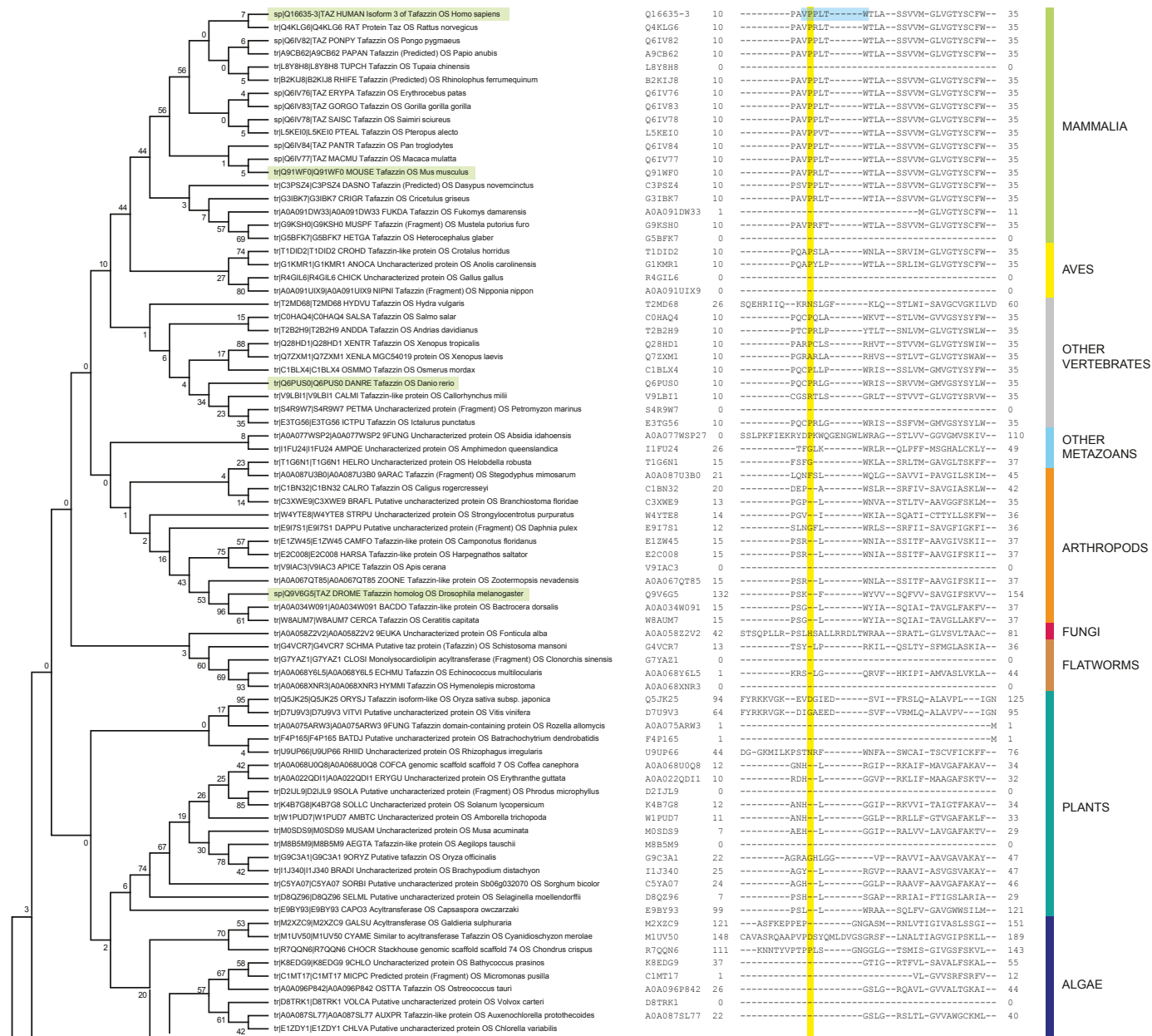


FIGURE 3.S1 Pro13 is conserved within mammals and some vertebrates but not fungi, bacteria, or plants. [Figure continued on next page.]

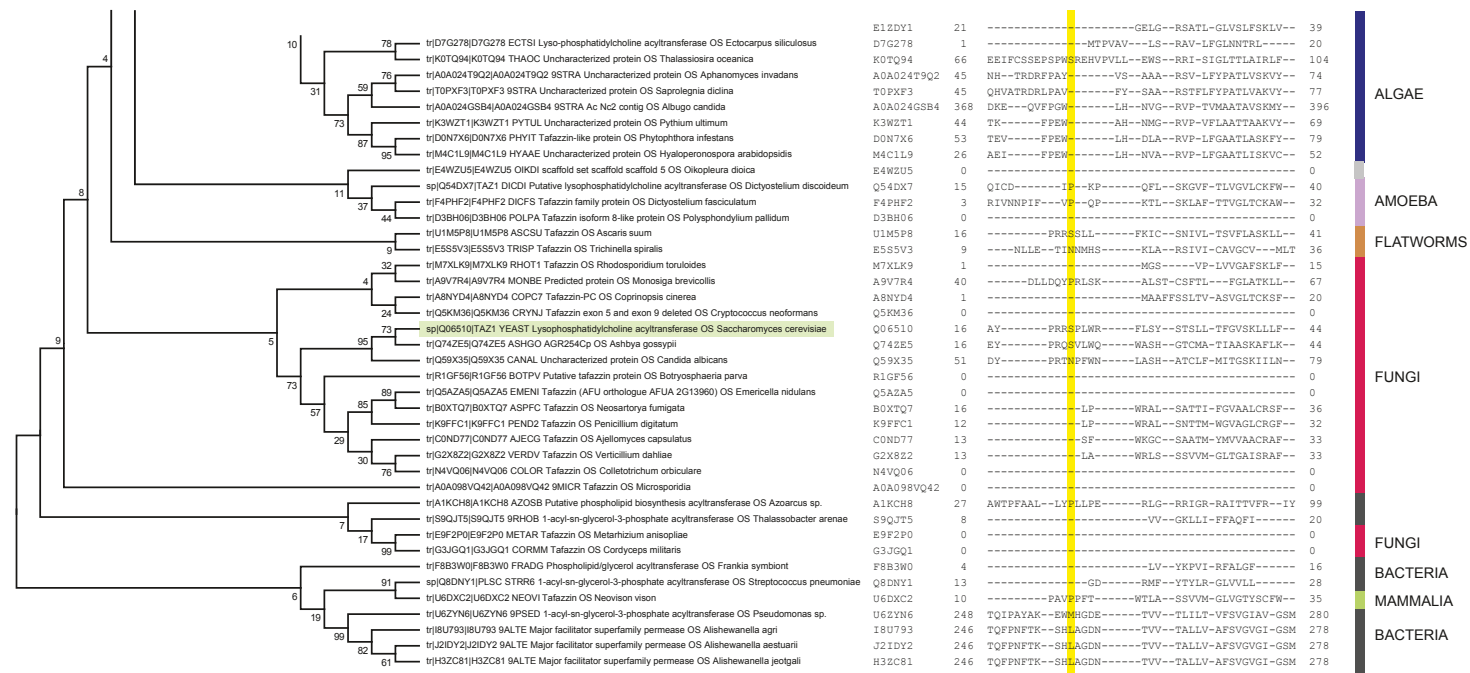


FIGURE 3.S1 Pro13 is conserved within mammals and some vertebrates but not fungi, bacteria, or plants. Sequence alignment of TAZ from humans and other organisms using COBALT (Papadopoulos and Agarwala, 2007). Only a section of the alignment encompassing human Pro13 is shown which is highlighted in yellow. The residues affected by TALEN-mediated disruption of 293 Flp-In cells are noted in blue in the sequence corresponding to human TAZ-ex5. Aligned sequences are then ordered according to the phylogenetic tree on the left. Organisms highlighted in green are those for which a BTHS (animal or cell) model is currently available. The evolutionary history was inferred by using the Maximum Likelihood (ML) method based on the JTT matrix-based model (Jones et al., 1992). The bootstrap consensus tree inferred from 500 replicates is taken to represent the evolutionary history of the taxa analyzed (Felsenstein, 1985). Branches corresponding to partitions produced in less than 50% bootstrap replicates are collapsed. The percentage of replicate trees in which the associated taxa clustered together in the bootstrap test is shown next to the branches. Initial tree(s) for the heuristic search were obtained by applying the Neighbor-Joining method to a matrix of pairwise distances estimated using a JTT model. The analysis involved 118 amino acid sequences. All positions with less than 95% site coverage were eliminated. That is, fewer than 5% alignment gaps, missing data, and ambiguous bases were allowed at any position. There were a total of 57 positions in the final dataset. Evolutionary analyses were conducted in MEGA6 (Tamura et al., 2013).

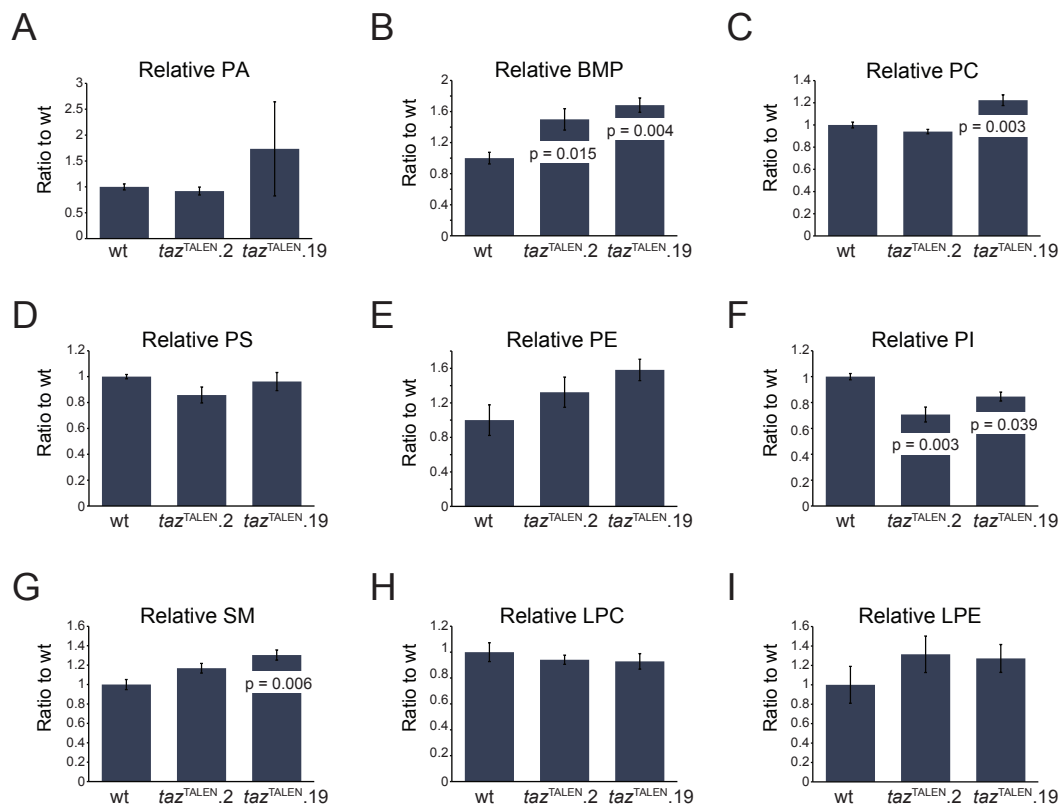


FIGURE 3.S2 Increased bis-monoacylglycerol phosphate (BMP) and decreased phosphatidylinositol (PI) in *taz*^{TALEN} mitochondria. The relative amounts of the indicated lipids in *taz*^{TALEN} compared to wt 293 Flp-In cells. All data are the mean \pm SEM (n = 3). Significant differences are indicated. PA, phosphatidic acid; PC, phosphatidylcholine; PS, phosphatidylserine;

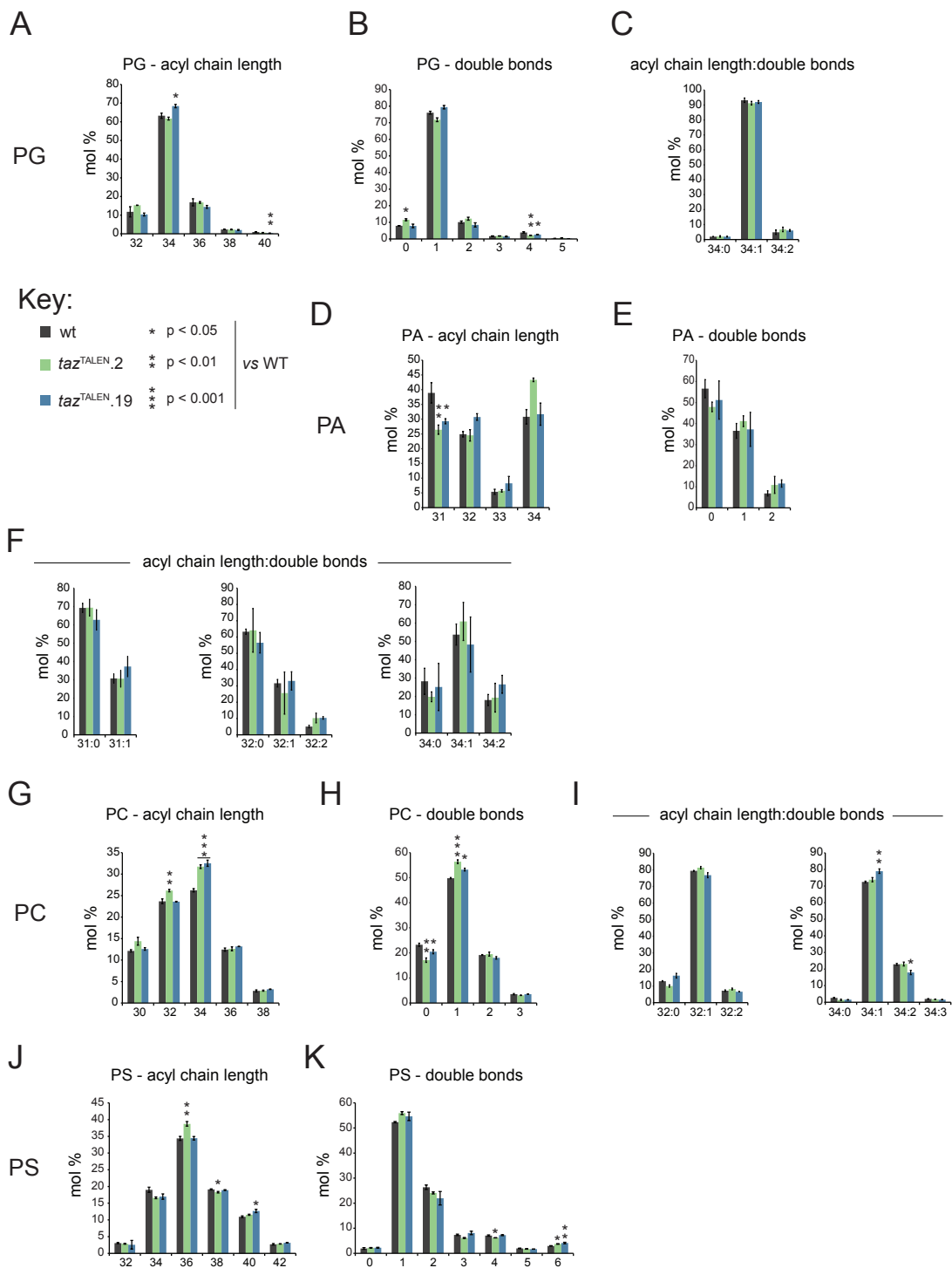


FIGURE 3.S3 *taz*^{TALEN} cells contain modest changes in acyl chain composition of the TAZ substrates, PE and PC. [See next page for L-S and figure legends.]

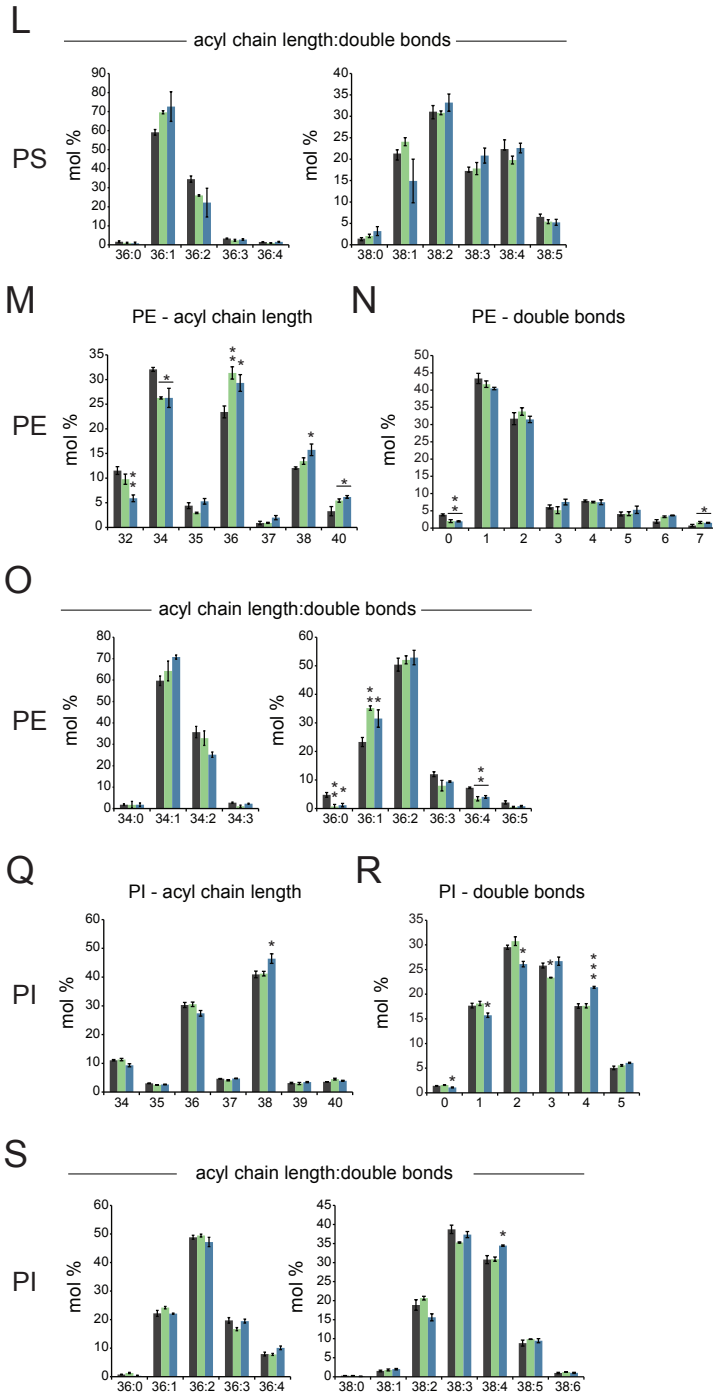
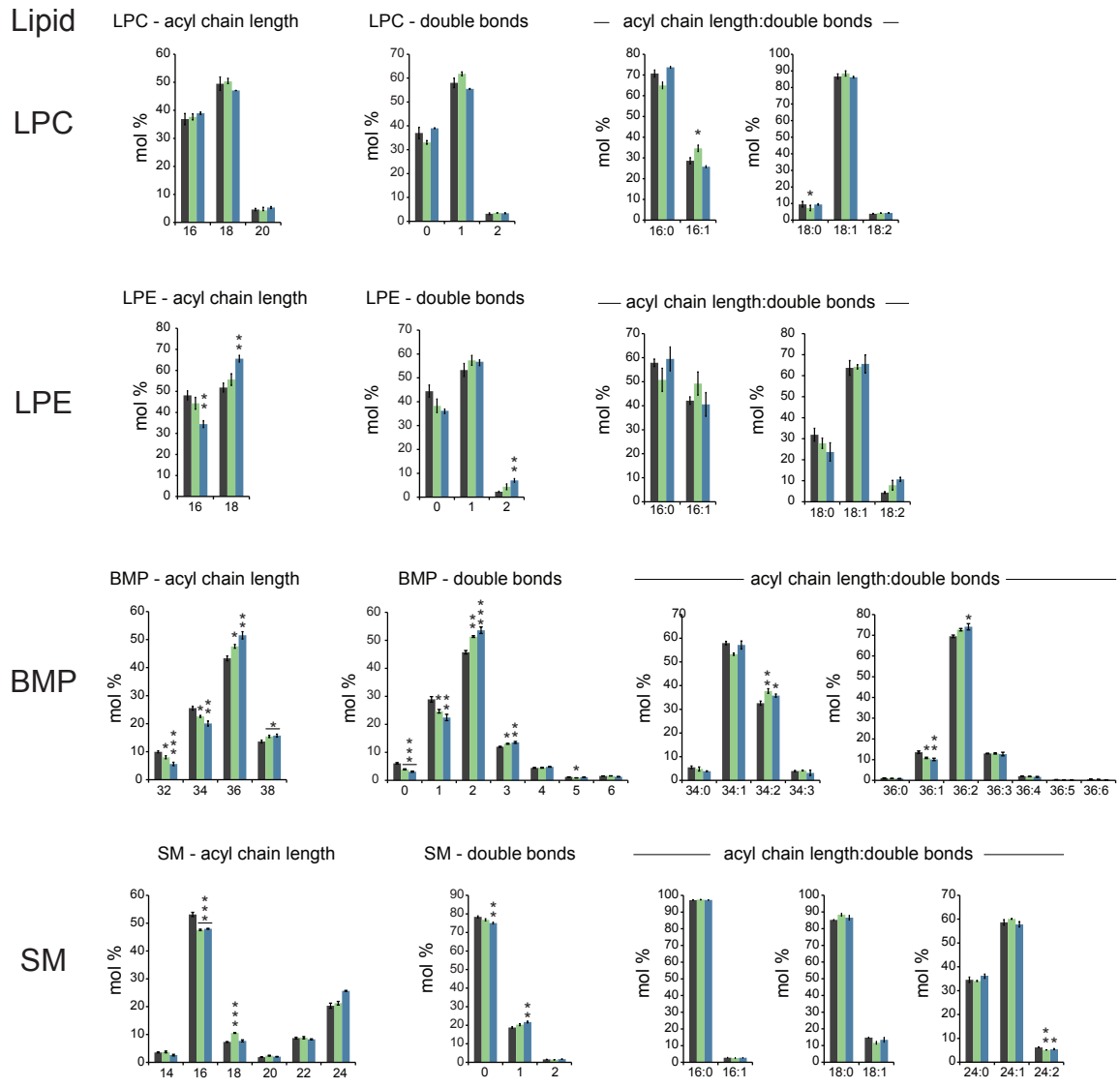


FIGURE 3.S3 *taz*^{TALEN} cells contain modest changes in acyl chain composition of the TAZ substrates, PE and PC. The acyl chain length, the number of double bonds, and the acyl chain length:double bond ratio for the indicated lipid species was determined as indicated in Figure 3.5. All data are the mean \pm SEM (n = 3). Significant differences are indicated.



Key:

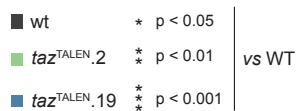


FIGURE 3.S4 Altered BMP acylation in mitochondria from *taz*^{TALEN} cells. The acyl chain length, the number of double bonds, and the acyl chain length:double bond ratio for the indicated lipid species were determined as indicated in Figure 3.5. All data are the mean ± SEM (n = 3). Significant differences are indicated.

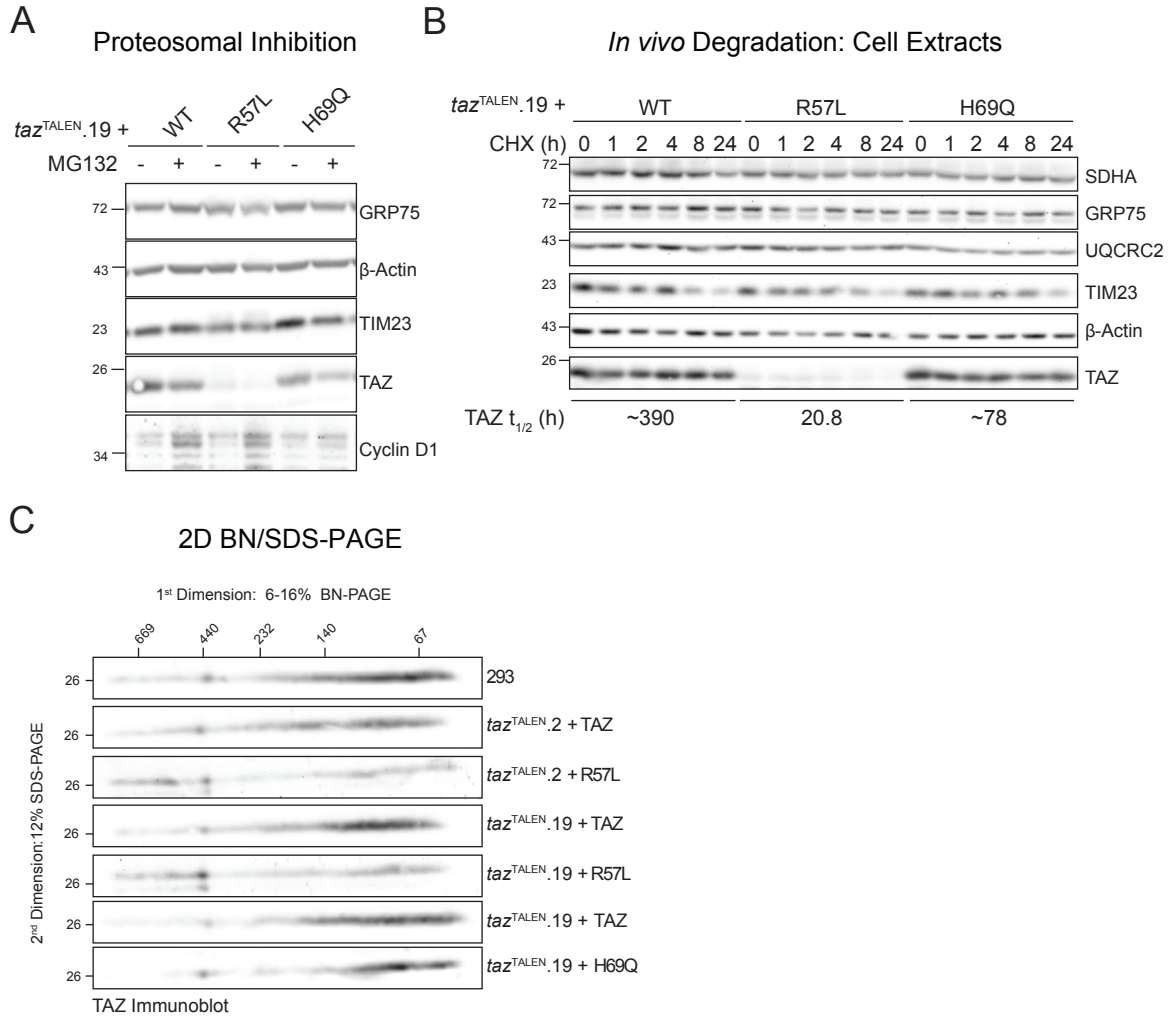


FIGURE 3.S5 The unstable R57L allele and the catalytically-null H69Q mutant assemble in high molecular weight complexes. (A) *taz*^{TALEN.19} cells overexpressing WT, R57L and H69Q alleles were incubated for 4 hours with 20 μ M of MG132. 40 μ g of whole cell lysates were resolved by SDS-PAGE and immunoblotted for the indicated proteins. (B) Mitochondrial extracts from 293 Flp-In and *taz*^{TALEN} cells overexpressing WT, R57L, or H69Q (200 μ g) were solubilized with digitonin, resolved by 2D BN/SDS-PAGE, and immunoblotted for TAZ. (C) The R57L allele has a relatively short half-life. Whole cell extracts (20 μ g) were collected after incubation with cycloheximide for the indicated times, and the amount of TAZ remaining assessed by immunoblot. The half-lives of the indicated TAZ alleles were calculated using the mean of five individual repetitions.

REFERENCES

- 1 Claypool, S.M. and Koehler, C.M. (2012) The complexity of cardiolipin in health and disease. *Trends in biochemical sciences*, **37**, 32-41.
- 2 Zhang, J., Guan, Z., Murphy, A.N., Wiley, S.E., Perkins, G.A., Worby, C.A., Engel, J.L., Heacock, P., Nguyen, O.K., Wang, J.H. *et al.* (2011) Mitochondrial phosphatase PTPMT1 is essential for cardiolipin biosynthesis. *Cell metabolism*, **13**, 690-700.
- 3 Claypool, S.M. (2009) Cardiolipin, a critical determinant of mitochondrial carrier protein assembly and function. *Biochimica et biophysica acta*, **1788**, 2059-2068.
- 4 Gebert, N., Joshi, A.S., Kutik, S., Becker, T., McKenzie, M., Guan, X.L., Mooga, V.P., Stroud, D.A., Kulkarni, G., Wenk, M.R. *et al.* (2009) Mitochondrial cardiolipin involved in outer-membrane protein biogenesis: implications for Barth syndrome. *Current biology : CB*, **19**, 2133-2139.
- 5 Kutik, S., Rissler, M., Guan, X.L., Guiard, B., Shui, G., Gebert, N., Heacock, P.N., Rehling, P., Dowhan, W., Wenk, M.R. *et al.* (2008) The translocator maintenance protein Tam41 is required for mitochondrial cardiolipin biosynthesis. *J. Cell Biol.*, **183**, 1213-1221.
- 6 Lange, C., Nett, J.H., Trumpower, B.L. and Hunte, C. (2001) Specific roles of protein-phospholipid interactions in the yeast cytochrome bc1 complex structure. *The EMBO journal*, **20**, 6591-6600.
- 7 Acín-Pérez, R., Fernández-Silva, P., Peleato, M.L., Pérez-Martos, A. and Enriquez, J.A. (2008) Respiratory Active Mitochondrial Supercomplexes. *Mol. Cell*, **32**, 529-539.
- 8 Pfeiffer, K., Gohil, V., Stuart, R.A., Hunte, C., Brandt, U., Greenberg, M.L. and Schagger, H. (2003) Cardiolipin stabilizes respiratory chain supercomplexes. *The Journal of biological chemistry*, **278**, 52873-52880.
- 9 Zhang, M., Mileykovskaya, E. and Dowhan, W. (2002) Gluing the respiratory chain together. Cardiolipin is required for supercomplex formation in the inner mitochondrial membrane. *The Journal of biological chemistry*, **277**, 43553-43556.
- 10 DeVay, R.M., Dominguez-Ramirez, L., Lackner, L.L., Hoppins, S., Stahlberg, H. and Nunnari, J. (2009) Coassembly of Mgm1 isoforms requires cardiolipin and mediates mitochondrial inner membrane fusion. *J. Cell Biol.*, **186**, 793-803.
- 11 Montessuit, S., Somasekharan, S.P., Terrones, O., Lucken-Ardjomande, S., Herzig, S., Schwarzenbacher, R., Manstein, D.J., Bossy-Wetzel, E., Basanez, G., Meda, P. *et al.* (2010) Membrane remodeling induced by the dynamin-related protein Drp1 stimulates Bax oligomerization. *Cell*, **142**, 889-901.

- 12 Chu, C.T., Ji, J., Dagda, R.K., Jiang, J.F., Tyurina, Y.Y., Kapralov, A.A., Tyurin, V.A., Yanamala, N., Shrivastava, I.H., Mohammadyani, D. *et al.* (2013) Cardiolipin externalization to the outer mitochondrial membrane acts as an elimination signal for mitophagy in neuronal cells. *Nature cell biology*, **15**, 1197-1205.
- 13 Gonzalvez, F., Schug, Z.T., Houtkooper, R.H., MacKenzie, E.D., Brooks, D.G., Wanders, R.J., Petit, P.X., Vaz, F.M. and Gottlieb, E. (2008) Cardiolipin provides an essential activating platform for caspase-8 on mitochondria. *J. Cell Biol.*, **183**, 681-696.
- 14 Baile, M.G., Lu, Y.W. and Claypool, S.M. (2014) The topology and regulation of cardiolipin biosynthesis and remodeling in yeast. *Chemistry and physics of lipids*, **179**, 25-31.
- 15 Schlame, M., Ren, M., Xu, Y., Greenberg, M.L. and Haller, I. (2005) Molecular symmetry in mitochondrial cardiolipins. *Chemistry and physics of lipids*, **138**, 38-49.
- 16 Xu, Y., Malhotra, A., Ren, M. and Schlame, M. (2006) The enzymatic function of tafazzin. *The Journal of biological chemistry*, **281**, 39217-39224.
- 17 Barth, P.G., Scholte, H.R., Berden, J.A., Van der Klei-Van Moorsel, J.M., Luyt-Houwen, I.E., Van 't Veer-Korthof, E.T., Van der Harten, J.J. and Sobotka-Plojhar, M.A. (1983) An X-linked mitochondrial disease affecting cardiac muscle, skeletal muscle and neutrophil leucocytes. *Journal of the neurological sciences*, **62**, 327-355.
- 18 Bione, S., D'Adamo, P., Maestrini, E., Gedeon, A.K., Bolhuis, P.A. and Toniolo, D. (1996) A novel X-linked gene, G4.5. is responsible for Barth syndrome. *Nature genetics*, **12**, 385-389.
- 19 Valianpour, F., Mitsakos, V., Schlemmer, D., Towbin, J.A., Taylor, J.M., Ekert, P.G., Thorburn, D.R., Munnich, A., Wanders, R.J., Barth, P.G. *et al.* (2005) Monolysocardiolipins accumulate in Barth syndrome but do not lead to enhanced apoptosis. *Journal of lipid research*, **46**, 1182-1195.
- 20 Houtkooper, R.H., Turkenburg, M., Poll-The, B.T., Karall, D., Perez-Cerda, C., Morrone, A., Malvagia, S., Wanders, R.J., Kulik, W. and Vaz, F.M. (2009) The enigmatic role of tafazzin in cardiolipin metabolism. *Biochimica et biophysica acta*, **1788**, 2003-2014.
- 21 Dudek, J., Cheng, I.F., Balleininger, M., Vaz, F.M., Streckfuss-Bomeke, K., Hubscher, D., Vukotic, M., Wanders, R.J., Rehling, P. and Guan, K. (2013) Cardiolipin deficiency affects respiratory chain function and organization in an induced pluripotent stem cell model of Barth syndrome. *Stem cell research*, **11**, 806-819.
- 22 Gonzalvez, F., D'Aurelio, M., Boutant, M., Moustapha, A., Puech, J.P., Landes, T., Arnaune-Pelloquin, L., Vial, G., Taleux, N., Slomianny, C. *et al.* (2013) Barth syndrome: cellular compensation of mitochondrial dysfunction and apoptosis inhibition due to changes in cardiolipin remodeling linked to tafazzin (TAZ) gene mutation. *Biochimica et biophysica acta*, **1832**, 1194-1206.

- 23 McKenzie, M., Lazarou, M., Thorburn, D.R. and Ryan, M.T. (2006) Mitochondrial respiratory chain supercomplexes are destabilized in Barth Syndrome patients. *Journal of molecular biology*, **361**, 462-469.
- 24 Wang, G., McCain, M.L., Yang, L., He, A., Pasqualini, F.S., Agarwal, A., Yuan, H., Jiang, D., Zhang, D., Zangi, L. *et al.* (2014) Modeling the mitochondrial cardiomyopathy of Barth syndrome with induced pluripotent stem cell and heart-on-chip technologies. *Nature medicine*, **20**, 616-623.
- 25 Lu, Y.W. and Claypool, S.M. (2015) Disorders of phospholipid metabolism: an emerging class of mitochondrial disease due to defects in nuclear genes. *Frontiers in genetics*, **6**, 3.
- 26 Davey, K.M., Parboosingh, J.S., McLeod, D.R., Chan, A., Casey, R., Ferreira, P., Snyder, F.F., Bridge, P.J. and Bernier, F.P. (2006) Mutation of DNAJC19, a human homologue of yeast inner mitochondrial membrane co-chaperones, causes DCMA syndrome, a novel autosomal recessive Barth syndrome-like condition. *Journal of medical genetics*, **43**, 385-393.
- 27 Mayr, J.A., Haack, T.B., Graf, E., Zimmermann, F.A., Wieland, T., Haberberger, B., Superti-Furga, A., Kirschner, J., Steinmann, B., Baumgartner, M.R. *et al.* (2012) Lack of the mitochondrial protein acylglycerol kinase causes Sengers syndrome. *American journal of human genetics*, **90**, 314-320.
- 28 Richter-Dennerlein, R., Korwitz, A., Haag, M., Tatsuta, T., Dargazanli, S., Baker, M., Decker, T., Lamkemeyer, T., Rugarli, E.I. and Langer, T. (2014) DNAJC19, a mitochondrial cochaperone associated with cardiomyopathy, forms a complex with prohibitins to regulate cardiolipin remodeling. *Cell metabolism*, **20**, 158-171.
- 29 Wortmann, S.B., Vaz, F.M., Gardeitchik, T., Vissers, L.E., Renkema, G.H., Schuurs-Hoeijmakers, J.H., Kulik, W., Lammens, M., Christin, C., Kluijtmans, L.A. *et al.* (2012) Mutations in the phospholipid remodeling gene SERAC1 impair mitochondrial function and intracellular cholesterol trafficking and cause dystonia and deafness. *Nature genetics*, **44**, 797-802.
- 30 Claypool, S.M., McCaffery, J.M. and Koehler, C.M. (2006) Mitochondrial mislocalization and altered assembly of a cluster of Barth syndrome mutant tafazzins. *J. Cell Biol.*, **174**, 379-390.
- 31 Claypool, S.M., Whited, K., Srijumnong, S., Han, X. and Koehler, C.M. (2011) Barth syndrome mutations that cause tafazzin complex lability. *J. Cell Biol.*, **192**, 447-462.
- 32 Whited, K., Baile, M.G., Currier, P. and Claypool, S.M. (2013) Seven functional classes of Barth syndrome mutation. *Human molecular genetics*, **22**, 483-492.
- 33 Gonzalez, I.L. (2005) Barth syndrome: TAZ gene mutations, mRNAs, and evolution. *Am. J. Med. Genet. A*, **134**, 409-414.

- 34 Vaz, F.M., Houtkooper, R.H., Valianpour, F., Barth, P.G. and Wanders, R.J. (2003) Only one splice variant of the human TAZ gene encodes a functional protein with a role in cardiolipin metabolism. *The Journal of biological chemistry*, **278**, 43089-43094.
- 35 Houtkooper, R.H., Rodenburg, R.J., Thiels, C., van Lenthe, H., Stet, F., Poll-The, B.T., Stone, J.E., Steward, C.G., Wanders, R.J., Smeitink, J. *et al.* (2009) Cardiolipin and monolysocardiolipin analysis in fibroblasts, lymphocytes, and tissues using high-performance liquid chromatography-mass spectrometry as a diagnostic test for Barth syndrome. *Analytical biochemistry*, **387**, 230-237.
- 36 Claypool, S.M., Boonthung, P., McCaffery, J.M., Loo, J.A. and Koehler, C.M. (2008) The cardiolipin transacylase, tafazzin, associates with two distinct respiratory components providing insight into Barth syndrome. *Molecular biology of the cell*, **19**, 5143-5155.
- 37 Brandner, K., Mick, D.U., Frazier, A.E., Taylor, R.D., Meisinger, C. and Rehling, P. (2005) Taz1, an outer mitochondrial membrane protein, affects stability and assembly of inner membrane protein complexes: implications for Barth Syndrome. *Molecular biology of the cell*, **16**, 5202-5214.
- 38 Hung, V., Zou, P., Rhee, H.W., Udeshi, N.D., Cracan, V., Svinkina, T., Carr, S.A., Mootha, V.K. and Ting, A.Y. (2014) Proteomic mapping of the human mitochondrial intermembrane space in live cells via ratiometric APEX tagging. *Mol. Cell*, **55**, 332-341.
- 39 Lam, S.S., Martell, J.D., Kamer, K.J., Deerinck, T.J., Ellisman, M.H., Mootha, V.K. and Ting, A.Y. (2015) Directed evolution of APEX2 for electron microscopy and proximity labeling. *Nature methods*, **12**, 51-54.
- 40 Baile, M.G., Whited, K. and Claypool, S.M. (2013) Deacylation on the matrix side of the mitochondrial inner membrane regulates cardiolipin remodeling. *Molecular biology of the cell*, **24**, 2008-2020.
- 41 Baile, M.G., Sathappa, M., Lu, Y.W., Pryce, E., Whited, K., McCaffery, J.M., Han, X., Alder, N.N. and Claypool, S.M. (2014) Unremodeled and remodeled cardiolipin are functionally indistinguishable in yeast. *The Journal of biological chemistry*, **289**, 1768-1778.
- 42 Schlame, M., Acehan, D., Berno, B., Xu, Y., Valvo, S., Ren, M., Stokes, D.L. and Eppand, R.M. (2012) The physical state of lipid substrates provides transacylation specificity for tafazzin. *Nature chemical biology*, **8**, 862-869.
- 43 Merkwirth, C., Dargazanli, S., Tatsuta, T., Geimer, S., Lower, B., Wunderlich, F.T., von Kleist-Retzow, J.C., Waisman, A., Westermann, B. and Langer, T. (2008) Prohibitins control cell proliferation and apoptosis by regulating OPA1-dependent cristae morphogenesis in mitochondria. *Genes & development*, **22**, 476-488.

- 44 Ho, S.N., Hunt, H.D., Horton, R.M., Pullen, J.K. and Pease, L.R. (1989) Site-directed mutagenesis by overlap extension using the polymerase chain reaction. *Gene*, **77**, 51-59.
- 45 Claypool, S.M., Oktay, Y., Boonthung, P., Loo, J.A. and Koehler, C.M. (2008) Cardiolipin defines the interactome of the major ADP/ATP carrier protein of the mitochondrial inner membrane. *J. Cell Biol.*, **182**, 937-950.
- 46 Panneels, V., Schussler, U., Costagliola, S. and Sinning, I. (2003) Choline head groups stabilize the matrix loop regions of the ATP/ADP carrier ScAAC2. *Biochemical and biophysical research communications*, **300**, 65-74.
- 47 Claypool, S.M., Dickinson, B.L., Yoshida, M., Lencer, W.I. and Blumberg, R.S. (2002) Functional reconstitution of human FcRn in Madin-Darby canine kidney cells requires co-expressed human beta 2-microglobulin. *The Journal of biological chemistry*, **277**, 28038-28050.
- 48 Frezza, C., Cipolat, S. and Scorrano, L. (2007) Organelle isolation: functional mitochondria from mouse liver, muscle and cultured fibroblasts. *Nature protocols*, **2**, 287-295.
- 49 O'Shea, K.M., Khairallah, R.J., Sparagna, G.C., Xu, W., Hecker, P.A., Robillard-Frayne, I., Des Rosiers, C., Kristian, T., Murphy, R.C., Fiskum, G. *et al.* (2009) Dietary omega-3 fatty acids alter cardiac mitochondrial phospholipid composition and delay Ca²⁺-induced permeability transition. *Journal of molecular and cellular cardiology*, **47**, 819-827.
- 50 Palmer, J.W., Tandler, B. and Hoppel, C.L. (1977) Biochemical properties of subsarcolemmal and interfibrillar mitochondria isolated from rat cardiac muscle. *The Journal of biological chemistry*, **252**, 8731-8739.
- 51 Untergasser, A., Nijveen, H., Rao, X., Bisseling, T., Geurts, R. and Leunissen, J.A. (2007) Primer3Plus, an enhanced web interface to Primer3. *Nucleic acids research*, **35**, W71-74.
- 52 Chambers, M.C., Maclean, B., Burke, R., Amodei, D., Ruderman, D.L., Neumann, S., Gatto, L., Fischer, B., Pratt, B., Egertson, J. *et al.* (2012) A cross-platform toolkit for mass spectrometry and proteomics. *Nat. Biotech.*, **30**, 918-920.
- 53 Smith, C.A., Want, E.J., O'Maille, G., Abagyan, R. and Siuzdak, G. (2006) XCMS: processing mass spectrometry data for metabolite profiling using nonlinear peak alignment, matching, and identification. *Analytical chemistry*, **78**, 779-787.
- 54 Schneider, C.A., Rasband, W.S. and Eliceiri, K.W. (2012) NIH Image to ImageJ: 25 years of image analysis. *Nature methods*, **9**, 671-675.

- 55 Reynolds, S.M., Kall, L., Riffle, M.E., Bilmes, J.A. and Noble, W.S. (2008) Transmembrane topology and signal peptide prediction using dynamic bayesian networks. *PLoS computational biology*, **4**, e1000213.
- 56 Hirokawa, T., Boon-Chieng, S. and Mitaku, S. (1998) SOSUI: classification and secondary structure prediction system for membrane proteins. *Bioinformatics*, **14**, 378-379.
- 57 Krogh, A., Larsson, B., von Heijne, G. and Sonnhammer, E.L. (2001) Predicting transmembrane protein topology with a hidden Markov model: application to complete genomes. *Journal of molecular biology*, **305**, 567-580.
- 58 Tusnady, G.E. and Simon, I. (2001) The HMMTOP transmembrane topology prediction server. *Bioinformatics*, **17**, 849-850.
- 59 Cao, B., Porollo, A., Adamczak, R., Jarrell, M. and Meller, J. (2006) Enhanced recognition of protein transmembrane domains with prediction-based structural profiles. *Bioinformatics*, **22**, 303-309.
- 60 Kall, L., Krogh, A. and Sonnhammer, E.L. (2004) A combined transmembrane topology and signal peptide prediction method. *Journal of molecular biology*, **338**, 1027-1036.
- 61 Juretic, D., Zoranic, L. and Zucic, D. (2002) Basic charge clusters and predictions of membrane protein topology. *Journal of chemical information and computer sciences*, **42**, 620-632.
- 62 Hennerdal, A. and Elofsson, A. (2011) Rapid membrane protein topology prediction. *Bioinformatics*, **27**, 1322-1323.
- 63 Viklund, H. and Elofsson, A. (2008) OCTOPUS: improving topology prediction by two-track ANN-based preference scores and an extended topological grammar. *Bioinformatics*, **24**, 1662-1668.
- 64 Bernsel, A., Viklund, H., Falk, J., Lindahl, E., von Heijne, G. and Elofsson, A. (2008) Prediction of membrane-protein topology from first principles. *Proceedings of the National Academy of Sciences of the United States of America*, **105**, 7177-7181.
- 65 Viklund, H. and Elofsson, A. (2004) Best alpha-helical transmembrane protein topology predictions are achieved using hidden Markov models and evolutionary information. *Protein science : a publication of the Protein Society*, **13**, 1908-1917.
- 66 Cserzo, M., Eisenhaber, F., Eisenhaber, B. and Simon, I. (2004) TM or not TM: transmembrane protein prediction with low false positive rate using DAS-TMfilter. *Bioinformatics*, **20**, 136-137.
- 67 Pashou, E.E., Litou, Z.I., Liakopoulos, T.D. and Hamodrakas, S.J. (2004) waveTM: wavelet-based transmembrane segment prediction. *In silico biology*, **4**, 127-131.

- 68 Claros, M.G. and von Heijne, G. (1994) TopPred II: an improved software for membrane protein structure predictions. *Computer applications in the biosciences : CABIOS*, **10**, 685-686.
- 69 Hofmann, K. and Stoffel, W. (1993) TMbase - A database of membrane spanning proteins segments. *Biol. Chem. Hoppe-Seyler*, **374**.
- 70 Emanuelsson, O., Nielsen, H., Brunak, S. and von Heijne, G. (2000) Predicting subcellular localization of proteins based on their N-terminal amino acid sequence. *Journal of molecular biology*, **300**, 1005-1016.
- 71 Claros, M.G. and Vincens, P. (1996) Computational method to predict mitochondrially imported proteins and their targeting sequences. *European journal of biochemistry / FEBS*, **241**, 779-786.
- 72 Gavel, Y. and von Heijne, G. (1990) Cleavage-site motifs in mitochondrial targeting peptides. *Protein engineering*, **4**, 33-37.
- 73 Horton, P. and Nakai, K. (1997) Better prediction of protein cellular localization sites with the k nearest neighbors classifier. *Proceedings / ... International Conference on Intelligent Systems for Molecular Biology ; ISMB. International Conference on Intelligent Systems for Molecular Biology*, **5**, 147-152.
- 74 Fariselli, P., Savojardo, C., Martelli, P.L. and Casadio, R. (2009) Grammatical-Restrained Hidden Conditional Random Fields for Bioinformatics applications. *Algorithms for molecular biology : AMB*, **4**, 13.
- 75 Small, I., Peeters, N., Legeai, F. and Lurin, C. (2004) Predotar: A tool for rapidly screening proteomes for N-terminal targeting sequences. *Proteomics*, **4**, 1581-1590.
- 76 Bannai, H., Tamada, Y., Maruyama, O., Nakai, K. and Miyano, S. (2002) Extensive feature detection of N-terminal protein sorting signals. *Bioinformatics*, **18**, 298-305.
- 77 Fukasawa, Y., Tsuji, J., Fu, S.C., Tomii, K., Horton, P. and Imai, K. (2015) MitoFates: improved prediction of mitochondrial targeting sequences and their cleavage sites. *Molecular & cellular proteomics : MCP*, **14**, 1113-1126.
- 78 Diehl, J.A., Zindy, F. and Sherr, C.J. (1997) Inhibition of cyclin D1 phosphorylation on threonine-286 prevents its rapid degradation via the ubiquitin-proteasome pathway. *Genes & development*, **11**, 957-972.

SUPPLEMENTAL REFERENCES

- 1 Papadopoulos, J.S. and Agarwala, R. (2007) COBALT: constraint-based alignment tool for multiple protein sequences. *Bioinformatics*, **23**, 1073-1079.
- 2 Jones, D.T., Taylor, W.R. and Thornton, J.M. (1992) The rapid generation of mutation data matrices from protein sequences. *Comput Appl Biosci*, **8**, 275-282.
- 3 Felsenstein, J. (1985) Confidence limits on phylogenies: an approach using the bootstrap. *Evolution*, **39**, 783-791.
- 4 Tamura, K., Stecher, G., Peterson, D., Filipski, A. and Kumar, S. (2013) MEGA6: Molecular Evolutionary Genetics Analysis version 6.0. *Mol Biol Evol*, **30**, 2725-2729.

CHAPTER 4

Future Directions

FUTURE DIRECTIONS

The fortuitous development of antibodies against endogenous human and rodent tafazzin (TAZ) in our lab has enabled the biochemical and cell biologic characterization of human TAZ detailed in the previous chapter. Mammalian TAZ is localized to IMS-facing leaflets of the outer (OMM) and inner (IMM) mitochondrial membranes, just like its yeast counterpart. The protein is membrane associated, likely in an interfacial manner, with both termini protruding into the IMS. Based on its extreme protease-resistance, the entire protein, including appendages added to the C-terminus, adopts a tightly-folded final structure. Having characterized the TAZ monoclonal antibodies and the cell biology of TAZ, we sought to establish a BTHS cell model whereby the loss-of-function mechanisms can be systematically dissected biochemically, at the protein level. Using TALEN-mediated genome editing in HEK293 Flp-In cells, *taz*^{TALEN} mutants were obtained that lacked detectable TAZ protein or activity. In these backgrounds, WT, R57L, and H69Q TAZ alleles were introduced by FLP recombination at the FRT site. Importantly, expression of WT TAZ in *taz*^{TALEN} cells restored the MLCL:CL ratio that is a hallmark of the disease to wt 293 levels. In contrast, the expression of the pathogenic R57L and H69Q alleles could not restore the lipid abnormalities in *taz*^{TALEN} cells to WT TAZ levels. In fact, the mutant alleles exhibited phenotypes that were consistent with that of equivalent mutations when modeled in yeast (1); H69Q is catalytically-dead, as expected, and R57L is functional but unstable with a short half-life. The corresponding K65L in yeast is temperature-sensitive (1). These observations are intriguing and suggest that for certain pathogenic mutations, such as R57L, drugs that can maximize the mutant allele's residual activity by stabilizing the polypeptide structure or retarding its

accelerated turnover may provide viable treatment options. Moreover, these results confirm that our BTHS cell model can serve as a convenient platform that can be used to further interrogate the mechanisms that underlie the spectrum of BTHS patient mutants.

The beauty of science and the process of discovery is that every question answered represents the beginning of many more that will emerge. So while we demonstrate that the subcellular localization of mammalian TAZ and the loss of function mechanisms of the R57L and H69Q alleles are conserved with its yeast counterpart, our characterization of TAZ is but one piece of a larger puzzle. Can the other patient mutations be recapitulated and studied in our *taz*^{TALEN} system? What is the respiratory capacity of *taz*^{TALEN} cells relative to the parental 293, or that of *taz*^{TALEN}s expressing WT versus mutant alleles? How do TAZ mRNA expression compare to that of steady state protein levels? Is there a correlation? And if not, is TAZ expression regulated translationally or post-translationally? Does TAZ interact with other proteins? How may these interactions, if they exist, affect TAZ function? These are but a few of the questions that arise with the end of the previous chapter. Below are potential directions, grouped thematically, that can be pursued.

Function

To address some of the immediate issues that were beyond the capacity of Chapter 2, a logical next step would be to subject *taz*^{TALEN}s expressing WT- or mutant TAZ to a battery of tests (including, and not limited to, ATP turnover, proton leak, maximal respiratory capacity, substrate preference) for respiratory function. It has been noted by several groups that *taz* models contain destabilized respiratory supercomplexes (2-4) and reduced electron transport chain activities (5) that likely compromise energetic

output. Indeed, the expression of WT TAZ in our *taz*^{TALEN} system is able to rescue the lipid defect that defines the syndrome, however, by quantifying the respiratory function in our novel BTHS cell model lacking TAZ protein and function, a baseline respiratory capacity can be established to investigate how other pathogenic BTHS missense mutations influence energy production. Using classical methods such as the oxygen electrode and individual respiratory activity assays, the effect of various *taz* lesions can be assessed. For instance, oxygen consumption by mitochondria can be monitored in cells after the selective permeabilization of the plasma membrane with minute levels of digitonin and upon the addition of respiratory complex-linked substrates (6, 7). In this manner, the rate of oxygen consumption becomes a measure of the electron flux through the system. Cells with defective TAZ have respiratory impairments (3, 5, 8-10); therefore, it is expected that respiratory defects will be revealed with the use of an oxygen electrode or with the Extracellular Flux instrument for high throughput analysis. Alternative methods to confirm the respiratory defect could also involve in-gel activity assays. Respiratory activities can be followed colorimetrically by supplying exogenous substrates or artificial electron donors to native gels providing insight into both function and assembly.

The major ADP/ATP carrier in yeast, Aac2p, interacts with a number of protein complexes as well as respiratory supercomplexes. Notably, these interactions are CL-dependent and functionally important; when *CRD1* (cardiolipin synthase) is ablated, Aac2p's interactions with respiratory supercomplexes are destabilized and respiratory functionality is decreased (11, 12). In Δ *taz1* yeast, Aac2p's interaction with the respiratory supercomplex is reduced or destabilized, and while there is respiratory

dysfunction, it is less severe than in the complete absence of CL (11). Therefore, we sought to study the assembly of adenine nucleotide translocases (ANT; orthologous to ADP/ATP carrier) in our novel TAZ deficient mammalian model. Preliminary results suggest that the MLCL:CL imbalance in the *taz*^{TALEN} cells may compromise ANT2's high molecular weight interactions (data not shown). This suggests that a portion of the mammalian ANT2 interactome is either dependent on the acyl chain composition of CL and/or sensitive to elevated levels of MLCL since the relative CL levels are not different between WT 293 and the *taz*^{TALEN} cells. As ANT2 and other ANT isoforms are necessary for ADP/ATP flux between the mitochondria and the rest of the cell (13), the metabolic consequences of this quarternary defect need to be further investigated. The resultant baseline analyses will provide the framework by which we can systematically, and veritably, define the degree of energetic dysfunction that is a consequence of a particular patient allele (and its lipid aberrations).

Characterizing mutants

When R57L and H69Q alleles were overexpressed in our *taz*^{TALEN} cell model, the cells phenocopied $\Delta taz1$ yeast that expressed the equivalent K65L and H77Q mutations. This provides proof-of-principle for the use of our cell model in characterizing other known pathogenic mutations. R57L, an unstable protein, and the catalytically-null H69Q are mutations that cover two types of loss-of-function mechanisms from a list of seven described using 21 missense mutations that are identical or conserved between yeast and humans (1, 14). The loss-of-function mechanisms additionally include: non-functional truncated products resulting from frameshifts or aberrant splicing; mislocalized within mitochondria and aggregation-prone; aberrantly assembled; hypomorphic alleles with

residual transacylase activity; and unable to engage in stable productive assemblies. A variant(s) from each class can be selected and studied for conserved loss-of-function mechanisms. For instance, mutations that are described to be mislocalized and/or aggregation-prone when modeled in yeast can be confirmed with APEX2 tagging and subsequent electron microscopy, hypomorphic alleles can be subject to transacylase assays, while native PAGE can reveal aberrant TAZ assemblies. Further, our *taz*^{TALEN} system can be used to characterize other pathogenic alleles that cannot be modeled in yeast due to lack of sequence conservation (ClustalOmega alignment of yeast Taz1p and human TAZ revealed an 18.878% identity; Figure 4.1).

Role of modifying factors

It has become clear from the numerous case studies of BTHS patients and those afflicted with other mitochondrial diseases that strict genotype-phenotype correlations do not always exist (15, 16). Modifying factors such as age, gender, genetic and (epigenetic) modifiers (17, 18), degree of mitochondrial DNA (mtDNA) penetrance (or mosaicism), and mtDNA haplotype likely act as key determinants of BTHS pathogenicity and disease progression. It has been demonstrated by several groups that mtDNA haplotypes can define gene expression (19) and contribute significantly to the predisposition to and severity of mitochondrial diseases (20). Although technically challenging, the introduction of various *taz* alleles into cybrids harboring mtDNA of different haplotypes may be required to draw solid genotype-phenotype relationships in BTHS pathogenesis.

Structure

Another defining feature of TAZ, which has only complicated our analyses, is its protease-resistance. Mammalian TAZ can be degraded by pronase E, a protease mixture,

only after the addition of detergent to mitochondria. When human TAZ was heterologously expressed in *Δtaz1* yeast, a similar protease accessibility profile was observed (Figure 4.2) and bolstered our original interpretation of TAZ's submitochondrial localization, which placed the protein on the matrix-facing leaflet of the matrix. However, this conclusion was arrived at using a classical biochemical approach that requires the target protein to be protease sensitive in order to interrogate its topology. Unfortunately, TAZ happens to be resistant to numerous proteases and behaves as a tightly folded protein. When endogenous or overexpressed TAZ is boiled in the presence of detergent prior to protease treatment, TAZ becomes more easily degraded, demonstrating that if TAZ is first denatured by heat and remains unfolded in the presence of detergent, TAZ becomes susceptible to proteolytic degradation. Interestingly, yeast Taz1p also contains a core structure that is resistant to proteinase K degradation (up to 1 mg/ml) in the presence of 0.1% Triton X-100 (21), pointing to structural conservation across eukaryotes.

It is curious as to why TAZ is so obstinate to proteolysis (protease treatment and overall turnover) despite numerous cleavages that are allowed by thermolysin (85 cleavage sites), proteinase K (141 sites), and trypsin (33 sites) when the PeptideCutter algorithm was used (22). For instance, proteins that can resist the action of proteinase K are rare as this serine protease exhibits broad substrate specificity and potent proteolytic activity in the presence of detergents and over a wide pH range. Exceptions include the well-known Protease-resistant protein, PrP, pathogenic aggregates such as α -synuclein, and the protease itself. Since (endogenous) TAZ is not present in aggregates and participates in a range of high molecular weight interactions, TAZ's intrinsic resistance

towards proteases likely has functional implications. Perhaps TAZ needs to remain tightly folded as a consequence of its localization and function; it is anchored to the membrane but exposed to the soluble IMS. Further, it catalyzes the transfer of fatty acyl chains between phospholipids at the interface of the hydrophobic core of the membrane bilayer and the hydrophilic lipid head groups. As TAZ needs to function dynamically at this water-lipid interface on multiple fronts it may be critical that the protein remains ordered, folded, and resistant to changes in the electrostatic environment to ensure function. For example, residues participating in disulfide bonding and metal coordination in copper and zinc superoxide dismutases, which are critical for function, are largely SDS-resistant, characteristics that likely evolved as a way to preserve structural integrity and function in the face of its oxidatively damaging substrates (free radicals, superoxide anions, etc).

Unfortunately, a structure for TAZ is lacking and antibodies against endogenous TAZ have been unavailable (until now), precluding structure-function analyses that would be helpful in dissecting the mechanisms underlying the various loss-of-function mutations. A cursory examination of full-length human TAZ using ProtParam (22) shows that behind leucine (11.0%) and glycine (7.5%), proline (7.2%) is the third most abundant amino acid represented in TAZ's sequence (Figure 4.3). Prolines in peptide chains can influence the conformation and folding of the peptide backbone by virtue of its unique cyclic and imino structure. As a result, its rigidity prevents it from occupying many of the main-chain conformations that can be adopted by other amino acids. Further, there is evidence that suggests that di-proline motifs in the C' terminus of a protein (TAZ has two di-prolines, one close to each termini of the protein) or prolines, in general, may decrease

the proteins susceptibility to proteolytic enzymes (23, 24). In fact, of the 38 proteases tested by PeptideCutter, none are predicted to cleave TAZ's di-proline pair (22); proline endopeptidases have been reported to cleave di-proline bonds, but only substrates whose sequences do not exceed 30 amino acids (25). Thus, the preponderance of prolines is striking and worth investigating as they may be involved in conferring TAZ its unique structural characteristics.

Membrane association

Another aspect of TAZ that remains elusive are the amino acids that mediate the protein's membrane association. As TAZ does not contain an N' terminal targeting signal and does not undergo processing during mitochondrial import, the protein is likely targeted to its final localization via hydrophobic stretches that may act as internal stop-transfer signals. As mentioned briefly in Chapter II, algorithms that are commonly used to predict transmembrane (TM) domains show conflicting results for TAZ. In the absence of any solid structural data, it could be helpful to generate deletions in regions of the protein that exhibit high hydrophobicity (TM-like) to arrive at residues involved in membrane interactions. Subsequently, carbonate extraction and/or digitonin fractionation of the various TM mutants, along with APEX2-tagging, if need be, can be performed to zero in on TAZ's putative "membrane anchor(s)". In yeast, mutations modeled at V223D, V224R, and I226P are thought to disrupt a hydrophobic stretch of the protein that may be involved in membrane anchoring, resulting in mutant Taz1 proteins that are partially mistargeted to the mitochondrial matrix, aggregation-prone, and fail to function (14, 21). As these mutants can be translated and properly imported, at least in yeast, residues at the equivalent human positions, I209, L210, and L212, should be mutagenized and

introduced into *taz*^{TALEN} cells to assess the phospholipid and metabolic consequences of these mutations. Besides systematically mutating and/or deleting portions of the protein to identify sequences important for membrane association, other modes of membrane association such as myristoylation, prenylation, and palmitoylation should also be explored. TAZ contains two cysteines, Cys33 and Cys118, that are predicted to be palmitoylated (26). Further, Cys33 is invariant between yeast and humans. Notably, BTHS patients harboring Cys118 missense mutations exist (27, 28) and since the residue is not conserved between yeast and humans, would serve as an ideal candidate to investigate using our *taz*^{TALEN} system.

An interesting idea to consider is the effect of TAZ mislocalization or “re-localization” within the mitochondrion. TAZ’s current placement on the IMS-facing leaflet of the IMM and/or OMM is difficult to reconcile with CL’s predominance in the matrix-facing leaflet, the site of its biosynthesis. On the surface, it seems energetically costly to flip-flop CL across the IMM for multiple rounds of remodeling by an enzyme that does not exhibit intrinsic substrate specificity (29). Thus, it may be worthwhile to investigate the effects of a matrix-localized TAZ that would place the protein in the same compartment as the core CL biosynthetic machinery. A starting point might involve mutating the I209, L210, and L212 residues to less disruptive amino acids such as alanine (i.e. “targeted” alanine scanning mutagenesis). Since the introduction of charged or kinked residues within and/or flanking the hydrophobic “anchor” may actually repel membrane association or disrupt TAZ’s overall protein fold and stability (in addition to causing its mislocalization), mutagenesis to alanine may reveal ameliorated phenotypes.

TAZ interactions

In yeast, Taz1p has been shown to interact with the major ADP/ATP carrier, Aac2p, and the ATP synthase, both of which are key components in the supply and flux of energy intermediates across the mitochondrial IM (30). However, in mammals, not much is known about TAZ's interactome. Using the STRING database that includes known and predicted protein interactions, be it direct or indirect, a query for human TAZ revealed hits such as phospholipases, PLA2G6 and PLA2G4A, as well as HADHB, DNAJC19, and OPA3 (31). Most of the listed interactions are identified by textmining published abstracts rather than actual experimentation and therefore, would need to be interrogated using biochemical and cell biological techniques such as immunoprecipitation, co-expression, and or proteomics. Interestingly, of the multiple large-scale mammalian mitochondrial proteomes that are available in the literature (32-41), only one study (42) was able to identify TAZ as a component and resident of the mitochondrion, and only in mouse liver mitochondria. In hindsight, the lack of TAZ in these proteomic studies might hark back to TAZ's inherent structural stability and resistance towards tryptic digests (and therefore preclude peptide identification by MS/MS).

For a more directed approach at identifying proteins that interact with TAZ, cells expressing CNAP-TAZ or TAZ-3XFLAG can be used. As their expression restores the lipid aberrations in *taz*^{TALEN} cells, TAZ function is not adversely affected by either added tag. The N' terminal CNAP-tag (containing His and Protein C epitopes) appended onto TAZ has been successfully used to define the yeast Aac2p interactome (12) and the human ANT1 and ANT2 interactome (data not shown). In the latter experiment, cells expressing tagged and untagged ANTs were differentially cultured in either labeled

“heavy” medium or unlabeled “light” medium; mitochondrial lysates were affinity purified and mixed prior to gel resolution and subsequent LC-MS/MS. By coupling SILAC (stable isotope labeling of amino acids in cell culture) labeling with conventional MS/MS-based proteomics, quantitative levels of hits can be obtained and non-specific hits can be largely eliminated (43). If somehow digitonin-solubilized TAZ adversely affects protein binding (in light of evidence suggesting that TAZ’s specificity is determined by the physical state of its lipid macroenvironment (29)), APEX2-tagged TAZ constructs that are already generated and characterized can be used. The engineered peroxidase tag is capable of biotinylation *in vivo* proteins proximal to TAZ in the presence of biotin-phenol and H₂O₂ (34). The labeled proteins can then be enriched with the use of streptavidin-conjugated resin. Presumably, the high binding affinity of biotin for streptavidin would allow for the identification of partners that may otherwise be transient interactions or present at low abundance. The limitation of the APEX2 proteomic approach is that the peroxidase is highly promiscuous and lacks specificity, as such, not all proteins can be labeled and if identified, might not be true interactors but highly abundant and/or reactive proteins (44). Another issue that has to be considered is whether or not appending the APEX2 tag onto the highly folded and protease resistant C’ termini would affect APEX2’s function and hamper accessibility to proximal proteins due to steric hindrance.

TAZ expression and regulation

TAZ expression has been largely documented on the mRNA level (45-47); in humans, at least 6 alternatively spliced isoforms (FL, -ex5, -ex7, -ex5,7, -ex6,7, and -ex5,6,7) are thought to exist (47, 48). When *TAZ* mRNA expression was surveyed in a

variety of tissues, the mRNA expression pattern was similar for most isoforms except for TAZ-ex6,7 (overall low abundance) and did not necessarily correlate to tissues that are primarily affected in BTHS pathology (i.e. heart and skeletal muscle) (48). Further, when various *TAZ* isoforms were expressed in BTHS patient fibroblasts, none of the isoforms, individually, were able to thoroughly rescue the lipid defect (though there is a slight improvement) (48), pointing to functional contributions of each of the spliced variants. However, in $\Delta taz1$ yeast, only the heterologous expression of human TAZ variant lacking exon 5 can restore the lipid defects; full-length human TAZ can only partially restore the CL profile (49).

As is, the relative importance of each splice variant remains unclear. Thus, using our TAZ mAbs, which conveniently recognize epitopes in three different exons, the relationship between mRNA expression and steady state protein levels can be explored. In our *taz*^{TALEN} system, *TAZ* mRNA levels are unchanged between wt 293 and *taz*^{TALEN} cells despite the absence of a protein product in the latter. mRNA analysis of *TAZ* splice variants in patient fibroblasts show a wide spectrum of transcript levels – some alleles have increased mRNA expression that might be caused by transcriptional upregulation but other alleles had unaffected, decreased, or even absent *TAZ* transcript levels (48). These results suggest that TAZ is unlikely to be regulated at the transcriptional level, like that posited for CL metabolism (50, 51), as there seems to not be any conclusive transcriptional upregulation in the absence of TAZ activity.

If TAZ is not regulated at the transcriptional level, translational and post-translational mechanisms could be in play. Importantly, TAZ-ex5 is the only variant expressed in 293 cells and its reintroduction into *taz*^{TALEN}.2 and .19 clearly rescued the

MLCL:CL imbalance. Even though our quantitative RT-PCR did not distinguish between the different *TAZ* mRNA that might be present, isoform-specific primers can be designed to determine the relative expression of each variant in 293 cells. If multiple *TAZ* isoforms are present and yet only TAZ-ex5 is translated, translational regulation of TAZ clearly exists, perhaps in a tissue-specific manner. Regardless of the mRNA transcripts that are present, the absence of functional TAZ in our *taz*^{TALEN} system can provide a clean background to evaluate the individual contributions of each isoform when overexpressed.

Currently, it remains to be determined if TAZ undergoes any form of PTM. Using PTM prediction algorithms, 9 phosphorylated sites (NetPhos 2.0, (52)), 6 glycation sites (NetGlycate, (53)), 9 C' terminal mannosylation sites (NetCGlyc, (54)), and ubiquitination at position 135 (CPLM, (55)) were identified. Using an antibody against acetylated lysine motifs, K149 of human TAZ was identified as acetylated based on proteomic discovery-mode mass spectrometry (56). While the existence and functional relevance of these candidate sites are unknown, for instance, acylation in mitochondria may be a chemical event facilitated by alkaline pH and acyl-CoA concentrations in the matrix rather than an enzyme-dependent event (57), unconventional PTMs are still worth considering. Glycation is hypothesized to participate in mitochondrial pathologies (58) and mannosylation could be mediated by mitochondrial mannosyltransferases that are activated by phospholipids such as CL (59). Even carbamylation, which occurs on mitochondrial glutamate dehydrogenase and increases susceptibility to proteinases (60), could be a potential regulatory modification. No N' terminal acetylation (61), myristoylation (Myristoylator, (62)), or prenylation sites (PrePS, (63)) were predicted.

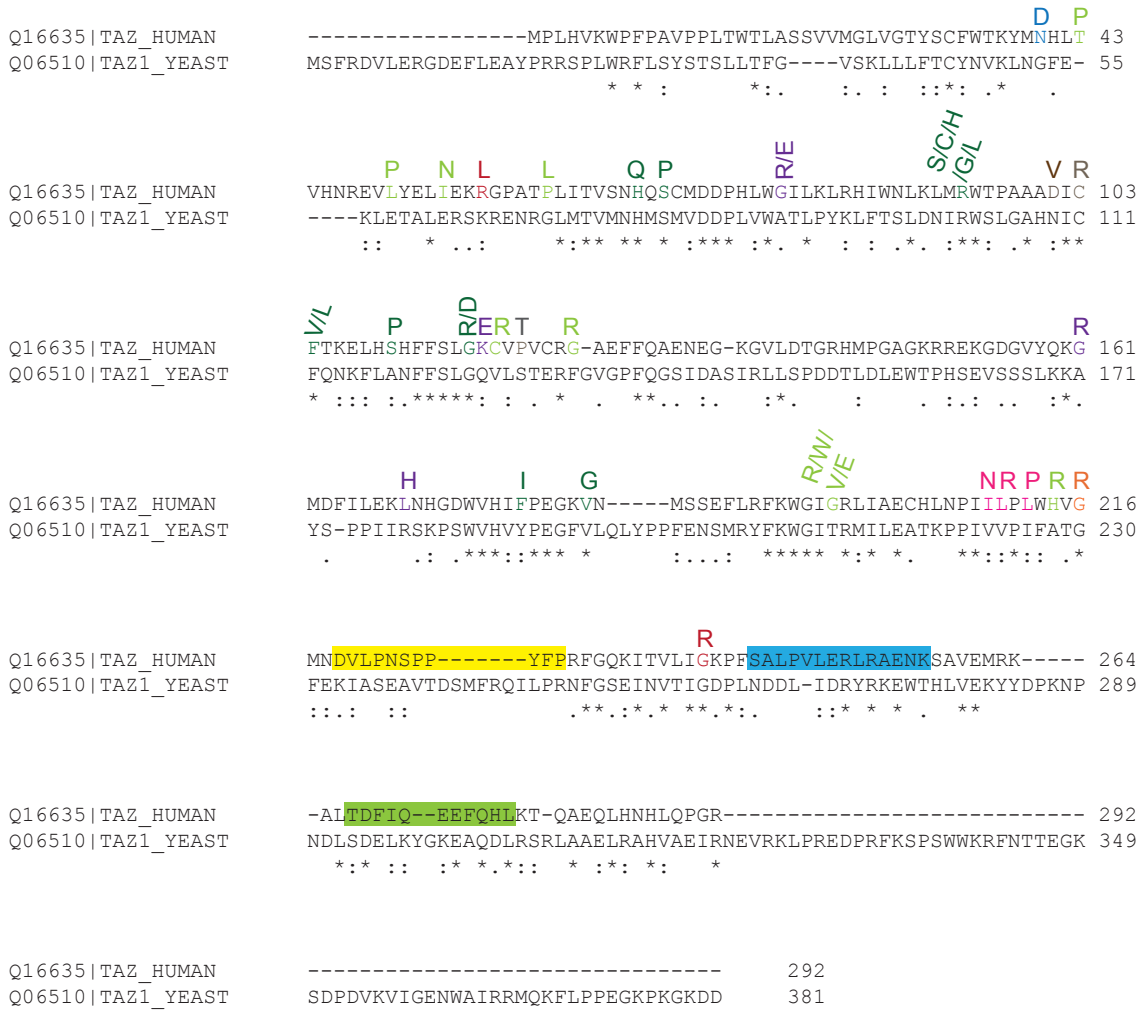
Final words

Named after the masochistic Italian comic who finds immense joy in beating his jockstrap with a water bottle, TAZ has certainly lived up to its name. During my graduate career coddling and prodding this enigmatic lipid remodeler, TAZ and I have had a tumultuous relationship filled with excitement, novelty, joy, confusion, deceit, and finally acceptance (pun intended). But at the end of all of it, I can only thank TAZ for taking me on an unforgettable scientific adventure. If there is anything that I have learned it is that:

“Do not believe in anything simply because you have heard it. Do not believe in anything simply because it is spoken and rumored by many. Do not believe in anything simply because it is found written in your religious books. Do not believe in anything merely on the authority of your teachers and elders. Do not believe in tradition because they have been handed down for many generations. But after observation and analysis, when you find that anything agrees with reason and is conducive to the good and benefit of one and all, then accept it and live up to it.”

– Hindu Prince Gautama Siddharta, the founder of Buddhism, 563-483 BC)

CLUSTAL O(1.2.1) multiple sequence alignment



Exon	Amino Acids
1	1-26
2	27-79
3	80-95
4	96-124
5	125-154
6	155-179
7	182-195
8	196-216
9	217-233
10	234-259
11	260-292

TAZ mAbs

- = 3D7F11 epitope
- = 2C2C9 epitope
- = 2G3F7 epitope

Nonconserved BTBS Mutants

Conserved uncharacterized BTBS Mutants

Yeast BTBS Mutant Class

- WT Function
- Class 2: Low Fidelity Sorting and Aggregation-Prone
- Class 3: Aberrant Assembly
- Class 4: Catalytically Null
- Class 5: Functional Hypomorph
- Class 6: Complex Liability
- Class 7: Temperature-Sensitive

FIGURE 4.1 Clustal Omega (1.2.1) alignment of human and yeast tafazzin. Sequences corresponding to yeast.Taz1p (Q06510) and full-length human TAZ (Q16635) were retrieved from Uniprot and aligned using CLUSTAL O(1.2.1). The epitopes recognized by each of the three mAbs are highlighted within the sequence alignment. Characterized and uncharacterized BTBS mutants are noted in various colors.

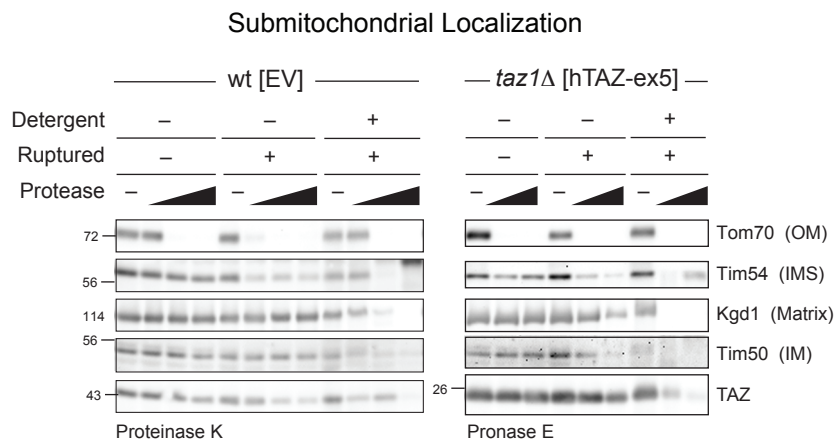


FIGURE 4.2 Protease accessibility of human TAZ lacking exon 5 heterologously expressed in *taz1Δ*.

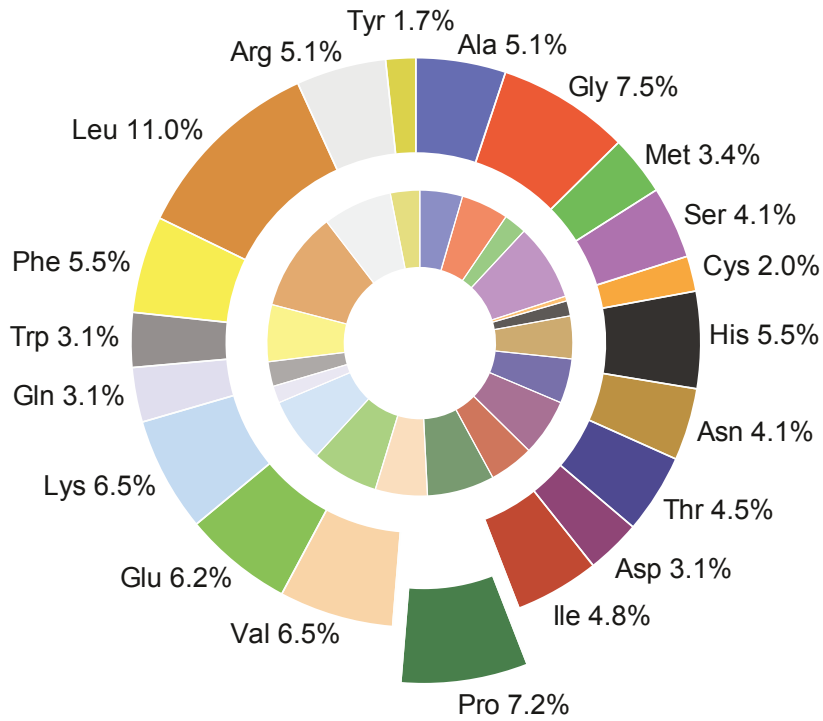


FIGURE 4.3 Amino acid compositions of human and yeast tafazzin. The relative contributions of each amino acid to the final protein. The outer ring represents the amino acid breakdown for human TAZ (Q16635) and the inner ring is that of yeast Taz1p (Q06510).

REFERENCES

- 1 Whited, K., Baile, M.G., Currier, P. and Claypool, S.M. (2013) Seven functional classes of Barth syndrome mutation. *Human molecular genetics*, **22**, 483-492.
- 2 McKenzie, M., Lazarou, M., Thorburn, D.R. and Ryan, M.T. (2006) Mitochondrial respiratory chain supercomplexes are destabilized in Barth Syndrome patients. *Journal of molecular biology*, **361**, 462-469.
- 3 Gonzalez, F., D'Aurelio, M., Boutant, M., Moustapha, A., Puech, J.P., Landes, T., Arnaune-Pelloquin, L., Vial, G., Taleux, N., Slomianny, C. *et al.* (2013) Barth syndrome: cellular compensation of mitochondrial dysfunction and apoptosis inhibition due to changes in cardiolipin remodeling linked to tafazzin (TAZ) gene mutation. *Biochimica et biophysica acta*, **1832**, 1194-1206.
- 4 Dudek, J., Cheng, I.F., Balleininger, M., Vaz, F.M., Streckfuss-Bomeke, K., Hubscher, D., Vukotic, M., Wanders, R.J., Rehling, P. and Guan, K. (2013) Cardiolipin deficiency affects respiratory chain function and organization in an induced pluripotent stem cell model of Barth syndrome. *Stem Cell Res*, **11**, 806-819.
- 5 Powers, C., Huang, Y., Strauss, A. and Khuchua, Z. (2013) Diminished Exercise Capacity and Mitochondrial bc1 Complex Deficiency in Tafazzin-Knockdown Mice. *Front Physiol*, **4**, 74.
- 6 Salabei, J.K., Gibb, A.A. and Hill, B.G. (2014) Comprehensive measurement of respiratory activity in permeabilized cells using extracellular flux analysis. *Nature protocols*, **9**, 421-438.

- 7 Divakaruni, A.S., Rogers, G.W. and Murphy, A.N. (2014) Measuring Mitochondrial Function in Permeabilized Cells Using the Seahorse XF Analyzer or a Clark-Type Oxygen Electrode. *Curr Protoc Toxicol*, **60**, 25 22 21-25 22 16.
- 8 Hsu, P., Liu, X., Zhang, J., Wang, H.G., Ye, J.M. and Shi, Y. (2015) Cardiolipin remodeling by TAZ/tafazzin is selectively required for the initiation of mitophagy. *Autophagy*, **11**, 643-652.
- 9 Barth, P.G., Van den Bogert, C., Bolhuis, P.A., Scholte, H.R., van Gennip, A.H., Schutgens, R.B. and Ketel, A.G. (1996) X-linked cardioskeletal myopathy and neutropenia (Barth syndrome): respiratory-chain abnormalities in cultured fibroblasts. *J Inherit Metab Dis*, **19**, 157-160.
- 10 Xu, Y., Sutachan, J.J., Plesken, H., Kelley, R.I. and Schlame, M. (2005) Characterization of lymphoblast mitochondria from patients with Barth syndrome. *Laboratory investigation; a journal of technical methods and pathology*, **85**, 823-830.
- 11 Baile, M.G., Sathappa, M., Lu, Y.W., Pryce, E., Whited, K., McCaffery, J.M., Han, X., Alder, N.N. and Claypool, S.M. (2014) Unremodeled and remodeled cardiolipin are functionally indistinguishable in yeast. *The Journal of biological chemistry*, **289**, 1768-1778.
- 12 Claypool, S.M., Oktay, Y., Boonthung, P., Loo, J.A. and Koehler, C.M. (2008) Cardiolipin defines the interactome of the major ADP/ATP carrier protein of the mitochondrial inner membrane. *The Journal of cell biology*, **182**, 937-950.
- 13 Pfaff, E. and Klingenberg, M. (1968) Adenine nucleotide translocation of mitochondria. 1. Specificity and control. *European journal of biochemistry / FEBS*, **6**, 66-79.

- 14 Claypool, S.M., Whited, K., Srijumnong, S., Han, X. and Koehler, C.M. (2011) Barth syndrome mutations that cause tafazzin complex lability. *The Journal of cell biology*, **192**, 447-462.
- 15 Johnston, J., Kelley, R.I., Feigenbaum, A., Cox, G.F., Iyer, G.S., Funanage, V.L. and Proujansky, R. (1997) Mutation characterization and genotype-phenotype correlation in Barth syndrome. *Am J Hum Genet*, **61**, 1053-1058.
- 16 Ronvelia, D., Greenwood, J., Platt, J., Hakim, S. and Zaragoza, M.V. (2012) Intrafamilial variability for novel TAZ gene mutation: Barth syndrome with dilated cardiomyopathy and heart failure in an infant and left ventricular noncompaction in his great-uncle. *Mol Genet Metab*, **107**, 428-432.
- 17 Vatta, M., Mohapatra, B., Jimenez, S., Sanchez, X., Faulkner, G., Perles, Z., Sinagra, G., Lin, J.H., Vu, T.M., Zhou, Q. *et al.* (2003) Mutations in Cypher/ZASP in patients with dilated cardiomyopathy and left ventricular non-compaction. *J Am Coll Cardiol*, **42**, 2014-2027.
- 18 Marziliano, N., Mannarino, S., Nespoli, L., Diegoli, M., Pasotti, M., Malattia, C., Grasso, M., Pilotto, A., Porcu, E., Raisaro, A. *et al.* (2007) Barth syndrome associated with compound hemizyosity and heterozyosity of the TAZ and LDB3 genes. *American journal of medical genetics. Part A*, **143A**, 907-915.
- 19 Kelly, R.D., Rodda, A.E., Dickinson, A., Mahmud, A., Nefzger, C.M., Lee, W., Forsythe, J.S., Polo, J.M., Trounce, I.A., McKenzie, M. *et al.* (2013) Mitochondrial DNA haplotypes define gene expression patterns in pluripotent and differentiating embryonic stem cells. *Stem Cells*, **31**, 703-716.

- 20 Kenney, M.C., Chwa, M., Atilano, S.R., Falatoonzadeh, P., Ramirez, C., Malik, D., Tarek, M., Del Carpio, J.C., Nesburn, A.B., Boyer, D.S. *et al.* (2014) Molecular and bioenergetic differences between cells with African versus European inherited mitochondrial DNA haplogroups: implications for population susceptibility to diseases. *Biochimica et biophysica acta*, **1842**, 208-219.
- 21 Claypool, S.M., McCaffery, J.M. and Koehler, C.M. (2006) Mitochondrial mislocalization and altered assembly of a cluster of Barth syndrome mutant tafazzins. *The Journal of cell biology*, **174**, 379-390.
- 22 Gasteiger, E., Hoogland, C., Gattiker, A., Duvaud, S.e., Wilkins, M., Appel, R. and Bairoch, A. (2005) Walker, J. (ed.), In *The Proteomics Protocols Handbook*. Humana Press, in press., pp. 571-607.
- 23 Vanhoof, G., Goossens, F., De Meester, I., Hendriks, D. and Scharpe, S. (1995) Proline motifs in peptides and their biological processing. *FASEB J*, **9**, 736-744.
- 24 Markert, Y., Koditz, J., Ulbrich-Hofmann, R. and Arnold, U. (2003) Proline versus charge concept for protein stabilization against proteolytic attack. *Protein Eng*, **16**, 1041-1046.
- 25 Fulop, V., Bocskei, Z. and Polgar, L. (1998) Prolyl oligopeptidase: an unusual beta-propeller domain regulates proteolysis. *Cell*, **94**, 161-170.
- 26 Ren, J., Wen, L., Gao, X., Jin, C., Xue, Y. and Yao, X. (2008) CSS-Palm 2.0: an updated software for palmitoylation sites prediction. *Protein Eng Des Sel*, **21**, 639-644.
- 27 Ichida, F., Tsubata, S., Bowles, K.R., Haneda, N., Uese, K., Miyawaki, T., Dreyer, W.J., Messina, J., Li, H., Bowles, N.E. *et al.* (2001) Novel gene mutations in patients with left ventricular noncompaction or Barth syndrome. *Circulation*, **103**, 1256-1263.

- 28 Schlame, M., Kelley, R.I., Feigenbaum, A., Towbin, J.A., Heerdt, P.M., Schieble, T., Wanders, R.J., DiMauro, S. and Blanck, T.J. (2003) Phospholipid abnormalities in children with Barth syndrome. *J Am Coll Cardiol*, **42**, 1994-1999.
- 29 Schlame, M., Acehan, D., Berno, B., Xu, Y., Valvo, S., Ren, M., Stokes, D.L. and Epand, R.M. (2012) The physical state of lipid substrates provides transacylation specificity for tafazzin. *Nature chemical biology*, **8**, 862-869.
- 30 Claypool, S.M., Boonthung, P., McCaffery, J.M., Loo, J.A. and Koehler, C.M. (2008) The cardiolipin transacylase, tafazzin, associates with two distinct respiratory components providing insight into Barth syndrome. *Molecular biology of the cell*, **19**, 5143-5155.
- 31 Jensen, L.J., Kuhn, M., Stark, M., Chaffron, S., Creevey, C., Muller, J., Doerks, T., Julien, P., Roth, A., Simonovic, M. *et al.* (2009) STRING 8--a global view on proteins and their functional interactions in 630 organisms. *Nucleic acids research*, **37**, D412-416.
- 32 Pagliarini, D.J., Calvo, S.E., Chang, B., Sheth, S.A., Vafai, S.B., Ong, S.E., Walford, G.A., Sugiana, C., Boneh, A., Chen, W.K. *et al.* (2008) A mitochondrial protein compendium elucidates complex I disease biology. *Cell*, **134**, 112-123.
- 33 Rhee, H.W., Zou, P., Udeshi, N.D., Martell, J.D., Mootha, V.K., Carr, S.A. and Ting, A.Y. (2013) Proteomic mapping of mitochondria in living cells via spatially restricted enzymatic tagging. *Science*, **339**, 1328-1331.
- 34 Hung, V., Zou, P., Rhee, H.W., Udeshi, N.D., Cracan, V., Svinkina, T., Carr, S.A., Mootha, V.K. and Ting, A.Y. (2014) Proteomic mapping of the human mitochondrial intermembrane space in live cells via ratiometric APEX tagging. *Mol Cell*, **55**, 332-341.

- 35 Kislinger, T., Cox, B., Kannan, A., Chung, C., Hu, P., Ignatchenko, A., Scott, M.S., Gramolini, A.O., Morris, Q., Hallett, M.T. *et al.* (2006) Global survey of organ and organelle protein expression in mouse: combined proteomic and transcriptomic profiling. *Cell*, **125**, 173-186.
- 36 Mootha, V.K., Bunkenborg, J., Olsen, J.V., Hjerrild, M., Wisniewski, J.R., Stahl, E., Bolouri, M.S., Ray, H.N., Sihag, S., Kamal, M. *et al.* (2003) Integrated analysis of protein composition, tissue diversity, and gene regulation in mouse mitochondria. *Cell*, **115**, 629-640.
- 37 Taylor, S.W., Fahy, E., Zhang, B., Glenn, G.M., Warnock, D.E., Wiley, S., Murphy, A.N., Gaucher, S.P., Capaldi, R.A., Gibson, B.W. *et al.* (2003) Characterization of the human heart mitochondrial proteome. *Nat Biotechnol*, **21**, 281-286.
- 38 Zhang, J., Li, X., Mueller, M., Wang, Y., Zong, C., Deng, N., Vondriska, T.M., Liem, D.A., Yang, J.I., Korge, P. *et al.* (2008) Systematic characterization of the murine mitochondrial proteome using functionally validated cardiac mitochondria. *Proteomics*, **8**, 1564-1575.
- 39 Gaucher, S.P., Taylor, S.W., Fahy, E., Zhang, B., Warnock, D.E., Ghosh, S.S. and Gibson, B.W. (2004) Expanded coverage of the human heart mitochondrial proteome using multidimensional liquid chromatography coupled with tandem mass spectrometry. *J Proteome Res*, **3**, 495-505.
- 40 Reifschneider, N.H., Goto, S., Nakamoto, H., Takahashi, R., Sugawa, M., Dencher, N.A. and Krause, F. (2006) Defining the mitochondrial proteomes from five rat organs in a physiologically significant context using 2D blue-native/SDS-PAGE. *J Proteome Res*, **5**, 1117-1132.

- 41 Forner, F., Foster, L.J., Campanaro, S., Valle, G. and Mann, M. (2006) Quantitative proteomic comparison of rat mitochondria from muscle, heart, and liver. *Mol Cell Proteomics*, **5**, 608-619.
- 42 Lotz, C., Lin, A.J., Black, C.M., Zhang, J., Lau, E., Deng, N., Wang, Y., Zong, N.C., Choi, J.H., Xu, T. *et al.* (2014) Characterization, design, and function of the mitochondrial proteome: from organs to organisms. *J Proteome Res*, **13**, 433-446.
- 43 Ong, S.E., Blagoev, B., Kratchmarova, I., Kristensen, D.B., Steen, H., Pandey, A. and Mann, M. (2002) Stable isotope labeling by amino acids in cell culture, SILAC, as a simple and accurate approach to expression proteomics. *Mol Cell Proteomics*, **1**, 376-386.
- 44 Lam, S.S., Martell, J.D., Kamer, K.J., Deerinck, T.J., Ellisman, M.H., Mootha, V.K. and Ting, A.Y. (2015) Directed evolution of APEX2 for electron microscopy and proximity labeling. *Nature methods*, **12**, 51-54.
- 45 Bione, S., D'Adamo, P., Maestrini, E., Gedeon, A.K., Bolhuis, P.A. and Toniolo, D. (1996) A novel X-linked gene, G4.5. is responsible for Barth syndrome. *Nature genetics*, **12**, 385-389.
- 46 Gonzalez, I.L. (2005) Barth syndrome: TAZ gene mutations, mRNAs, and evolution. *American journal of medical genetics. Part A*, **134**, 409-414.
- 47 Lu, B., Kelher, M.R., Lee, D.P., Lewin, T.M., Coleman, R.A., Choy, P.C. and Hatch, G.M. (2004) Complex expression pattern of the Barth syndrome gene product tafazzin in human cell lines and murine tissues. *Biochemistry and cell biology = Biochimie et biologie cellulaire*, **82**, 569-576.
- 48 Houtkooper, R.H., Turkenburg, M., Poll-The, B.T., Karall, D., Perez-Cerda, C., Morrone, A., Malvagia, S., Wanders, R.J., Kulik, W. and Vaz, F.M. (2009) The

enigmatic role of tafazzin in cardiolipin metabolism. *Biochimica et biophysica acta*, **1788**, 2003-2014.

49 Vaz, F.M., Houtkooper, R.H., Valianpour, F., Barth, P.G. and Wanders, R.J. (2003) Only one splice variant of the human TAZ gene encodes a functional protein with a role in cardiolipin metabolism. *The Journal of biological chemistry*, **278**, 43089-43094.

50 Athesa, Y., Viollet, B., Mateo, P., Rousseau, D., Novotova, M., Garnier, A., Vaulont, S., Wilding, J.R., Grynberg, A., Veksler, V. *et al.* (2007) AMP-activated protein kinase alpha2 deficiency affects cardiac cardiolipin homeostasis and mitochondrial function. *Diabetes*, **56**, 786-794.

51 Jiang, Y.J., Lu, B., Xu, F.Y., Gartshore, J., Taylor, W.A., Halayko, A.J., Gonzalez, F.J., Takasaki, J., Choy, P.C. and Hatch, G.M. (2004) Stimulation of cardiac cardiolipin biosynthesis by PPARalpha activation. *J Lipid Res*, **45**, 244-252.

52 Blom, N., Gammeltoft, S. and Brunak, S. (1999) Sequence and structure-based prediction of eukaryotic protein phosphorylation sites. *Journal of molecular biology*, **294**, 1351-1362.

53 Johansen, M.B., Kiemer, L. and Brunak, S. (2006) Analysis and prediction of mammalian protein glycation. *Glycobiology*, **16**, 844-853.

54 Julenius, K. (2007) NetCGlyc 1.0: prediction of mammalian C-mannosylation sites. *Glycobiology*, **17**, 868-876.

55 Liu, Z., Wang, Y., Gao, T., Pan, Z., Cheng, H., Yang, Q., Cheng, Z., Guo, A., Ren, J. and Xue, Y. (2014) CPLM: a database of protein lysine modifications. *Nucleic acids research*, **42**, D531-536.

- 56 Hornbeck, P.V., Kornhauser, J.M., Tkachev, S., Zhang, B., Skrzypek, E., Murray, B., Latham, V. and Sullivan, M. (2012) PhosphoSitePlus: a comprehensive resource for investigating the structure and function of experimentally determined post-translational modifications in man and mouse. *Nucleic acids research*, **40**, D261-270.
- 57 Wagner, G.R. and Payne, R.M. (2013) Widespread and enzyme-independent Nepsilon-acetylation and Nepsilon-succinylation of proteins in the chemical conditions of the mitochondrial matrix. *The Journal of biological chemistry*, **288**, 29036-29045.
- 58 Pun, P.B. and Murphy, M.P. (2012) Pathological significance of mitochondrial glycation. *Int J Cell Biol*, **2012**, 843505.
- 59 Ardail, D., Gateau, O., Morelis, R. and Louisot, P. (1985) Glycosyltransferase activities in liver mitochondria. Phospholipid-dependence of inner membrane mannosyltransferase. *European journal of biochemistry / FEBS*, **149**, 497-502.
- 60 Hood, W., de la Morena, E. and Grisolia, S. (1977) Increased susceptibility of carbamylated glutamate dehydrogenase to proteolysis. *Acta Biol Med Ger*, **36**, 1667-1672.
- 61 Kiemer, L., Bendtsen, J.D. and Blom, N. (2005) NetAcet: prediction of N-terminal acetylation sites. *Bioinformatics*, **21**, 1269-1270.
- 62 Bologna, G., Yvon, C., Duvaud, S. and Veuthey, A.L. (2004) N-Terminal myristoylation predictions by ensembles of neural networks. *Proteomics*, **4**, 1626-1632.
- 63 Maurer-Stroh, S., Koranda, M., Benetka, W., Schneider, G., Sirota, F.L. and Eisenhaber, F. (2007) Towards complete sets of farnesylated and geranylgeranylated proteins. *PLoS computational biology*, **3**, e66.

APPENDIX I

Unremodeled and remodeled cardiolipin are functionally indistinguishable in yeast

This contents of this appendix is published in:

Baile MG, Sathappa M[#], **Lu YW[#]**, Pryce E, Whited K, McCaffery JM, Han X, Alder NN, and Claypool SM. Unremodeled and remodeled cardiolipin are functionally indistinguishable in yeast. *J Biol Chem.* 2014 Jan 17; 289(3): 1768-78.

[#]co-second authors

SUMMARY

After biosynthesis, an evolutionarily conserved acyl chain remodeling process generates a final highly homogenous and yet tissue-specific molecular form of the mitochondrial lipid cardiolipin. Hence cardiolipin molecules in different organisms, and even different tissues within the same organism, contain a distinct collection of attached acyl chains. This observation is the basis for the widely accepted paradigm that the acyl chain composition of cardiolipin is matched to the unique mitochondrial demands of a tissue. For this hypothesis to be correct, cardiolipin molecules with different acyl chain compositions should have distinct functional capacities and cardiolipin that has been remodeled should promote cardiolipin-dependent mitochondrial processes better than its unremodeled form. However, functional disparities between different molecular forms of cardiolipin have never been established. Here we interrogate this simple but crucial prediction utilizing the best available model to do so, *Saccharomyces cerevisiae*. Specifically, we compare the ability of unremodeled and remodeled cardiolipin, which differ markedly in their acyl chain composition, to support mitochondrial activities known to require cardiolipin. Surprisingly, defined changes in the acyl chain composition of cardiolipin do not alter either mitochondrial morphology or oxidative phosphorylation. Importantly, preventing cardiolipin remodeling initiation in yeast lacking *TAZI*, an ortholog of the causative gene in Barth syndrome, ameliorates mitochondrial dysfunction. Thus, our data do not support the prevailing hypothesis that unremodeled cardiolipin is functionally distinct from remodeled cardiolipin, at least for the functions examined, suggesting alternative physiological roles for this conserved pathway.

INTRODUCTION

Cardiolipin (CL), a mitochondrial phospholipid with two phosphate headgroups and four acyl chains, is required for the optimal function of numerous mitochondrial processes, including oxidative phosphorylation (OXPHOS) (Acehan et al., 2011; Claypool et al., 2008b; Eble et al., 1990; Fry and Green, 1980; Fry and Green, 1981; Gomez and Robinson, 1999; Koshkin and Greenberg, 2000; Koshkin and Greenberg, 2002; Pfeiffer et al., 2003; Schwall et al., 2012; Sedlak and Robinson, 1999; Zhang et al., 2002; Zhang et al., 2005), protein import (Gebert et al., 2009; Jiang et al., 2000; Marom et al., 2009; van der Laan et al., 2007), establishment of cristae morphology (Claypool et al., 2006; Mileykovskaya and Dowhan, 2009), fission and fusion (Ban et al., 2010; DeVay et al., 2009; Montessuit et al., 2010), and apoptosis (Gonzalvez et al., 2008; Ostrander et al., 2001). Despite limited acyl chain specificity of the CL biosynthetic enzymes (de Kroon et al., 2013; Houtkooper et al., 2006), the acyl chain composition of CL within an organism or cell type displays a remarkable degree of homogeneity (Schlame et al., 2005). This is achieved via acyl chain remodeling that is initiated by a lipase(s), generating monolyso-CL (MLCL, CL lacking one acyl chain), and completed by a transacylase or an acyltransferase which reacylates MLCL (Claypool and Koehler, 2012).

Mutations in the MLCL transacylase tafazzin cause Barth syndrome, resulting in cardiac and skeletal myopathy, cyclic neutropenia, and respiratory chain defects (Barth et al., 1983; Bione et al., 1996; Schlame and Ren, 2006). In Barth syndrome patients and models of Barth syndrome, CL levels are decreased, MLCL accumulates, and the remaining CL contains an altered acyl chain composition (Gu et al., 2004; Schlame et al., 2003; Soustek et al., 2011; Valianpour et al., 2005; Whited et al., 2012; Xu et al., 2006a),

although which lipid alteration either individually or in combination leads to mitochondrial dysfunction has not been thoroughly investigated.

While the pathophysiological importance of defective CL remodeling is firmly established, the physiological importance of this pathway represents a largely unaddressed issue that is preventing a comprehensive molecular understanding of how this evolutionarily conserved and clinically relevant process promotes mitochondrial function. The most widely accepted hypothesis is based on the highly intriguing observation that the final homogeneous molecular form of CL varies between organisms or even between tissues within the same organism (Cheng et al., 2008; Schlame et al., 2005). As such, it is postulated that CL molecules with different acyl chain compositions are functionally distinct, and that the molecular form of CL specifically fits the demands of its host cell (Cheng et al., 2008; Houtkooper et al., 2009; Kiebish et al., 2012; Schlame et al., 2002). However, as of yet, this provocative hypothesis has not been directly tested in any model organism.

At present, yeast are not merely the best, but also the only model available capable of directly comparing the functionality of distinct molecular forms of CL in otherwise isogenic cells. Three CL remodeling pathways have been identified in higher eukaryotes, although their relative contribution to establishing the final molecular form of CL is unclear (Claypool and Koehler, 2012; Schlame, 2013). In contrast, yeast only undergo tafazzin-mediated CL remodeling. Recently, the phospholipase that initiates CL remodeling was identified in yeast as Cld1p (Beranek et al., 2009). Cld1p has no homolog in higher eukaryotes; however its function, the removal of an acyl chain from CL to form MLCL, is conserved. A similar phenomenon is seen with the

phosphatidylglycerolphosphate phosphatase in CL biosynthesis: the yeast (Gep4p) and mammalian (PTPMT1) enzymes are phylogenetically unrelated despite catalyzing the same reaction (Osman et al., 2010; Zhang et al., 2011a). A calcium-independent phospholipase A₂ has been identified as a CL phospholipase in flies (iPLA₂-VIA) and mammals (iPLA₂γ) (Malhotra et al., 2009; Mancuso et al., 2007; Schlame et al., 2012b). However, murine iPLA₂γ is not the lipase that provides the substrate MLCL utilized by tafazzin (Kiebish et al., 2013). Consequently, the exact role of these lipases in CL remodeling is unclear. Therefore, in higher eukaryotes, not only are there multiple potential CL remodeling pathways, but additionally, a complete inventory of all of the involved players has not been established. As such, it is currently not possible to compare the functionality of distinct molecular forms of CL in metazoans.

In contrast, Cld1p localizes exclusively to mitochondria and is the only lipase that initiates tafazzin-mediated CL remodeling in yeast (Baile et al., 2013; Beranek et al., 2009). Here, we utilized $\Delta cld1$ yeast to determine if cardiolipin molecules with different acyl chain compositions—in this case unremodeled *versus* remodeled cardiolipin—have distinct functional capacities, a central prediction of the prevailing hypothesis. Unexpectedly, unremodeled CL functioned as well as remodeled CL in maintaining mitochondrial morphology and promoting OXPHOS. Further, mutating *CLDI*, and thus preventing the initiation of CL remodeling, was able to suppress the defects of $\Delta taz1$ yeast. Thus, we conclude that in yeast, unremodeled CL can support known CL-dependent mitochondrial functions as well as remodeled CL.

RESULTS

CLD1 functions upstream of TAZ1 in CL remodeling

The initial characterization of *CLD1* revealed that $\Delta cld1$ and $\Delta cld1\Delta taz1$ yeast contained identical mitochondrial phospholipid profiles (Beranek et al., 2009), indicating that *CLD1* is epistatic to *TAZ1* (the yeast homolog of tafazzin) in the same pathway. In contrast, growth on respiratory media, where ethanol and glycerol are the only available carbon sources thus requiring ATP generated by OXPHOS, suggested that *CLD1* functions in a pathway parallel to, or distinct from, *TAZ1* (Beranek et al., 2009).

In an attempt to resolve this, we analyzed CL biosynthesis and remodeling mutants in multiple independent yeast strains. As expected, in mitochondria isolated from yeast lacking cardiolipin synthase ($\Delta crd1$), CL was absent and its precursor PG accumulated (Figure A.1). Importantly, the same phospholipid profile was seen in the double mutant, $\Delta crd1\Delta cld1$, indicating that *CLD1* functions after *CRD1*, in one pathway. The $\Delta cld1$ mutant displayed a lipid profile similar to that of wild type, while $\Delta taz1$ resulted in a reduction of CL and an accumulation of MLCL. The double mutant $\Delta cld1\Delta taz1$ phenocopied $\Delta cld1$ and wild type. Thus, in agreement with previous studies (Baile et al., 2013; Beranek et al., 2009), analysis of mitochondrial phospholipids indicates that *CLD1* functions upstream of *TAZ1* and downstream of *CRD1* in the CL remodeling pathway.

The placement of *CLD1* between *CRD1* and *TAZ1* was also analyzed by growth on respiratory media (Figure A.2). $\Delta crd1$ yeast displayed a growth defect, and both $\Delta crd1\Delta cld1$ and $\Delta crd1\Delta taz1$ mimicked this phenotype, confirming that *CRD1* is upstream of both *CLD1* and *TAZ1*. $\Delta taz1$ yeast also displayed a growth defect on

respiratory media, but only at elevated temperature. Consistent with Berenak *et al*, $\Delta cld1$ yeast grew as well as wild type, but in contrast to their results, our analysis showed that $\Delta cld1\Delta taz1$ did not exhibit a growth defect and phenocopied $\Delta cld1$. To rule out strain-specific differences, this epistasis analysis was confirmed in two additional genetic backgrounds (Figures A.1 and A.2). Therefore, *CLDI* functions upstream of *TAZI* in a single biochemical pathway.

$\Delta cld1$ mitochondria contain unremodeled CL

CL from $\Delta cld1$ yeast was previously shown by GC/MS to contain more C_{16:0} fatty acyl chains than wild type at the expense of C_{18:1} and C_{16:1} (Berenak *et al.*, 2009). This is consistent with the presence of unremodeled CL in $\Delta cld1$ mitochondria, and prompted us to analyze more comprehensively the acyl chain composition of CL in remodeling mutants by shotgun lipidomics (Figures A.3A and Tables 4 and 5). The acyl chain composition of CL from $\Delta cld1$ or $\Delta taz1$ mitochondria was clearly altered compared to wild type, and the CL species that accumulated in $\Delta cld1$ were similar to that of $\Delta cld1\Delta taz1$, consistent with *CLDI* functioning upstream of *TAZI*.

Unremodeled CL in yeast is characterized in part by saturated acyl chains of increased heterogeneity. To quantify this, the molecular species of CL from each strain was categorized by the number of saturated acyl chains, and expressed as the percent of total CL (Figure A.3B). CL from wild type mitochondria contained mostly unsaturated fatty acyl chains; only 8% contained one saturated acyl chain while the remaining 92% of CL contained no saturated acyl chains. In contrast, only 20% of CL from $\Delta cld1$ contained no unsaturated acyl chains, whereas 51% and 28% of CL contained one or two saturated acyl chains, respectively.

Interestingly, the presence of CL with no saturated acyl chains in both $\Delta cld1$ and $\Delta taz1$ mitochondria suggests that either an alternate (albeit minor) CL remodeling pathway exists, or instead that a subpopulation of newly synthesized CL already contains four unsaturated acyl chains. While the relative amounts of mature (e.g. a remodeled-like acyl chain composition) CL vary between $\Delta cld1$ and $\Delta taz1$ mitochondria, the absolute amounts are similar (Figures A.3C and D), implying that Cld1p is able to specifically deacylate unremodeled CL. This is further supported by the molecular species of MLCL present in $\Delta taz1$; although 28% of CL in $\Delta cld1$ contains 2 saturated acyl chains, none of the molecular forms of MLCL in $\Delta taz1$ contained 2 saturated acyl chains (Figure A.3E and Table 5), suggesting that Cld1p preferentially removes saturated acyl chains from CL.

Thus, we have provided the most extensive analysis to date of the CL acyl chain composition in CL remodeling mutants. CL molecules from $\Delta cld1$ yeast contain more saturated acyl chains than wild type, consistent with unremodeled CL. Accordingly, $\Delta cld1$ is a genetic tool to determine if CL molecules with different acyl chain compositions are functionally distinct in a strain that is otherwise isogenic to wild type yeast.

CL remodeling is not required to maintain mitochondrial morphology

Altered mitochondrial morphology has been observed in $\Delta crd1$ and $\Delta taz1$ yeast (Claypool et al., 2008a; Mileykovskaya and Dowhan, 2009). To determine what role, if any, CL remodeling plays in the establishment and/or maintenance of mitochondrial morphology, CL remodeling mutants were analyzed by EM (Figures A.4 and A.5).

No overt morphological differences were observed between mitochondria in wild type and $\Delta cld1$ yeast (Figure A.4A). Surprisingly, the morphology of mitochondria in $\Delta crd1$ and $\Delta taz1$ also appeared unaffected, although measurement of mitochondrial membranes indicated that both mutants contained longer cristae membranes than wild type or $\Delta cld1$ (Figures A.4B and C). Additionally, no difference in the number of aberrant mitochondria, which display exaggerated cristae, was observed between wild type and any CL remodeling mutant (Figures A.4D and E).

To confirm these results, mitochondria from CL remodeling mutants derived from the W303 genetic background were also analyzed (Figure A.5). While no remarkable morphological defects were observed (Figure A.5A), mitochondria from $\Delta crd1$ and $\Delta cld1$ (but not $\Delta taz1$) yeast displayed longer cristae membranes than wild type, and all of the mutants displayed longer OMM membranes than wild type (Figures A.5B and C). Additionally, in the W303 background, no aberrant mitochondria were observed in wild type (Figures A.5D and E), unlike the mutants which contained a small fraction of aberrant mitochondria.

The mitochondrial morphology in $\Delta crd1$, $\Delta cld1$, and $\Delta taz1$ yeast remained largely unperturbed, although subtle differences were noted. Importantly, studies which previously reported abnormal mitochondrial morphology in $\Delta crd1$ and $\Delta taz1$ yeast never reported the penetrance of the observed defects (Claypool et al., 2008a; Mileykovskaya and Dowhan, 2009). Furthermore, our results indicate that the genetic background contributes to mitochondrial morphology. Thus, we conclude that there is not a general morphological phenotype in mitochondria lacking either remodeled CL or CL entirely.

CL remodeling is not required for optimal OXPHOS function

CL is required for the optimal function of respiratory complexes (Fry and Green, 1980; Fry and Green, 1981; Gomez and Robinson, 1999; Koshkin and Greenberg, 2000; Koshkin and Greenberg, 2002; Schwall et al., 2012; Sedlak and Robinson, 1999), as well as for the stability of respiratory supercomplexes (Claypool and Koehler, 2012; Claypool et al., 2008b; Pfeiffer et al., 2003; Zhang et al., 2002; Zhang et al., 2005). Respiratory supercomplexes, which in yeast consist of two copies of complex III and either one (III₂IV) or two (III₂IV₂) copies of complex IV, increase the efficiency of electron flux through the electron transport chain *via* substrate channeling (Cruciat et al., 2000; Lapuente-Brun et al., 2013). Thus, we used $\Delta cld1$ to determine the ability of unremodeled CL to support OXPHOS.

In $\Delta crd1$ (and $\Delta crd1\Delta cld1$) mitochondria, respiratory supercomplexes were destabilized due to the absence of CL, as seen by the decreased abundance of the III₂IV₂ supercomplex and the resultant increase in the III₂IV supercomplex, as well as the liberated complex III dimer and free complex IV (Figure A.6A). Additionally, the ADP/ATP carrier (Aac2p) did not assemble into higher molecular weight complexes, including with respiratory complexes, in the absence of CL (Claypool et al., 2008b). In $\Delta taz1$, respiratory supercomplex stability was not affected, although the association of Aac2p with the supercomplex was diminished. In $\Delta cld1$ however, the stability of respiratory supercomplexes, including those containing Aac2p, was preserved, indicating that the acyl chain composition of CL does not affect respiratory supercomplex stability.

We further investigated the role of the molecular form of CL in OXPHOS by measuring the rate of O₂ consumption in isolated mitochondria. The P/O ratio (a measure of OXPHOS efficiency) in $\Delta cld1$ mitochondria was indistinguishable from wild type, but

was decreased in $\Delta crd1$, $\Delta crd1\Delta cld1$, and $\Delta taz1$ mitochondria (Figure A.6B). Likewise, no change in the respiratory control ratio (RCR; a measure of OXPHOS coupling) was observed in $\Delta cld1$ compared to wild type (Figure A.6C). Notably, the OXPHOS defects observed in $\Delta taz1$ mitochondria were suppressed after the additional deletion of *CLD1*.

As an alternative method to measure OXPHOS function, we tracked the membrane potential ($\Delta\psi_m$) of isolated mitochondria using the potentiometric fluorescent probe TMRM (Figure A.6D). $\Delta\psi_m$ was established *via* NADH addition, and state 3 respiration was induced by adding ADP, which caused a transient depolarization due to the utilization of the proton gradient to drive ADP/ATP transport by Aac2p and ATP production by complex V. After the ADP was consumed, the inner membrane repolarized and state 4 respiration resumed. $\Delta cld1$ and $\Delta cld1\Delta taz1$ mitochondria were able to repolarize at rates identical to wild type, whereas $\Delta crd1$, $\Delta crd1\Delta cld1$ and $\Delta taz1$ mitochondria repolarized more slowly (Figure A.6E). Taken together, these results indicate that OXPHOS coupling is not dependent on the acyl chain composition of CL that is generated by tafazzin-mediated remodeling.

Interestingly, the individual state 3 and state 4 respiration rates in $\Delta crd1$ and $\Delta taz1$ mitochondria were higher than in wild type (Figure A.7A), which is consistent with some reports, but different from others (Claypool et al., 2008b; Jiang et al., 2000; Koshkin and Greenberg, 2000; Koshkin and Greenberg, 2002; Ma et al., 2004). This observation potentially could be due to a lower steady-state $\Delta\psi_m$ for mitochondria from these strains which, due to respiratory control, would result in higher respiration rates (e.g. easier to pump protons against a lower electrochemical potential); but relative $\Delta\psi_m$ measurements in $\Delta crd1$ and $\Delta crd1\Delta cld1$ mitochondria were not significantly different

from wild type (Figure A.7B). However, TMRM time traces revealed that immediately after establishing the $\Delta\psi_m$, $\Delta crd1$, $\Delta crd1\Delta cld1$, and $\Delta taz1$ mitochondria began to depolarize, whereas those from the other strains maintained a high $\Delta\psi_m$ (Figure A.6D). This depolarization may originate from breaches in the inner membrane permeability barrier that, although not large enough to resolve on measurements of relative steady-state $\Delta\psi_m$ (Figure A.7B), could be resolved on individual traces (Figure A.6D). To identify the source of the putative proton leak, we tested the effects of inhibiting two key OXPHOS components, complex V using oligomycin and Aac2p using carboxyatracyloside (Figure A.7C); both of which create regulated aqueous conduits in the membrane and require CL for assembly (Acehan et al., 2011; Claypool et al., 2008b). The lack of transient depolarization after ADP addition confirmed the efficacy of both oligomycin and carboxyatracyloside. Interestingly, both inhibitors curtailed the immediate depolarization in $\Delta crd1$, $\Delta crd1\Delta cld1$ and $\Delta taz1$ mitochondria, suggesting that in these strains, the time-dependent decrease in $\Delta\psi_m$ was mediated by proton leak through complex V and Aac2p.

When respiration was analyzed under uncoupled conditions to measure maximum electron transport capacity, a small but significant decrease in mitochondria lacking *CRDI* was measured, but no decrease was seen in $\Delta taz1$ or $\Delta cld1$ (Figure A.8A). Measurement of individual complex III and complex IV activities revealed that the defect was specific to complex III (Figures A.8B and C), consistent with CL participating in its catalytic mechanism (Wenz et al., 2009). Further, the steady state abundance of respiratory complex subunits (as well as other mitochondrial proteins) was not affected in any mutant (Figure A.8D). Thus, unremodeled and remodeled CL, which differ

significantly in their acyl chain composition, have the same capacity to promote the expression, assembly, and activity of the OXPHOS system.

DISCUSSION

Despite the pervasiveness of the hypothesis that CL remodeling establishes a molecular form of CL that is optimized to support mitochondrial function, direct evidence for this proposition is lacking. Using *Δcld1* yeast, which cannot initiate CL remodeling, we have provided the most comprehensive comparison to date of the intrinsic functional capacity of distinct molecular forms of CL—remodeled vs. unremodeled CL—in otherwise isogenic cells. Our data indicate that in yeast unremodeled and remodeled CL are equally able to maintain mitochondrial morphology and promote OXPHOS and are thus at variance with the prevailing model that CL remodeling is critical for mitochondrial function. Still, it is possible that the acyl chain composition in mammals plays a larger role in controlling OXPHOS function than in yeast and that this capacity has been a relatively recent addition to the functionality of this remodeling pathway. Consistent with this possibility is that cardiolipin remodeling attributed to acyl-CoA:lysocardiolipin acyltransferase-1, which localizes to the endoplasmic reticulum, is associated with mitochondrial dysfunction (Cao et al., 2004; Cao et al., 2009; Li et al., 2010). Alternatively, mitochondrial processes other than OXPHOS that are presently not known and thus not interrogated in the present study, may be dependent on a specific CL acyl chain composition.

Our results, however, suggest that CL remodeling evolved to achieve other biological outcomes instead of simply establishing a tissue-specific molecular form of

CL. The ability to remodel CL acyl chains may be more important than the establishment of a specific molecular form. CL is susceptible to oxidative damage due to its tight association with respiratory complexes, the major sites of reactive oxygen species production in a cell (Kim et al., 2011). Thus, CL remodeling may be used as a repair mechanism that removes and replaces damaged acyl chains, restoring OXPHOS capacity (Baile et al., 2013; Musatov, 2006). Indeed, increased oxidative damage is observed in *Δtaz1* yeast and Barth syndrome lymphoblasts (Chen et al., 2008; Gonzalvez et al., 2013). Why then, do most tissues/organisms contain only a few molecular forms of CL? Tafazzin has no acyl chain specificity (Xu et al., 2006b). Thus, the acyl chain composition of remodeled CL may instead reflect the acyl chain composition of the surrounding lipids in the microenvironment containing tafazzin (Schlame et al., 2012a). Additionally, when compared to *Δcld1*, the acyl chain composition of CL in *Δtaz1* suggests that saturated acyl chains are the preferred substrate of Cld1p. As such, the specificity of the lipase may also contribute to the final molecular form of CL in a given tissue/cell (Zhang et al., 2011b).

These results have important implications regarding the pathological causes of Barth syndrome. Great emphasis has been placed on the altered CL acyl chain composition, but Barth syndrome patients (and models) also exhibit decreased levels of CL with concurrent increases in MLCL (Gu et al., 2004; Schlame et al., 2003; Soustek et al., 2011; Valianpour et al., 2005; Whited et al., 2012; Xu et al., 2006a). Our data suggest that the absolute levels of lipids (either decreased CL or increased MLCL) and/or the absence of an active remodeling pathway may exert a larger role in contributing to the disease state than simple changes in the final acyl chain composition. These conclusions

have therapeutic implications. For instance, if alterations in the levels of CL and MLCL are the major drivers of mitochondrial dysfunction, then therapies promoting the accumulation of CL and/or depletion of MLCL may alleviate the symptoms of Barth syndrome. An obvious target to inhibit is the lipase that initiates CL remodeling, as we have shown that the $\Delta cld1\Delta taz1$ yeast strain phenocopies wild type. Interestingly, Barth syndrome patient lymphoblasts treated with the iPLA₂ inhibitor bromoenol lactone partially corrects the MLCL:CL ratio, as does knocking out iPLA₂ in *TAZ*^{-/-} flies (Malhotra et al., 2009). However, this strategy is currently hampered in patients since the relevant lipase(s) that functions upstream of tafazzin has not been molecularly identified (Kiebish et al., 2013). Thus further investigation into the basic biology of CL remodeling is required before plausible treatments can be realized.

MATERIALS AND METHODS

Yeast strains and growth conditions

All yeast strains used in this study were isogenic to GA74-1A (*MATa*, *his3-11,15*, *leu2*, *ura3*, *trp1*, *ade8* [*rho*⁺, *mit*⁺]) except where indicated, and have been described previously (Baile et al., 2013; Claypool et al., 2008a; Claypool et al., 2008b; Jarosch et al., 1996), except $\Delta crd1\Delta cld1$, which was generated by replacing the entire open reading frame of *CLD1* with *HIS3MX6* and *CRD1* with *TRP1* (Wach et al., 1994). Strains derived from W303 (*MATa*, *ade2-1*, *ura3-1,15*, *his3-11*, *trp1-1*, *can1-100* [*rho*⁺, *mit*⁺]) were generated by replacing *CRD1* with *TRP1*, *CLD1* with *HIS3MX6*, and/or *TAZ1* with *URA3MX*. Strains derived from PTY144 (*MAT α* , *leu2-3,112*, *ura3-52*, *trp1- Δ 1*, *lys2*, *his3::hisg* [*rho*⁺, *LYS2*]) (Thorsness et al., 2002) were generated by replacing *CRD1*, *CLD1*, or *TAZ1* with *HIS3MX6*, except $\Delta cld1\Delta taz1$ in which *CLD1* was replaced with

HIS3MX6 and *TAZI* with *URA3MX*. Yeast were grown in rich lactate media (1% yeast extract, 2% tryptone, 0.05% dextrose, 2% lactic acid, 3.4 mM CaCl₂-2H₂O, 8.5 mM NaCl, 2.95 mM MgCl₂-6H₂O, 7.35 mM KH₂PO₄, 18.7 mM NH₄Cl, pH 5.5), except for growth analysis where overnight YPD (1% yeast extract, 2% peptone, 2% dextrose) cultures were spotted on synthetic media (0.17% yeast nitrogen base, 0.5% ammonium sulfate, 0.2% complete amino acid mix with either 2% dextrose or 3% glycerol/1% ethanol). Genetic knockouts constructed for this study were generated by replacing the entire open reading frame of the gene using PCR-mediated gene replacement (Wach et al., 1994).

Multidimensional mass spectrometry-based shotgun lipidomic analysis of mitochondrial lipids

A modified Bligh and Dyer procedure was used to extract lipids from each yeast mitochondrial preparation. Each lipid extract was reconstituted with a volume of 200 µl/mg mitochondrial protein in chloroform/methanol (1:1; v/v). Internal standards for quantification of individual molecular species of lipid classes were added prior to lipid extraction (Christie and Han, 2010). Shotgun lipidomics analyses were performed with a QqQ mass spectrometer (Thermo Fisher Scientific TSQ Vantage, San Jose, CA) equipped with an automated nanospray device (Triversa Nanomate, Advion Biosciences, Ithaca, NY) and operated with Xcalibur software as previously described (Han et al., 2008). Identification and quantification of lipid molecular species were performed using an automated software program as previously described (Yang et al., 2009).

Electron Microscopy

Cells were harvested and fixed in 3% glutaraldehyde contained in 0.1 M Na cacodylate, pH 7.4, 5 mM CaCl₂, 5 mM MgCl₂, and 2.5% (w/v) sucrose for 1 hour at room temperature with gentle agitation; spheroplasted; embedded in 2% ultra low temperature agarose (prepared in water); cooled; and subsequently cut into small pieces (~1mm³). The cells were then post-fixed in 1% OsO₄, 1% potassium ferrocyanide contained in 0.1 M Na cacodylate, 5mM CaCl₂, pH 7.4 for 30 minutes at room temperature. The blocks were washed thoroughly 4X with ddH₂O, 10 minutes total; transferred to 1% thiocarbohydrazide at room temperature for 3 minutes; washed in ddH₂O (4X, 1 minute each); and transferred to 1% OsO₄, 1% potassium ferrocyanide in 0.1 M Na cacodylate, pH 7.4 for an additional 3 min at room temperature. The cells were washed 4X with ddH₂O (15 minutes total); en bloc stained in Kellenberger's uranyl acetate (UA) for 2 hr to overnight; dehydrated through a graded series of ethanol; and subsequently embedded in Spurr resin. Sections were cut on a Reichert Ultracut T ultramicrotome; post-stained with UA and lead citrate; and observed on an FEI Tecnai 12 TEM at 100kV. Images were recorded with a Soft Imaging System Megaview III digital camera; and figures were assembled in Adobe Photoshop with only linear adjustments in contrast and brightness.

Assessment of $\Delta\psi_m$

The lipophilic cationic dye tetramethylrhodamine methyl ester (TMRM, Molecular Probes), which accumulates in mitochondria in accordance with a Nernstian distribution, was used in quench mode. 2 ml samples of mitochondria (0.1 mg mitochondrial protein per ml) in measurement buffer (MB; 20 mM Tris-HCl, pH 7.2, 20 mM KCl, 3mM MgCl₂, 4mM KH₂PO₄ and 250 mM sucrose) containing 50 nM TMRM

(from DMSO stocks, final DMSO concentration 1.0% (v/v)) were added to stirred cuvettes. TMRM emission (λ_{ex} 547 nm; λ_{em} 570 nm; slits at 4 nm) was measured over a time course that included the successive addition of: (i) respiratory substrate (2 mM NADH) at 100 s; (ii) 45 μM ADP, pH 7.5 at 300 s and 700 s, and (iii) 2.5 μM valinomycin at 1000 s to completely dissipate the potential. The relative measure of $\Delta\psi_{\text{m}}$ was based on the difference in fluorescence intensity (ΔF) prior to respiratory substrate addition and after establishment of the maximal $\Delta\psi_{\text{m}}$. The time dependence of return to state 4 respiration following the initiation of a phosphorylation cycle was calculated graphically (Kaleidagraph) as the time between ADP addition and stable re-establishment of the maximal $\Delta\psi_{\text{m}}$. Carboxyatractyloside and oligomycin, each at final concentration of 10 μM were incubated with mitochondria at 4°C for 5 min either separately or together. After incubation, TMRM emission was measured over a time course as described above.

Complex III and complex IV activity measurements

Complex III and IV activities were measured as described (Tzagoloff et al., 1975) with a few modifications. To measure complex III activity, 1-25 μg mitochondria solubilized in 0.5% (w/v) *n*-dodecyl β -D-maltoside were added to reaction buffer (50 mM KPi , 2 mM EDTA, pH 7.4) with 0.008% (w/v) horse heart cytochrome *c* and 1 mM potassium cyanide. The reaction was started by adding 100 μM decylubiquinol, and the reduction of cytochrome *c* followed at 550 nm. Complex IV activity was measured by adding mitochondrial extracts to reaction buffer with 0.008% (w/v) ferro-cytochrome *c* and following cytochrome *c* oxidation at 550 nm.

Antibodies

Most antibodies used in this study were generated in our laboratory or the Schatz (J. Schatz, University of Basel, Basel, Switzerland) or Koehler (C. Koehler, University of California, Los Angeles, Los Angeles, CA) laboratories and have been described previously (Baile et al., 2013; Claypool et al., 2006; Daum et al., 1982; Maccacchini et al., 1979; Ohashi et al., 1982; Poyton and Schatz, 1975; Riezman et al., 1983; Whited et al., 2012). Other antibodies used were mouse anti-Aac2p clone 6H8 (Panneels et al., 2003), and horseradish peroxidase-conjugated (Thermo Fisher Scientific) or fluorescent-conjugated (Pierce) secondary antibodies.

Miscellaneous

Isolation of mitochondria, preparation of yeast cell extracts, blue native-PAGE, mitochondrial respiration, phospholipid analysis, and immunoblotting were performed as previously described (Claypool et al., 2008a; Claypool et al., 2006; Claypool et al., 2008b). Statistical comparisons were performed by one-way analysis of variance compared to wild type using SigmaPlot 11 software (Systate Software, San Jose, CA). All graphs show the mean \pm SEM.

ACKNOWLEDGEMENTS

We would like to thank Drs. Jeff Schatz and Carla Koehler for antibodies, and Dr. Peter Thorsness for the PTY144 strain. This work was supported by National Institutes of Health grants R00HL089185 and 1R01HL108882 (SMC), National Science Foundation MCB-1024908 (NNA), NCRN SRR022588A (JMM), and intramural institutional research funds (XH). MGB and YL are predoctoral fellows of the American Heart Association.

TABLE 4 Molecular species of CL

Table 3.1. Molecular species of CL

Molecular species	60:3	60:2	62:3	62:2	64:4	64:3	64:2	66:4	66:3	66:2	68:4	68:3	68:2	70:4	70:3	72:4	72:3	Total CL	MLCL:CL	
Acyl chain composition	14:0-14:1-16:1-16:1	14:0-14:0-16:1-16:1	14:0-16:1-16:1-16:1	14:0-16:1-16:1-16:0	16:1-16:1-16:1-16:1	16:0-16:1-16:1-16:1, 14:0-16:1-16:1-18:1	16:0-16:1-16:1-16:0, 14:0-16:1-16:1-18:0	16:1-16:1-16:1-18:1	16:0-16:1-16:1-18:1, 14:0-16:1-18:1-18:1, 16:1-16:1-16:1-18:0	16:0-16:0-16:1-18:1, 16:0-16:1-18:1-18:0	16:1-16:1-18:1-18:1	16:0-16:1-18:1-18:1	16:0-16:0-18:1-18:1, 16:0-16:1-18:1-18:0	16:1-18:1-18:1-18:1	16:1-18:1-18:1-18:1	16:1-18:1-18:0, 16:0-18:1-18:1-18:1	18:1-18:1-18:1-18:1	18:1-18:1-18:1-18:0		
Mass	644.92	645.93	658.94	659.95	671.95	672.95	673.96	685.96	686.97	687.98	699.98	700.99	701.99	713.99	715.00	728.01	729.02			
WT prep 1 ^a	0.00		0.19		0.96	0.25		6.42	0.48		15.23	1.06		11.30	0.69	2.94	0.22	39.74	0.022	
WT prep 2	0.07		0.35		0.56	0.37		4.67	0.35		12.01	0.79		11.98	0.85	3.98	0.26	36.24	0.024	
WT prep 3	0.11		0.42		0.71	0.39		5.41	0.22		13.57	0.79		14.12	0.90	3.28	0.24	40.17	0.035	
Ataz1 prep 1								1.51	0.77		4.01	1.93	0.53	1.25	0.69	0.11	0.09	10.92	2.057	
Ataz1 prep 2								1.09	0.60		4.14	2.29	0.72	1.50	1.14	0.12	0.14	11.75	1.828	
Ataz1 prep 3								0.77	0.35		3.17	1.64	0.52	1.10	0.76	0.14	0.12	8.57	2.507	
Acld1 prep 1		0.00		0.00		0.63	0.60	1.33	4.01	2.68	3.40	7.48	4.64	1.59	3.28	0.24	0.30	30.17	0.012	
Acld1 prep 2		0.03		0.14		0.60	0.59	1.13	3.88	3.09	3.17	8.22	5.86	1.51	3.37	0.21	0.30	32.11	0.008	
Acld1 prep 3		0.01		0.08		0.47	0.42	0.91	2.86	2.17	2.73	7.09	4.91	1.46	2.99	0.21	0.29	26.60	0.010	
Ataz1 Acld1 prep 1		0.00		0.14		0.53	0.52	1.23	4.22	3.74	3.15	8.97	7.04	1.37	3.32	0.14	0.26	34.63	0.050	
Ataz1 Acld1 prep 2		0.04		0.09		0.48	0.54	1.01	3.59	3.22	3.29	8.61	6.96	1.16	3.01	0.11	0.23	32.33	0.045	
Ataz1 Acld1 prep 3		0.00		0.00		0.32	0.38	1.00	3.62	2.97	3.48	9.02	7.10	1.26	3.14	0.15	0.25	32.71	0.039	
Significance ^b								yes	no		yes	yes		yes	no	yes	yes	yes	yes	
WT vs taz								yes	no		yes	yes		yes	no	yes	yes	yes	yes	
WT vs cld						no		yes	yes		yes	yes		yes	yes	yes	yes	yes	no	
WT vs cldtaz						no		yes	yes		yes	yes		yes	yes	no	yes	yes	no	
taz vs cld						no		no	yes		no	yes	yes	no	yes	no	yes	yes	yes	
taz vs cldtaz						no		no	yes		no	yes	yes	no	yes	no	yes	yes	yes	
cld vs cldtaz		no		no		no	no	no	no	no	no	yes	yes	no	no	no	yes	no	no	

^anmol CL /mg protein

^bSignificance determined by one-way analysis of variance

TABLE 5 Molecular species of MLCL.

Table 3.2. Molecular species of MLCL

Molecular species	46:2	48:3	48:2	50:3	50:2	52:3	52:2	54:3	54:2	
Acyl chain composition	14:0-16:1-16:1	16:1-16:1-16:1	16:1-16:1-16:0	16:1-16:1-18:1	16:1-16:1-18:0, 16:0-16:1-18:1	16:1-18:1-18:1	16:0-18:1-18:1	16:1-18:1-18:1	18:1-18:1-18:0	
Mass	540.83	553.84	554.85	567.86	568.86	581.87	582.88	595.89	596.89	TOTAL MLCL
WT prep 1 ^a		0.03		0.29		0.41	0.02	0.11		0.85
WT prep 2		0.03		0.26		0.40	0.03	0.16		0.87
WT prep 3		0.04		0.42		0.70	0.02	0.21		1.40
Δ taz1 prep 1	0.05	0.51	0.45	4.30	2.49	8.29	4.24	1.37	0.75	22.45
Δ taz1 prep 2	0.09	0.29	0.32	3.38	2.22	7.88	4.79	1.54	0.97	21.49
Δ taz1 prep 3	0.09	0.30	0.31	3.44	2.07	8.22	4.57	1.56	0.91	21.47
Δ cld1 prep 1				0.07	0.13	0.07	0.09			0.35
Δ cld1 prep 2				0.02	0.13	0.03	0.07			0.26
Δ cld1 prep 3				0.02	0.14	0.03	0.09			0.27
Δ taz1 Δ cld1 prep 1			0.09	0.20	0.46	0.38	0.54	0.02	0.04	1.72
Δ taz1 Δ cld1 prep 2			0.05	0.19	0.38	0.31	0.47	0.02	0.04	1.46
Δ taz1 Δ cld1 prep 3			0.01	0.16	0.37	0.27	0.41	0.00	0.05	1.27
Significance^b										
WT vs taz		yes		yes		yes	yes	yes		yes
WT vs cld				no		yes	no			no
WT vs cldtaz				no		no	yes	yes		no
taz vs cld				yes	yes	yes	yes			yes
taz vs cldtaz			yes	yes	yes	yes	yes	yes	yes	yes
cld vs cldtaz				no	yes	no	yes			yes

^anmol MLCL /mg protein

^bSignificance determined by one-way analysis of variance

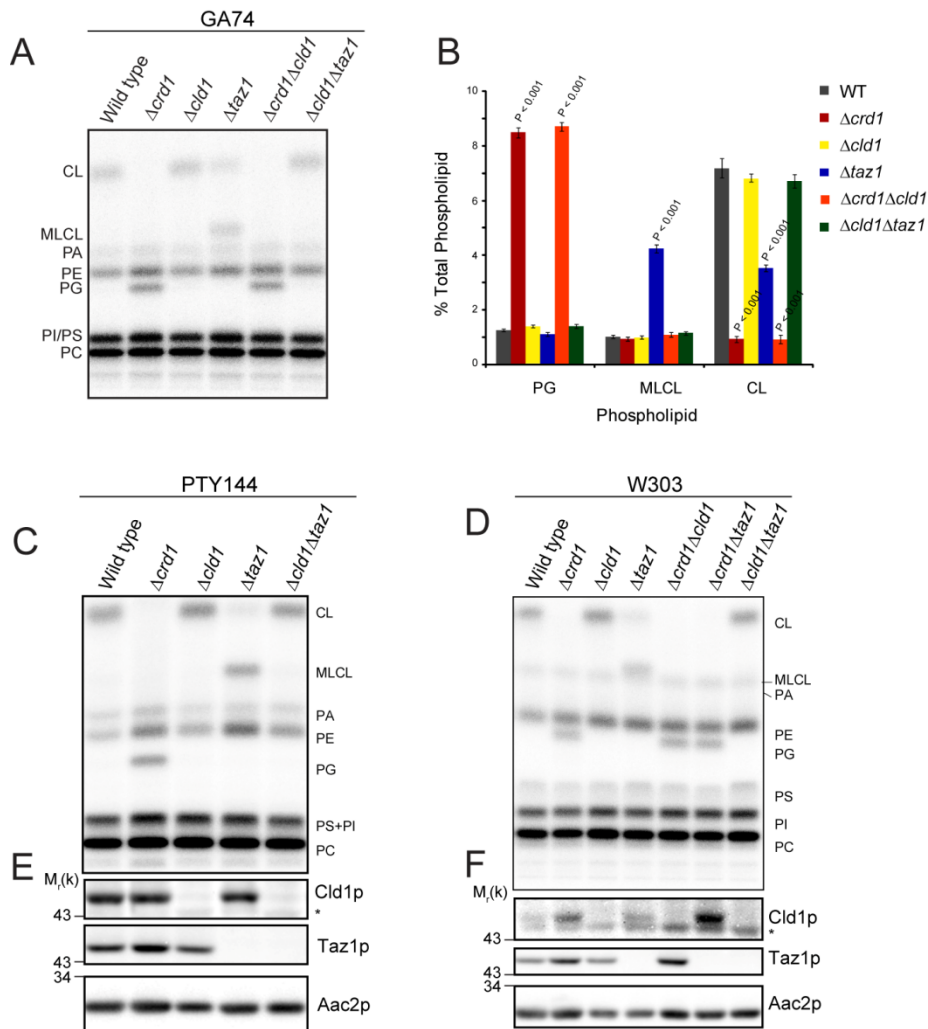


FIGURE A.1. *CLD1* is epistatic to *TAZ1* in the CL remodeling pathway by mitochondrial phospholipid analysis. (A) Mitochondrial phospholipids from the indicated strains derived from GA74-1A were labeled with $^{32}\text{P}_i$ and separated by TLC. (B) Quantification of (A). $n = 5-6$. *** $p < 0.001$ Mitochondrial phospholipids from the indicated strains derived from (C) PTY144 and (D) W303 were analyzed as in (A). Whole cell extracts from the indicated strains derived from (E) PTY144 and (F) W303 were immunoblotted. * indicates a non-specific cross reaction of the Cld1p antisera. PA, phosphatidic acid; PE, phosphatidylethanolamine; PG, phosphatidylglycerol; PS, phosphatidylserine; PI, phosphatidylinositol; PC, phosphatidylcholine.

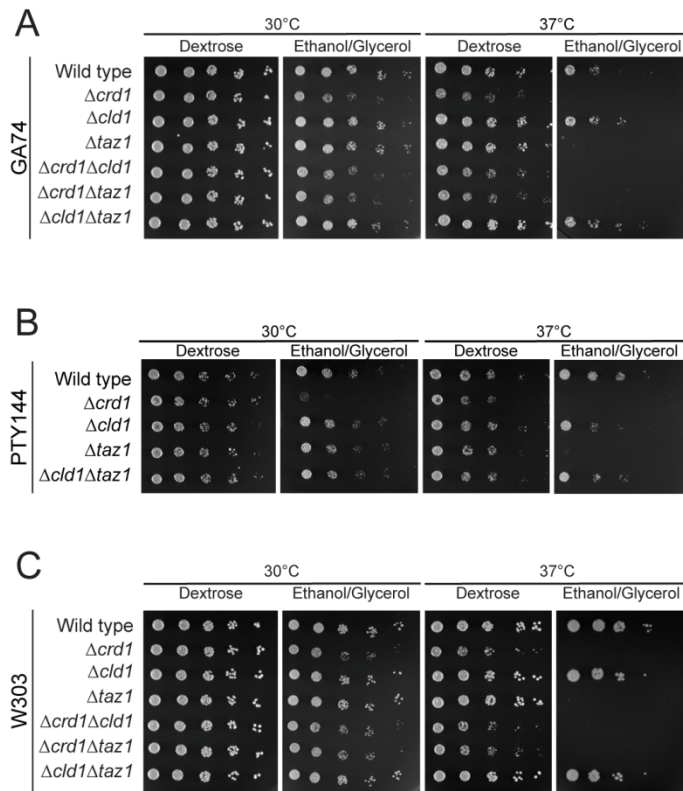


FIGURE A.2. *CLD1* is epistatic to *TAZ1* in the CL remodeling pathway by respiratory growth analysis. 1:4 serial dilutions of the indicated strains derived from (A) GA74-1A, (B) PTY144, or (C) W303 were spotted on the indicated media and incubated at 30°C or 37°C.

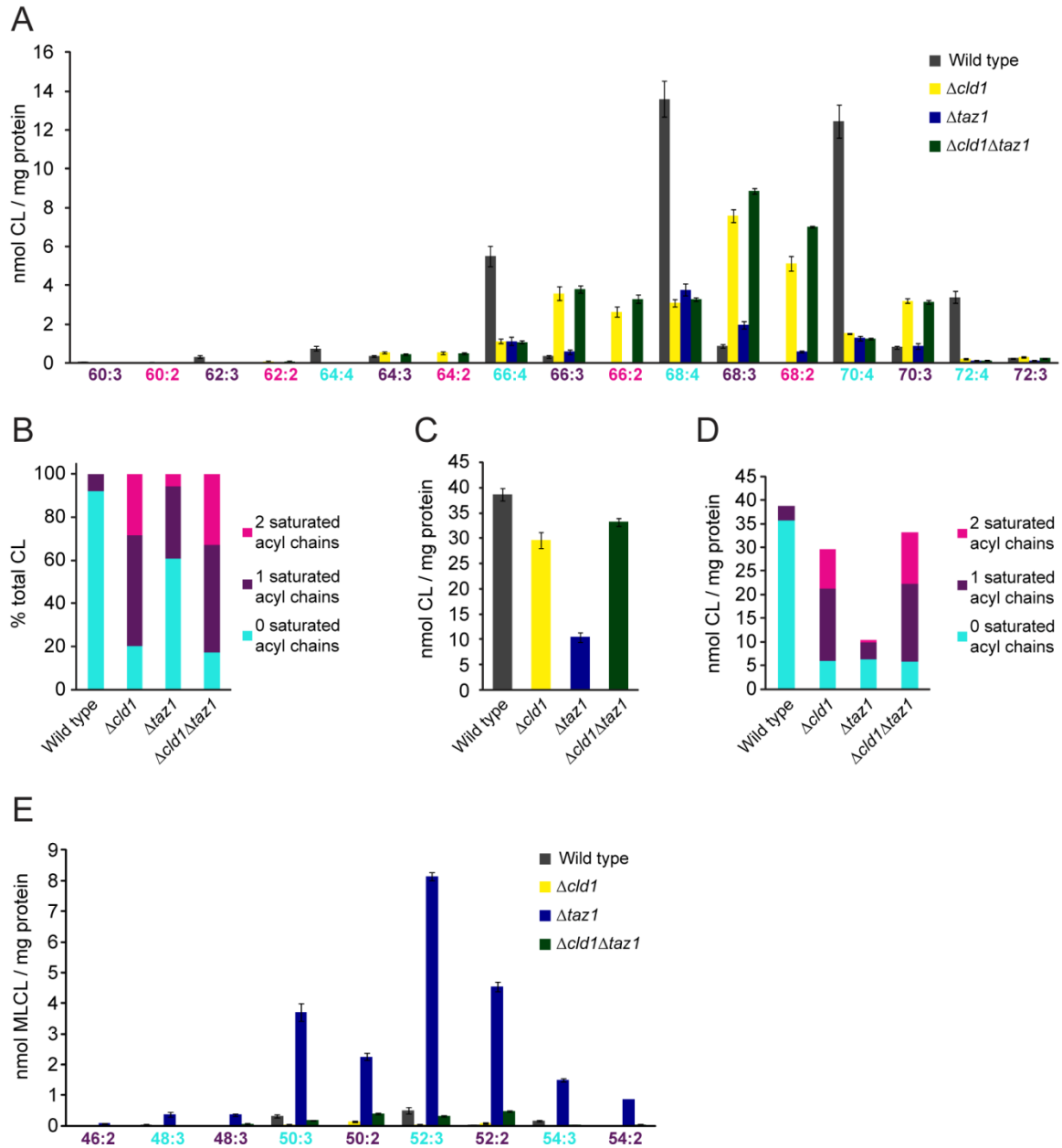


FIGURE A.3. $\Delta cld1$ contains unremodeled CL. (A) The acyl chain composition of CL was determined by multidimensional mass spectrometric array analysis. $n=3$ (B) CL was categorized by the number of saturated acyl chains and expressed as a % of the total CL. (C) Quantification of the total amount of CL per mg of protein. (D) CL was categorized by the number of saturated acyl chains and expressed as the amount of CL per mg protein. (E) The acyl chain composition of MLCL was determined by multidimensional mass spectrometric array analysis. $n=3$.

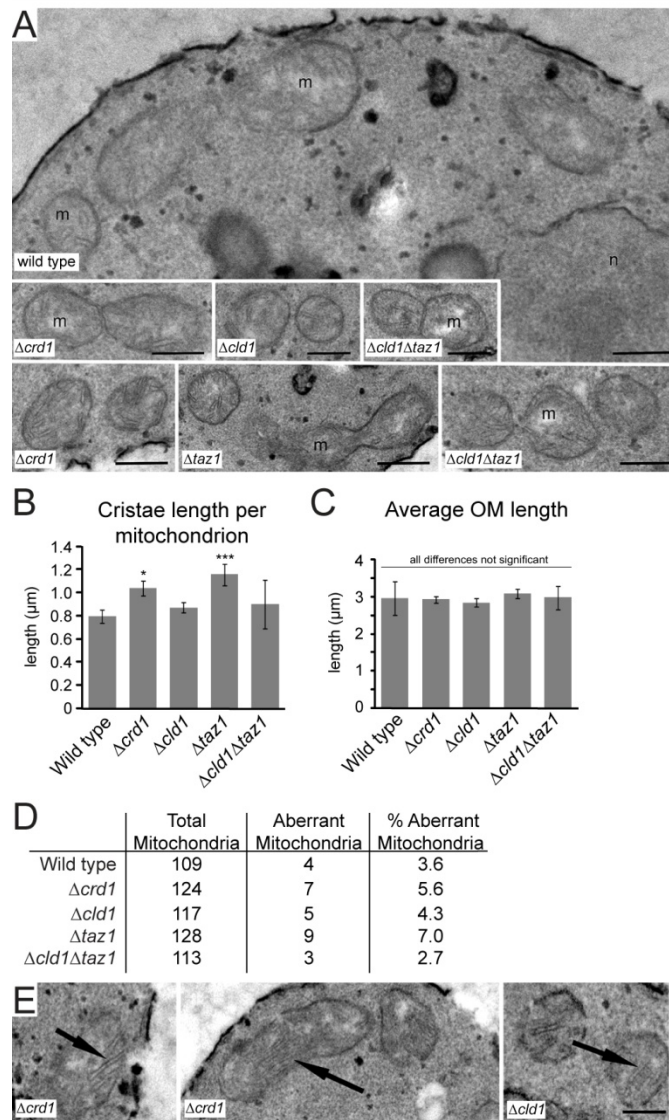


FIGURE A.4. Mitochondrial morphology is not affected by unremodeled CL in GA74 yeast. Mitochondria from the indicated strains derived GA74 were analyzed by TEM. (A) Representative micrographs from the indicated strains. m = mitochondria, n = the nucleus. Bars = 0.5 μm . (B) Quantification of cristae length per mitochondrion. (C) Quantification of OM length per mitochondrion. (D) Quantification of aberrant mitochondria for each strain, defined as the appearance of exaggerated cristae $>0.5 \mu\text{m}$ in length. Number of mitochondria analyzed is indicated for each strain. (E) Examples of mitochondria with exaggerated cristae. Bars = 0.5 μm . * $p < 0.05$, *** $p \leq 0.001$

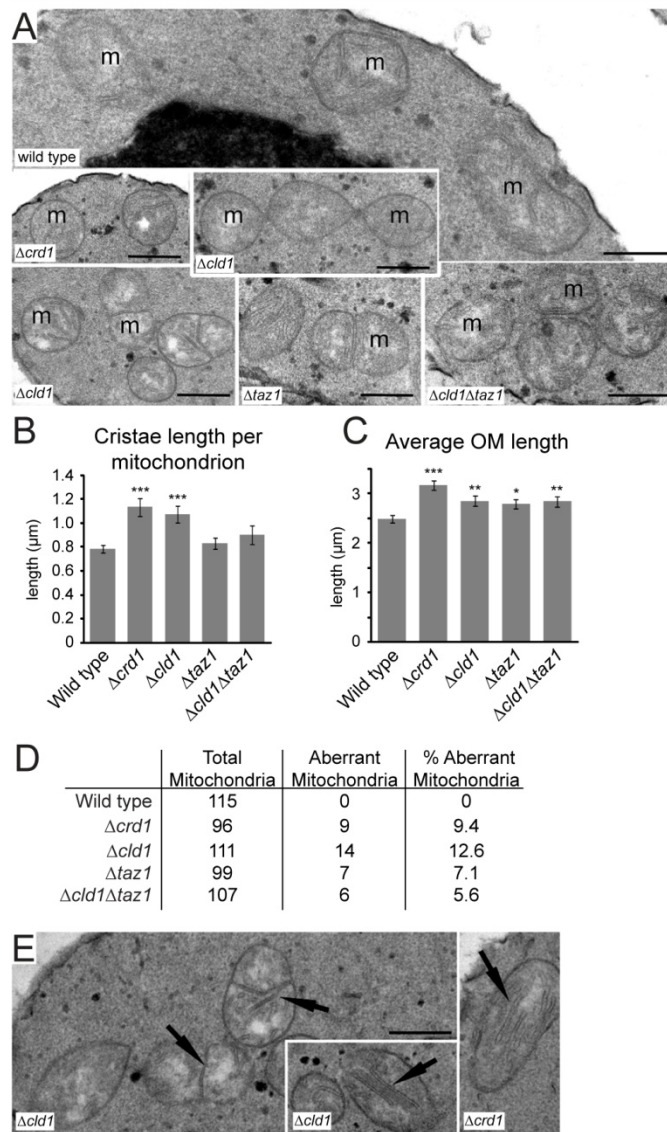


FIGURE A.5. Mitochondrial morphology is not affected by unremodeled CL in W303 yeast. Mitochondria from the indicated strains derived GA74 were analyzed by TEM. (A) Representative micrographs from the indicated strains. m = mitochondria. Bars = 0.5 μ m. (B) Quantification of cristae length per mitochondrion. (C) Quantification of OMM length per mitochondrion. (D) Quantification of aberrant mitochondria for each strain, defined as the appearance of exaggerated cristae $>0.5 \mu$ m in length. Number of mitochondria analyzed is indicated for each strain. (E) Examples of mitochondria with exaggerated cristae. Bars = 0.5 μ m. * $p < 0.05$, ** $p \leq 0.01$, *** $p \leq 0.001$

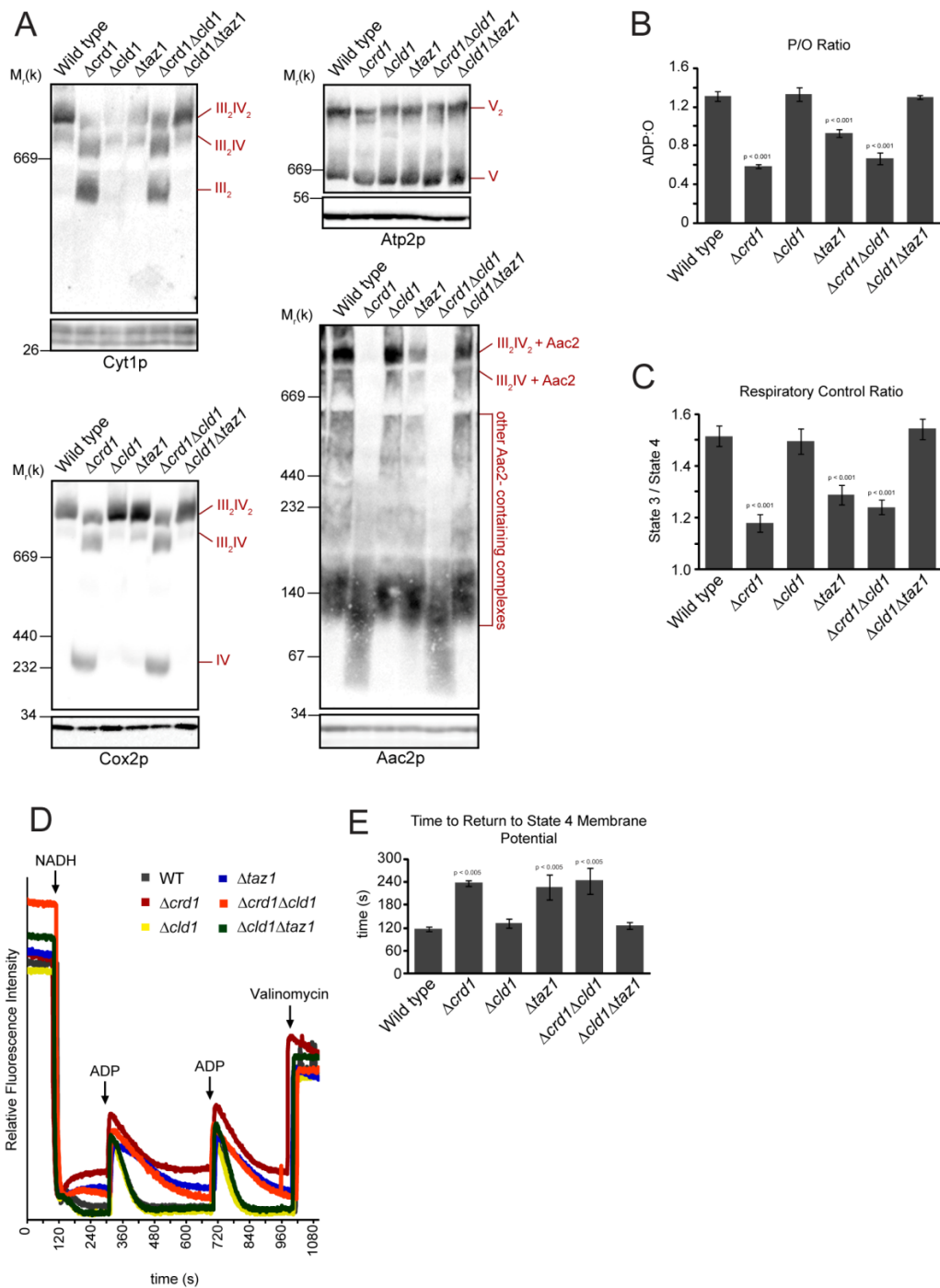


FIGURE A.6. OXPHOS function is not affected by unremodeled CL. (A) Mitochondria were solubilized with digitonin, separated by blue native-PAGE (top panels), and immunoblotted for Cyt1p (complex III), Cox2p (complex IV), Atp2p (complex V), and Aac2p. Bottom panels are immunoblots following SDS-PAGE which serve as loading controls. (B and C) Respiration measured in the presence of 2 mM NADH. $n = 6-9$. (B) P/O ratios. (C) Respiratory control ratios. (D) Representative TMRM time traces of mitochondria isolated from the indicated yeast strains following the addition of 2 mM NADH (to establish the $\Delta\psi_m$) and two sequential additions of 45 μ M ADP to induce phosphorylation cycles, manifest as transient depolarizations. (E) The average times required for the re-establishment of maximal (state 4) $\Delta\psi_m$ following ADP addition for the yeast strains indicated. * $p < 0.05$, *** $p < 0.001$

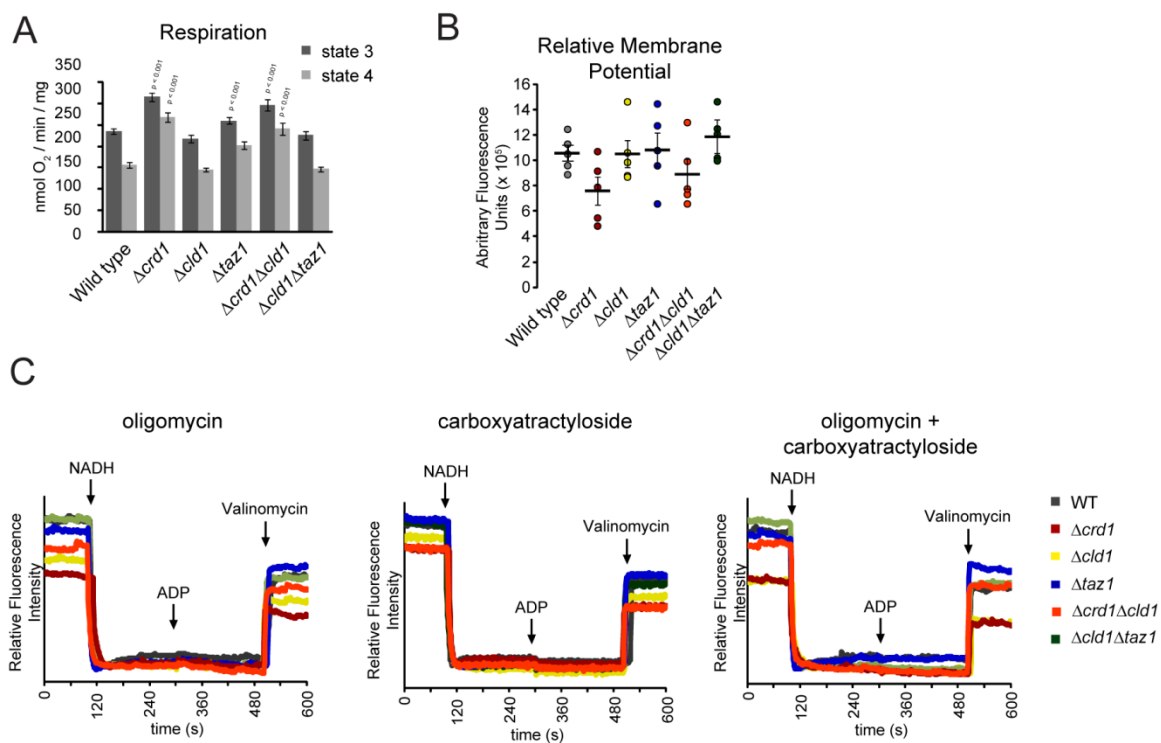


FIGURE A.7. Mitochondrial proton leak is increased in the absence of CL. (A) Respiration of isolated mitochondria measured in the presence of NADH (state 4) or NADH and ADP (state 3). *** $p < 0.001$ (B) The relative membrane potentials from 5 independent experiments were plotted (circles). The mean \pm SEM are displayed as black bars. (C) Membrane potential of the indicated strains measured in the presence of oligomycin (left), carboxyatractyloside (middle), or oligomycin + carboxyatractyloside (right).

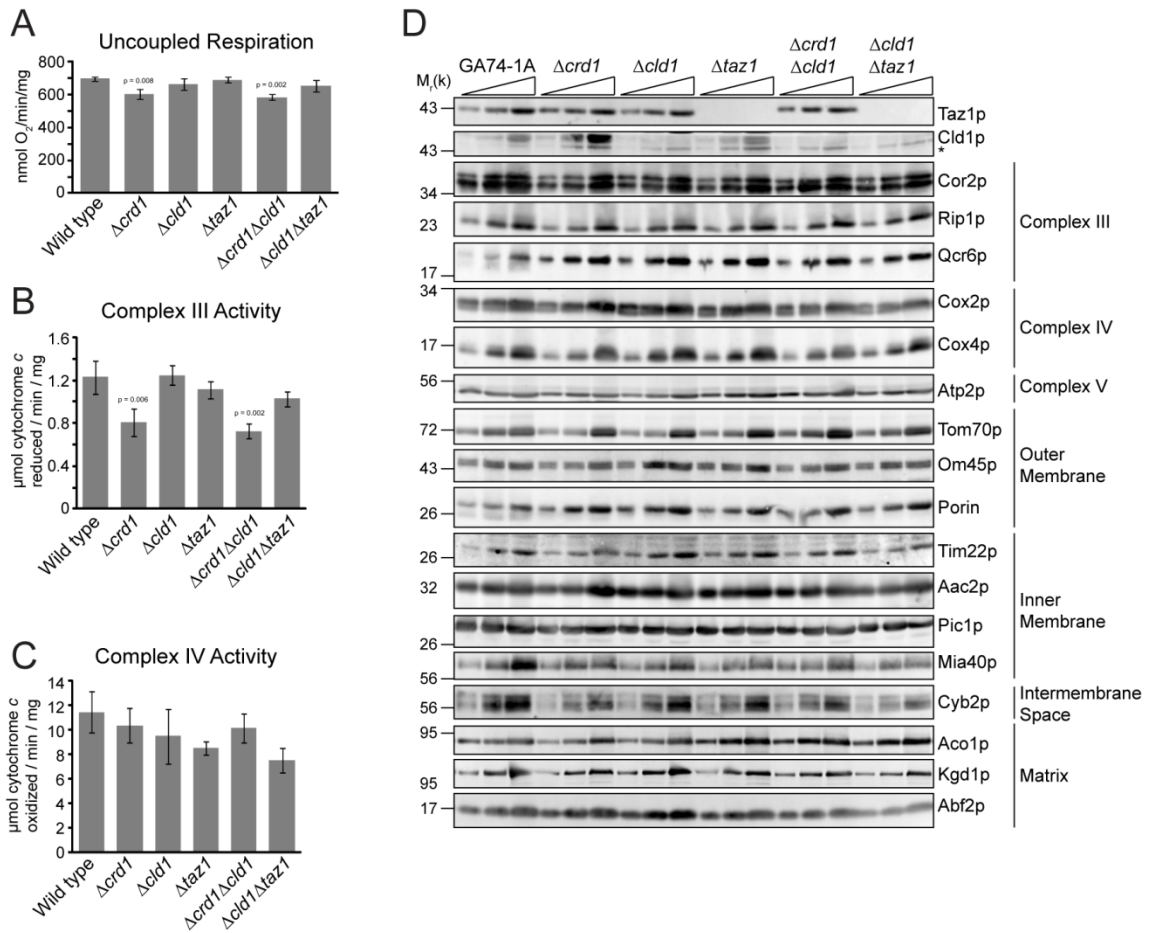


FIGURE A.8. The individual components of OXPHOS are not affected by unremodeled CL. (A) Uncoupled respiration measured in the presence of 2 mM NADH and 10 μM CCCP. (B) Complex III and (C) complex IV activity, measured in DDM mitochondrial extracts. ** $p < 0.01$ (D) Mitochondrial proteins from the indicated strains were separated by SDS-PAGE and immunoblotted. * indicates a non-specific cross reaction of the Cld1p antisera

REFERENCES

- Acehan, D., A. Malhotra, Y. Xu, M. Ren, D.L. Stokes, and M. Schlame. 2011. Cardiolipin affects the supramolecular organization of ATP synthase in mitochondria. *Biophys J.* 100:2184-92.
doi: 10.1016/j.bpj.2011.03.031
- Baile, M.G., K. Whited, and S.M. Claypool. 2013. Deacylation on the matrix side of the mitochondrial inner membrane regulates cardiolipin remodeling. *Mol Biol Cell.* 24:2008-20.
doi: 10.1091/mbc.E13-03-0121
- Ban, T., J.A. Heymann, Z. Song, J.E. Hinshaw, and D.C. Chan. 2010. OPA1 disease alleles causing dominant optic atrophy have defects in cardiolipin-stimulated GTP hydrolysis and membrane tubulation. *Hum Mol Genet.* 19:2113-22.
doi: 10.1093/hmg/ddq088
- Barth, P.G., H.R. Scholte, J.A. Berden, J.M. Van der Klei-Van Moorsel, I.E. Luyt-Houwen, E.T. Van 't Veer-Korthof, J.J. Van der Harten, and M.A. Sobotka-Plojhar. 1983. An X-linked mitochondrial disease affecting cardiac muscle, skeletal muscle and neutrophil leucocytes. *J Neurol Sci.* 62:327-55.
- Beranek, A., G. Rechberger, H. Knauer, H. Wolinski, S.D. Kohlwein, and R. Leber. 2009. Identification of a cardiolipin-specific phospholipase encoded by the gene CLD1 (YGR110W) in yeast. *J Biol Chem.* 284:11572-8.
doi: 10.1074/jbc.M805511200
- Bione, S., P. D'Adamo, E. Maestrini, A.K. Gedeon, P.A. Bolhuis, and D. Toniolo. 1996. A novel X-linked gene, G4.5, is responsible for Barth syndrome. *Nat Genet.* 12:385-9.

doi:10.1038/ng0496-385

Cao, J., Y. Liu, J. Lockwood, P. Burn, and Y. Shi. 2004. A novel cardiolipin-remodeling pathway revealed by a gene encoding an endoplasmic reticulum-associated acyl-CoA:lysocardiolipin acyltransferase (ALCAT1) in mouse. *J Biol Chem.* 279:31727-34.

doi:10.1074/jbc.M402930200

Cao, J., W. Shen, Z. Chang, and Y. Shi. 2009. ALCAT1 is a polyglycerophospholipid acyltransferase potently regulated by adenine nucleotide and thyroid status. *Am J Physiol Endocrinol Metab.* 296:E647-53.

doi: 10.1152/ajpendo.90761.2008

Chen, S., Q. He, and M.L. Greenberg. 2008. Loss of tafazzin in yeast leads to increased oxidative stress during respiratory growth. *Mol Microbiol.* 68:1061-72.

doi: 10.1111/j.1365-2958.2008.06216.x

Cheng, H., D.J. Mancuso, X. Jiang, S. Guan, J. Yang, K. Yang, G. Sun, R.W. Gross, and X. Han. 2008. Shotgun lipidomics reveals the temporally dependent, highly diversified cardiolipin profile in the mammalian brain: temporally coordinated postnatal diversification of cardiolipin molecular species with neuronal remodeling. *Biochemistry.* 47:5869-80.

doi:10.1021/bi7023282

Christie, W., and X. Han. 2010. Lipid Analysis: Isolation, Separation, Identification and Lipidomic Analysis. The Oily Press, Bridgewater, England. 448 pp.

- Claypool, S.M., P. Boonthung, J.M. McCaffery, J.A. Loo, and C.M. Koehler. 2008a. The cardiolipin transacylase, tafazzin, associates with two distinct respiratory components providing insight into Barth syndrome. *Mol Biol Cell*. 19:5143-55. doi: 10.1091/mbc.E08-09-0896
- Claypool, S.M., and C.M. Koehler. 2012. The complexity of cardiolipin in health and disease. *Trends Biochem Sci*. 37:32-41. doi: 10.1016/j.tibs.2011.09.003
- Claypool, S.M., J.M. McCaffery, and C.M. Koehler. 2006. Mitochondrial mislocalization and altered assembly of a cluster of Barth syndrome mutant tafazzins. *J Cell Biol*. 174:379-90. doi: 10.1083/jcb.200605043
- Claypool, S.M., Y. Oktay, P. Boonthung, J.A. Loo, and C.M. Koehler. 2008b. Cardiolipin defines the interactome of the major ADP/ATP carrier protein of the mitochondrial inner membrane. *J Cell Biol*. 182:937-50. doi: 10.1083/jcb.200801152
- Cruciat, C.M., S. Brunner, F. Baumann, W. Neupert, and R.A. Stuart. 2000. The cytochrome bc1 and cytochrome c oxidase complexes associate to form a single supracomplex in yeast mitochondria. *J Biol Chem*. 275:18093-8. doi:10.1074/jbc.M001901200
- Daum, G., P.C. Bohni, and G. Schatz. 1982. Import of proteins into mitochondria. Cytochrome b2 and cytochrome c peroxidase are located in the intermembrane space of yeast mitochondria. *J Biol Chem*. 257:13028-33.

- de Kroon, A.I., P.J. Rijken, and C.H. De Smet. 2013. Checks and balances in membrane phospholipid class and acyl chain homeostasis, the yeast perspective. *Prog Lipid Res.* 52:374-394.
doi: 10.1016/j.plipres.2013.04.006
- DeVay, R.M., L. Dominguez-Ramirez, L.L. Lackner, S. Hoppins, H. Stahlberg, and J. Nunnari. 2009. Coassembly of Mgm1 isoforms requires cardiolipin and mediates mitochondrial inner membrane fusion. *J Cell Biol.* 186:793-803.
doi: 10.1083/jcb.200906098
- Eble, K.S., W.B. Coleman, R.R. Hantgan, and C.C. Cunningham. 1990. Tightly associated cardiolipin in the bovine heart mitochondrial ATP synthase as analyzed by ³¹P nuclear magnetic resonance spectroscopy. *J Biol Chem.* 265:19434-40.
- Fry, M., and D.E. Green. 1980. Cardiolipin requirement by cytochrome oxidase and the catalytic role of phospholipid. *Biochem Biophys Res Commun.* 93:1238-46.
doi:0006-291X(80)90622-1
- Fry, M., and D.E. Green. 1981. Cardiolipin requirement for electron transfer in complex I and III of the mitochondrial respiratory chain. *J Biol Chem.* 256:1874-80.
- Gebert, N., A.S. Joshi, S. Kutik, T. Becker, M. McKenzie, X.L. Guan, V.P. Mooga, D.A. Stroud, G. Kulkarni, M.R. Wenk, P. Rehling, C. Meisinger, M.T. Ryan, N. Wiedemann, M.L. Greenberg, and N. Pfanner. 2009. Mitochondrial cardiolipin involved in outer-membrane protein biogenesis: implications for Barth syndrome. *Curr Biol.* 19:2133-9.
doi: 10.1016/j.cub.2009.10.074

- Gomez, B., Jr., and N.C. Robinson. 1999. Phospholipase digestion of bound cardiolipin reversibly inactivates bovine cytochrome bc1. *Biochemistry*. 38:9031-8.
doi:10.1021/bi990603r
- Gonzalvez, F., M. D'Aurelio, M. Boutant, A. Moustapha, J.P. Puech, T. Landes, L. Arnaure, G. Vial, N. Talleux, C. Slomianny, R.J. Wanders, R.H. Houtkooper, P. Belenger, I.M. Moller, E. Gottlieb, F.M. Vaz, G. Manfredi, and P.X. Petit. 2013. Barth syndrome: Cellular compensation of mitochondrial dysfunction and apoptosis inhibition due to changes in cardiolipin remodeling linked to tafazzin gene mutation. *Biochim Biophys Acta*. 1832:1194-206.
doi: 10.1016/j.bbadis.2013.03.005
- Gonzalvez, F., Z.T. Schug, R.H. Houtkooper, E.D. MacKenzie, D.G. Brooks, R.J. Wanders, P.X. Petit, F.M. Vaz, and E. Gottlieb. 2008. Cardiolipin provides an essential activating platform for caspase-8 on mitochondria. *J Cell Biol*. 183:681-96.
doi: 10.1083/jcb.200803129
- Gu, Z., F. Valianpour, S. Chen, F.M. Vaz, G.A. Hakkaart, R.J. Wanders, and M.L. Greenberg. 2004. Aberrant cardiolipin metabolism in the yeast taz1 mutant: a model for Barth syndrome. *Mol Microbiol*. 51:149-58.
- Han, X., K. Yang, and R.W. Gross. 2008. Microfluidics-based electrospray ionization enhances the intrasource separation of lipid classes and extends identification of individual molecular species through multi-dimensional mass spectrometry: development of an automated high-throughput platform for shotgun lipidomics. *Rapid Commun Mass Spectrom*. 22:2115-24.

doi:10.1002/rcm.3595

Houtkooper, R.H., H. Akbari, H. van Lenthe, W. Kulik, R.J. Wanders, M. Frentzen, and F.M. Vaz. 2006. Identification and characterization of human cardiolipin synthase. *FEBS Lett.* 580:3059-64.

doi: 10.1016/j.febslet.2006.04.054

Houtkooper, R.H., M. Turkenburg, B.T. Poll-The, D. Karall, C. Perez-Cerda, A. Morrone, S. Malvagia, R.J. Wanders, W. Kulik, and F.M. Vaz. 2009. The enigmatic role of tafazzin in cardiolipin metabolism. *Biochim Biophys Acta.* 1788:2003-14.

doi: 10.1016/j.bbamem.2009.07.009

Jarosch, E., G. Tuller, G. Daum, M. Waldherr, A. Voskova, and R.J. Schweyen. 1996. Mrs5p, an essential protein of the mitochondrial intermembrane space, affects protein import into yeast mitochondria. *J Biol Chem.* 271:17219-25.

Jiang, F., M.T. Ryan, M. Schlame, M. Zhao, Z. Gu, M. Klingenberg, N. Pfanner, and M.L. Greenberg. 2000. Absence of cardiolipin in the *crd1* null mutant results in decreased mitochondrial membrane potential and reduced mitochondrial function. *J Biol Chem.* 275:22387-94.

doi:10.1074/jbc.M909868199

Kiebish, M.A., K. Yang, X. Liu, D.J. Mancuso, S. Guan, Z. Zhao, H.F. Sims, R. Cerqua, W.T. Cade, X. Han, and R.W. Gross. 2013. Dysfunctional cardiac mitochondrial bioenergetic, lipidomic, and signaling in a murine model of Barth syndrome. *J Lipid Res.* 54:1312-25.

doi: 10.1194/jlr.M034728

- Kiebish, M.A., K. Yang, H.F. Sims, C.M. Jenkins, X. Liu, D.J. Mancuso, Z. Zhao, S. Guan, D.R. Abendschein, X. Han, and R.W. Gross. 2012. Myocardial regulation of lipidomic flux by cardiolipin synthase: setting the beat for bioenergetic efficiency. *J Biol Chem.* 287:25086-97.
doi: 10.1074/jbc.M112.340521
- Kim, J., P.E. Minkler, R.G. Salomon, V.E. Anderson, and C.L. Hoppel. 2011. Cardiolipin: characterization of distinct oxidized molecular species. *J Lipid Res.* 52:125-35.
doi: 10.1194/jlr.M010520
- Koshkin, V., and M.L. Greenberg. 2000. Oxidative phosphorylation in cardiolipin-lacking yeast mitochondria. *Biochem J.* 347 Pt 3:687-91.
- Koshkin, V., and M.L. Greenberg. 2002. Cardiolipin prevents rate-dependent uncoupling and provides osmotic stability in yeast mitochondria. *Biochem J.* 364:317-22.
- Lapiente-Brun, E., R. Moreno-Loshuertos, R. Acin-Perez, A. Latorre-Pellicer, C. Colas, E. Balsa, E. Perales-Clemente, P.M. Quiros, E. Calvo, M.A. Rodriguez-Hernandez, P. Navas, R. Cruz, A. Carracedo, C. Lopez-Otin, A. Perez-Martos, P. Fernandez-Silva, E. Fernandez-Vizarra, and J.A. Enriquez. 2013. Supercomplex assembly determines electron flux in the mitochondrial electron transport chain. *Science.* 340:1567-70.
doi: 10.1126/science.1230381
- Li, J., C. Romestaing, X. Han, Y. Li, X. Hao, Y. Wu, C. Sun, X. Liu, L.S. Jefferson, J. Xiong, K.F. Lanoue, Z. Chang, C.J. Lynch, H. Wang, and Y. Shi. 2010.

Cardiolipin remodeling by ALCAT1 links oxidative stress and mitochondrial dysfunction to obesity. *Cell Metab.* 12:154-65.

doi: 10.1016/j.cmet.2010.07.003

Ma, L., F.M. Vaz, Z. Gu, R.J. Wanders, and M.L. Greenberg. 2004. The human TAZ gene complements mitochondrial dysfunction in the yeast taz1Delta mutant. Implications for Barth syndrome. *J Biol Chem.* 279:44394-9.

doi:10.1074/jbc.M405479200

Maccacchini, M.L., Y. Rudin, G. Blobel, and G. Schatz. 1979. Import of proteins into mitochondria: precursor forms of the extramitochondrially made F1-ATPase subunits in yeast. *Proc Natl Acad Sci U S A.* 76:343-7.

Malhotra, A., I. Edelman-Novemsky, Y. Xu, H. Plesken, J. Ma, M. Schlame, and M. Ren. 2009. Role of calcium-independent phospholipase A2 in the pathogenesis of Barth syndrome. *Proc Natl Acad Sci U S A.* 106:2337-41.

doi: 10.1073/pnas.0811224106

Mancuso, D.J., H.F. Sims, X. Han, C.M. Jenkins, S.P. Guan, K. Yang, S.H. Moon, T. Pietka, N.A. Abumrad, P.H. Schlesinger, and R.W. Gross. 2007. Genetic ablation of calcium-independent phospholipase A2gamma leads to alterations in mitochondrial lipid metabolism and function resulting in a deficient mitochondrial bioenergetic phenotype. *J Biol Chem.* 282:34611-22.

doi: 10.1074/jbc.M707795200

Marom, M., R. Safonov, S. Amram, Y. Avneon, E. Nachliel, M. Gutman, K. Zohary, A. Azem, and Y. Tsfadia. 2009. Interaction of the Tim44 C-terminal domain with

negatively charged phospholipids. *Biochemistry*. 48:11185-95.

doi:10.1021/bi900998v

Mileykovskaya, E., and W. Dowhan. 2009. Cardiolipin membrane domains in prokaryotes and eukaryotes. *Biochim Biophys Acta*. 1788:2084-91.

doi: 10.1016/j.bbamem.2009.04.003

Montessuit, S., S.P. Somasekharan, O. Terrones, S. Lucken-Ardjomande, S. Herzig, R. Schwarzenbacher, D.J. Manstein, E. Bossy-Wetzel, G. Basanez, P. Meda, and J.C. Martinou. 2010. Membrane remodeling induced by the dynamin-related protein Drp1 stimulates Bax oligomerization. *Cell*. 142:889-901.

doi: 10.1016/j.cell.2010.08.017

Musatov, A. 2006. Contribution of peroxidized cardiolipin to inactivation of bovine heart cytochrome c oxidase. *Free Radic Biol Med*. 41:238-46.

doi: 10.1016/j.freeradbiomed.2006.03.018

Ohashi, A., J. Gibson, I. Gregor, and G. Schatz. 1982. Import of proteins into mitochondria. The precursor of cytochrome c1 is processed in two steps, one of them heme-dependent. *J Biol Chem*. 257:13042-7.

Osman, C., M. Haag, F.T. Wieland, B. Brugger, and T. Langer. 2010. A mitochondrial phosphatase required for cardiolipin biosynthesis: the PGP phosphatase Gep4. *EMBO J*. 29:1976-87.

doi: 10.1038/emboj.2010.98

Ostrander, D.B., G.C. Sparagna, A.A. Amoscato, J.B. McMillin, and W. Dowhan. 2001. Decreased cardiolipin synthesis corresponds with cytochrome c release in

palmitate-induced cardiomyocyte apoptosis. *J Biol Chem.* 276:38061-7.

doi:10.1074/jbc.M107067200

Panneels, V., U. Schussler, S. Costagliola, and I. Sinning. 2003. Choline head groups stabilize the matrix loop regions of the ATP/ADP carrier ScaAAC2. *Biochem Biophys Res Commun.* 300:65-74.

Pfeiffer, K., V. Gohil, R.A. Stuart, C. Hunte, U. Brandt, M.L. Greenberg, and H. Schagger. 2003. Cardiolipin stabilizes respiratory chain supercomplexes. *J Biol Chem.* 278:52873-80.

doi:10.1074/jbc.M308366200

Poyton, R.O., and G. Schatz. 1975. Cytochrome c oxidase from bakers' yeast. IV. Immunological evidence for the participation of a mitochondrially synthesized subunit in enzymatic activity. *J Biol Chem.* 250:762-6.

Riezman, H., R. Hay, S. Gasser, G. Daum, G. Schneider, C. Witte, and G. Schatz. 1983. The outer membrane of yeast mitochondria: isolation of outside-out sealed vesicles. *EMBO J.* 2:1105-11.

Schlame, M. 2013. Cardiolipin remodeling and the function of tafazzin. *Biochim Biophys Acta.* 1831:582-8.

doi: 10.1016/j.bbalip.2012.11.007

Schlame, M., D. Acehan, B. Berno, Y. Xu, S. Valvo, M. Ren, D.L. Stokes, and R.M. Epand. 2012a. The physical state of lipid substrates provides transacylation specificity for tafazzin. *Nat Chem Biol.* 8:862-9.

doi: 10.1038/nchembio.1064

- Schlame, M., S. Blais, I. Edelman-Novemsky, Y. Xu, F. Montecillo, C.K. Phoon, M. Ren, and T.A. Neubert. 2012b. Comparison of cardiolipins from *Drosophila* strains with mutations in putative remodeling enzymes. *Chem Phys Lipids*. 165:512-9.
doi: 10.1016/j.chemphyslip.2012.03.001
- Schlame, M., R.I. Kelley, A. Feigenbaum, J.A. Towbin, P.M. Heerdt, T. Schieble, R.J. Wanders, S. DiMauro, and T.J. Blanck. 2003. Phospholipid abnormalities in children with Barth syndrome. *J Am Coll Cardiol*. 42:1994-9.
doi:S0735109703012403
- Schlame, M., and M. Ren. 2006. Barth syndrome, a human disorder of cardiolipin metabolism. *FEBS Lett*. 580:5450-5.
doi: 10.1016/j.febslet.2006.07.022
- Schlame, M., M. Ren, Y. Xu, M.L. Greenberg, and I. Haller. 2005. Molecular symmetry in mitochondrial cardiolipins. *Chem Phys Lipids*. 138:38-49.
doi:10.1016/j.chemphyslip.2005.08.002
- Schlame, M., J.A. Towbin, P.M. Heerdt, R. Jehle, S. DiMauro, and T.J. Blanck. 2002. Deficiency of tetralinoleoyl-cardiolipin in Barth syndrome. *Ann Neurol*. 51:634-7.
doi:10.1002/ana.10176
- Schwall, C.T., V.L. Greenwood, and N.N. Alder. 2012. The stability and activity of respiratory Complex II is cardiolipin-dependent. *Biochim Biophys Acta*. 1817:1588-96.
doi: 10.1016/j.bbabbio.2012.04.015

- Sedlak, E., and N.C. Robinson. 1999. Phospholipase A(2) digestion of cardiolipin bound to bovine cytochrome c oxidase alters both activity and quaternary structure. *Biochemistry*. 38:14966-72.
doi:bi9914053
- Soustek, M.S., D.J. Falk, C.S. Mah, M.J. Toth, M. Schlame, A.S. Lewin, and B.J. Byrne. 2011. Characterization of a transgenic short hairpin RNA-induced murine model of Tafazzin deficiency. *Hum Gene Ther*. 22:865-71.
doi:10.1089/hum.2010.199
- Thorsness, M.K., K.H. White, and P.E. Thorsness. 2002. Migration of mtDNA into the nucleus. *Methods Mol Biol*. 197:177-86.
doi: 10.1385/1-59259-284-8:177
- Tzagoloff, A., A. Akai, and R.B. Needleman. 1975. Assembly of the mitochondrial membrane system: isolation of nuclear and cytoplasmic mutants of *Saccharomyces cerevisiae* with specific defects in mitochondrial functions. *J Bacteriol*. 122:826-31.
- Valianpour, F., V. Mitsakos, D. Schlemmer, J.A. Towbin, J.M. Taylor, P.G. Ekert, D.R. Thorburn, A. Munnich, R.J. Wanders, P.G. Barth, and F.M. Vaz. 2005. Monolysocardiolipins accumulate in Barth syndrome but do not lead to enhanced apoptosis. *J Lipid Res*. 46:1182-95.
doi: 10.1194/jlr.M500056-JLR200
- van der Laan, M., M. Meinecke, J. Dudek, D.P. Hutu, M. Lind, I. Perschil, B. Guiard, R. Wagner, N. Pfanner, and P. Rehling. 2007. Motor-free mitochondrial presequence

- translocase drives membrane integration of preproteins. *Nat Cell Biol.* 9:1152-9.
doi: 10.1038/ncb1635
- Wach, A., A. Brachat, R. Pohlmann, and P. Philippsen. 1994. New heterologous modules for classical or PCR-based gene disruptions in *Saccharomyces cerevisiae*. *Yeast.* 10:1793-808.
- Wenz, T., R. Hielscher, P. Hellwig, H. Schagger, S. Richers, and C. Hunte. 2009. Role of phospholipids in respiratory cytochrome bc(1) complex catalysis and supercomplex formation. *Biochim Biophys Acta.* 1787:609-16.
doi: 10.1016/j.bbabbio.2009.02.012
- Whited, K., M.G. Baile, P. Currier, and S.M. Claypool. 2012. Seven functional classes of Barth syndrome mutation. *Hum Mol Genet.* 22:483-92.
doi: 10.1093/hmg/dds447
- Xu, Y., M. Condell, H. Plesken, I. Edelman-Novemsky, J. Ma, M. Ren, and M. Schlame. 2006a. A *Drosophila* model of Barth syndrome. *Proc Natl Acad Sci U S A.* 103:11584-8.
doi: 10.1073/pnas.0603242103
- Xu, Y., A. Malhotra, M. Ren, and M. Schlame. 2006b. The enzymatic function of tafazzin. *J Biol Chem.* 281:39217-24.
doi: 10.1074/jbc.M606100200
- Yang, K., H. Cheng, R.W. Gross, and X. Han. 2009. Automated lipid identification and quantification by multidimensional mass spectrometry-based shotgun lipidomics. *Anal Chem.* 81:4356-68.
doi:10.1021/ac900241u

- Zhang, J., Z. Guan, A.N. Murphy, S.E. Wiley, G.A. Perkins, C.A. Worby, J.L. Engel, P. Heacock, O.K. Nguyen, J.H. Wang, C.R. Raetz, W. Dowhan, and J.E. Dixon. 2011a. Mitochondrial phosphatase PTPMT1 is essential for cardiolipin biosynthesis. *Cell Metab.* 13:690-700.
doi: 10.1016/j.cmet.2011.04.007
- Zhang, L., R.J. Bell, M.A. Kiebish, T.N. Seyfried, X. Han, R.W. Gross, and J.H. Chuang. 2011b. A mathematical model for the determination of steady-state cardiolipin remodeling mechanisms using lipidomic data. *PLoS One.* 6:e21170.
doi:10.1371/journal.pone.0021170
- Zhang, M., E. Mileykovskaya, and W. Dowhan. 2002. Gluing the respiratory chain together. Cardiolipin is required for supercomplex formation in the inner mitochondrial membrane. *J Biol Chem.* 277:43553-6.
doi:10.1074/jbc.C200551200
- Zhang, M., E. Mileykovskaya, and W. Dowhan. 2005. Cardiolipin is essential for organization of complexes III and IV into a supercomplex in intact yeast mitochondria. *J Biol Chem.* 280:29403-8.
doi: 10.1074/jbc.M504955200

CURRICULUM VITAE

Ya-Wen Lu

Department of Physiology
Johns Hopkins University
School of Medicine
725 N Wolfe St, Hunterian 207
Baltimore, MD 21205

phone 413.884.2405
email ylu15@jhmi.edu
yawenlu@gmail.com

Education

- 08/2009 – 12/2015 Ph.D., Biochemistry, Cellular, and Molecular Biology (Physiology), Johns Hopkins University School of Medicine, Baltimore, MD
Mentor: Steven M. Claypool, Ph.D.
- 09/2005 – 05/2009 B.A., Chemistry and Art History *cum laude*, Williams College, Williamstown, MA
Mentor: Amy M. Gehring, Ph.D.
- 08/1993 – 06/2005 K-12, Ruamrudee International School, Bangkok, Thailand

Research experience

- 04/2010 – 12/2015 Graduate research. Lab of Steven M. Claypool, Ph.D. Department of Physiology, JHUSOM
- 01/2010 – 03/2010 Research rotation. Lab of Svetlana Lutsenko, Ph.D. Department of Physiology, JHUSOM
- 09/2009 – 12/2009 Research rotation. Lab of Geraldine Seydoux, Ph.D., Department of Molecular Biology and Genetics. JHUSOM
- Summers 2007, 2008 Summer Research Assistant. Lab of Amy M. Gehring, Ph.D., Department of Chemistry, Williams College
- 09/2008 – 06/2009 Senior Thesis research. Lab of Amy M. Gehring, Ph.D., Department of Chemistry, Williams College
- Summers 2005, 2006 Summer Intern. Lab of Dr. Hao-Hueng Chang, M.D., Department of Dentistry, National Taiwan University Hospital, Taipei, Taiwan

Fellowships

- 07/2012 – 06/2014 American Heart Association Pre-doctoral Fellowship, Mid-Atlantic Affiliate
- 09/2008 – 06/2009 Edgar M. Bronfman '50 International Fellowship, Williams College

Honors and awards

- 2015 Best Poster Award. Gordon Research Conference on Molecular and Cellular Biology of Lipids. The same poster was awarded the Best Poster Award (presented by and awarded to Claypool SM) at the Lipids – In vivo dynamics, Protein Partners, and Signaling Section of the American Society for Biochemistry and Molecular Biology 2015 Annual Meeting.
- 2014 Poster Travel Award. 7th International Barth Syndrome Scientific, Medical and Family Conference.
- 2008 Frederick C. Hagedorn, Jr. '71 Premedical Prize. Williams College

Publications

Lu YW, Acoba MG, Kandasamy S, Sathappa M, Alder NN, Claypool SM. The role of CL-binding motifs in mediating heterologous interactions of mitochondrial carriers. *Manuscript in preparation*.

Lu YW, Galbraith L, Herndon JD, Lu YL, Pras-Raves M, Vervaart M, van Kampen A, Luyf A, Koehler CM, Gottlieb E, Vaz FM, Claypool SM. Defining functional classes of Barth syndrome mutation in humans. *In revision at Human Molecular Genetics*.

Bhattacharjee A, Duffy M, Robinson E, Conrad-Antoville A, **Lu YW**, Mangels C, Capps T, Vogt S, Murphy MP, Lutsenko S, Ralle M. Activity of menkes disease protein ATP7A is essential for redox balance in the mitochondria. *In revision at Journal of Biological Chemistry*.

Lu YW, Claypool SM. Disorders of phospholipid metabolism: an emerging class of mitochondrial disease due to defects in nuclear genes. *Frontiers in Genetics* (Invited review). 2015 Feb 3; 6: 3. [PMCID: PMC4315098]

Baile MG, **Lu YW**, Claypool SM. The topology and regulation of cardiolipin biosynthesis and remodeling in yeast. *Chemistry and Physics of Lipids* (Invited review). 2014 Apr; 179: 25-31. [PMCID: PMC3947685]

Baile MG, Sathappa M, **Lu YW**, Pryce E, Whited K, McCaffery JM, Han X, Alder NN, Claypool SM. Unremodeled and remodeled cardiolipin are functionally indistinguishable in yeast. *Journal of Biological Chemistry*. 2014 Jan 17; 289(3): 1768-78. [PMCID: PMC3894353]

Lu YW, San Roman AK, Gehring AM. Role of phosphopantetheinyl transferase genes in antibiotic production by *Streptomyces coelicolor*. *Journal of Bacteriology*. 2008 Oct; 190(20): 6903-8. [PMCID: PMC2566214]

Oral Presentation – National conferences

- 04/2015 Selected speaker. Topological differences but dysfunctional conservation of cardiolipin remodeling. Navigating Lipid Research in Baltimore: from Cell to System, 2nd Annual Meeting, Carnegie Institution, Baltimore, MD
- 06/2014 Selected speaker. Biochemical characterization of human and murine Tafazzin. 7th International Barth Syndrome Scientific, Medical and Family Conference, Biennial Meeting, Clearwater, FL

Oral Presentations – Local meetings

- 10/2014 Selected speaker. Biochemical characterization of human and murine Tafazzin. Annual BCMB Graduate Program Retreat, Baltimore MD
- 02/2012 The role of cardiolipin in defining the interactome of the ADP/ATP carrier. Johns Hopkins Yeast Club. JHUSOM, Baltimore, MD
- 01/2012 The role of cardiolipin in defining the interactome of the ADP/ATP carrier. BCMB Graduate Program Colloquium Series. JHUSOM, Baltimore, MD

Poster abstracts

Lu YW, Galbraith L, Gottlieb E, Vaz FM, Claypool SM. 2014. Topological Difference but Dysfunctional Conservation of Cardiolipin Remodeling in Yeast and Mammals. Molecular & Cellular Biology of Lipids, Gordon Research Conference, Waterville Valley, NH, July 26-31.

Lu YW, Galbraith L, Gottlieb E, Vaz FM, Claypool SM. 2014. Biochemical characterization of human and murine Tafazzin. 7th International Barth Syndrome Scientific, Medical and Family Conference, Clearwater, FL, June 23-28.

Lu YW, Baile MG, Huang TC, Pandey A, Claypool SM. 2013. The role of cardiolipin in defining the mammalian ANT interactome. American Society for Biochemistry and Molecular Biology, Boston, MA, April 20-24.

Teaching

- 01/2016 – 03/2016 Teaching Assistant for ME:340.703 Cell Structure and Dynamics. Department of Cell Biology, JHUSOM, Baltimore, MD
Supervisor: Hiromi Sesaki Ph.D.
- 01/2015 – 03/2015 Teaching Assistant for ME:340.703 Cell Structure and Dynamics. Department of Cell Biology, JHUSOM, Baltimore, MD
Supervisor: Hiromi Sesaki Ph.D.
- 01/2014 – 03/2014 Teaching Assistant for ME:340.703 Cell Structure and Dynamics. Department of Cell Biology, JHUSOM, Baltimore, MD
Supervisor: Peter Espenshade Ph.D.
- 10/2013 Teaching Assistant for ME:800.600 Cell Physiology block of Scientific Foundations of Medicine (first year medical student core curriculum), Department of Cell Biology, JHUSOM, Baltimore, MD
Supervisor: Erika Matunis Ph.D.
- 02/2008 – 05/2009 Laboratory Teaching Assistant for CHEM 151: Concepts of Chemistry and CHEM 256: Introduction to Physical and Inorganic Chemistry. Department of Chemistry, Williams College, Williamstown, MA
Supervisor: Enrique Peacock-Lopez Ph.D.

Mentoring

09/2014 – 12/2014 Thomas Lin (JHU undergraduate)
01/2015 – present Michelle Acoba (Cellular and Molecular Physiology rotation student and a now graduate student in the Claypool Lab)

List of References

Steven M. Claypool, Ph.D.
Associate Professor of Physiology
Director, Graduate Program in Cellular and Molecular Physiology
Department of Physiology
725 N Wolfe St, Hunterian 207
Baltimore, MD 21205
Phone: +1 (410) 614-1786
Fax: +1 (410) 955-0461
Email: sclaypo1@jhmi.edu

Rajini Rao, Ph.D.
Professor of Physiology
Director, Center for Membrane Transport
Director, Graduate Program in Cellular and Molecular Medicine
725 N Wolfe St, WBSB 201
Baltimore, MD 21205
Phone: +1 (410) 955-4732
Fax: +1 (410) 955-0461
Email: rrao@jhmi.edu

Michael J. Wolfgang, Ph.D.
Associate Professor of Biological Chemistry
855 N Wolfe St, Rangos 475
Baltimore, MD 21205
Phone: +1 (443) 287-7680
Fax: +1 (410) 614-8033
Email: mwolfgal@jhmi.edu

Daniel M. Raben, Ph.D.
Professor of Biological Chemistry, Physiology, and Oncology
725 N Wolfe St, Hunterian 502
Baltimore, MD 21205
Phone: +1 (410) 955-1289
Fax: +1 (410) 614-8729
Email: draben@jhmi.edu